Progression of Neuroanatomical Abnormalities in Psychosis

By

Theophilus Narteh Akudjedu., MSc, BSc.

A thesis submitted to the National University of Ireland Galway, as fulfilment of the requirements for a Degree of Doctor of Philosophy

Discipline of Psychiatry
School of Medicine
College of Medicine, Nursing and Health Sciences

October 2019

Research Supervisors
Dr. Brian Hallahan
Dr. Dara Cannon
Prof. Colm McDonald

TABLE OF CONTENTS

AUTHORS DECLARATION

I declare that all of the work presented in this thesis is entirely my own work, except where otherwise indicated by reference in the text. I further declare that this original work was carried out in accordance with the rules and regulations of the National University of Ireland Galway and has not been submitted previously as an exercise at this or any other institution for any other academic award.

The original data for both studies focusing on the comparative analyses of segmentation techniques and progression of brain changes after first-episode of psychosis were acquired prior to commencement of the current PhD research. Acquisition of MRI and clinical data was done by Dr. Cathy Scanlon, Dr. John McFarland and Dr. Shane McInerney. My responsibilities included conducting all pre-processing and quality control of MRI data and imaging analyses with support particularly during study 1 on various segmentation techniques as follows: Stereology – (Emma McDermott and Peter Dockery), Manual tracing (Sarah Hehir, Helen Casey, Srinath Ambati, Joanne Kenney and Stefani O'Donoghue) and FSL-FIRST (Leila Nabulsi). All statistical and other imaging analyses and writing of the thesis was conducted entirely by me under the supervision of Dr Brian Hallahan, Dr Dara Cannon and Prof Colm McDonald.

Signed: Date:

Theophilus Narteh Akudjedu 04/10/2019

ACKNOWLEDGEMENTS

I would like to give a special mention to my supervisor, Dr. Brian Hallahan, whose guidance and support through the PhD was immeasurable. I have benefitted a lot from his open door policy that allowed me to just walk in whenever he is available. To my most supportive co-supervisors – Dr. Dara Cannon and Prof Colm McDonald who equally provided great support and guidance throughout the PhD process - I have gained great insight and understanding of psychiatry, anatomy and clinical neuroscience from you all, for which I am grateful. You have been a brilliant team of stimulating mentors during the past few years.

I would like to extend my gratitude to my fellow PhD students and members of the Clinical Neuroimaging Laboratory who have always been supportive and provided a conducive and friendly atmosphere for the hard work of PhD to be done. Thanks for the laughs, the jokes and the help throughout the period……!

Next, I would like to thank the NUI Galway College of Medicine, Nursing and Health Sciences for funding my PhD training through the Postgraduate Scholarship Scheme. I would also like to thank all of the participants and their families for their involvement in the Research Programme of the Clinical Neuroimaging laboratory, NUI Galway.

Finally, and most importantly, I'd like to thank all my family for all the love and support from far and near during my PhD. Particularly, I would like to extend a most special and warm mention to my wife – Trish, who stuck with me, and this process, through hills and valleys. She gave me support, encouragement and provided me with nice distractions when I needed them to ease the process. Thank you for everything – this thesis is dedicated to you.

LIST OF PUBLICATIONS AND PRESENTATIONS

Peer-reviewed Publications

1. **Akudjedu, T.N.,** Nabulsi, L., Makelyte, M., Scanlon, C., Hehir, S., Casey, H., Ambati, S., Kenney, J., O'Donoghue, S., et al., 2018. A comparative study of segmentation techniques for the quantification of brain subcortical volume. Brain Imaging and Behavior 12(6), 1678-1695. PMID: 29442273 DOI: 10.1007/s11682-018-9835-y **(Published).**

2. **Akudjedu, T.N.,** Tronchin, G., Scanlon, C., Kenney, J., McInerney, S., McFarland, J., Barker, G.J., McCarthy, P., Cannon, D.M., Hallahan, B., McDonald C., 2019. Progression of subcortical changes after first-episode of psychosis: A 3-year longitudinal structural magnetic resonance imaging study. Schizophrenia Research **(Submitted).**

3. **Akudjedu, T.N.,** Tronchin, G., Scanlon, C., Kenney, J., McInerney, S., McFarland, J., Barker, G.J., McCarthy, P., Cannon, D.M., Hallahan, B., McDonald C., 2019. Progression of cortical changes after first-episode of psychosis: A 3-year longitudinal structural magnetic resonance imaging study. Psychological Medicine **(In Preparation).**

Abstracts

Oral Presentations

1. **Akudjedu, T.N.,** Nabulsi, L., Makelyte, M., Scanlon, C., Hehir, S., Casey, H., Ambati, S., Kenney, J., O'Donoghue, S., et al., 2018. A comparative study of segmentation techniques for the quantification of brain subcortical volume. 10th Neuroscience Ireland Conference in NUI Galway, Republic of Ireland. August 28th - 29th 2017.

Poster Presentations

1. **Akudjedu, T.N.,** Tronchin, G., Scanlon, C., Kenney, J., McInerney, S., McFarland, J., Barker, G.J., McCarthy, P., Cannon, D.M., Hallahan, B., McDonald C. Progression of subcortical changes after first-episode of psychosis: A 3-year longitudinal structural magnetic resonance imaging study. Poster Presentation at the 74th Annual Meeting of the Society of Biological Psychiatry in Chicago, United States of America, May 16th – 18th 2019. **(Published).**

2. **Akudjedu, T.N.,** Nabulsi, L., Makelyte, M., Scanlon, C., Hehir, S., Casey, H., Ambati, S., Kenney, J., O'Donoghue, S., et al., 2018. A comparative study of segmentation techniques for the quantification of brain subcortical volume. 10th Neuroscience Ireland Conference, NUI Galway, Republic of Ireland. August 28th - 29th 2017.

3. **Akudjedu, T.N.,** Nabulsi, L., Makelyte, M., Scanlon, C., Hehir, S., Casey, H., Ambati, S., Kenney, J., O'Donoghue, S., et al., 2018. A comparative study of segmentation techniques for the quantification of brain subcortical volume. Galway Neuroscience Centre Annual Research Day, NUI Galway, Republic of Ireland. December 2nd, 2016.

4. **Akudjedu, T.N.,** Nabulsi, L., Makelyte, M., Scanlon, C., Hehir, S., Casey, H., Ambati, S., Kenney, J., O'Donoghue, S., et al., 2018. A comparative study of segmentation techniques for the quantification of brain subcortical volume. College of Medicine, Nursing & Health Sciences Postgraduate Research Day, NUI Galway, Republic of Ireland. June 3rd, 2016.

LIST OF FIGURES

LIST OF TABLES

STRUCTURE OF THE THESIS

This thesis is organised into five chapters involving three main studies. The first chapter provides a general introduction to the background of psychosis with focus on aetiology, epidemiology and neuroanatomical abnormalities. It reviews further, the brain segmentation approaches employed in the field of neuropsychiatry and explore the basic principles of structural MRI image acquisition and analyses. The second chapter (study 1), systematically investigated the accuracy of segmentation techniques at delineating subcortical structures in a large heterogenous sample of major psychiatric disorders. Based on the recommendations of chapter 1, an optimal segmentation technique (FreeSurfer) was employed in chapter 3 (study 2) to investigate the progression of changes in the ventricles and subcortical structures over time and the association of these changes with clinical and functional measures in FEP patients relative to a healthy control population. The fourth chapter (study 3), examined in the same sample as in study 2, the cortical changes longitudinally and the association of these changes with clinical and functional measures. Finally, chapter 5, integrates the findings from the three studies and discusses the strengths and limitations of the studies and recommends directions for future research.

Overall, three manuscripts have emerged from the current PhD research and are presented in this thesis, the first is titled “A comparative study of segmentation techniques for the quantification of brain subcortical volume” was accepted and published in Brain Imaging & Behavior (Dec 2018). The second, submitted to Schizophrenia Research is titled “Progression of subcortical changes after first-episode of psychosis: A 3-year longitudinal sMRI study”. Finally, the third manuscript titled “Progression of cortical changes after first-episode of psychosis: A 3-year longitudinal sMRI study” is in preparation for submission to Psychological Medicine.

THESIS ABSTRACT

Background: Structural brain changes and their cross-sectional relationships with clinical and functional measures have been demonstrated several times using magnetic resonance imaging at the onset of first-episode of psychosis (FEP) (Vita *et al.* 2006; Dazzan *et al.* 2012). However, few studies have carried out longitudinal analyses to clarify the extent and location of progressive changes and their associations over time and thus, findings in this area remain unclear. We investigated the progressive profile of ventricular and cortico-subcortical regions over a 3-year period in individuals following FEP compared with healthy controls (HC), and whether these progressive neuroanatomical changes were related to a number of clinical factors including severity of symptoms, antipsychotic medications and level of functioning. In order to choose an optimal tool to fully elucidate these neuroanatomical changes, the performance of various brain segmentation techniques were compared in terms of their anatomical accuracy, consistency and labour intensity.

Methods: For the comparative study of segmentation techniques, high resolution 1.5 Tesla T1-weighted MR images were obtained from 177 patients with major psychiatric disorders and 104 HCs. The relative consistency (partial correlation), absolute agreement (intraclass correlation coefficient (ICC) and potential technique bias (Bland-Altman plots) of each technique was compared with manual segmentation.

The studies (2 and 3) focusing on progressive neuroanatomical changes after FEP, similarly employed 1.5T T1-weighted MR images from 28 FEP patients and 28 HCs at baseline and 3-year follow-up. The longitudinal FreeSurfer pipeline (v.5.3.0) was used for regional volumetric analyses and cortical reconstructions by creating an unbiased anatomical template for improved sensitivity to detecting subtle changes over time. Repeated-measures ANCOVA and vertex-wise linear regression analyses were used to compare progressive changes in relation to subcortical structures/ventricles and thickness across the cortical mantle, respectively, between groups. Independent group analyses of covariance was used to compare rates of thickness change of the abnormal cortical regions (ROI). Partial correlations were used to determine associations of progressive neuroanatomical change with clinical and functional characteristics. Age, gender and intracranial volume (only in the case of volume) were included as covariates.

Results: In relation to the segmentation techniques, all yielded high correlations and moderate ICC's relative to manual segmentation for the caudate. For the hippocampus, stereology yielded good consistency and ICC, whereas automated and semi-automated

techniques yielded poor ICC and moderate consistency. Bias was least using stereology for segmentation of the hippocampus and using FreeSurfer for segmentation of the caudate.

In the analyses relating to progressive changes after FEP, a significant group by time interaction was found indicating progressively reduced volume of the caudate, putamen and thalamus in FEP patients relative to controls, with a trend for increased lateral ventricular volume more prominent on the right. Additionally, in FEP patients relative to HCs, there was a significantly increased rate of cortical thinning at a mean difference of 0.844% [95% CI (0.095, 1.593)] (Fig.4.3A) in the left lateral orbitofrontal region (LLOFR) over the 3-year period. We observed further that increasing lateral ventricular volume over time was associated with worsening negative symptoms and poorer global assessment of functioning over time.

Conclusions: In a typical neuropsychiatric MRI dataset, automated segmentation techniques provide good accuracy for an *easy-to-segment* structure such as the caudate, whereas for the hippocampus, a reasonable correlation with volume but poor absolute agreement was demonstrated. This indicates manual or stereological volume estimation should be considered for studies that require high levels of precision such as those with small sample size. This finding should inform the field especially in decision making on each type of segmentation technique to use especially for the now standard, large-scale brain morphometric studies ongoing in the field of neuropsychiatry.

Our results from the studies (2 and 3) focusing on FEP and MRI techniques utilised in study 1 demonstrate existence of localised progressive cortical thinning in the LLOFR characterised by volume deficits in the dorsal striatum, thalamic regions and right lateral ventricular enlargement across the psychosis phenotype after the early years following the first presentation of illness. This is suggestive of a structural disturbance in the subnetwork of the cortico-striato-thalamo-cortical circuitry in a progressive manner after FEP. Furthermore, increasing ventricular volumes are neuroanatomical markers of poorer clinical outcome. These findings lend weight to the evidence of early progressive brain changes in psychotic disorders and thus, this knowledge could potentially contribute to the identification of imaging biomarkers for timely intervention.

ABBREVIATIONS

ANCOVA Analysis of covariance

ARMS At risk mental state

DISC 1 Disrupted in schizophrenia 1

DSM Diagnostic and statistical manual

CB1 Cannabinoid 1

CPZ Chlorpromazine

CT Computed tomography

FEP First Episode of Psychosis

FU Follow-up

GM Grey Matter

GWAS Genome-wide association study

HC Healthy Controls

ICV Intracranial Volume

LLOFR Left lateral orbitofrontal region

LV Lateral ventricle

MPRAGE Magnetisation-Prepared Rapid Acquisition of Gradient Echo

MRI Magnetic Resonance Imaging

NOS not otherwise specified

PANSS Positive and Negative Syndrome Scale

PC1 Percentage change

QDEC Query Design Estimate Contrast

ROI Region of interest

SCID Structured Clinical Interview for DSM-IV

SPC symmetrised percentage change

UHG University Hospital Galway

WM White Matter

Chapter 1

General Introduction

1.1 Introduction

Psychotic symptoms are present across a wide range of mental health disorders and are likely to cause considerable distress and disability for the individual experiencing the symptoms and their family or carer (National Institute for health Care and Excellence (NICE, 2014)). The presence of a psychotic disorder is associated with a high socioeconomic burden (Gustavsson *et al.* 2011; Wittchen *et al.* 2011). The onset of psychosis often occurs during a period critical to the cognitive, social and emotional development and can adversely impact the individual in relation to their vocational, educational and normal developmental needs (Birchwood *et al.* 1998). Psychotic symptoms are broadly categorised into positive and negative symptoms with positive symptoms typically encompassing hallucinations and delusions whilst negative symptoms include amotivation or concentration decline, social withdrawal and anhedonia (Owen *et al.* 2016).

Psychotic disorders can be categorised based on if the primary disorder is a mood disorder (affective psychosis) or not (non-affective psychosis). Affective psychotic disorders include bipolar I disorder and major depressive disorder while non-affective psychotic disorders include schizophrenia, schizoaffective disorder, psychotic disorder not otherwise specified (NOS), substance induced psychosis and delusional disorder as were previously defined (Kenney *et al.* 2015). Furthermore, psychosis is also classified based on the cause of the psychotic symptoms, thus, it can be organic or functional in nature. Organic psychosis arises due to a known physical disorder such as severe head trauma or a brain tumour. For example, Dutschke and colleagues (2017) in a case report, observed psychotic symptoms in a patient with a localised tumour in the region of the posterior thalamus and internal capsule. On the other hand, functional psychosis represents psychosis occurring in the absence of a known physical abnormality or cause (Ganguli *et al.* 2011). In a series of anthropological reports by Castillo (1997; 2001; 2003), a relationship was observed between cultural beliefs, meditative trance and functional psychoses. In highly experienced yogis from an Indian tribe, many years of meditative trance seems to have produced a state of permanently altered consciousness characterised by recurrent religious visions and beliefs (Castillo, 2003). In a modern western culture, these beliefs would otherwise be considered delusional. Of note, other psychotic symptoms could be secondary to a general medical condition or substance use, including illicit and medicinal drugs. Generally, the term first-episode of psychosis (FEP) is used to describe the first psychotic episode. In this research, our operational definition for FEP included patients diagnosed with either an affective or non-affective psychotic disorder.

Participants were minimally medicated (<3 weeks) prior to recruitment and fulfilled the following criteria of not currently having; 1) an existing or history of neurological disorders, 2) learning disability, 3) life-time substance dependency (as defined by DSM-IV-TR), 4) a history of head injury resulting in loss of consciousness for over 5 minutes and 5) oral steroid use in the past 3 months. We recruited a broader psychosis phenotype rather than non-affective psychosis alone to reflect the day-to-day clinical practice in a real-world setting.

1.2 Epidemiology of psychosis

The prevalence of psychosis has been estimated in several studies in an attempt to accurately quantify the consequent socioeconomic and clinical burden on the general population. These attempts were mostly based on a broad definition of psychosis which contributed to a wide range of results. In a meta-analysis by Perala and colleagues (2007), the estimated global lifetime prevalence of all psychotic disorders was 3.48%. This estimated global average comprised a lifetime prevalence for schizophrenia (0.87%), substance-induced psychotic disorders (0.42%), major depressive disorder where psychotic symptoms are present (0.35%), bipolar 1 disorder (0.34%), schizoaffective disorder (0.32%), organic causes (0.21%), delusional disorder and schizophreniform disorder (0.07%). These findings are consistent with other studies (Baldwin *et al.* 2005; Gynther *et al.* 2019) that report non-affective psychoses to be more common than affective psychoses. Schizophrenia is the most common psychotic disorder with an illness onset usually between 18 and 30 years. Often beginning in early adulthood, psychotic disorders often prevail and progress throughout a person's entire life, substantially lowering life expectancy by heightening the risk of deaths related to suicide and substance abuse (Jongsma *et al.* 2019). In an indigenous Australian population, an age-standardised annual psychosis prevalence of 1·7% was observed, approximately two times higher in men than women (Gynther *et al.* 2019). This is consistent with the findings of a meta-analysis (Jongsma *et al.* 2019) that similarly reported higher risks of all psychotic disorders in men (incidence rate ratio 1·44 C.I [1·27–1·62]).

Of note, prevalence of psychosis varies by culture, location and the presence of an ongoing psychotic symptoms greatly depends on the availability of treatment and even response to treatment as well as how psychosis was defined (Bhugra, 2005; Jongsma *et al.* 2019). Therefore, it is increasingly evident that one prevalence study does not fit all, and clinicians need to focus most on local rates of prevalence in order to best treat their population and identify risk factors and individuals at high risk (Goldner *et al.* 2000; Jongsma *et al.* 2019). The prevailing high prevalence of psychotic disorders is associated with considerable clinical

and socioeconomic burden (Gustavsson *et al.* 2011; Wittchen *et al.* 2011). In Ireland, approximately 3% of the population experience a psychotic disorder during their lifetime with an onset frequency in late adolescence or early adulthood (Health Service Executive, 2019). The Cavan-Monaghan First-Episode Study (Baldwin *et al.* 2005) noted a younger mean age at first psychotic episode in males compared to females. Kirkbride and colleagues (2017) similarly observed high incidence rate for first psychotic episode in males before twenty years of age with further increased rates in ethnic minority groups (incidence rate ratio: 1.4; 95% CI=1.1–1.6) as well as those with lower socioeconomic status (incidence rate ratio: 1.3; 95% CI=1.2–1.4).

1.3 Aetiology of psychosis

The precise aetiology of psychotic disorders remain unclear, however, several factors have been implicated. These may be broadly categorised into underlying genetic factors that predispose individuals to primary psychotic disorders and environmental exposures that potentially cause structural neuroanatomical damages to the brain (Tyrer, 2015) including trauma, disease and drugs or chemicals.

A population based family study (Lichtenstein *et al.* 2009) observed an increased risk of both schizophrenia (64% heritability) and bipolar disorder (59% heritability) to first degree relatives of probands with either disorder in a sample of over 9 million unique individuals from a Swedish health registry. Of note, Lichtenstein and colleagues (2009) further demonstrate heritability risks for either disorder or their co-morbidity to be higher in those with biological relationships relative to adoptive relations. A meta-analysis of twin studies (Sullivan *et al.* 2003) reported 81% (95% confidence interval, 73%-90%) point estimate of heritability in liability to schizophrenia. This is consistent with another similar study (Cardino and Gottesman, 2000) that reported heritability estimates of approximately 80-85% and proband-wise concordance rates of 41-65% in monozygotic twins and 0-28% in dizygotic twins. Given that monozygotic twins (sharing 100% of their genes) and dizygotic twins (sharing 50% of their genes) share the environment they are raised in, higher concordance rates in monozygotic over dizygotic twins most likely result from genetic similarity (Henriksen *et al.* 2017). Furthermore, longitudinal twin studies have also demonstrated that progressive global brain volume reduction (Brans *et al.* 2009) and thinning of the cortex, particularly of the left superior temporal cortex (Hedman *et al.* 2016) in patients are partly due to genetic liability for schizophrenia. Structural brain changes implicated in psychotic illness will be discussed further in this chapter.

Several genome wide association (GWAS) studies demonstrate strong evidence for risk genes of psychotic disorders such as schizophrenia (Ripke *et al.* 2014; Cosgrove *et al.* 2018; Holland *et al.* 2019) and bipolar disorder (Stahl *et al.* 2019). For example, the ZNF804A (zinc finger binding protein 804A) and CACNA1C (calcium channel, voltage-dependent, L type, alpha 1C subunit) loci appear to influence the risk for both schizophrenia and bipolar disorder (Andrade *et al.* 2019). This finding lends weight to the hypothesis that schizophrenia and bipolar disorder are not aetiologically distinct. McDonald and colleagues (2004) demonstrated an association between genetic liability and distinct grey matter volume deficits in the bilateral fronto-striato-thalamic and left lateral temporal regions in schizophrenia and the right anterior cingulate gyrus and ventral striatum in bipolar disorder. Similarly, other studies suggest that variants of neurodevelopment-related genes such as the disrupted in schizophrenia 1 (DISC 1) and neuregulin 1 (NRG1) genes can contribute to brain abnormalities including cortical thinning (Vázquez-Bourgon *et al.* 2016) and lateral ventricular enlargement (Suarez-Pinilla *et al.* 2015), respectively, in the early and progressive phases of schizophrenia. These structural neuroanatomical variations and their associations with genetic risks across the brain in patients contradicts the hypothesis of aetiological distinction in affective and non-affective psychosis by Andrade and colleagues (2019). Despite these inconsistencies, a genetic component to the development of psychosis has been demonstrated by several family, twin and adoption studies to confirm its role as a predisposing factor.

Furthermore, steadily accumulating evidence indicate a strong association between traumatic experiences and the later development of psychosis (Hardy, 2017; Redman *et al.* 2017). For example, Kilcommons and Morrison (2005) found a strong association between severity and prevalence of lifetime traumatic experiences and later development of a psychotic disorder in a heterogenous sample.

Psychotic episodes may be secondary to a general medical condition or substance use, including illicit and medicinal drugs. For example, psychotic episodes were previously reported in multiple sclerosis patients to be associated with left temporal lobe lesions (Reiss *et al.* 2006), secondary to a localised brain tumour in the region of the posterior thalamus and internal capsule (Dutschke *et al.* 2017) and in severe traumatic brain injury (Fujii and Ahmed, 2001). Environmental insults like cannabis misuse have also been demonstrated to mediate cortical thinning of the anterior cingulate and dorsolateral prefrontal cortices (Rais

et al. 2010), volume reductions of grey matter (Rais *et al.* 2008; Yucel *et al.* 2008; Welch *et al.* 2011) and enlargement of lateral and third ventricular volumes (Rais *et al.* 2008; Olabi *et al.* 2011) in psychotic patients. Of note, these brain regions have all been independently associated with psychosis in structural MRI studies in the absence of cannabis misuse (Cahn *et al.* 2002; Fornito *et al.* 2008; Andreasen *et al.* 2011; Volpe *et al.* 2012).
The aetiology of psychosis is still not understood, however, drawing on emerging evidence thus far, the aetiology of psychosis seem to be modulated by a gene-environment interaction as a risk factor for developing psychotic illness.

Furthermore, alterations in neurotransmitter levels and in particular dopamine have been demonstrated in psychosis (as reviewed, Kesby *et al.* 2018). There are hypotheses of schizophrenia that attempt to explain the role of altered signalling of dopamine, glutamate and other neurotransmitters, as well as associations with neural synaptic connectivity and environmental insults during the neurodevelopmental stages in psychosis. The dopamine hypothesis of schizophrenia attributes symptoms of the illness to altered signalling of dopamine and draws evidence from observations of several studies demonstrating the antagonistic dopamine-receptor effects of antipsychotic medications (Kesby *et al.* 2018). Dopaminergic hypofrontality is seen in the dorsolateral prefrontal cortex of psychotic patients (Howes *et al.* 2015), showing a complexity of dopaminergic disturbances rather than just an excess of dopamine in the brain. However, some studies suggest that alterations in the dopamine systems of the mesolimbic pathway may contribute to positive symptoms whereas such alterations in the mesocortical pathway may be responsible for the negative symptoms of schizophrenia (Kesby *et al.* 2018).

1.4 Structural imaging in psychosis

Despite, the assertion by some critics for the lack of a clear taxonomic classification for psychosis (Claridge and Barrantes-Vital, 2011), it has been argued that one of the greatest achievements in the field of psychiatry and clinical neuroscience has been the understanding that psychosis could be explained in terms of structural brain dysfunctions (Tyrer, 2015). Structural brain changes have been demonstrated with imaging techniques to have largely influenced brain function during the development of schizophrenia and other psychotic disorders (Lawrie *et al.* 2008). Structural imaging studies have complemented clinical, neuropsychological and post-mortem investigations by exploring neuroanatomical case-control differences in the study of psychosis. However, early neuroimaging studies (Johnstone *et al.* 1976; Weinberger *et al.* 1979; Tanaka *et al.* 1981) focussed more on the

cross-sectional volume differences between groups using computed tomography (CT) and manual segmentation approaches for image acquisition and analyses, respectively. For example, the pioneering work of Johnstone and colleagues (1976) employed CT scans to demonstrate ventricular volume enlargement in schizophrenia. In fact, this cross-sectional study marks the beginning of research into structural neuroanatomical abnormalities in psychotic disorders. Although cross-sectional study designs allow for the detection of between-group differences, they are limited in their ability to track the progression of these abnormalities over time. Thus, the need for longitudinal neuroimaging studies, with the earliest of such studies employing CT scans over time but suffered gross methodological challenges (as reviewed, DeLisi, 1999) including lacking a comparison group, inconsistent follow-up times as well as a relatively poor image acquisition and segmentation approaches. Some of these challenges are unrelated to CT studies alone; however, CT studies are hampered mainly, by the relatively poor image acquisition and analysis techniques. In the last three decades, research has predominantly employed the use of magnetic resonance imaging (MRI) due to it's potential of consistently providing higher resolution images of structural neuroanatomical changes in patients with psychosis (Shenton *et al.* 2001; Wright *et al.* 2000).

1.4.1 Structural magnetic resonance imaging in psychosis

Despite extensive research progress in the field, the neurobiological underpinnings of psychotic illness still remain unclear (Thompson *et al.* 2008). However, improvement in MRI sequences have allowed further detailed *in vivo* brain examination of patients with psychotic illness. Structural magnetic resonance imaging depends on hydrogen atoms present in both water and brain tissue to create an electromagnetic field for MR image production. The magnetic moments of hydrogen atoms align parallel or anti-parallel to the static magnetic field of an MRI scanner. These forces cancel out, leaving a relatively small portion in parallel alignment with the magnetic field of the scanner, referred to as the net magnetisation of hydrogen atoms. Thus, a stronger magnetic field results in greater magnetisation within the tissue, and ultimately higher resolution of the acquired images. More specifically, the MRI scanner applies an electromagnetic wave called a radiofrequency pulse to perturb the hydrogen atoms in the water molecules of brain tissues to a higher energy state and out of alignment with the magnetic field of the MRI scanner. This is only achieved at a frequency matching the frequency of the hydrogen atom's precession, known as the Larmor frequency.

The pulse causes a portion of hydrogen atoms to move out of the longitudinal (parallel) and into the transverse (anti-parallel) plane. Thus, this results in a reduction of longitudinal magnetisation and an induced temporary state of transverse magnetisation. As the radiofrequency pulse decays, the transverse magnetisation also decays and the longitudinal magnetisation returns to its initial state, both exponentially. The longitudinal relaxation time (T1) is measured as the time taken for the longitudinal magnetisation to return to 63% of its maximum after being perturbed by the radiofrequency pulse. This happens differently in different tissue types, based on the local differences in water content which serve to outline the shape and size of brain subregions for detailed research analyses or interpretation. For example, T1 is longer for tissues with higher water content when compared with tissues with higher fat content. Voxels that have a longer T1 will have relatively lower longitudinal magnetisation than those with shorter T1 and therefore become darker in a T1-weighted MR image. In the brain, this produces contrast between grey and white matter areas, offering the possibility to investigate structural neuroanatomical changes.

Structural MRI sequences are widely used in clinical practice (Symms *et al.* 2004) and thus, MRI imaging may be considered good practice in the routine initial assessment of FEP patients, although it is not part of standardised national guidelines (Lehman *et al.* 2004; Falkenberg *et al.* 2017). The application of structural MR imaging in the field of clinical neuroscience research has allowed for more valid and reliable data with greater power regarding sensitivity and specificity of the images produced. This would potentially help identify neuroimaging biomarkers for early disease detection and targeted therapies at the early stages of psychosis (Kempton *et al.* 2015). In this thesis, all participants therefore underwent structural MR imaging in a 1.5 Tesla Siemens Magnetom Symphony scanner equipped with a 4-channel head coil. The acquired structural data included a volumetric T1-weighted magnetisation-prepared rapid acquisition of gradient echo (MPRAGE) sequence. The T1-weighted image was then employed for studying changes in ventricles and sub/cortical regions of the brain by exploring metrics such as volume and cortical thickness using a semi-automated brain segmentation tool (FreeSurfer). Cortical thickness change has been demonstrated to strongly influence volumetric reductions (Panizzon *et al.* 2009). Given that cortical thickness is highly heritable and may be influenced by specific cellular mechanisms (Winkler *et al.* 2010) such as synaptic pruning and myelination (Goldstone *et al.* 2018), it therefore represents an important morphometric measure for the identification of prognostically meaningful biological markers in patients experiencing their FEP. In relation to

the deep grey subcortical structures, volumetric changes will be employed in this thesis with suggestion for future studies to consider shape changes over time.

1.5 Some brain segmentation techniques applied in neuropsychiatry

The complexity of disorders that involve the brain require meticulous attempts to fully understand its structure and function. Thus far, advances in *in vivo* brain imaging acquisition and analyses have allowed for volumetric quantification of neuroanatomical structures in MRI datasets for the investigation of case-control differences and even disease progression using neuromorphometric properties. In an attempt to understand neuroanatomical changes, voxels of high resolution structural MRI images are classified based on intensity, orientation and knowledge of anatomy in the process of segmentation (Erickson and Avula, 1998). Accurate segmentation is therefore a step towards understanding the neuroanatomical basis of several psychiatric disorders and the influence of gene-environment interactions on the brain (Kapur *et al.* 1996; Morey *et al.* 2009). However, there are numerous segmentation techniques available within the field and currently are broadly categorised as manual (e.g. ITK-SNAP [http://www.itksnap.org/, Yushkevich *et al.* 2006], 3D-Slicer [https://www.slicer.org/, Fedorov *et al.* 2012]), semi-automated (e.g. FreeSurfer [http://surfer.nmr.mgh.harvard.edu, Fischl *et al.* 2002]) and fully automated (e.g. FSL-FIRST [http://fsl.fmrib.ox.ac.uk, Patenaude *et al.* 2011], volBrain [http://volbrain.upv.es, Manjon and Coupe, 2016], voxel-based morphometry [http://www.neuro.uni-jena.de, Ashburner and Friston, 2000) techniques depending on the level of manual intervention required by the user in the process of segmenting a region of interest. Furthermore, stereology (e.g. Measure® [a specialised interactive software developed at John's Hopkins - Maryland, Barta *et al.* 1995]), a long-standing reliable method for the estimation of volume of structures, has also been employed with MR imaging and previously been demonstrated to deliver consistent findings when compared to manual tracing for both smooth (Ertekin *et al.* 2015) and complex (Sheline *et al.* 1999) structures. In this thesis (chapter 2), the caudate and hippocampus were chosen as representative subcortical structures to be examined to test the performance of segmentation techniques, given that these two structures are implicated in several psychiatric disorders including schizophrenia, bipolar disorder (Ellison-Wright *et al.* 2008; Adriano *et al.* 2012) etc. and are at either end of the spectrum in relation to their ease of segmentation. Thus, findings in relation to these structures are likely generalisable to several other brain structures.

The application of cytoarchitectonic probability maps for segmentation was previously suggested by Bokde and colleagues (2005) for improved definition of brain changes. Although cytoarchitectonics is emerging as a standard for evaluating *in vivo* measurement methods (Craddock *et al.* 2018), manual segmentation is currently considered a gold standard for brain segmentation (Morey *et al.* 2009; Doring *et al.* 2011; Sanchez-Benavides *et al.* 2010). However, such procedure is associated with a number of limitations including the requirement for substantial anatomical and methodological expertise by the tracer(s), with associated inter- and intra-rater reliability concerns, although the strict use of protocols combined with anatomical expertise and training can minimise these. In addition, manual tracing is associated with significant time requirements, potentially limiting the feasibility of this technique for the volumetric quantification of large datasets. Automated approaches are increasingly used due to their significantly reduced time and labour requirements with excellent reproducibility and less training or anatomical knowledge required for the end-user (Bokde *et al.* 2002; 2005). However, most automated techniques operate under the assumption of the existence of no or minimal neuroanatomical variability which may be more pronounced in patient populations (Bokde *et al.* 2005). Thus, uncertainty is present in relation to anatomical accuracy and consistency of the various automated techniques at segmenting regional brain structures.

1.6 Structural brain abnormalities in first-episode of psychosis

Structural neuroanatomical alterations have been studied using both cross-sectional and longitudinal study designs to demonstrate changes both in chronic and in the early phases of psychotic illnesses compared to HCs (Gur *et al.* 1998; Ellison-Wright *et al.* 2008) when assessed using neuroimaging techniques. Although some of these reported neuroanatomical alterations overlap at certain brain regions, they differ mostly in the extent and location across various cohorts depending on several clinical factors. Recently, methodological factors such as the variability in brain image acquisition and analysis techniques have been demonstrated to influence some of these reported neuroanatomical changes observed in psychosis (Stankiewicz *et al.* 2011; Schoemaker *et al.* 2016; Makowski *et al.* 2018).

1.6.1 Cross-sectional structural neuroimaging findings in first-episode of psychosis

Findings from several cross-sectional studies examining brain changes at the time of FEP relative to healthy controls (HCs) document widespread neuroanatomical alterations at global and regional levels. Meta-analyses of cross-sectional studies focusing on non-affective FEP patients demonstrate volumetric reductions in the hippocampus (Adriano *et al.* 2012;

Steen *et al.* 2006; Vita and De Peri, 2007; Vita *et al.* 2006) comparable in magnitude to those at the chronic phase of illness (Cohen's d ranging from −0.47 to −0.66) (Adriano *et al.* 2012; Vita *et al.* 2006). Although this finding is biased considering the narrow diagnostic phenotype of the samples involved, the known gradual downward linear trajectory of hippocampal volume after adolescence (Shaw *et al.* 2008), suggest that this morphometric alterations at the early phases of illness may be a biological trait marker.

In another meta-analytic study of voxel-based structural MRI studies of FEP and chronic schizophrenia relative to HCs, significant neuroanatomical changes were observed to largely coincide with the basal ganglia-thalamocortical circuitry (Ellison-Wright *et al.* 2008). Specifically, these findings include bilateral reductions in caudate head gray matter, thalamus, the left uncus/amygdala region, the insula bilaterally, and the anterior cingulate with evidence for progression of cortical changes.

To date, the most consistently reported changes after FEP relative to HCs are reductions in whole brain volume and bilateral increments in lateral ventricular (LV) volume (effect size range = 0.47–0.61) (De Peri *et al.* 2012; Steen *et al.* 2006; Vita *et al.* 2006). Furthermore, although not consistent findings, other meta-analyses have reported grey matter volume reductions of the insula, caudate, operculum, superior temporal, medial frontal, cerebellum, prefrontal and anterior cingulate cortices (Chan *et al.* 2011; Fusar-Poli *et al.* 2012, 2014; Radua *et al.* 2012). Of note, all these are robust findings considering the relatively large number of patients (N range = 271-965) examined.

Of particular note, is the relative preservation of the temporo-limbic structures in FEP (Wood *et al.* 2001; Vita and de Peri, 2007) such as amygdala and temporal lobe. However, this may be related only to FEP rather than more chronic psychoses. For example, significant grey matter volume reductions of the amygdala have been found in a meta-analysis of individuals with established schizophrenia (Glahn *et al.* 2008). Furthermore, schizophrenia patients had smaller amygdala volume relative to those with psychotic bipolar disorder (Mahon *et al.* 2012). Thus, these findings may suggest that amygdala volume alterations may represent a morphologic feature in staging and distinguishing (affective vs. non-affective) psychotic illness. Indeed, neuroanatomical changes which become evident during the early-stages of psychosis are important to the study of the illness over time as they may conceivably be reflective of the principal brain regions of neuropathological deviance in psychotic disorder and further suggest that the brain undergoes a time of active structural regional changes at

illness onset. However, the debate regarding the progression of these structural abnormalities remains active. Thus, a fundamental goal of research in this area remains to identify the existence and extent of progression of these baseline brain changes at disease onset to establish a clinical time framework for intervention.

1.6.2 Longitudinal structural neuroimaging findings in first-episode of psychosis

The controversy of whether the neuroanatomical changes observed in cross-sectional studies at disease onset are static or progressive or even reversible over the evolution of the disorder (Keshavan *et al.* 1998; Schaufelberger *et al.* 2011; Olabi *et al.* 2011) is still active. Structural longitudinal neuroimaging studies of FEP may provide an opportunity to examine these questions using neuromorphometric measures to assess the state of brain structures and their associations with clinical measures over time. Indeed, FEP has been associated with a number of longitudinal brain changes with the most consistent of these relating to progressive LV enlargement (Steen *et al.* 2006; Cahn *et al.* 2009; Kempton *et al.* 2010; Olabi *et al.* 2011), and a progressive reduction in total GM volume (Steen *et al.* 2006; Zipparo *et al.* 2008; Olabi *et al.* 2011; Gutierrez-Galve *et al.* 2014), with findings in relation to other brain regions being somewhat inconsistent (Schaufelberger *et al.* 2011; Haukvik *et al.* 2016).

In a meta-analytic investigation of longitudinal MRI studies (N=500) of FEP schizophrenia, a significant pattern of progressive grey matter volume reduction in the frontal, temporal and parietal lobes and in the Heschl's gyrus relative to healthy controls (HCs) were observed (Vita *et al.* 2012). Sun and colleagues (2009) also demonstrate cortical surface contraction particularly in the dorsal regions of the frontal lobes of FEP patients to be occurring at twice the rate as that observed in HCs over a period of 1–4 years, suggestive of an altered pattern of development in FEP by way of excessive cortical thinning. Furthermore, a longitudinal comparison conducted by Pantelis and colleagues (2003), reported significant reduction in grey matter in the left parahippocampal, fusiform, orbitofrontal, cerebellar cortices and the cingulate gyri in individuals who had developed psychosis over time compared to HC's. In other longitudinal FEP studies, cortical thinning was observed in the frontal and prefrontal regions over time (Andreasen *et al.* 2011; Roiz-Santianez *et al.* 2014; Gutiérrez-Galve *et al.* 2014) with significant volume reductions in the frontal, temporal and parietal cortices in HCs over time (de Castro-Manglano *et al.* 2011). However, this is not a consistent finding with no significant change in cortical grey matter volume over time also noted (Dickey *et al.* 2004; Haukvik *et al.* 2016). Similarly, reports of progressive change in subcortical volumes in individuals with psychosis have been inconsistent, with studies reporting conflicting results

for the caudate (Lang *et al.* 2001; Lieberman *et al.* 2001; Roiz-Santiánez *et al.* 2014), hippocampus (Schaufelberger *et al.* 2011; Ebdrup *et al.* 2011; Lappin *et al.* 2014) and thalamus (Theberge *et al.* 2007; van Haren *et al.* 2007; Andreasen *et al.* 2011).

These inconsistencies regarding neuroanatomical progression after FEP are potentially due to embedded study heterogeneities of a clinical (e.g. variable clinical severity, antipsychotic medication use and follow-up times) and methodological (e.g. different image acquisition and analysis techniques) nature. Although longitudinal studies are complicated by additional practical factors such as MRI scanner upgrades and the challenge of re-recruitment, they remain a powerful approach in monitoring intra-individual changes within a cohort over time (Whitwell, 2008). Whilst, several studies have investigated the relationship between neuroanatomical changes and clinical/functional measures in FEP, findings have been inconsistent with few studies carried out to further clarify the extent and location of progressive changes and their associations over time.

1.6.3 The cortico-striato-thalamo-cortical circuitry in psychosis

It can be postulated that neuroanatomical changes reported to date in FEP broadly aligned to the cortico-striato-thalamo-cortical circuitry. These changes include bilateral reductions in subcortical grey matter structures of the basal ganglia, thalamus and to a lesser extent, the hippocampus and amygdala (Ellison-Wright *et al.* 2008). Furthermore, cortical changes, predominantly in the frontal and temporo-limbic regions have been reported with some studies demonstrating evidence for progression of these changes over time (Pantelis *et al.* 2003). The cortico-striato-thalamo-cortical circuitry describes projections that bypass the pallidum, connecting directly the striatum and thalamus before returning to the cortical regions of the brain. There are three subnetworks within this circuitry (Fig.1.1), namely, a) motor, b) associative and c) limbic.

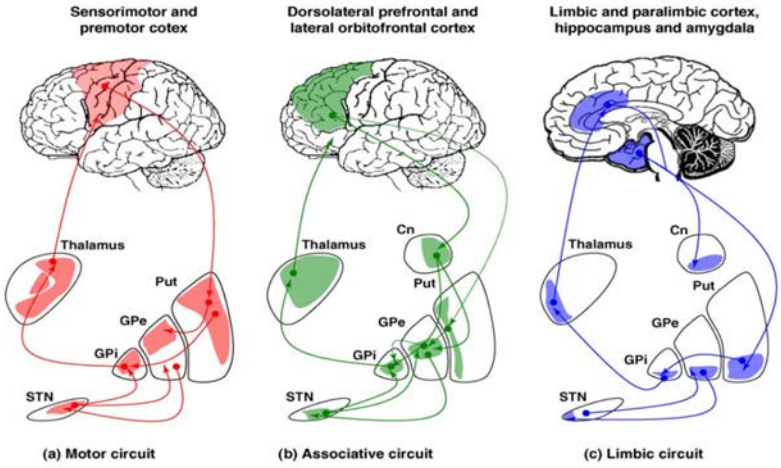

Fig.1.1 The cortico-striato-thalamo-cortical circuitry within the human brain (Krack *et al.* 2010). GPi = internal globus pallidus, GPe = globus pallidus pars externa, STN = subthalamic nucleus, Cn = Caudate, Put = Putamen.

As shown in Fig.1.1 the motor circuit (a) comprises neuronal projections extending from the sensorimotor cortex to the posterolateral putamen (Put). A direct connection extends from the putamen to the internal globus pallidus (GPi) with an indirect connection extending from the posterior putamen to the globus pallidus pars externa (GPe), the subthalamic nucleus (STN) and the GPi. Of note, the GPi is the primary output nucleus of the basal ganglia to the cortex via the ventrolateral thalamus. The associative circuit (b) originates from the dorsolateral prefrontal and lateral orbitofrontal cortices and project to the caudate nucleus (Cn) and the anteromedial portion of the putamen. Projections from the caudate and putamen (striatum) are connected to the dorsomedial region of the GPi and anteromedial parts of the GPe and STN to converge onto the GPi and back to the cortex through the ventral anterior nuclei of the thalamus. Finally, the limbic circuit (c) originating from the hippocampus, amygdala, paralimbic and limbic cortices project to the ventral striatum (ventral portion of the caudate and putamen). The ventral striatum projects to the limbic portion of the GPe and medioventral STN and ventral GPi and to the cortex through the mediodorsal nucleus of the thalamus. The literature review thus far indicates a strong likelihood of a structural disturbance in the associative subnetwork of the cortico-striato-thalamo-cortical circuitry after a FEP.

1.7 Longitudinal neuroimaging findings and associations with clinical/confounding factors

Studying psychosis at the time of FEP is optimal for examining the latent pathophysiological mechanisms of the illness as the influence of potential confounders inherent to the nature of psychosis are absent or at their minimum during this stage. This is especially relevant to this naturalistic observation study, designed to investigate progression of neuroanatomical

changes over time. Several clinical factors have been implicated to impact regional brain volumes, including the administration of antipsychotic medication (Ho *et al.* 2011; Vita *et al.* 2012; Fusar-Poli *et al.* 2013) and genetic susceptibility (Andreassen *et al.* 2013) among others. However, studying individuals at the at-risk mental state (ARMS) or with a first episode of psychosis prior to treatment with psychotropic medication have been undertaken to avoid the potential confounding of psychotropic medication use. The first-episode psychosis cohort examined for this thesis was minimally exposed to medication treatments (< 3weeks) and indeed, the sample has been clinically diagnosed with psychosis unlike in ARMS, where approaching 40% of these individuals do not transition to psychosis (Fusar-Poli *et al.* 2012). Longitudinal neuroimaging investigations that integrate neuroanatomical and clinical measures may help to further clarify the aetiopathogenesis of psychosis. Brain changes emerging longitudinally after FEP are frequently reported (Steen *et al.* 2006; Cahn *et al.* 2009), however the extent of the clinical and functional measures associated with such brain changes remain inconsistent and have yet to be comprehensively examined. Several clinical factors have been reported to affect regional neuroanatomy longitudinally subsequent to a FEP. These potential factors that may affect brain change over time include clinical symptom severity, antipsychotic treatment and cannabis use (Zipursky *et al.* 2013).

Cannabis use has previously been implicated to impact on progressive cortical thinning in a first-episode schizophrenia cohort. Rais and colleagues (2010) demonstrated additional cortical thinning in cannabinoid 1 (CB1) receptor enhanced brain regions of the anterior cingulate and dorsolateral prefrontal cortices of patient cannabis users relative to non-users. In the same cohort, significant volume reductions of grey matter and larger increases in lateral and third ventricular volumes were observed which were more pronounced in patients with schizophrenia who continued to use cannabis during the first five years of antipsychotic treatment (Rais *et al.* 2008). Similarly, longitudinal volume reductions in the CB1 receptor enhanced areas of the thalamus were also observed in FEP patients who ingested cannabinoids (Welch et al. 2011). Furthermore, a systematic review (Rapp *et al.* 2012) of *in vivo* structural neuroimaging and postmortem studies, reported structural abnormalities in CB1 receptor enhanced brain areas such as the cingulate, prefrontal cortices and the cerebellum in patients relative to healthy samples. Taken together, patients with psychosis or those at risk for developing psychosis may be particularly vulnerable to brain volume loss and/or ventricular volume enlargement due to cannabis exposure. However, this is not a consistent finding. In contrast, continued cannabis use did not have any major volumetric effect on grey matter changes after 3-years of follow-up, although

volume of some left medial temporal lobe structures (i.e. hippocampus, amygdala, superior temporal gyrus) were associated with cannabis use over time (Koenders *et al.* 2016).

Additionally, the amount of antipsychotic medication administered and duration of treatment prior to recruitment may potentially moderate the inherent disease process and have been associated with greater GM deficits (Cahn *et al.* 2002; Ho *et al.* 2011; Ebdrup *et al.* 2013). Indeed, a meta-regression analyses of MRI studies indicated that GM volume deficits were influenced by greater overall levels of antipsychotic medication use irrespective of antipsychotic type (Radua *et al.* 2012). In a large schizophrenia cohort (N=211) followed-up soon after illness onset and at multiple times (2 - 5) over an average period of approximately 7.2 years, greater grey matter tissue loss and ventricular enlargement was associated with more antipsychotic use and longer duration of treatment (Ho *et al.* 2011). In addition, progressive decreases in white matter volume was also most prominent among patients who received higher cumulative dosages of antipsychotic treatment. Furthermore, other studies have linked increased striatal volume in chronic schizophrenia (Corson *et al.* 1999; Okugawa *et al.* 2007; van Haren *et al.* 2007) to the relatively long exposure to antipsychotic medications.

The influence of illness chronicity and symptom severity on observed regional brain changes have been demonstrated after the first-episode of psychosis. The neuroanatomical alterations at the early phases of psychosis differ from those reported at the chronic and established phases of the illness (Gur *et al.* 1998; Ellison-Wright *et al.* 2008) when assessed using neuroimaging techniques. Although some of these reported neuroanatomical alterations overlap at certain brain regions, they differ mostly in the extent and location across various cohorts depending on the stage of psychosis when patients were recruited (Gur *et al.* 1998; Pantelis *et al.* 2003) or the clinical symptom severity of the illness (Lieberman *et al.* 2001). Furthermore, symptom severity has also been associated with several regional brain volume alterations over time in individuals with FEP (Lieberman *et al.* 2005; van Haren *et al.* 2008; Ho *et al.* 2011). For example, progressive LV enlargement has been associated with greater overall psychopathology (Rais *et al.* 2008; Cahn *et al.* 2009). Additionally, less reduction of bilateral hippocampal volume was associated with good clinical, cognitive and functional outcome (Lappin *et al.* 2013) while greater volume reduction of the caudate was associated with greater clinical improvement (Lappin *et al.* 2013; Roiz-Santiáñez *et al.* 2014).Taken together, the progression of morphometric abnormalities in the initial years after the onset of psychotic illness may be inherent to the

pathogenesis of the illness as well as environmental factors such as cannabis use (Rais *et al.* 2008; Rais *et al.* 2010) and clinical factors such as cumulative antipsychotic medication usage (Lieberman *et al.* 2005; Ho *et al.* 2011; Vita *et al.* 2012) and genetic susceptibility (Andreassen *et al.* 2013; Vazquez-Bourgon *et al.* 2016; Hedman *et al.* 2016) among others. Thus, to fully elucidate the issue of progressive neuroanatomical deficits, longitudinal studies must reliably follow patients throughout the trajectory of their illness, optimally beginning as early as illness onset.

1.8 Aims of the thesis

The central focus of this research builds on from previous studies that examined FEP patients and aims to determine if there were progressive changes in ventricles, cortical and subcortical regions over a 3-year follow-up period and to ascertain if any changes were related to clinical variables including severity of symptoms, use of antipsychotic medications and level of functioning. As the search for reliant imaging biomarkers continues in the early diagnosis of psychosis (Kempton *et al.* 2015), this research will augment existing knowledge of disease progression and association with clinical factors in FEP. Given the broad psychotic phenotype of the diagnostic group under consideration for this research, who were minimally medicated (<3 weeks) prior to recruitment and followed-up after a relatively long time, findings from this study will serve to provide a better understanding of early brain changes in psychotic disorders. In order to choose an optimal tool for this study, the performance (accuracy, consistency, labour intensity etc) of various brain segmentation techniques were initially compared.

These research aims were developed through three studies embodied in this thesis (study 1, 2 and 3). The specific aims and hypotheses are presented in detail in each chapter, respectively. Briefly, the aims of each study are outlined below.

Study 1 – aims to systematically examine the performance (accuracy, consistency, labour intensity etc) of fully-automated (model-based) (FSL-FIRST v.5.0.4), fully-automated (patch-based) (volBrain v.1.0), semi–automated (FreeSurfer v.5.1) and stereological (Measure®) segmentation techniques against manual segmentation (ITK-SNAP v.1.8) for the quantification of the caudate and hippocampus in a large clinically heterogeneous sample of adult MR images.

Study 2 – aims to determine if there were progressive changes in subcortical and ventricular volumes over a 3-year follow-up period and to ascertain if any such changes were related to particular clinical variables including severity of symptoms, use of antipsychotic medications and level of functioning.

Study 3 – aims to investigate the progressive profile of cortical changes in individuals with FEP compared to HCs over a 3-year period and to ascertain if any such changes are related to a number of clinical variables including severity of symptoms, antipsychotic medications and level of functioning.

References

1. Adriano, F., Caltagirone, C., Spalletta, G., 2011. Hippocampal Volume Reduction in First-Episode and Chronic Schizophrenia: A Review and Meta-Analysis. The Neuroscientist 18(2), 180-200.
2. Andrade, A., Brennecke, A., Mallat, S., Brown, J., Gomez-Rivadeneira, J., Czepiel, N., Londrigan, L., 2019. Genetic Associations between Voltage-Gated Calcium Channels and Psychiatric Disorders. Int J Mol Sci 20(14), 3537.
3. Andreasen, N.C., Nopoulos, P., Magnotta, V., Pierson, R., Ziebell, S., Ho, B.-C., 2011. Progressive brain change in schizophrenia: a prospective longitudinal study of first-episode schizophrenia. Biological psychiatry 70(7), 672-679.
4. American Psychiatric Association., 2013. Diagnostic and statistical manual of mental disorders (5th ed.). https://doi.org/10.1176/appi.books.9780890425596.dsm05
5. Andreassen, O.A., Thompson, W.K., Schork, A.J., Ripke, S., Mattingsdal, M., Kelsoe, J.R., Kendler, K.S., O'Donovan, M.C., Rujescu, D., Werge, T., Sklar, P., The Psychiatric Genomics, C., Bipolar, D., Schizophrenia Working, G., Roddey, J.C., Chen, C.-H., McEvoy, L., Desikan, R.S., Djurovic, S., Dale, A.M., 2013. Improved Detection of Common Variants Associated with Schizophrenia and Bipolar Disorder Using Pleiotropy-Informed Conditional False Discovery Rate. PLOS Genetics 9(4), e1003455.
6. Ashburner, J., Friston, K.J., 2000. Voxel-Based Morphometry—The Methods. Neuroimage 11(6), 805-821.
7. Baldwin, P., Browne, D., Scully, P.J., Quinn, J.F., Morgan, M.G., Kinsella, A., Owens, J.M., Russell, V., O'Callaghan, E., Waddington, J.L., 2005. Epidemiology of First-Episode Psychosis: Illustrating the Challenges Across Diagnostic Boundaries Through the Cavan-Monaghan Study at 8 Years. Schizophrenia Bulletin 31(3), 624-638.
8. Barta, P.E., Petty, R.G., McGilchrist, I., Lewis, R.W., Jerram, M., Casanova, M.F., Powers, R.E., Brill, L.B., Pearlson, G.D., 1995. Asymmetry of the planum temporale: methodological considerations and clinical associations. Psychiatry Research: Neuroimaging 61(3), 137-150.
9. Bhugra, D., 2005. The global prevalence of schizophrenia. PLoS Med 2(5), e151-e175.
10. Bokde, A.L.W., Teipel, S.J., Schwarz, R., Leinsinger, G., Buerger, K., Moeller, T., Möller, H.-J., Hampel, H., 2005. Reliable manual segmentation of the frontal, parietal, temporal, and occipital lobes on magnetic resonance images of healthy subjects. Brain Research Protocols 14(3), 135-145.
11. Bokde, A.L.W., Teipel, S.J., Zebuhr, Y., Leinsinger, G., Gootjes, L., Schwarz, R., Buerger, K., Scheltens, P., Moeller, H.J., Hampel, H., 2002. A new rapid landmark-based regional MRI segmentation method of the brain. Journal of the Neurological Sciences 194(1), 35-40.
12. Birchwood, M., Todd, P., Jackson, C., 1998. Early intervention in psychosis: the critical-period hypothesis. International Clinical Psychopharmacology 13, S31-S40.
13. Brans, R.G.H., van Haren, N.E.M., van Baal, G.C.M., Schnack, H.G., Kahn, R.S., Pol, H.E.H., 2008. Heritability of Changes in Brain Volume Over Time in Twin Pairs Discordant for Schizophrenia. JAMA Psychiatry 65(11), 1259-1268.
14. Cahn, W., Pol, H.E.H., Lems, E.B.T.E., van Haren, N.E.M., Schnack, H.G., van der Linden, J.A., Schothorst, P.F., van Engeland, H., Kahn, R.S., 2002. Brain Volume Changes in First-Episode Schizophrenia: A 1-Year Follow-up Study. JAMA Psychiatry 59(11), 1002-1010.
15. Cannon, T.D., Chung, Y., He, G., Sun, D., Jacobson, A., van Erp, T.G.M., McEwen, S., Addington, J., Bearden, C.E., Cadenhead, K., Cornblatt, B., Mathalon, D.H., McGlashan, T., Perkins, D., Jeffries, C., Seidman, L.J., Tsuang, M., Walker, E., Woods,

S.W., Heinssen, R., 2015. Progressive Reduction in Cortical Thickness as Psychosis Develops: A Multisite Longitudinal Neuroimaging Study of Youth at Elevated Clinical Risk. Biological Psychiatry 77(2), 147-157.
16. Cardno, A.G., Gottesman, I.I., 2000. Twin studies of schizophrenia: From bow-and-arrow concordances to Star Wars Mx and functional genomics. American Journal of Medical Genetics 97(1), 12-17.
17. Castillo, R.J., 2003. Trance, Functional Psychosis, and Culture. Psychiatry: Interpersonal and Biological Processes 66(1), 9-21.
18. Castillo, R. J., (1997) Dissociation. In W.S. Tseng and J. Streltzer, eds., Culture and Psychopathology: A Guide to clinical Assessment (pp. 101 – 123). Brunner/Mazel.1997.
19. Castillo, R. J., (2001) Lessons from folk healing practices. In W.S. Tseng and J. Streltzer, eds., Culture and Psychopathology: A Guide to clinical Assessment (pp. 81 - 101). American Psychiatric Press, 2001.
20. Chan, R.C.K., Di, X., McAlonan, G.M., Gong, Q.-y., 2011. Brain anatomical abnormalities in high-risk individuals, first-episode, and chronic schizophrenia: an activation likelihood estimation meta-analysis of illness progression. Schizophrenia bulletin 37(1), 177-188.
21. Claridge, G., Barrantes-Vidal, N., 2018. The classification of psychosis. British Journal of Psychiatry 198(4), 323-324.
22. Cobia, D.J., Smith, M.J., Salinas, I., Ng, C., Gado, M., Csernansky, J.G., Wang, L., 2017. Progressive deterioration of thalamic nuclei relates to cortical network decline in schizophrenia. Schizophrenia research 180, 21-27.
23. Corson, P.W., Nopoulos, P., Del D. Miller, D.D., Arndt, S., Nancy C. Andreasen, N. C., 1999. Change in Basal Ganglia Volume Over 2 Years in Patients with Schizophrenia: Typical Versus Atypical Neuroleptics. American Journal of Psychiatry 156(8), 1200-1204.
24. Cosgrove, D., Mothersill, D.O., Whitton, L., Harold, D., Kelly, S., Holleran, L., Holland, J., Anney, R., Consortium, T.W.T.C.C., Richards, A., Mantripragada, K., Owen, M., O'Donovan, M.C., Gill, M., Corvin, A., Morris, D.W., Donohoe, G., 2018. Effects of MiR-137 genetic risk score on brain volume and cortical measures in patients with schizophrenia and controls. American Journal of Medical Genetics Part B: Neuropsychiatric Genetics 177(3), 369-376.
25. Craddock, R.C., Bellec, P., Jbabdi, S., 2018. Neuroimage special issue on brain segmentation and parcellation - Editorial. Neuroimage 170, 1-4.
26. Crespo-Facorro, B., Kim, J.-J., Andreasen, N.C., O'Leary, D.S., Magnotta, V., 2000. Regional frontal abnormalities in schizophrenia: a quantitative gray matter volume and cortical surface size study. Biological Psychiatry 48(2), 110-119.
27. Fujii, D.E., & Ahmed, I., 2001. Risk Factors in Psychosis Secondary to Traumatic Brain Injury. The Journal of Neuropsychiatry and Clinical Neurosciences 13(1), 61-69.
28. de Castro-Manglano, P., Mechelli, A., Soutullo, C., Gimenez-Amaya, J., Ortuño, F., McGuire, P., 2011. Longitudinal changes in brain structure following the first episode of psychosis. Psychiatry Research: Neuroimaging 191(3), 166-173.
29. De Peri, L., Alessandra, C., Giacomo, D., Paolo, F.-P., Emilio, S., Antonio, V., 2012. Brain Structural Abnormalities at the Onset of Schizophrenia and Bipolar Disorder: A Meta-analysis of Controlled Magnetic Resonance Imaging Studies. Curr Pharm Des 18(4), 486-494.
30. DeLisi, L.E., 1999. Defining the course of brain structural change and plasticity in schizophrenia. Psychiatry Research: Neuroimaging 92(1), 1-9.
31. DeLisi, L.E., Sakuma, M., Ge, S., Kushner, M., 1998. Association of brain structural change with the heterogeneous course of schizophrenia from early childhood

through five years subsequent to a first hospitalization. Psychiatry Research: Neuroimaging 84(2), 75-88.
32. Dickey, C.C., Salisbury, D.F., Nagy, A.I., Hirayasu, Y., Lee, C.U., McCarley, R.W., Shenton, M.E., 2004. Follow-up MRI study of prefrontal volumes in first-episode psychotic patients. Schizophrenia research 71(2-3), 349-351.
33. Lang, D. J., Kopala, L.C., Robert A. Vandorpe, R.A., Rui, Q., Smith, G.N., Goghari, V.M., Honer, W. G., 2001. An MRI Study of Basal Ganglia Volumes in First-Episode Schizophrenia Patients Treated with Risperidone. American Journal of Psychiatry 158(4), 625-631.
34. Doring, T.M., Kubo, T.T.A., Cruz Jr, L.C.H., Juruena, M.F., Fainberg, J., Domingues, R.C., Gasparetto, E.L., 2011. Evaluation of hippocampal volume based on MR imaging in patients with bipolar affective disorder applying manual and automatic segmentation techniques. Journal of Magnetic Resonance Imaging 33(3), 565-572.
35. Dutschke, L.L., Steinau, S., Wiest, R., Walther, S., 2017. Brain Tumor-Associated Psychosis and Spirituality-A Case Report. Front Psychiatry 8, 237-237.
36. Ebdrup, B.H., Skimminge, A., Rasmussen, H., Aggernaes, B., Oranje, B., Lublin, H., Baaré, W., Glenthøj, B., 2011. Progressive striatal and hippocampal volume loss in initially antipsychotic-naive, first-episode schizophrenia patients treated with quetiapine: relationship to dose and symptoms. International Journal of Neuropsychopharmacology 14(1), 69-82.
37. Erickson, B.J., Avula, R.T., 1998. An algorithm for automatic segmentation and classification of magnetic resonance brain images. J Digit Imaging 11(2), 74-82.
38. Ertekin, T., Acer, N., İçer, S., Vurdem, Ü.E., Çınar, Ş., Özçelik, Ö., 2015. Volume estimation of the subcortical structures in Parkinson's disease using magnetic resonance imaging: A methodological study. Neurology Asia 20(2), 143-153.
39. Falkenberg, I., Benetti, S., Raffin, M., Wuyts, P., Pettersson-Yeo, W., Dazzan, P., Morgan, K.D., Murray, R.M., Marques, T.R., David, A.S., Jarosz, J., Simmons, A., Williams, S., McGuire, P., 2018. Clinical utility of magnetic resonance imaging in first-episode psychosis. British Journal of Psychiatry 211(4), 231-237.
40. Fedorov, A., Beichel, R., Kalpathy-Cramer, J., Finet, J., Fillion-Robin, J.-C., Pujol, S., Bauer, C., Jennings, D., Fennessy, F., Sonka, M., Buatti, J., Aylward, S., Miller, J.V., Pieper, S., Kikinis, R., 2012. 3D Slicer as an image computing platform for the Quantitative Imaging Network. Magn Reson Imaging 30(9), 1323-1341.
41. Fischl, B., Salat, D.H., Busa, E., Albert, M., Dieterich, M., Haselgrove, C., van der Kouwe, A., Killiany, R., Kennedy, D., Klaveness, S., Montillo, A., Makris, N., Rosen, B., Dale, A.M., 2002. Whole Brain Segmentation: Automated Labeling of Neuroanatomical Structures in the Human Brain. Neuron 33(3), 341-355.
42. Fornito, A., Yung, A.R., Wood, S.J., Phillips, L.J., Nelson, B., Cotton, S., Velakoulis, D., McGorry, P.D., Pantelis, C., Yücel, M., 2008. Anatomic Abnormalities of the Anterior Cingulate Cortex Before Psychosis Onset: An MRI Study of Ultra-High-Risk Individuals. Biological Psychiatry 64(9), 758-765.
43. Fusar-Poli, P., Bonoldi, I., Yung, A.R., Borgwardt, S., Kempton, M.J., Valmaggia, L., Barale, F., Caverzasi, E., McGuire, P., 2012. Predicting Psychosis: Meta-analysis of Transition Outcomes in Individuals at High Clinical Risk. JAMA Psychiatry 69(3), 220-229.
44. Fusar-Poli, P., Smieskova, R., Serafini, G., Politi, P., Borgwardt, S., 2014. Neuroanatomical markers of genetic liability to psychosis and first episode psychosis: A voxelwise meta-analytical comparison. The World Journal of Biological Psychiatry 15(3), 219-228.
45. Ganguli, M., Blacker, D., Blazer, D.G., Grant, I., Jeste, D.V., Paulsen, J.S., Petersen, R.C., Sachdev, P.S., 2011. Classification of neurocognitive disorders in DSM-5: a work in progress. Am J Geriatr Psychiatry 19(3), 205-210.

46. Glahn, D.C., Laird, A.R., Ellison-Wright, I., Thelen, S.M., Robinson, J.L., Lancaster, J.L., Bullmore, E., Fox, P.T., 2008. Meta-Analysis of Gray Matter Anomalies in Schizophrenia: Application of Anatomic Likelihood Estimation and Network Analysis. Biological Psychiatry 64(9), 774-781.
47. Goldner, E.M., Hsu, L., Waraich, P., Somers, J.M., 2002. Prevalence and Incidence Studies of Schizophrenic Disorders: A Systematic Review of the Literature. The Canadian Journal of Psychiatry 47(9), 833-843.
48. Goldstone, A., Willoughby, A.R., de Zambotti, M., Franzen, P.L., Kwon, D., Pohl, K.M., Pfefferbaum, A., Sullivan, E.V., Müller-Oehring, E.M., Prouty, D.E., Hasler, B.P., Clark, D.B., Colrain, I.M., Baker, F.C., 2018. The mediating role of cortical thickness and gray matter volume on sleep slow-wave activity during adolescence. Brain Struct Funct 223(2), 669-685.
49. Gur, R.E., Cowell, P., Turetsky, B.I., Gallacher, F., Cannon, T., Bilker, W., Gur, R.C., 1998. A Follow-up Magnetic Resonance Imaging Study of Schizophrenia: Relationship of Neuroanatomical Changes to Clinical and Neurobehavioral Measures. JAMA Psychiatry 55(2), 145-152.
50. Gustavsson, A., Svensson, M., Jacobi, F., Allgulander, C., Alonso, J., Beghi, E., Dodel, R., Ekman, M., Faravelli, C., Fratiglioni, L., Gannon, B., Jones, D.H., Jennum, P., Jordanova, A., Jönsson, L., Karampampa, K., Knapp, M., Kobelt, G., Kurth, T., Lieb, R., Linde, M., Ljungcrantz, C., Maercker, A., Melin, B., Moscarelli, M., Musayev, A., Norwood, F., Preisig, M., Pugliatti, M., Rehm, J., Salvador-Carulla, L., Schlehofer, B., Simon, R., Steinhausen, H.-C., Stovner, L.J., Vallat, J.-M., den Bergh, P.V., van Os, J., Vos, P., Xu, W., Wittchen, H.-U., Jönsson, B., Olesen, J., 2011. Cost of disorders of the brain in Europe 2010. European Neuropsychopharmacology 21(10), 718-779.
51. Gutiérrez-Galve, L., Chu, E.M., Leeson, V.C., Price, G., Barnes, T.R.E., Joyce, E.M., Ron, M.A., 2014. A longitudinal study of cortical changes and their cognitive correlates in patients followed up after first-episode psychosis. Psychological Medicine 45(1), 205-216.
52. Gynther, B., Charlson, F., Obrecht, K., Waller, M., Santomauro, D., Whiteford, H., Hunter, E., 2019. The Epidemiology of Psychosis in Indigenous Populations in Cape York and the Torres Strait. EClinicalMedicine 10, 68-77.
53. Hardy, A., 2017. Pathways from Trauma to Psychotic Experiences: A Theoretically Informed Model of Posttraumatic Stress in Psychosis. Frontiers in Psychology 8(697).
54. Haukvik, U.K., Hartberg, C.B., Nerland, S., Jørgensen, K.N., Lange, E.H., Simonsen, C., Nesvåg, R., Dale, A.M., Andreassen, O.A., Melle, I., Agartz, I., 2015. No progressive brain changes during a 1-year follow-up of patients with first-episode psychosis. Psychological Medicine 46(3), 589-598.
55. Health Service Executive (HSE)., 2019. HSE launches National Model of Care for Early Intervention in Psychosis - HSE.ie. [online] Available at: https://www.hse.ie/eng/services/news/media/pressrel/hse-launches-national-model-of-care-for-early-intervention-in-psychosis.html [Accessed 7 Sep. 2019].
56. Hedman, A.M., van Haren, N.E.M., van Baal, G.C.M., Brouwer, R.M., Brans, R.G.H., Schnack, H.G., Kahn, R.S., Hulshoff Pol, H.E., 2016. Heritability of cortical thickness changes over time in twin pairs discordant for schizophrenia. Schizophrenia Research 173(3), 192-199.
57. Henriksen, M.G., Nordgaard, J., Jansson, L.B., 2017. Genetics of Schizophrenia: Overview of Methods, Findings and Limitations. Front Hum Neurosci 11, 322-322.
58. Ho, B.-C., Andreasen, N.C., Ziebell, S., Pierson, R., Magnotta, V., 2011. Long-term Antipsychotic Treatment and Brain Volumes: A Longitudinal Study of First-Episode

Schizophrenia Long-term Antipsychotics and Brain Volumes. JAMA Psychiatry 68(2), 128-137.
59. Holland, J.F., Cosgrove, D., Whitton, L., Harold, D., Corvin, A., Gill, M., Mothersill, D.O., Morris, D.W., Donohoe, G., 2019. Beyond C4: Analysis of the complement gene pathway shows enrichment for IQ in patients with psychotic disorders and healthy controls. Genes, Brain and Behavior 0(0), e12602.
60. Howes, O., McCutcheon, R., Stone, J., 2015. Glutamate and dopamine in schizophrenia: an update for the 21st century. J Psychopharmacol 29(2), 97-115.
61. Ian Ellison-Wright , M.R.C.P., David C. Glahn , P.D., Angela R. Laird , P.D., Sarah M. Thelen , B.S., Ed Bullmore , P.D., 2008. The Anatomy of First-Episode and Chronic Schizophrenia: An Anatomical Likelihood Estimation Meta-Analysis. American Journal of Psychiatry 165(8), 1015-1023.
62. Iglesias, J.E., Van Leemput, K., Augustinack, J., Insausti, R., Fischl, B., Reuter, M., Alzheimer's Disease Neuroimaging, I., 2016. Bayesian longitudinal segmentation of hippocampal substructures in brain MRI using subject-specific atlases. Neuroimage 141, 542-555.
63. Johnstone, E., Frith, C.D., Crow, T.J., Husband, J., Kreel, L., 1976. CEREBRAL VENTRICULAR SIZE AND COGNITIVE IMPAIRMENT IN CHRONIC SCHIZOPHRENIA. The Lancet 308(7992), 924-926.
64. Jongsma, H.E., Turner, C., Kirkbride, J.B., Jones, P.B., 2019. International incidence of psychotic disorders, 2002–17: a systematic review and meta-analysis. The Lancet Public Health 4(5), e229-e244.
65. Kapur, T., Grimson, W.E.L., Wells, W.M., Kikinis, R., 1996. Segmentation of brain tissue from magnetic resonance images. Medical Image Analysis 1(2), 109-127.
66. Kempton, M.J., McGuire, P., 2015. How can neuroimaging facilitate the diagnosis and stratification of patients with psychosis? Eur Neuropsychopharmacol 25(5), 725-732.
67. Kempton, M.J., Stahl, D., Williams, S.C.R., DeLisi, L.E., 2010. Progressive lateral ventricular enlargement in schizophrenia: A meta-analysis of longitudinal MRI studies. Schizophrenia Research 120(1), 54-62.
68. Kenney, J., Anderson-Schmidt, H., Scanlon, C., Arndt, S., Scherz, E., McInerney, S., McFarland, J., Byrne, F., Ahmed, M., Donohoe, G., Hallahan, B., McDonald, C., Cannon, D.M., 2015. Cognitive course in first-episode psychosis and clinical correlates: A 4year longitudinal study using the MATRICS Consensus Cognitive Battery. Schizophrenia Research 169(1), 101-108.
69. Kesby, J.P., Eyles, D.W., McGrath, J.J., Scott, J.G., 2018. Dopamine, psychosis and schizophrenia: the widening gap between basic and clinical neuroscience. Translational Psychiatry 8(1), 30.
70. Keshavan, M.S., Haas, G.L., Kahn, C.E., Eduardo, A., Dick, E.L., Schooler, N.R., Sweeney, J.A., Pettegrew, J.W., 1998. Superior temporal gyrus and the course of early schizophrenia: Progressive, static, or reversible? Journal of Psychiatric Research 32(3), 161-167.
71. Kilcommons, A.M., Morrison, A.P., 2005. Relationships between trauma and psychosis: an exploration of cognitive and dissociative factors. Acta Psychiatrica Scandinavica 112(5), 351-359.
72. Kirkbride, J.B., Yasir Hameed, Gayatri Ankireddypalli, Konstantinos Ioannidis, Carolyn M. Crane, Mukhtar Nasir, Nikolett Kabacs, Antonio Metastasio, Oliver Jenkins, Ashkan Espandian, Styliani Spyridi, Danica Ralevic, Suneetha Siddabattuni, Ben Walden, Adewale Adeoye, Jesus Perez, Peter B. Jones., 2017. The Epidemiology of First-Episode Psychosis in Early Intervention in Psychosis Services: Findings from the Social Epidemiology of Psychoses in East Anglia [SEPEA] Study. American Journal of Psychiatry 174(2), 143-153.

73. Koenders, L., Cousijn, J., Vingerhoets, W.A.M., van den Brink, W., Wiers, R.W., Meijer, C.J., Machielsen, M.W.J., Veltman, D.J., Goudriaan, A.E., de Haan, L., 2016. Grey Matter Changes Associated with Heavy Cannabis Use: A Longitudinal sMRI Study. PLOS ONE 11(5), e0152482.
74. Krack, P., Hariz, M.I., Baunez, C., Guridi, J., Obeso, J.A., 2010. Deep brain stimulation: from neurology to psychiatry? Trends in Neurosciences 33(10), 474-484.
75. Kuperberg, G.R., Broome, M.R., McGuire, P.K., David, A.S., Eddy, M., Ozawa, F., Goff, D., West, W.C., Williams, S.C.R., van der Kouwe, A.J.W., Salat, D.H., Dale, A.M., Fischl, B., 2003. Regionally Localized Thinning of the Cerebral Cortex in Schizophrenia. JAMA Psychiatry 60(9), 878-888.
76. Lappin, J.M., Morgan, C., Chalavi, S., Morgan, K.D., Reinders, A.A.T.S., Fearon, P., Heslin, M., Zanelli, J., Jones, P.B., Murray, R.M., Dazzan, P., 2013. Bilateral hippocampal increase following first-episode psychosis is associated with good clinical, functional and cognitive outcomes. Psychological Medicine 44(6), 1279-1291.
77. Lawrie, S.M., 2018. Are structural brain changes in schizophrenia related to antipsychotic medication? A narrative review of the evidence from a clinical perspective. Ther Adv Psychopharmacol 8(11), 319-326.
78. Lawrie, S.M., McIntosh, A.M., Hall, J., Owens, D.G.C., Johnstone, E.C., 2008. Brain Structure and Function Changes During the Development of Schizophrenia: The Evidence from Studies of Subjects at Increased Genetic Risk. Schizophrenia Bulletin 34(2), 330-340.
79. Lehman, AF, Lieberman, JA, Dixon, LB, McGlashan, TH, Miller, AL, Perkins, DO, Kreyenbuhl, J, McIntyre, JS, Charles, SC, Altshuler, K, Cook, I, Cross, CD, Mellman, L, Moench, LA, Norquist, G, Twemlow, SW, Woods, S, Yager, J, Gray, SH, Askland, K, Pandya, R, Prasad, K, Johnston, R, Nininger, J, Peele, R, Anzia, DJ, Benson, RS, Lurie, L, Walker, RD, Kunkle, R, Simpson, A, Fochtmann, LJ, Hart, C & Regier, D 2004, 'Practice Guideline for the Treatment of Partients with Schizophrenia, Second Edition', American Journal of Psychiatry, vol. 161, no. 2 SUPPL.
80. Lesh, T.A., Tanase, C., Geib, B.R., Niendam, T.A., Yoon, J.H., Minzenberg, M.J., Ragland, J.D., Solomon, M., Carter, C.S., 2015. A Multimodal Analysis of Antipsychotic Effects on Brain Structure and Function in First-Episode Schizophrenia Antipsychotics in First-Episode Schizophrenia Antipsychotics in First-Episode Schizophrenia. JAMA Psychiatry 72(3), 226-234.
81. Lichtenstein, P., Yip, B.H., Björk, C., Pawitan, Y., Cannon, T.D., Sullivan, P.F., Hultman, C.M., 2009. Common genetic determinants of schizophrenia and bipolar disorder in Swedish families: a population-based study. Lancet 373(9659), 234-239.
82. Lieberman, J.A., Chakos, M., Wu, H., Alvir, J., Hoffman, E., Robinson, D., Bilder, R., 2001. Longitudinal study of brain morphology in first episode schizophrenia. Biological Psychiatry 49(6), 487-499.
83. Lieberman, J.A., Tollefson, G.D., Charles, C., Zipursky, R., Sharma, T., Kahn, R.S., Keefe, R.S.E., Green, A.I., Gur, R.E., McEvoy, J., Perkins, D., Hamer, R.M., Gu, H., Tohen, M., Group, H.S., 2005. Antipsychotic Drug Effects on Brain Morphology in First-Episode Psychosis. JAMA Psychiatry 62(4), 361-370.
84. Mahon, P.B., Eldridge, H., Crocker, B., Notes, L., Gindes, H., Postell, E., King, S., Potash, J.B., Ratnanather, J.T., Barta, P.E., 2012. An MRI study of amygdala in schizophrenia and psychotic bipolar disorder. Schizophrenia research 138(2-3), 188-191.
85. Makowski, C., Béland, S., Kostopoulos, P., Bhagwat, N., Devenyi, G.A., Malla, A.K., Joober, R., Lepage, M., Chakravarty, M.M., 2018. Evaluating accuracy of striatal,

pallidal, and thalamic segmentation methods: Comparing automated approaches to manual delineation. Neuroimage 170, 182-198.
86. Manjón, J.V., Coupé, P., 2016. volBrain: An Online MRI Brain Volumetry System. Frontiers in Neuroinformatics 10(30).
87. McDonald, C., Bullmore, E.T., Sham, P.C., Chitnis, X., Wickham, H., Bramon, E., Murray, R.M., 2004. Association of Genetic Risks for Schizophrenia and Bipolar DisorderWith Specific and Generic Brain Structural Endophenotypes. JAMA Psychiatry 61(10), 974-984.
88. Morey, R.A., Petty, C.M., Xu, Y., Pannu Hayes, J., Wagner, H.R., Lewis, D.V., LaBar, K.S., Styner, M., McCarthy, G., 2009. A comparison of automated segmentation and manual tracing for quantifying hippocampal and amygdala volumes. Neuroimage 45(3), 855-866.
89. National Institute for health Care and Excellence (NICE), 2014. Psychosis and schizophrenia in adults: treatment and management. NICE clinical guideline 178. London: NICE; 2014.
90. Navari, S., Dazzan, P., 2009. Do antipsychotic drugs affect brain structure? A systematic and critical review of MRI findings. Psychological Medicine 39(11), 1763-1777.
91. Okugawa, G., Nobuhara, K., Takase, K., Saito, Y., Yoshimura, M., Kinoshita, T., 2007. Olanzapine Increases Grey and White Matter Volumes in the Caudate Nucleus of Patients with Schizophrenia. Neuropsychobiology 55(1), 43-46.
92. Olabi, B., Ellison-Wright, I., McIntosh, A.M., Wood, S.J., Bullmore, E., Lawrie, S.M., 2011. Are There Progressive Brain Changes in Schizophrenia? A Meta-Analysis of Structural Magnetic Resonance Imaging Studies. Biological Psychiatry 70(1), 88-96.
93. Owen, M.J., Sawa, A., Mortensen, P.B., 2016. Schizophrenia. The Lancet 388(10039), 86-97.
94. Palaniyappan, L., Das, T.K., Winmill, L., Hough, M., James, A., 2019. Progressive post-onset reorganisation of MRI-derived cortical thickness in adolescents with schizophrenia. Schizophrenia Research 208, 477-478.
95. Panizzon, M.S., Fennema-Notestine, C., Eyler, L.T., Jernigan, T.L., Prom-Wormley, E., Neale, M., Jacobson, K., Lyons, M.J., Grant, M.D., Franz, C.E., Xian, H., Tsuang, M., Fischl, B., Seidman, L., Dale, A., Kremen, W.S., 2009. Distinct Genetic Influences on Cortical Surface Area and Cortical Thickness. Cerebral Cortex 19(11), 2728-2735.
96. Pantelis, C., Velakoulis, D., McGorry, P.D., Wood, S.J., Suckling, J., Phillips, L.J., Yung, A.R., Bullmore, E.T., Brewer, W., Soulsby, B., Desmond, P., McGuire, P.K., 2003. Neuroanatomical abnormalities before and after onset of psychosis: a cross-sectional and longitudinal MRI comparison. The Lancet 361(9354), 281-288.
97. Patenaude, B., Smith, S.M., Kennedy, D.N., Jenkinson, M., 2011. A Bayesian model of shape and appearance for subcortical brain segmentation. Neuroimage 56(3), 907-922.
98. Radua, J., Borgwardt, S., Crescini, A., Mataix-Cols, D., Meyer-Lindenberg, A., McGuire, P.K., Fusar-Poli, P., 2012. Multimodal meta-analysis of structural and functional brain changes in first episode psychosis and the effects of antipsychotic medication. Neuroscience & Biobehavioral Reviews 36(10), 2325-2333.
99. Rapp, C., Bugra, H., Riecher-Rössler, A., Tamagni, C., Borgwardt, S., 2012. Effects of cannabis use on human brain structure in psychosis: a systematic review combining in vivo structural neuroimaging and postmortem studies. Curr Pharm Des 18(32), 5070-5080.

100. Redman, S.L., Corcoran, C.M., Kimhy, D., Malaspina, D., 2017. Effects of early trauma on psychosis development in clinical high-risk individuals and stability of trauma assessment across studies: a review. Arch Psychol (Chic) 1(3), 28.
101. Reiss, J.P., Sam, D., Sareen, J., 2006. Psychosis in multiple sclerosis associated with left temporal lobe lesions on serial MRI scans. Journal of Clinical Neuroscience 13(2), 282-284.
102. Ripke, S., Neale, B.M., Corvin, A., Walters, J.T.R., Farh, K.-H., Holmans, P.A., Lee, P., Bulik-Sullivan, B., Collier, D.A., Huang, H., Pers, T.H., Agartz, I., Agerbo, E., Albus, M., Alexander, M., Amin, F., Bacanu, S.A., Begemann, M., Belliveau Jr, R.A., Bene, J., Bergen, S.E., Bevilacqua, E., Bigdeli, T.B., Black, D.W., Bruggeman, R., Buccola, N.G., Buckner, R.L., Byerley, W., Cahn, W., Cai, G., Campion, D., Cantor, R.M., Carr, V.J., Carrera, N., Catts, S.V., Chambert, K.D., Chan, R.C.K., Chen, R.Y.L., Chen, E.Y.H., Cheng, W., Cheung, E.F.C., Ann Chong, S., Robert Cloninger, C., Cohen, D., Cohen, N., Cormican, P., Craddock, N., Crowley, J.J., Curtis, D., Davidson, M., Davis, K.L., Degenhardt, F., Del Favero, J., Demontis, D., Dikeos, D., Dinan, T., Djurovic, S., Donohoe, G., Drapeau, E., Duan, J., Dudbridge, F., Durmishi, N., Eichhammer, P., Eriksson, J., Escott-Price, V., Essioux, L., Fanous, A.H., Farrell, M.S., Frank, J., Franke, L., Freedman, R., Freimer, N.B., Friedl, M., Friedman, J.I., Fromer, M., Genovese, G., Georgieva, L., Giegling, I., Giusti-Rodríguez, P., Godard, S., Goldstein, J.I., Golimbet, V., Gopal, S., Gratten, J., de Haan, L., Hammer, C., Hamshere, M.L., Hansen, M., Hansen, T., Haroutunian, V., Hartmann, A.M., Henskens, F.A., Herms, S., Hirschhorn, J.N., Hoffmann, P., Hofman, A., Hollegaard, M.V., Hougaard, D.M., Ikeda, M., Joa, I., Julià, A., Kahn, R.S., Kalaydjieva, L., Karachanak-Yankova, S., Karjalainen, J., Kavanagh, D., Keller, M.C., Kennedy, J.L., Khrunin, A., Kim, Y., Klovins, J., Knowles, J.A., Konte, B., Kucinskas, V., Ausrele Kucinskiene, Z., Kuzelova-Ptackova, H., Kähler, A.K., Laurent, C., Lee Chee Keong, J., Hong Lee, S., Legge, S.E., Lerer, B., Li, M., Li, T., Liang, K.-Y., Lieberman, J., Limborska, S., Loughland, C.M., Lubinski, J., Lönnqvist, J., Macek Jr, M., Magnusson, P.K.E., Maher, B.S., Maier, W., Mallet, J., Marsal, S., Mattheisen, M., Mattingsdal, M., McCarley, R.W., McDonald, C., McIntosh, A.M., Meier, S., Meijer, C.J., Melegh, B., Melle, I., Mesholam-Gately, R.I., Metspalu, A., Michie, P.T., Milani, L., Milanova, V., Mokrab, Y., Morris, D.W., Mors, O., Murphy, K.C., Murray, R.M., Myin-Germeys, I., Müller-Myhsok, B., Nelis, M., Nenadic, I., Nertney, D.A., Nestadt, G., Nicodemus, K.K., Nikitina-Zake, L., Nisenbaum, L., Nordin, A., O'Callaghan, E., O'Dushlaine, C., O'Neill, F.A., Oh, S.-Y., Olincy, A., Olsen, L., Van Os, J., Pantelis, C., Papadimitriou, G.N., Papiol, S., Parkhomenko, E., Pato, M.T., Paunio, T., Pejovic-Milovancevic, M., Perkins, D.O., Pietiläinen, O., Pimm, J., Pocklington, A.J., Powell, J., Price, A., Pulver, A.E., Purcell, S.M., Quested, D., Rasmussen, H.B., Reichenberg, A., Reimers, M.A., Richards, A.L., Roffman, J.L., Roussos, P., Ruderfer, D.M., Salomaa, V., Sanders, A.R., Schall, U., Schubert, C.R., Schulze, T.G., Schwab, S.G., Scolnick, E.M., Scott, R.J., Seidman, L.J., Shi, J., Sigurdsson, E., Silagadze, T., Silverman, J.M., Sim, K., Slominsky, P., Smoller, J.W., So, H.-C., Spencer, C.A., Stahl, E.A., Stefansson, H., Steinberg, S., Stogmann, E., Straub, R.E., Strengman, E., Strohmaier, J., Scott Stroup, T., Subramaniam, M., Suvisaari, J., Svrakic, D.M., Szatkiewicz, J.P., Söderman, E., Thirumalai, S., Toncheva, D., Tosato, S., Veijola, J., Waddington, J., Walsh, D., Wang, D., Wang, Q., Webb, B.T., Weiser, M., Wildenauer, D.B., Williams, N.M., Williams, S., Witt, S.H., Wolen, A.R., Wong, E.H.M., Wormley, B.K., Simon Xi, H., Zai, C.C., Zheng, X., Zimprich, F., Wray, N.R., Stefansson, K., Visscher, P.M., Trust Case-Control Consortium, W., Adolfsson, R., Andreassen, O.A., Blackwood, D.H.R., Bramon, E., Buxbaum, J.D., Børglum, A.D., Cichon, S., Darvasi, A., Domenici, E., Ehrenreich, H., Esko, T., Gejman, P.V., Gill, M., Gurling, H., Hultman, C.M., Iwata, N., Jablensky, A.V., Jönsson, E.G., Kendler, K.S., Kirov, G., Knight, J., Lencz, T., Levinson, D.F., Li, Q.S., Liu, J., Malhotra, A.K., McCarroll, S.A., McQuillin, A., Moran, J.L., Mortensen, P.B.,

Mowry, B.J., Nöthen, M.M., Ophoff, R.A., Owen, M.J., Palotie, A., Pato, C.N., Petryshen, T.L., Posthuma, D., Rietschel, M., Riley, B.P., Rujescu, D., Sham, P.C., Sklar, P., St Clair, D., Weinberger, D.R., Wendland, J.R., Werge, T., Daly, M.J., Sullivan, P.F., O'Donovan, M.C., 2014. Biological insights from 108 schizophrenia-associated genetic loci. Nature 511, 421.

103. Roiz-Santiáñez, R., Ayesa-Arriola, R., Tordesillas-Gutiérrez, D., Ortiz-García de la Foz, V., Pérez-Iglesias, R., Pazos, A., Sánchez, E., Crespo-Facorro, B., 2013. Three-year longitudinal population-based volumetric MRI study in first-episode schizophrenia spectrum patients. Psychological Medicine 44(8), 1591-1604.
104. Roiz-Santiáñez, R., Ortiz-García de la Foz, V., Ayesa-Arriola, R., Tordesillas-Gutiérrez, D., Jorge, R., Varela-Gómez, N., Suárez-Pinilla, P., Córdova-Palomera, A., Navasa-Melado, J.M., Crespo-Facorro, B., 2015. No progression of the alterations in the cortical thickness of individuals with schizophrenia-spectrum disorder: a three-year longitudinal magnetic resonance imaging study of first-episode patients. Psychological Medicine 45(13), 2861-2871.
105. Sánchez-Benavides, G., Gómez-Ansón, B., Sainz, A., Vives, Y., Delfino, M., Peña-Casanova, J., 2010. Manual validation of FreeSurfer's automated hippocampal segmentation in normal aging, mild cognitive impairment, and Alzheimer Disease subjects. Psychiatry Research: Neuroimaging 181(3), 219-225.
106. Schaufelberger, M.S., Lappin, J.M., Duran, F.L.S., Rosa, P.G.P., Uchida, R.R., Santos, L.C., Murray, R.M., McGuire, P.K., Scazufca, M., Menezes, P.R., Busatto, G.F., 2010. Lack of progression of brain abnormalities in first-episode psychosis: a longitudinal magnetic resonance imaging study. Psychological Medicine 41(8), 1677-1689.
107. Schoemaker, D., Buss, C., Head, K., Sandman, C.A., Davis, E.P., Chakravarty, M.M., Gauthier, S., Pruessner, J.C., 2016. Hippocampus and amygdala volumes from magnetic resonance images in children: Assessing accuracy of FreeSurfer and FSL against manual segmentation. Neuroimage 129, 1-14.
108. Shaw, P., Kabani, N.J., Lerch, J.P., Eckstrand, K., Lenroot, R., Gogtay, N., Greenstein, D., Clasen, L., Evans, A., Rapoport, J.L., Giedd, J.N., Wise, S.P., 2008. Neurodevelopmental Trajectories of the Human Cerebral Cortex. The Journal of Neuroscience 28(14), 3586-3594.
109. Sheline, Y.I., Sanghavi, M., Mintun, M.A., Gado, M.H., 1999. Depression Duration but Not Age Predicts Hippocampal Volume Loss in Medically Healthy Women with Recurrent Major Depression. The Journal of Neuroscience 19(12), 5034-5043.
110. Shenton, M.E., Dickey, C.C., Frumin, M., McCarley, R.W., 2001. A review of MRI findings in schizophrenia. Schizophrenia Research 49(1), 1-52.
111. Stahl, E.A., Breen, G., Forstner, A.J., McQuillin, A., Ripke, S., Trubetskoy, V., Mattheisen, M., Wang, Y., Coleman, J.R.I., Gaspar, H.A., de Leeuw, C.A., Steinberg, S., Pavlides, J.M.W., Trzaskowski, M., Byrne, E.M., Pers, T.H., Holmans, P.A., Richards, A.L., Abbott, L., Agerbo, E., Akil, H., Albani, D., Alliey-Rodriguez, N., Als, T.D., Anjorin, A., Antilla, V., Awasthi, S., Badner, J.A., Bækvad-Hansen, M., Barchas, J.D., Bass, N., Bauer, M., Belliveau, R., Bergen, S.E., Pedersen, C.B., Bøen, E., Boks, M.P., Boocock, J., Budde, M., Bunney, W., Burmeister, M., Bybjerg-Grauholm, J., Byerley, W., Casas, M., Cerrato, F., Cervantes, P., Chambert, K., Charney, A.W., Chen, D., Churchhouse, C., Clarke, T.-K., Coryell, W., Craig, D.W., Cruceanu, C., Curtis, D., Czerski, P.M., Dale, A.M., de Jong, S., Degenhardt, F., Del-Favero, J., DePaulo, J.R., Djurovic, S., Dobbyn, A.L., Dumont, A., Elvsåshagen, T., Escott-Price, V., Fan, C.C., Fischer, S.B., Flickinger, M., Foroud, T.M., Forty, L., Frank, J., Fraser, C., Freimer, N.B., Frisén, L., Gade, K., Gage, D., Garnham, J., Giambartolomei, C., Pedersen, M.G., Goldstein, J., Gordon, S.D., Gordon-Smith, K., Green, E.K., Green, M.J., Greenwood, T.A., Grove, J., Guan, W., Guzman-Parra, J., Hamshere, M.L., Hautzinger, M., Heilbronner, U., Herms, S., Hipolito, M., Hoffmann, P., Holland, D., Huckins, L., Jamain, S., Johnson, J.S., Juréus,

A., Kandaswamy, R., Karlsson, R., Kennedy, J.L., Kittel-Schneider, S., Knowles, J.A., Kogevinas, M., Koller, A.C., Kupka, R., Lavebratt, C., Lawrence, J., Lawson, W.B., Leber, M., Lee, P.H., Levy, S.E., Li, J.Z., Liu, C., Lucae, S., Maaser, A., MacIntyre, D.J., Mahon, P.B., Maier, W., Martinsson, L., McCarroll, S., McGuffin, P., McInnis, M.G., McKay, J.D., Medeiros, H., Medland, S.E., Meng, F., Milani, L., Montgomery, G.W., Morris, D.W., Mühleisen, T.W., Mullins, N., Nguyen, H., Nievergelt, C.M., Adolfsson, A.N., Nwulia, E.A., O'Donovan, C., Loohuis, L.M.O., Ori, A.P.S., Oruc, L., Ösby, U., Perlis, R.H., Perry, A., Pfennig, A., Potash, J.B., Purcell, S.M., Regeer, E.J., Reif, A., Reinbold, C.S., Rice, J.P., Rivas, F., Rivera, M., Roussos, P., Ruderfer, D.M., Ryu, E., Sánchez-Mora, C., Schatzberg, A.F., Scheftner, W.A., Schork, N.J., Shannon Weickert, C., Shehktman, T., Shilling, P.D., Sigurdsson, E., Slaney, C., Smeland, O.B., Sobell, J.L., Søholm Hansen, C., Spijker, A.T., St Clair, D., Steffens, M., Strauss, J.S., Streit, F., Strohmaier, J., Szelinger, S., Thompson, R.C., Thorgeirsson, T.E., Treutlein, J., Vedder, H., Wang, W., Watson, S.J., Weickert, T.W., Witt, S.H., Xi, S., Xu, W., Young, A.H., Zandi, P., Zhang, P., Zöllner, S., Adolfsson, R., Agartz, I., Alda, M., Backlund, L., Baune, B.T., Bellivier, F., Berrettini, W.H., Biernacka, J.M., Blackwood, D.H.R., Boehnke, M., Børglum, A.D., Corvin, A., Craddock, N., Daly, M.J., Dannlowski, U., Esko, T., Etain, B., Frye, M., Fullerton, J.M., Gershon, E.S., Gill, M., Goes, F., Grigoroiu-Serbanescu, M., Hauser, J., Hougaard, D.M., Hultman, C.M., Jones, I., Jones, L.A., Kahn, R.S., Kirov, G., Landén, M., Leboyer, M., Lewis, C.M., Li, Q.S., Lissowska, J., Martin, N.G., Mayoral, F., McElroy, S.L., McIntosh, A.M., McMahon, F.J., Melle, I., Metspalu, A., Mitchell, P.B., Morken, G., Mors, O., Mortensen, P.B., Müller-Myhsok, B., Myers, R.M., Neale, B.M., Nimgaonkar, V., Nordentoft, M., Nöthen, M.M., O'Donovan, M.C., Oedegaard, K.J., Owen, M.J., Paciga, S.A., Pato, C., Pato, M.T., Posthuma, D., Ramos-Quiroga, J.A., Ribasés, M., Rietschel, M., Rouleau, G.A., Schalling, M., Schofield, P.R., Schulze, T.G., Serretti, A., Smoller, J.W., Stefansson, H., Stefansson, K., Stordal, E., Sullivan, P.F., Turecki, G., Vaaler, A.E., Vieta, E., Vincent, J.B., Werge, T., Nurnberger, J.I., Wray, N.R., Di Florio, A., Edenberg, H.J., Cichon, S., Ophoff, R.A., Scott, L.J., Andreassen, O.A., Kelsoe, J., Sklar, P., e, Q.C., Consortium, B., the Bipolar Disorder Working Group of the Psychiatric Genomics, C., 2019. Genome-wide association study identifies 30 loci associated with bipolar disorder. Nature Genetics 51(5), 793-803.

112. Stankiewicz, J.M., Glanz, B.I., Healy, B.C., Arora, A., Neema, M., Benedict, R.H.B., Guss, Z.D., Tauhid, S., Buckle, G.J., Houtchens, M.K., Khoury, S.J., Weiner, H.L., Guttmann, C.R.G., Bakshi, R., 2011. Brain MRI lesion load at 1.5T and 3T versus clinical status in multiple sclerosis. J Neuroimaging 21(2), e50-e56.
113. Steen, R.G., Mull, C., McClure, R., Hamer, R.M., Lieberman, J.A., 2006. Brain volume in first-episode schizophrenia: Systematic review and meta-analysis of magnetic resonance imaging studies. British Journal of Psychiatry 188(6), 510-518.
114. Steullet, P., 2019. Thalamus-related anomalies as candidate mechanism-based biomarkers for psychosis. Schizophrenia Research.
115. Suárez-Pinilla, P., Roíz-Santiañez, R., Mata, I., Ortiz-García de la Foz, V., Brambilla, P., Fañanas, L., Valle-San Román, N., Crespo-Facorro, B., 2015. Progressive Structural Brain Changes and NRG1 Gene Variants in First-Episode Nonaffective Psychosis. Neuropsychobiology 71(2), 103-111.
116. Sullivan, P.F., Kendler, K.S., Neale, M.C., 2003. Schizophrenia as a Complex Trait: Evidence from a Meta-analysis of Twin Studies. JAMA Psychiatry 60(12), 1187-1192.
117. Sun, D., Phillips, L., Velakoulis, D., Yung, A., McGorry, P.D., Wood, S.J., van Erp, T.G.M., Thompson, P.M., Toga, A.W., Cannon, T.D., Pantelis, C., 2009. Progressive brain structural changes mapped as psychosis develops in 'at risk' individuals. Schizophrenia research 108(1-3), 85-92.

118. Symms, M., Jäger, H.R., Schmierer, K., Yousry, T.A., 2004. A review of structural magnetic resonance neuroimaging. Journal of Neurology, Neurosurgery & Psychiatry 75(9), 1235.
119. Tanaka, Y., Hazama, H., Kawahara, R., Kobayashi, K., 1981. Computerized tomography of the brain in schizophrenic patients: A CONTROLLED STUDY. Acta Psychiatrica Scandinavica 63(3), 191-197.
120. Théberge, J., Williamson, K.E., Aoyama, N., Drost, D.J., Manchanda, R., Malla, A.K., Northcott, S., Menon, R.S., Neufeld, R.W.J., Rajakumar, N., Pavlosky, W., Densmore, M., Schaefer, B., Williamson, P.C., 2007. Longitudinal grey-matter and glutamatergic losses in first-episode schizophrenia. British Journal of Psychiatry 191(4), 325-334.
121. Thompson, P.M., Bartzokis, G., Hayashi, K.M., Klunder, A.D., Lu, P.H., Edwards, N., Hong, M.S., Yu, M., Geaga, J.A., Toga, A.W., Charles, C., Perkins, D.O., McEvoy, J., Hamer, R.M., Tohen, M., Tollefson, G.D., Lieberman, J.A., Group, t.H.S., 2008. Time-Lapse Mapping of Cortical Changes in Schizophrenia with Different Treatments. Cerebral Cortex 19(5), 1107-1123.
122. Tyrer, P., 2015. Mental Illness, Etiology of, in: Wright, J.D. (Ed.), International Encyclopedia of the Social & Behavioral Sciences (Second Edition). Elsevier, Oxford, pp. 204-208.
123. van Haren, N.E.M., Pol, H.E.H., Schnack, H.G., Cahn, W., Brans, R., Carati, I., Rais, M., Kahn, R.S., 2008. Progressive Brain Volume Loss in Schizophrenia Over the Course of the Illness: Evidence of Maturational Abnormalities in Early Adulthood. Biological Psychiatry 63(1), 106-113.
124. Vázquez-Bourgon, J., Roiz-Santiañez, R., Papiol, S., Ferro, A., Varela-Gómez, N., Fañanás, L., Crespo-Facorro, B., 2016. Variations in Disrupted-in-Schizophrenia 1 gene modulate long-term longitudinal differences in cortical thickness in patients with a first-episode of psychosis. Brain Imaging and Behavior 10(3), 629-635.
125. Velakoulis, D., Wood, S.J., Wong, M.T.H., McGorry, P.D., Yung, A., Phillips, L., Smith, D., Brewer, W., Proffitt, T., Desmond, P., Pantelis, C., 2006. Hippocampal and Amygdala Volumes According to Psychosis Stage and Diagnosis: A Magnetic Resonance Imaging Study of Chronic Schizophrenia, First-Episode Psychosis, and Ultra–High-Risk Individuals. JAMA Psychiatry 63(2), 139-149.
126. Vita, A., de Peri, L., 2007. Hippocampal and amygdala volume reductions in first-episode schizophrenia. British Journal of Psychiatry 190(3), 271-271.
127. Vita, A., De Peri, L., Silenzi, C., Dieci, M., 2006. Brain morphology in first-episode schizophrenia: A meta-analysis of quantitative magnetic resonance imaging studies. Schizophrenia Research 82(1), 75-88.
128. Volpe, U., Mucci, A., Quarantelli, M., Galderisi, S., Maj, M., 2012. Dorsolateral prefrontal cortex volume in patients with deficit or nondeficit schizophrenia. Progress in Neuro-Psychopharmacology and Biological Psychiatry 37(2), 264-269.
129. Weinberger, D.R., Torrey, E.F., Neophytides, A.N., Wyatt, R.J., 1979. Lateral Cerebral Ventricular Enlargement in Chronic Schizophrenia. Archives of General Psychiatry 36(7), 735-739.
130. Welch, K.A., Stanfield, A.C., McIntosh, A.M., Whalley, H.C., Job, D.E., Moorhead, T.W., Owens, D.G.C., Lawrie, S.M., Johnstone, E.C., 2018. Impact of cannabis use on thalamic volume in people at familial high risk of schizophrenia. British Journal of Psychiatry 199(5), 386-390.
131. Whitwell, J.L., 2008. Longitudinal imaging: change and causality. Current Opinion in Neurology 21(4), 410-416.
132. Winkler, A.M., Kochunov, P., Blangero, J., Almasy, L., Zilles, K., Fox, P.T., Duggirala, R., Glahn, D.C., 2010. Cortical thickness or grey matter volume? The importance of selecting the phenotype for imaging genetics studies. NeuroImage 53(3), 1135-1146.

133. Wittchen, H.U., Jacobi, F., Rehm, J., Gustavsson, A., Svensson, M., Jönsson, B., Olesen, J., Allgulander, C., Alonso, J., Faravelli, C., Fratiglioni, L., Jennum, P., Lieb, R., Maercker, A., van Os, J., Preisig, M., Salvador-Carulla, L., Simon, R., Steinhausen, H.C., 2011. The size and burden of mental disorders and other disorders of the brain in Europe 2010. European Neuropsychopharmacology 21(9), 655-679.
134. Wood, S.J., Velakoulis, D., Smith, D.J., Bond, D., Stuart, G.W., McGorry, P.D., Brewer, W.J., Bridle, N., Eritaia, J., Desmond, P., Singh, B., Copolov, D., Pantelis, C., 2001. A longitudinal study of hippocampal volume in first episode psychosis and chronic schizophrenia. Schizophrenia Research 52(1), 37-46.
135. Wright, I.C., Rabe-Hesketh, S., Woodruff, P.W.R., David, A.S., Murray, R.M., Bullmore, E.T., 2000. Meta-analysis of regional brain volumes in schizophrenia. The American Journal of Psychiatry 157(1), 16-25.
136. Yucel, M., Solowij, N., Respondek, C., Whittle, S., Fornito, A., Pantelis, C., Lubman, D.I., 2008. Regional Brain Abnormalities Associated with Long-term Heavy Cannabis Use. JAMA Psychiatry 65(6), 694-701.
137. Yushkevich, P.A., Piven, J., Hazlett, H.C., Smith, R.G., Ho, S., Gee, J.C., Gerig, G., 2006. User-guided 3D active contour segmentation of anatomical structures: Significantly improved efficiency and reliability. Neuroimage 31(3), 1116-1128.
138. Zipparo, L., Whitford, T.J., Redoblado Hodge, M.A., Lucas, S., Farrow, T.F.D., Brennan, J., Gomes, L., Williams, L.M., Harris, A.W.F., 2008. Investigating the neuropsychological and neuroanatomical changes that occur over the first 2–3 years of illness in patients with first-episode schizophrenia. Progress in Neuro-Psychopharmacology and Biological Psychiatry 32(2), 531-538.
139. Zipursky, R.B., Reilly, T.J., Murray, R.M., 2013. The myth of schizophrenia as a progressive brain disease. Schizophrenia bulletin 39(6), 1363-1372.

Chapter 2

Study 1

A comparative study of segmentation techniques for the quantification of brain subcortical volume

Theophilus N. Akudjedu[1*], Leila Nabulsi[1], Migle Makelyte[1, 2], Cathy Scanlon[1], Sarah Hehir[1], Helen Casey[1], Srinath Ambati[1,] Joanne Kenney[1], Stefani O'Donoghue[1], Emma McDermott[1], Liam Kilmartin[2], Peter Dockery[1], Colm McDonald[1], Brian Hallahan[1], Dara M. Cannon[1].

[1]Centre for Neuroimaging & Cognitive Genomics (NICOG), Clinical Neuroimaging Laboratory, NCBES Galway Neuroscience Centre, Psychiatry & Anatomy, School of Medicine,College of Medicine Nursing and Health Sciences, National University of Ireland Galway, H91TK33 Galway, Ireland. [2]College of Engineering and Informatics, National University of Ireland Galway, H91TK33 Galway, Ireland.

Published in Brain Imaging & Behavior 2018 Dec;12(6):1678-1695.

Author's Contribution

The original data for this study was acquired prior to commencement of the current PhD research. Authors CMc, DMC and BH designed and supervised the general progress of the study. Acquisition of MRI and supervision of manual segmentation was done by CS and DMC. I carried out all pre-processing of the MRI images. The following author's contributed in relation to segmentation using stereology – (EMc and PD), manual tracing (SH, HC, SA, JK and SO) and FSL-FIRST (LN) and I carried out segmentation using volBrain, FreeSurfer, FSL-FIRST and quality checked all the manually segmented files. Furthermore, I performed statistical analyses and wrote the entire manuscript with the input of all authors who have approved the final work under the supervision of CMc, DMC and BH.

Abstract

Manual tracing of magnetic resonance imaging (MRI) represents the gold standard for segmentation in clinical neuropsychiatric research studies, however automated approaches are increasingly used due to its time limitations. The accuracy of segmentation techniques for subcortical structures has not been systematically investigated in large samples.

We compared the accuracy of fully automated [(i) model-based: FSL-FIRST; (ii) patch-based: volBrain], semi–automated (FreeSurfer) and stereological (Measure®) segmentation techniques with manual tracing (ITK-SNAP) for delineating volumes of the caudate (*easy-to-segment*) and the hippocampus (*difficult-to-segment*).

High resolution 1.5 Tesla T1-weighted MR images were obtained from 177 patients with major psychiatric disorders and 104 healthy participants. The relative consistency (partial correlation), absolute agreement (intraclass correlation coefficient, ICC) and potential technique bias (Bland-Altman plots) of each technique was compared with manual segmentation.

Each technique yielded high correlations (0.77 – 0.87, $p<0.0001$) and moderate ICC's (0.28 – 0.49) relative to manual segmentation for the caudate. For the hippocampus, stereology yielded good consistency (0.52 – 0.55, $p<0.0001$) and ICC (0.47-0.49), whereas automated and semi-automated techniques yielded poor ICC (0.07 – 0.10) and moderate consistency (0.35 – 0.62, $p<0.0001$). Bias was least using stereology for segmentation of the hippocampus and using FreeSurfer for segmentation of the caudate.

In a typical neuropsychiatric MRI dataset, automated segmentation techniques provide good accuracy for an *easy-to-segment* structure such as the caudate, whereas for the hippocampus, a reasonable correlation with volume but poor absolute agreement was demonstrated. This indicates manual or stereological volume estimation should be considered for studies that require high levels of precision such as those with small sample size.

Keywords FSL-FIRST, FreeSurfer, segmentation techniques, stereology, subcortical structures, volBrain

2.1 Introduction

In recent decades, significant advances in *in-vivo* brain imaging technologies have allowed for volumetric quantification of brain structures in large magnetic resonance imaging (MRI) datasets. This has enabled researchers to undertake large-scale world-wide studies examining brain anatomy and disease progression using morphometric properties. Several changes in cortical and subcortical morphometry are widely reported from clinical groups using segmentation techniques. Clinical neuromorphometric studies of cohorts including bipolar disorder (Quigley *et al.* 2015; Hibar *et al.* 2016; Sacchet *et al.* 2015; Mamah *et al.* 2016), first-episode psychosis (Scanlon *et al.* 2014; Cahn *et al.* 2002; Mamah *et al.* 2012), major depressive disorder (Schmaal *et al.* 2016; Sacchet *et al.* 2015; Renteria *et al.* 2017) and schizophrenia (van Erp *et al.* 2016; Okada *et al.* 2016; Mamah *et al.* 2016) have all employed various classes of segmentation processing techniques.

Manual segmentation techniques are currently considered the gold standard for volumetric quantification of regional brain structures (Morey *et al.* 2009; Rodionov *et al.* 2009; Doring *et al.* 2011; Sanchez-Benavides *et al.* 2010). However, such procedures are associated with a number of limitations including the requirement for substantial anatomical and methodological expertise by the tracer(s), with associated inter- and intra-rater reliability concerns, although the strict use of protocols combined with anatomical expertise and training can minimise these. In addition, manual tracing is associated with significant time requirements, potentially limiting the feasibility of this technique for the volumetric quantification of large datasets. Various automated techniques are now freely/commercially available to segment regional brain structures in order to overcome these limitations and have been employed in several large recent MRI collaborative studies (van Erp *et al.* 2016; Hibar *et al.* 2016; Franke *et al.* 2016).

Automated approaches for brain processing and segmentation have several potential advantages over manual segmentation. Advantages include a significant reduction in time and labour, excellent reproducibility and less training or anatomical knowledge for the end-user. Two automated, model-based approaches commonly used in the field currently are FreeSurfer (http://surfer.nmr.mgh.harvard.edu, Fischl *et al.* 2002) and "FIRST", which is provided as part of the FSL software library (http://fsl.fmrib.ox.ac.uk, Patenaude *et al.* 2011). FreeSurfer automatically assigns a label to each voxel from anatomical images based on probabilistic estimations relying on Markov random fields (MRFs). FIRST uses a probabilistic framework with boundaries of brain structures based on signal intensity of T1-images and

the expected shape of structures to be segmented. These model-based approaches assume that algorithms can reliably delineate anatomical regions irrespective of inter-individual differences or pathological changes in neuroanatomy and/or challenges of MR brain acquisition. In an attempt to address these concerns, fully automated multi-atlas label fusion approaches such as volBrain (http://volbrain.upv.es, Manjon and Coupe, 2016) have also been implemented. FreeSurfer additionally allows the user to edit the quality of segmentation determined automatically, unlike FIRST and volBrain, and can thus be considered a "semi-automated" technique.

Furthermore, stereology, a long-standing reliable method for the estimation of volume of structures, has been employed with MR imaging and previously been demonstrated to deliver consistent findings when compared to manual tracing for both smooth (Ertekin *et al.* 2015) and complex (Sheline *et al.* 1999) structures.

A number of previous studies (Sheline *et al.* 1999; Pardoe *et al.* 2009; Morey *et al.* 2009; Doring *et al.* 2011; Keller *et al.* 2012; Ertekin *et al.* 2015; Schoemaker *et al.* 2016; Makowski *et al.* 2017) have assessed the performance of automated methods and/or stereology compared to manual segmentation in relatively small populations. However, to our knowledge, no previous study has compared in such a large cohort of individuals across this wide range of segmentation techniques (fully-automated, semi-automated and stereology). The aim of the present analysis is to examine the performance of fully-automated (model-based) (FSL-FIRST v.5.0.4), fully-automated (patch-based) (volBrain v.1.0), semi–automated (FreeSurfer v.5.1) and stereological (Measure®) segmentation techniques against manual segmentation (ITK-SNAP v.1.8) (http://www.itksnap.org/) for the quantification of the caudate and hippocampus in a large heterogeneous sample of adult MR images. The caudate and the hippocampus were chosen as two representative structures that provide a smooth (*easy-to-segment*) and complex (*difficult-to-segment*) (Grimm *et al.* 2015) boundary for testing, respectively. Additionally, volumetric abnormalities in these regions have been implicated in numerous neuropsychiatric disorders.

2.2 Methods

2.2.1 Participants

Structural MR images (n=281), were obtained from individuals aged 16 – 60 years of age as part of the Clinical Neuroimaging Laboratory Research Programme at the National University of Ireland, Galway (NUI Galway). Participants included 189 males (67.3%) and had a mean age of 36 years (± 11 SD). They consisted of individuals with major psychiatric disorders

(n=177) and healthy participants (n=104). All participants provided written informed consent for the relevant studies and ethical approval was obtained from the NUI Galway, and Galway University Hospitals Research Ethics Committees.

2.2.2 MRI data acquisition

Clinical assessments and baseline protocols employed during recruitment have been described previously (Emsell *et al.* 2013; McFarland *et al.* 2013; Scanlon *et al.* 2014; Ahmed *et al.* 2015; Kenney *et al.* 2015). Briefly, MR data were acquired at University Hospital Galway (UHG) on a 1.5 Tesla Siemens Magnetom Symphony scanner (Erlangen, Germany) equipped with a 4-channel head coil. A standard localiser and T1-sagittal sequence was used to confirm participants' radiological position and placement of the image field-of-view in alignment with the anterior-posterior commissure (AC-PC) line. The weighted magnetisation-prepared rapid acquisition of gradient echo (MPRAGE) sequence was employed to acquire volumetric T1-weighted images (160 slices) with the following parameters: repetition time (TR): 1140 ms, echo time (TE): 4.38 ms, inversion time (TI): 600 ms, flip angle 15; matrix size 256×256; an in-plane pixel size of 0.9 mm × 0.9 mm and slice thickness of 0.9 mm.

2.2.3 Image pre-processing and quality analyses

The volumetric T1 images were visually examined for quality and underwent correction for intensity non-uniformity as described previously (Emsell *et al.* 2013; Scanlon *et al.* 2014; Ahmed *et al.* 2015). Non-parametric non-uniform intensity normalisation (N3) was performed to correct for intensity non-uniformity (Sled *et al.* 1998).

2.2.4 Volumetric quantification using manual segmentation with ITK-SNAP

The bilateral caudate nuclei and hippocampi were manually segmented by anatomically trained raters [JK, SA, SO and SH] using ITK-SNAP (v.1.8.0, Yushkevich *et al.* 2006) with inter-rater reliability [Caudate (Left: 0.97; Right: 0.96) and Hippocampus (Left: 0.89; Right: 0.94)] and intra-rater reliability scores greater than 0.85 for all raters.

ITK-SNAP displays the three orthogonal views of the MR image and a 3D view of the segmented structure. The pre-processed images underwent segmentation according to a strict anatomical protocol adapted from Looi *et al.* for the caudate (Looi *et al.* 2008) and from Velakoulis *et al.* and Strakowski *et al.* in the case of the hippocampus (Velakoulis *et al.* 2006; Strakowski *et al.* 1999).

The first slice included for the caudate was defined as that axial slice in which the grey matter (GM) of the caudate head was clearly distinguished from the surrounding frontal white matter (WM) anteriorly, the anterior commissure posteriorly, the internal capsule laterally, and a thin strip of WM medially. Tracing continued superiorly on every slice in which the GM of the caudate was bordered medially by the anterolateral portion of the lateral ventricle, anteriorly by the frontal WM and dorso-laterally by the internal capsule. The last slice was defined as the point at which the caudate body was no longer clearly visible laying medial to the lateral ventricle. Due care was taken to avoid inclusion of the nucleus accumbens.

The hippocampus was defined as consisting of the hippocampus proper (Ammon's horn), the dentate gyrus, and a portion of the subiculum. In order to limit inclusion to hippocampal GM, the alveus, fimbria, fornix and entorhinal cortex were excluded. Tracing was performed in the three orthogonal views mainly in the sagittal and coronal views with the axial view providing guidance. The anterior boundary was demarcated by the alveus acting as a WM border over the hippocampal head (Strakowski *et al.* 1999). The posterior boundary was defined by referring to the crus with tracing ending at the point where the greatest continuation of the fornix was visible as grey switches to WM (Velakoulis *et al.* 2006). The medial boundary was indicated by the open end of the hippocampal and uncal fissures and the medial aspect of the ambiens gyrus. The uncus and the ambient gyrus lie between the hippocampal complex and the ambient cistern in initial slices (Velakoulis *et al.* 2006). The lateral boundary was formed by the inferior horn of the lateral ventricle and adjacent WM (Altshuler *et al.* 1998, 2000). The superior boundary was the alveus and the inferior boundary was the WM between the hippocampus and the underlying parahippocampal gyrus (Brambilla *et al.* 2003).

Following segmentation according to the standardised protocols, the segmented regions were magnified by 7pixels/mm^3 simultaneously in all planes to examine accuracy of the segmentation surface. The segmented structures were further labelled (L/R) to maintain appropriate lateralisation according to their position. ITK-SNAP measured the volume of the structure by assigning each voxel a single label depending on whether the voxel was manually traced or not (Yushkevich *et al.* 2006). Thus, the number of voxels present within the traced area was used to compute the volume of the structure.

2.2.5 Volumetric quantification using stereological segmentation with Measure®

Stereology is a set of methodologies that ensure rigorous analysis of size, shape, and other quantitative parameters such as length, surface area and volume of three-dimensional objects based on observations in two dimensional sections (Garcia *et al.* 2007). Stereology has been employed as a novel alternative volumetric analysis technique for radiological anatomy. This technique is based on the Cavalieri principle and is robust, unbiased and efficient as it requires no assumptions about the structure (orientation or shape) under assessment (Gundersen *et al.* 1988).

Following this principle, the slices of the brain in which the caudate/hippocampus is present were examined. Careful observation by expert neuroanatomists [DC and CS] and a trained rater [EMcD] indicated that both structures appeared on approximately 60 slices of the images used for the study. Similarly, 10 randomly selected subjects were used to determine the intra-rater reliability [EMcD] for this study. The intra-rater reliability scores were 0.94 and 0.80 for the caudate and hippocampus respectively. The first slice was chosen randomly while the subsequent slices were selected at systematic intervals from the images. The grid size, number of slices, slice thickness and the structural boundaries for the caudate and the hippocampus were explicitly defined as per the manual segmentation technique [caudate (Looi *et al.* 2008) and hippocampus (Velakoulis *et al.* 2006 and Strakowski *et al.* 1999)]. A computer-generated point counting grid (stereological probe) was randomly superimposed on the image to automatically count and estimate the volume from the hippocampal or caudate profile bilaterally. To ensure accurate volumetric analysis, the hippocampus was sampled by a magnification of $7px/mm^3$ in the axial view. The scale bar was used to correct for the magnification on the image in comparison to real measurements. The above procedure was also used for the caudate bilaterally, however, at a magnification of $8px/mm^3$ in the axial view. Thus, the stereological parameters for the volumetric estimation of both structures were optimised to achieve minimal errors in measurement. The schematic illustration of the Cavalieri principle as applied for MRI segmentation was shown (see Fig.1; Mayer *et al.* 2016).

2.2.6 Volumetric quantification using fully-automatic (model-based) segmentation with FSL-FIRST

The fully automated segmentation of the volumes of the caudate and the hippocampus was carried out by employing FSL-FIRST (v.5.0.4, http://fsl.fmrib.ox.ac.uk/) after registration of images to a standard template (Centre for Morphometric Analysis (CMA), MGH, Boston).

These templates have been manually segmented as done previously (Filipek *et al.* 1994) to generate the models employed in FIRST. Following registration, the model-based approach using a Bayesian framework allows the probabilistic relationship of shape and intensity to be exploited in estimating volume (Patenaude, 2007; Patenaude *et al.* 2011). To ensure best fit for each of the structures of interest, the empirically optimised default settings for each structure were applied. The accuracy of the segmentation was visually checked from the labels for the specific structures (L/R) in native space to ensure good registration. The diagrammatic illustration of the transformation of the images from native space into standard space for the segmentation and back to native space for volumetric analysis was shown (see Fig.3; Morey *et al.* 2009). Eight subjects were removed from all further analyses due to poor registration and volume extraction errors.

2.2.7 Volumetric quantification using fully-automatic (patch-based) segmentation with volBrain

The volume of the caudate and the hippocampus was segmented by employing volBrain (v.1.0, http://volbrain.upv.es), another fully automated segmentation technique. The operational pipeline of this free online MRI brain volumetry system was described previously (Manjon and Coupe, 2016). Briefly, this technique employs the multi-atlas patch-based label fusion segmentation technology (Coupe *et al.* 2011) to segment anatomical structures. The system firstly pre-processes the images through a spatially adaptive non-local means of denoising and corrects for intensity inhomogeneity roughly. The images are then registered to MNI space and again corrected for inhomogeneity to achieve a fine normalised intensity. The pre-processing sets the input image in the same geometric and intensity space. The volumetric estimation of the various brain structures at different scales are then achieved through a non-local intracranial cavity extraction and tissue classification. Furthermore, segmentation of the hemispheres and then the subcortical structures (including caudate and hippocampus) were achieved by distinguishing each pixel or patch through the Optimised PAtchMatch Label fusion (OPAL) strategy (Giraud *et al.* 2016; Bao and Chung, 2016). Thus, subcortical labelling is based on a weighted label vote scheme through comparisons of pixels or patches. The image patch and the multi-atlas (manual labels) patches are compared after which weights are assigned according to patch similarity (Coupe *et al.* 2011; Giraud *et al.* 2016). This pipeline segments the hippocampus according to the EADC-ADNI Harmonised Protocol for Hippocampal Segmentation (Boccardi *et al.* 2015), the caudate was however segmented according to a local expert's definition at the algorithm/pipeline development site. This processing pipeline was shown in a schematic diagram (see Fig.1; Manjon and

Coupe, 2016). A segmentation failure rate (0.4%, n=1) was reported and this was removed from all further analysis.

2.2.8 Volumetric quantification using semi-automatic segmentation with FreeSurfer

The "recon-all" segmentation pipeline was employed for the delineation of both the caudate and the hippocampus bilaterally using FreeSurfer (v.5.1.0, http: //surfer. nmr.mgh.harvard.edu/). The technical operation of this free and documented volumetric image analysis suite was described previously (Fischl *et al.* 1999; Dale, 1999, Fischl and Dale, 2000; Fischl *et al.* 2002). Briefly, this technique segments by parcellating subcortical structures by affine registration to Talairach space depending on the differences in their voxel intensities. Thus, its estimations are based on the probability that each voxel will belong to a certain structure within the tissues of the brain. This pipeline is based on manual neuroanatomical segmentation protocols (Filipek *et al.* 1994) provided by the CMA. Schematic illustration of this outline was reported (see Fig. 3; Morey *et al.* 2009). The caudate and hippocampus volumes provided in the *aseg.stats* file were used in the analysis as they account for partial volume estimations and are deemed to be more accurate. Quality analyses included visual inspection of all the "recon-all" steps and the segmented structures as described in the established ENIGMA protocol (http://enigma.loni.ucla.edu/protocols/). Seventeen brain images were noted to have been inadequately skull stripped. These were corrected as described in the FreeSurfer guidelines by adjusting the watershed parameters using the [*recon-all -skullstrip -wsthresh XX -s XX*] and/or the *gcut* command without any further intervention manually. Three subjects were removed from all further analyses because of poor registration and extraction errors. The *aseg.mgz* volume files were converted from MGZ to NIFTI file format and transferred back into native space for visualisation.

2.2.9 Statistical analyses

Statistical analyses were performed with volumes in native space using the Statistical Package for Social Sciences (SPSS) version 23.0 for Windows (SPSS Inc., IBM, New York, USA). The Shapiro–Wilk's test was employed to test the normality of our data because of its relatively large power to detect normality (Razali and Wah 2011). In accordance with the comparative performance metrics outlined by Fenster and Chiu (2005), the degree to which the techniques agree with manual segmentation in accuracy, their level of consistency and efficiency were assessed.

2.2.9.1 Analysis of spatial overlap and volume difference

These are commonly used in medical image segmentation, especially for comparing new techniques against known references (Taha and Hanbury, 2015). As suggested for comparison of two techniques for inter-rater reliability by Collins *et al.* (1995), we investigated the level of agreement of each of the techniques with manual tracing in terms of their *percentage spatial overlap and volume difference* (Collins *et al.* 1995, Fischl *et al.* 2002; Han and Fischl, 2007). The percent spatial overlap (Dice score) was estimated for the volumes relative to the gold standard volumes. For a structure P, segmented using two techniques, the percent spatial overlap is defined in equation (1). Thus, P_1 is the volume as measured by the first technique and P_2 is the volume from the second technique (gold standard). This was computed for each subject, structure and volumes compared to the gold standard.

$$O(P_1,P_2) = [V(P_1) \cap V(P_2)/V(P_2)]*100\% \quad \textit{eqn (1)}$$

A maximum percent spatial overlap (100%) is achieved for identical volumes while less perfect spatial overlaps are assigned lower scores. Thus, slight shifts in the spatial location of a volume relative to another will cause a reduction in the overall percent spatial overlap between these volumes (Morey *et al.* 2009). Additionally, percent volume difference between volumes obtained with the other techniques and the gold standard were estimated as defined in equation (2). A positive volume difference indicates overestimation relative to the manually obtained volumes while a negative indicates underestimation and those approaching 0% indicate convergence of the volumes obtained from the other techniques and the gold standard.

$$D(P_1,P_2) = [V(P_1) - V(P_2)/V(P_2)]*100\% \quad \textit{eqn(2)}$$

We conducted a one-way ANOVA to compare the spatial overlaps and volumetric means obtained from the techniques. Tukey *post-hoc* test was conducted to indicate which of the techniques were significantly different from each other at 95% confidence interval (CI).

2.2.9.2 Correlation analysis between-techniques

Although these volume comparisons are paired, some confounding factors are likely to affect the algorithms/pipelines of the techniques differently. For example, differences in age, gender and intracranial volume are reported to influence the effect a segmentation method has on statistical results (Barnes *et al.* 2010; Nordenskjold *et al.* 2015). Partial correlation analysis controlling for age and gender were therefore conducted to determine the level of consistency between manual tracing and the other segmentation techniques for the global

sample. This statistical approach adjusts the crude correlation (Pearson's) scores by eliminating the effect of the confounding variables. Intracranial volume was however not included as part of the control variables in this study as group difference effect was not the main subject under investigation and the inclusion of intracranial volume corrections would have excluded the computation of practical performance metrics such as the percentage volume overlap which depends on the actual position of voxels (Sanchez-Benavides *et al.* 2010). The magnitudes of these correlation coefficients were compared for existence of significant differences to assess performance with reference to the manual technique using the *Fisher r-to-z transformation* (Watson, 2001). A total of six technique comparisons over the caudate and hippocampus were made to assess consistency bilaterally. An alpha adjustment at $p<0.01$ for statistical significance in accordance to the *Bonferroni procedure* for a two-tailed hypothesis was employed. Furthermore, the partial correlation coefficients obtained from the techniques relative to manual tracing were compared between the patient and control group for existence of significant differences in consistency. These differences helped to establish consistency of the various techniques within different cohorts using the *Fisher r-to-z transformation* (Watson, 2001).

Additionally, the intraclass correlation coefficient (ICC, single measures) was used to validate the absolute agreement between the techniques relative to the gold standard as done previously (Makowski *et al.* 2017; Schoemaker *et al.* 2016). ICC in this thesis was defined as the ratio of variability between segmentation technique measurements to the total variability including technique variability (TV), variability in repetition of measurement (VIR) and error variability (EV) (Kim, 2013). This is presented mathematically in equation (3).

$$\text{ICC (absolute agreement, number of techniques (k))} = TV / [TV + (VIR + EV)/k] \quad \textit{eqn (3)}$$

Thus, reliability based on absolute agreement unlike consistency or Pearson's correlation coefficient, is always lower as more stringent criteria based on variability in repetition is applied as shown in the above equation (3). A reliability score range of 0.75 - 0.90 is considered an optimum standard for adequate reproducibility and reliability (Hallgren, 2012; Koo and Li, 2016). The ICC was again used to determine the intra and inter-rater reliability between the raters for the manual and the stereological techniques.

2.2.9.3 Analysis of potential technique biases: Bland – Altman plots

The Bland-Altman plot is a popular statistical method for testing agreement of clinical techniques that measure continuous variables (Zaki *et al.* 2012). The systematic (built-in)

error which makes all relative measurements incorrect by a certain amount is referred to as bias (Zaki *et al.* 2012). Thus, biases found among techniques may be driven by several factors including differences in the neuroanatomical definitions employed. For instance, contrary to the protocols adopted by the automated techniques, the alveus and fimbria were excluded when segmenting the hippocampus using our protocol. In addition, the protocols employed by the automated techniques included variable amounts of grey matter from the hippocampal tail region (Andreas-Retzius and the Fasciolar gyrus) when segmenting the hippocampus. Although, the protocols employed for segmentation of the caudate are similar, the automated techniques seem to have excluded the boundary voxels at the head of the caudate (labelled as nucleus accumbens or surrounding white matter). In this study, bias was defined as the mean difference attained between manually traced volumes and volumes from the other techniques investigated. To further investigate the agreement and explore the extent of potential bias in the measurement of the volume of the subcortical structures by the techniques relative to the gold standard, we generated Bland-Altman plots (Bland and Altman, 1986, 1999). Contrary to the original assumptions for Bland-Altman plots, several recent studies (Schoemaker *et al.* 2016; Makowski *et al.* 2017), constructed the plots by computing the volumetric difference [$V(P_1) – V(P_2)$] relative to the manual and the other techniques for each structure per hemisphere against the corresponding manually traced volumes [$V(P_2)$] as proposed by Krouwer (2008). A regression line was further integrated to the plot for each technique to assess potential biases in the estimation of the volumes and to observe whether the definition of the structures studied influenced the discrepancy between the gold standard and the other techniques. Additionally, all the integrated regression lines were tested for significance to confirm the absence of zero slopes.

2.3 Results

2.3.1 Percentage spatial overlap between the manual and the other techniques

As shown in Table 2.1 and Fig. 2.1a, there was a statistical significant difference between spatial overlap of the various segmentation techniques relative to manual segmentation for all regions ($p<0.0001$) [right caudate $F(3,1039)=29.87$, left caudate $F(3, 1039)=33.47$; right hippocampus $F(3,1020)=555.49$ and left hippocampus $F(3,1020)=555.49$]. *Post-hoc* analysis further showed that the segmentation techniques were significantly different from each other ($p<0.0001$) in estimating the spatial locations of the left and right caudate except for comparisons between stereology and FSL-FIRST for the right ($p=0.99$) and left ($p=0.93$) caudate. The comparison between volBrain and FreeSurfer for the left caudate ($p=0.09$)

were statistically not different. All comparisons demonstrated significant differences ($p<0.0001$) from each other in estimating the spatial location of the hippocampus bilaterally.

2.3.2 Percentage volume difference between the manual and the other techniques

The volume estimates by each technique for the caudate and the hippocampus are presented in Table 2.1 and Fig. 2.1b. Compared to manual estimates, all techniques studied underestimated (-16 to -24%) volume of the right and left caudate. In contrast, compared to manual estimates, the volume of the hippocampus was comparable when segmented using stereology (-7 to 5%) and was substantially overestimated by 44-75% using automated and semi-automated approaches. These mean volumetric differences were statistically significant at 95% confidence interval at $p<0.0001$ for all regions [right caudate $F(4,1289)=168.92$; left caudate $F(4,1293)=138.05$; right hippocampus $F(4,1263)=1014.95$ and left hippocampus $F(4,1258)=843.10$]. *Post-hoc* comparisons demonstrated for the left and right caudate that the segmentation techniques were significantly different from each other in estimating volume ($p<0.0001$) except for comparisons between stereology and FSL-FIRST ($p=0.99$) and volBrain vs. FreeSurfer ($p=0.16$) for the right caudate. Similarly, for the left caudate, stereology vs. FSL-FIRST ($p=0.45$), stereology vs. volBrain ($p=0.08$) and volBrain vs. FreeSurfer ($p=0.09$) were not statistically different. All comparisons demonstrated significant differences from each other in estimating volumes of the hippocampus, with the least significant difference noted for comparisons between manual tracing and stereology for the left hippocampus ($p=0.02$).

2.3.3 Assessing consistency between the manual and the other techniques

Each of the four techniques were highly correlated (0.77 – 0.87) with manual segmentation for the caudate bilaterally, and moderately correlated (0.35 – 0.62) for the hippocampus (Table 2.1, Fig. 2.2, 2.3). Absolute between-technique agreement (ICC) relative to manual volume was generally fair (0.28 – 0.49) for the caudate. In contrast, hippocampal delineation by automated and semi-automated techniques gave poor (0.07 - 0.09) absolute agreement relative to manual segmentation, however, the stereologically acquired absolute hippocampal volumes agreed moderately (0.47 – 0.48).

The statistical comparison of the correlation coefficients of the global sample for each technique across the structures demonstrates that these are all not significantly different with the exception of FSL-FIRST vs. volBrain and FSL-FIRST vs. FreeSurfer for the caudate and

hippocampus bilaterally (Table 2.2). In contrast, the comparison between stereology and FSL-FIRST for the left hippocampus was statistically significant (Table 2.2).

Table 2.1: Comparison of relative and absolute volumes as derived from stereology, fully-automated and semi-automated techniques against manual tracing

Anatomy/Technique	**Structure Volume** (Mean mm^3 ± SD)	**Comparison of techniques to manual tracing**				**Diagnostic Groups** (*Partial Correlation)*	
		%Volume Difference ± SD	*%Volume Overlap± SD*	*Intraclass Correlation Coefficient (95% CI [Lower – Upper])*	*Partial Correlation **(n=281)** (r, p)*	*Healthy Controls **(n=104)** (r, p)*	*Patients **(n=177)** (r, p)*
Right Caudate							
ITK-SNAP	**4836±666**						
Stereology	3691±584	-24±6	81±4	0.30 [-0.03-0.67]	0.83, <0.0001	0.81, <0.0001	0.85, <0.0001
FSL-FIRST	3716±490	-23±7	81±5	0.28 [-0.05-0.64]	0.77, <0.0001	0.79, <0.0001	0.75, <0.0001
volBrain	3869±525	-20±6	83±6	0.37 [-0.05-0.73]	0.86, <0.0001	0.92, <0.0001	0.83, <0.0001
FreeSurfer	3978±590	-18±7	85±7	0.45 [-0.06-0.79]	0.85, <0.0001	0.89, <0.0001	0.83, <0.0001
Left Caudate							
ITK-SNAP	**4660±643**						
Stereology	3694±579	-21±6	83±4	0.36 [-0.04-0.73]	0.83, <0.0001	0.78, <0.0001	0.86, <0.0001
FSL-FIRST	3608±469	-23±7	82±5	0.30 [-0.05-0.65]	0.77, <0.0001	0.77, <0.0001	0.78, <0.0001
volBrain	3822±546	-20±6	85±5	0.45 [-0.05-0.79]	0.87, <0.0001	0.92, <0.0001	0.87, <0.0001
FreeSurfer	3920±582	-16±6	86±6	0.49 [-0.07-0.81]	0.85, <0.0001	0.87, <0.0001	0.85, <0.0001
Right Hippocampus							
ITK-SNAP	**2545±533**						
Stereology	2366±366	-7±18	93±7	0.49 [0.37-0.59]	0.52, <0.0001	0.38, <0.0001	0.56, <0.0001
FSL-FIRST	3732±445	47±30	68±13	0.10 [-0.06-0.30]	0.42, <0.0001	0.45, <0.0001	0.40, <0.0001
volBrain	4019±471	58±29	63±11	0.10 [-0.04-0.33]	0.61, <0.0001	0.52, <0.0001	0.67, <0.0001
FreeSurfer	4454±445	75±30	57±9	0.08 [-0.02-0.29]	0.62, <0.0001	0.56, <0.0001	0.63, <0.0001
Left Hippocampus							
ITK-SNAP	**2526±515**						
Stereology	2654±342	5±19	95±10	0.47 [0.30-0.60]	0.55, <0.0001	0.31, <0.001	0.61, <0.0001
FSL-FIRST	3649±432	44±31	69±13	0.08 [-0.06-0.26]	0.35, <0.0001	0.25, <0.0001	0.38, <0.0001
volBrain	3954±469	57±29	64±11	0.09 [-0.04-0.32]	0.60, <0.0001	0.40, <0.0001	0.69, <0.0001
FreeSurfer	4406±451	74±30	57±9	0.07 [-0.02-0.25]	0.56, <0.0001	0.38, <0.0001	0.61, <0.0001

Table 2.1 Legend: All volumes compared are in native space. For the partial correlation, age and gender were used as the co-variate. The reliability based on absolute agreement (ICC) unlike Pearson's (partial) correlation coefficient, is always lower because a more stringent criterion which depends on variability in repetition is applied as shown in equation 3.

Fig. 2.1a: Percentage volume overlap and standard deviations showing differences in estimating the spatial locations between techniques across structures

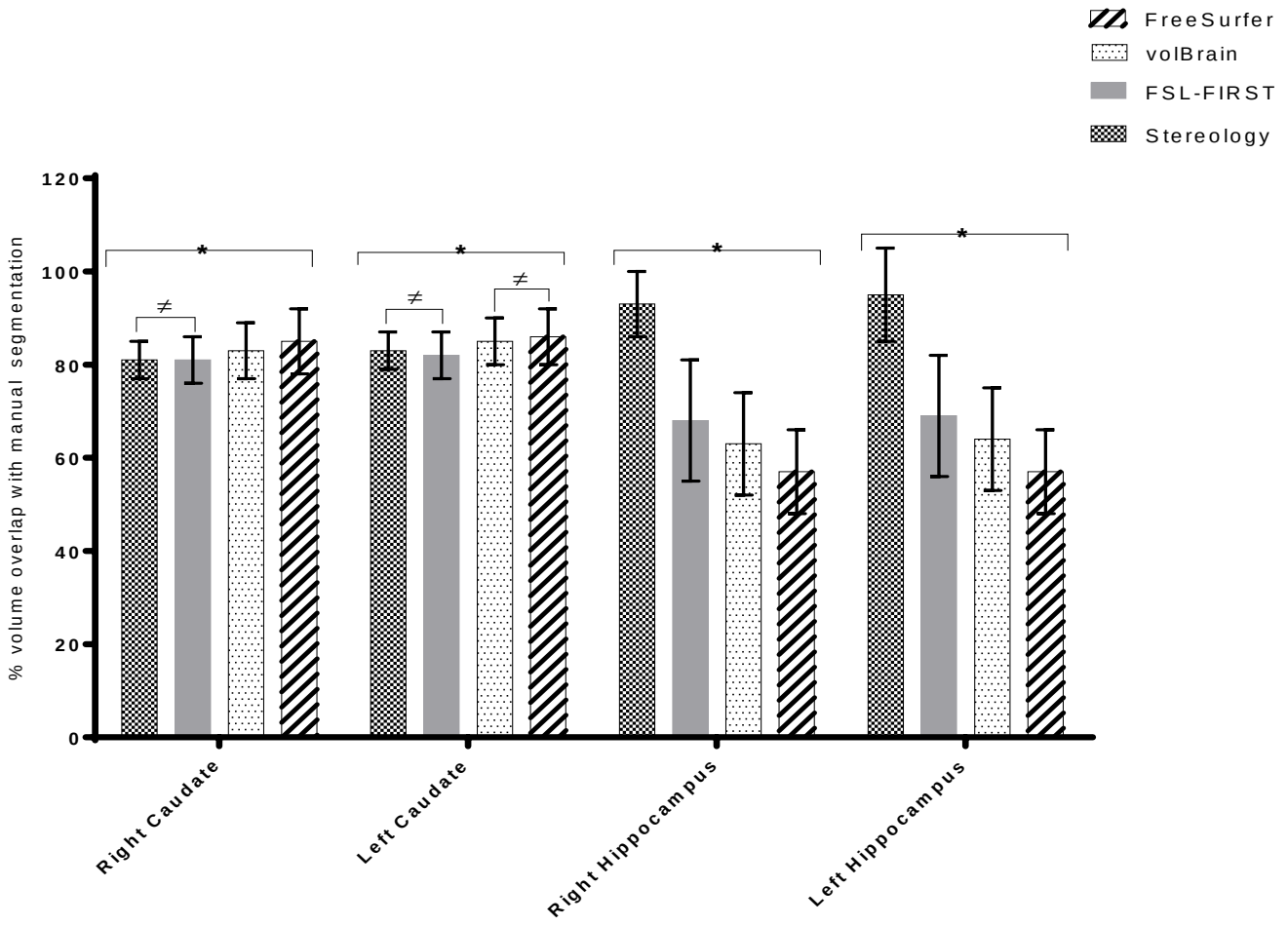

Fig. 2.1a Legend: Significant differences (*) were observed among the techniques relative to manual tracing across each structure. Tukey's post-hoc analysis revealed significant differences for all comparisons except for those marked by (≠)

Fig. 2.1b: Mean volumes and standard deviations showing volume differences between techniques across structures

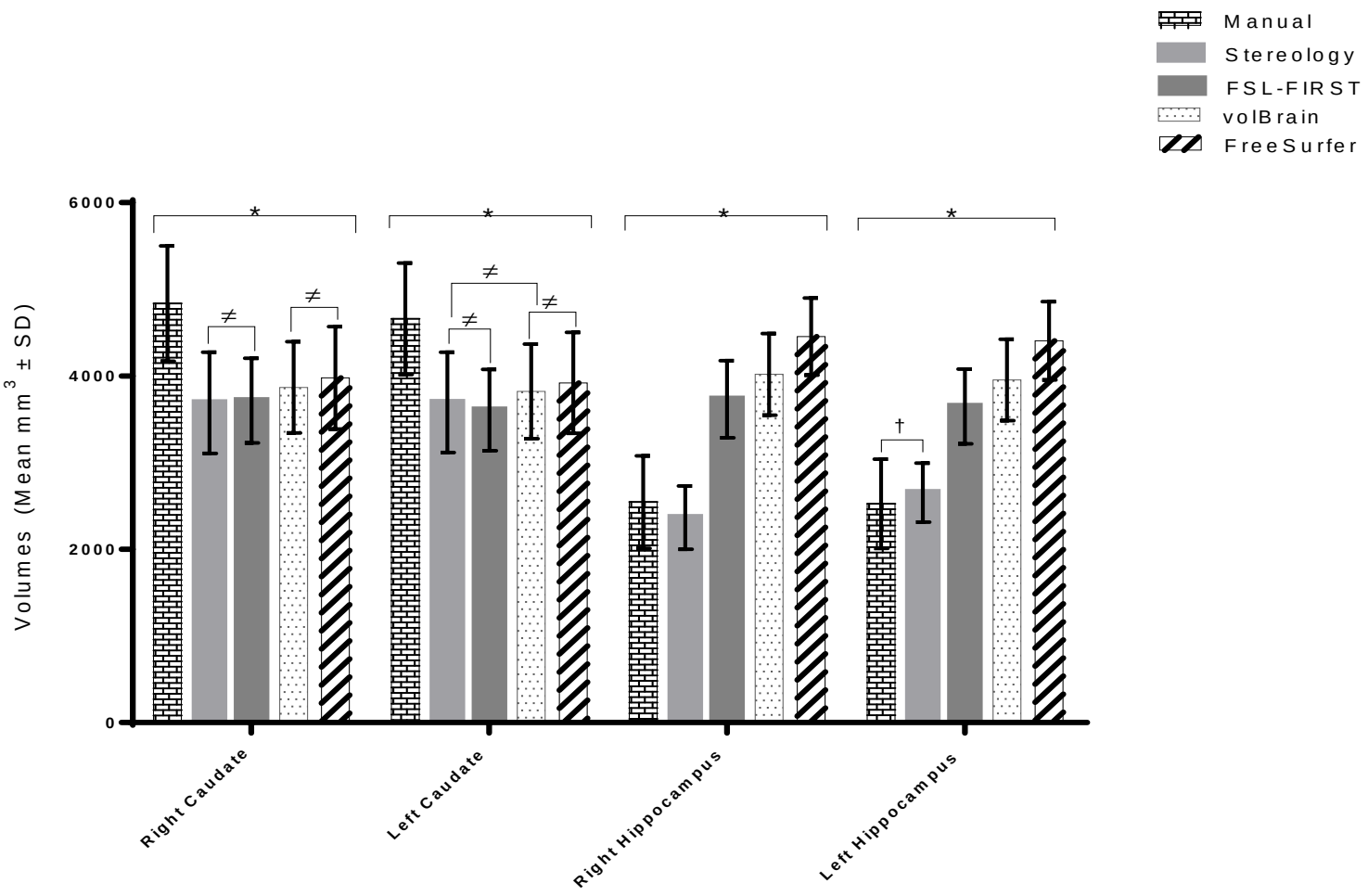

Fig. 2.1b Legend: Significant differences (*) were observed among the techniques across each structure. Tukey's post-hoc analysis revealed significant differences for all comparisons except for those marked (≠) and least significance noted (†)

Table 2.2: Comparison of segmentation techniques (correlations coefficients) within the global sample

	Right Caudate *(z, p)*	Left Caudate *(z, p)*	Right Hippocampus *(z, p)*	Left Hippocampus *(z, p)*
Stereology vs FSL-FIRST	1.75, 8.01×10^{-2}	1.77, 7.67×10^{-2}	1.31, 1.90×10^{-1}	2.57, 1.02×10^{-2}
Stereology vs volBrain	1.14, 2.54×10^{-1}	1.59, 1.12×10^{-1}	1.40, 1.62×10^{-1}	0.79, 4.30×10^{-1}
Stereology vs FreeSurfer	0.74, 4.59×10^{-1}	0.74, 4.59×10^{-1}	1.57, 1.16×10^{-1}	0.15, 8.81×10^{-1}
FSL-FIRST vs volBrain	2.89, 3.85×10^{-3}	3.35, 8.08×10^{-4}	2.73, 6.33×10^{-3}	3.42, 6.26×10^{-4}
FSL-FIRST vs FreeSurfer	2.50, 1.24×10^{-2}	2.52, 1.17×10^{-2}	2.90, 3.73×10^{-3}	2.78, 5.44×10^{-3}
FreeSurfer vs volBrain	0.41, 6.82×10^{-1}	0.85, 3.95×10^{-1}	0.18, 8.57×10^{-1}	0.65, 5.16×10^{-1}

Table 2.2 Legend: Fisher's r-to-z transformation was used to compare the partial correlation coefficients between techniques relative to manual

Fig. 2.2a: Scatterplots demonstrating values as assessed by manual segmentation in comparison to stereology and FSL-FIRST to assess consistency in the volume segmentation of the right caudate and hippocampus

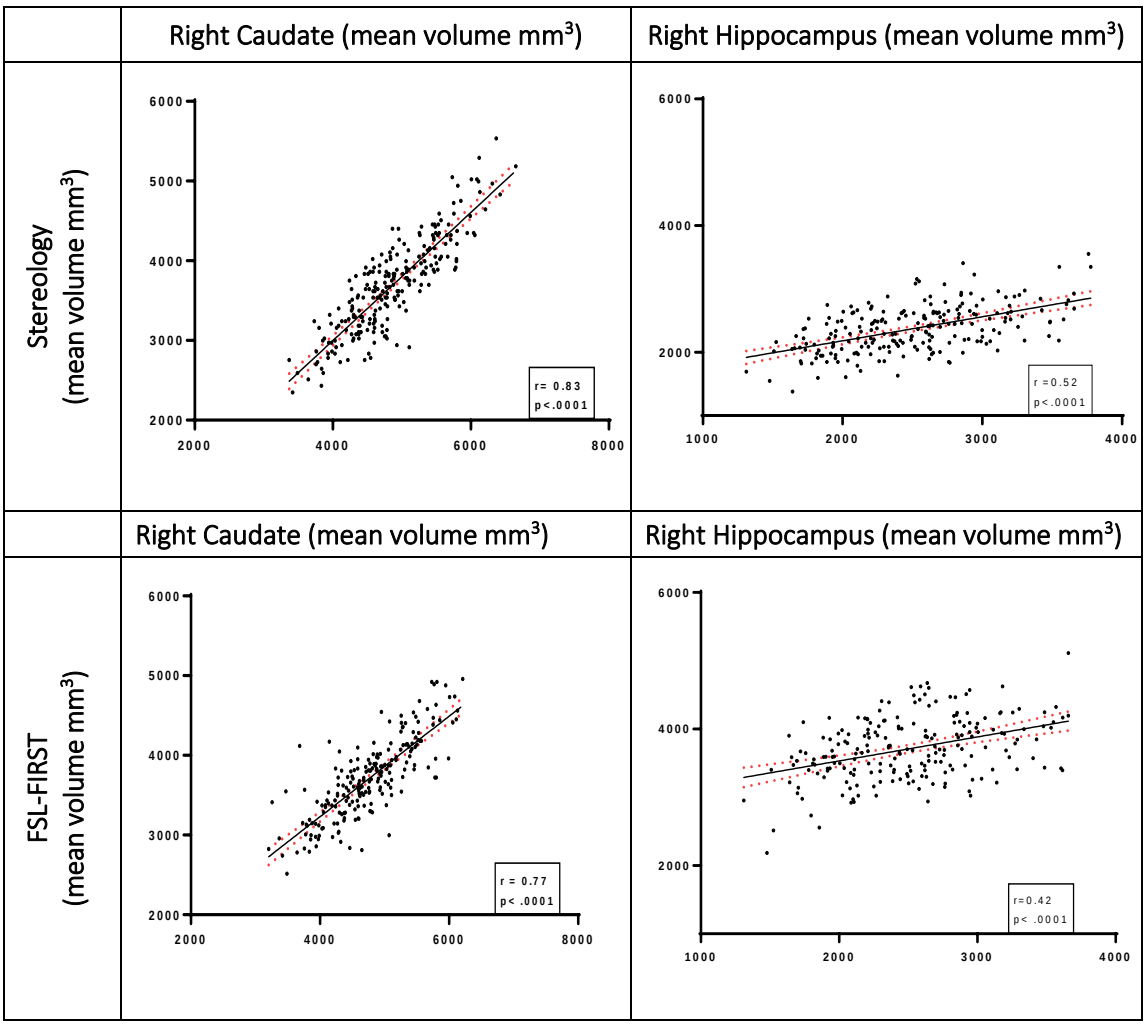

Fig. 2.2a Legend: The statistical values corresponding to the above correlations are presented in Table 1.

Fig. 2.2b: Scatterplots demonstrating values as assessed by manual segmentation in comparison to volBrain and FreeSurfer to assess consistency in the volume segmentation of the right caudate and hippocampus

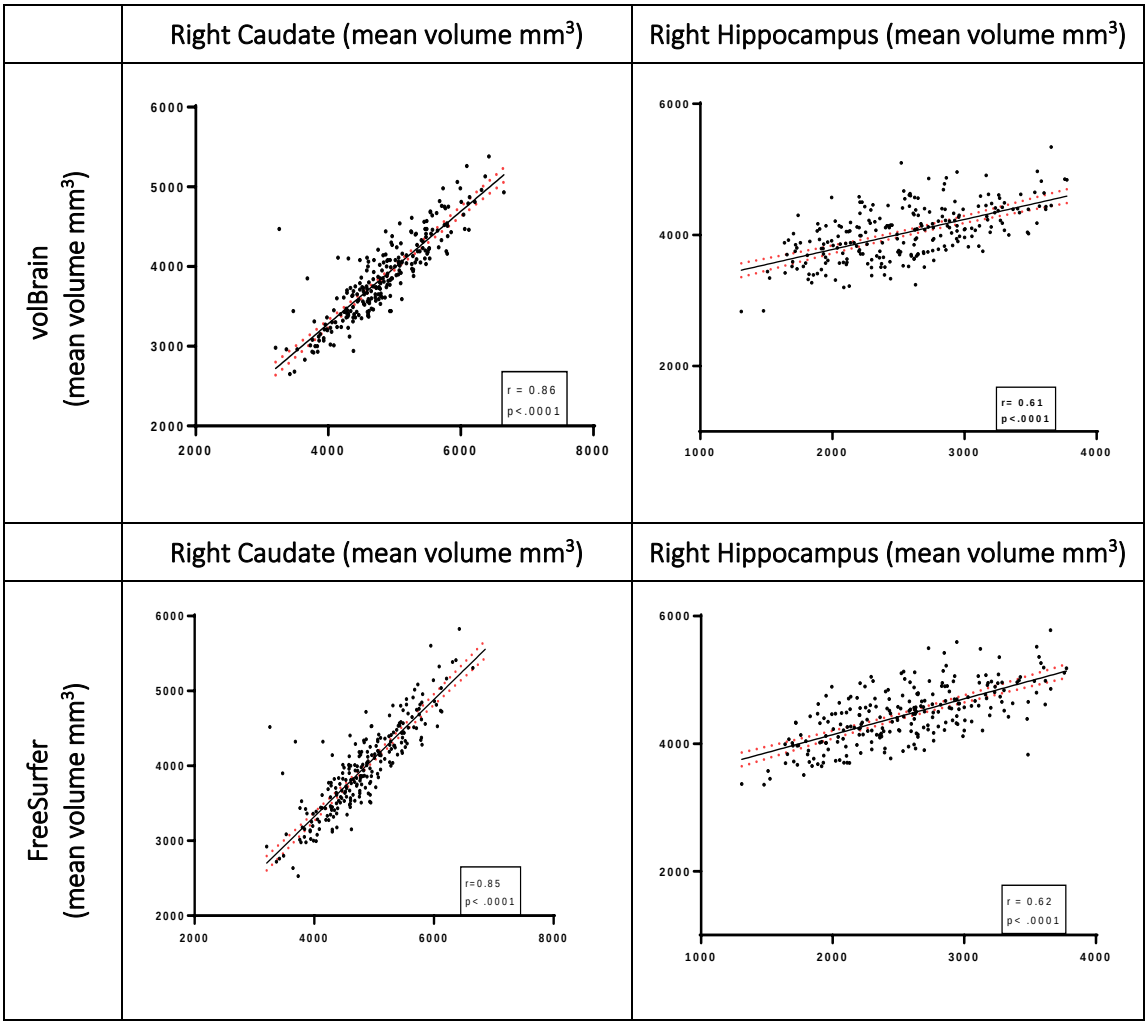

Fig. 2.2b Legend: The statistical values corresponding to the above correlations are presented in Table 1.

Fig. 2.3a: Scatterplots demonstrating values as assessed by manual segmentation in comparison to stereology and FSL-FIRST to assess consistency in the volume segmentation of the left caudate and hippocampus

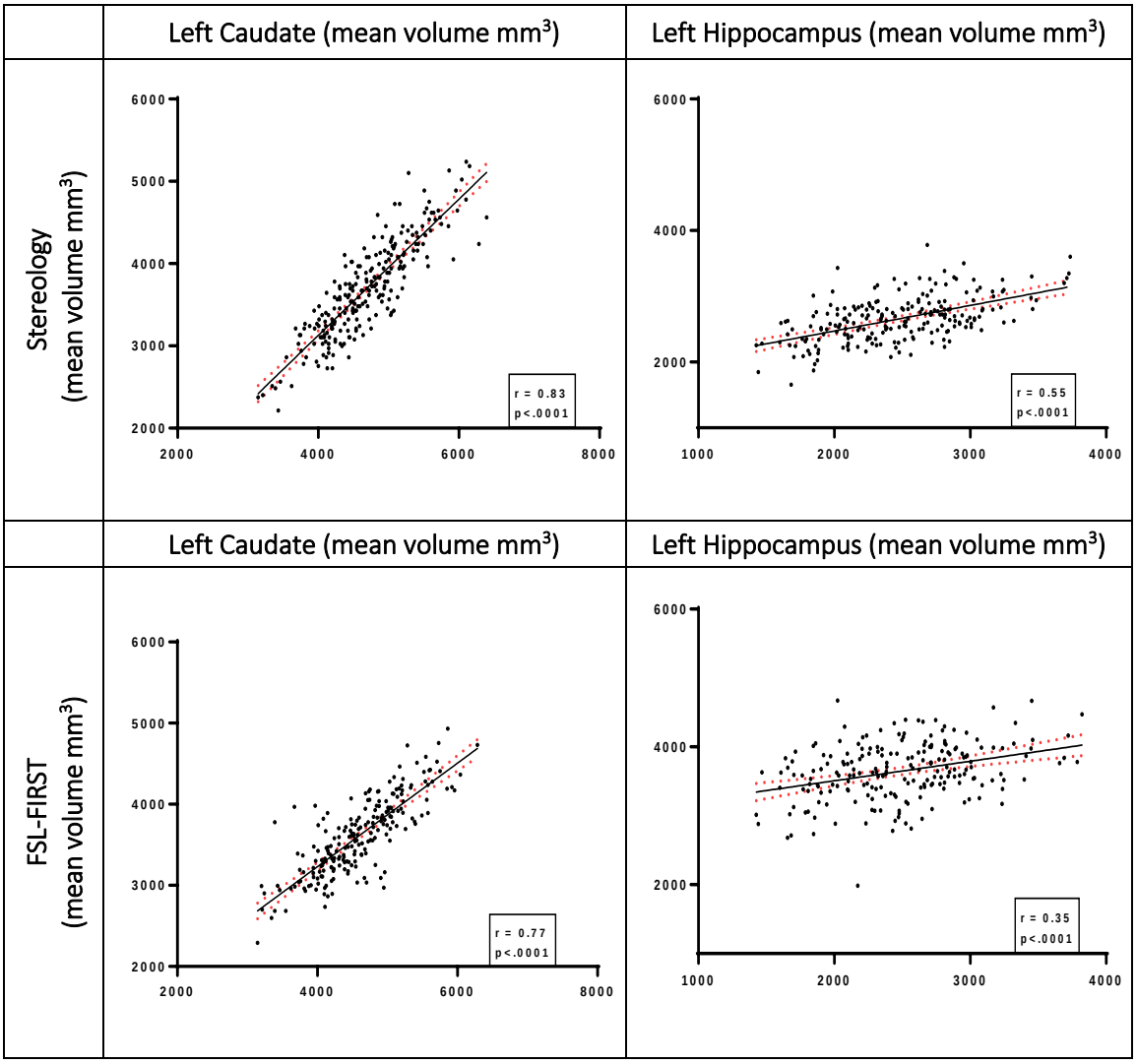

Fig. 2.3a Legend: The statistical values corresponding to the above correlations are presented in Table 1.

Fig. 2.3b: Scatterplots demonstrating values as assessed by manual segmentation in comparison to volBrain and FreeSurfer to assess consistency in the volume segmentation of the left caudate and hippocampus

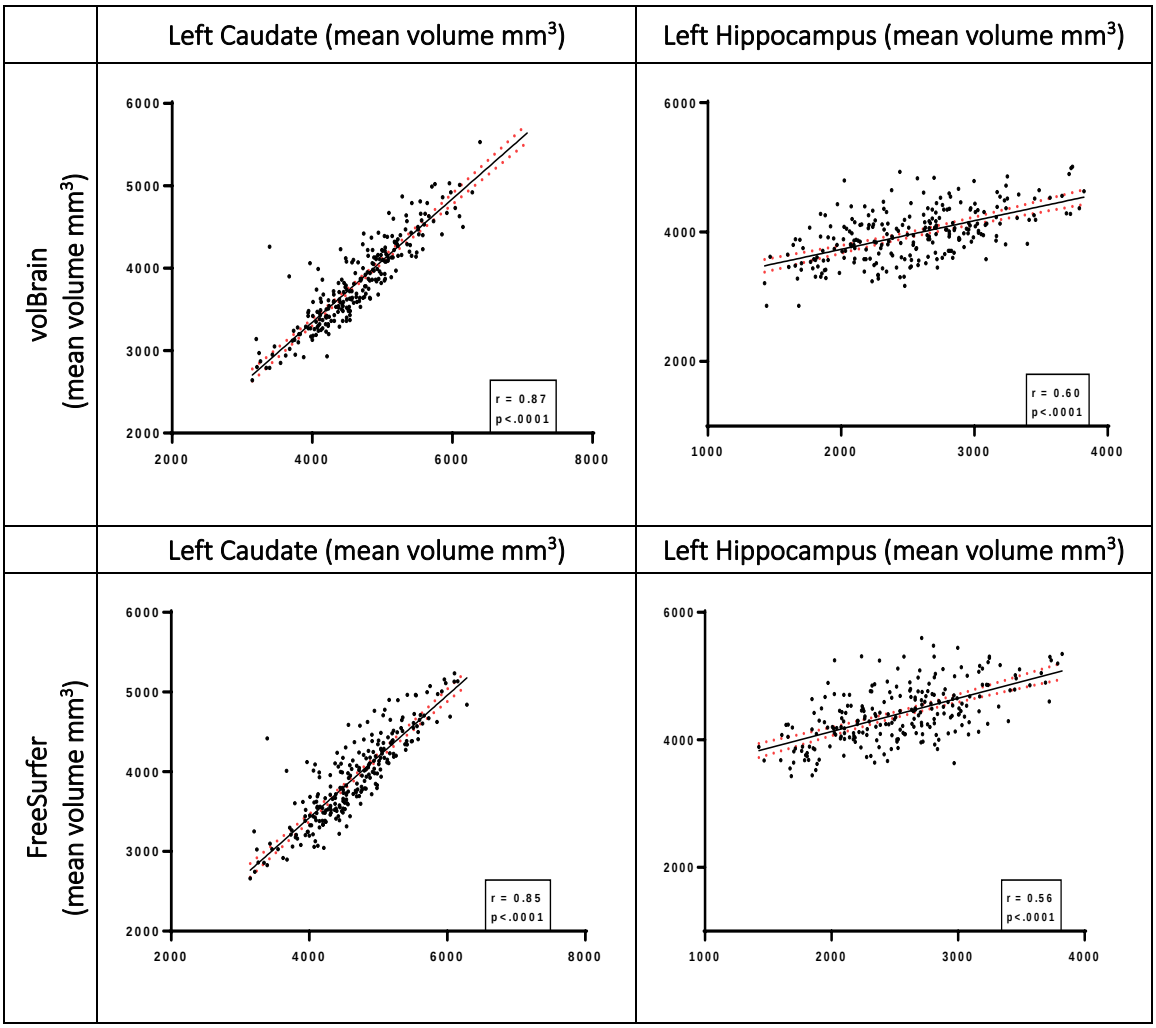

Fig. 2.3b Legend: The statistical values corresponding to the above correlations are presented in Table 1.

2.3.4 Comparing correlations between the cohort groups

The correlations obtained relative to the manual segmentation technique between patients and the healthy controls were compared between corresponding techniques to further assess consistency within the groups. The consistency of all the segmentation techniques within the groups were significantly not different from each other at estimating volumes except for stereology [left hippocampus (p=0.008)], volBrain [right caudate (p=0.003), left caudate (p=0.005) and the left hippocampus (p=0.002) and FreeSurfer [left hippocampus (p=0.025)] as shown in Table 2.3.

Table 2.3: Comparison of segmentation techniques (correlations coefficients) within patients and healthy controls relative to manual segmentation

	Right Caudate *(z, p)*	Left Caudate *(z, p)*	Right Hippocampus *(z, p)*	Left Hippocampus *(z, p)*
Stereology	0.93,3.52x10^{-1}	1.80,7.16x10^{-2}	1.59,1.12x10^{-1}	2.65,7.94x10^{-3}
FSL-FIRST	0.68,4.96x10^{-1}	0.18,8.61x10^{-1}	0.42,6.78x10^{-1}	0.99,3.25x10^{-1}
volBrain	2.98,2.90x10^{-3}	1.93,5.41x10^{-3}	1.72,8.47x10^{-2}	3.12,1.80x10^{-3}
FreeSurfer	1.74,8.13x10^{-2}	0.57,5.65x10^{-1}	0.80,4.25x10^{-1}	2.25,2.47x10^{-2}

Table 2.3 Legend: Fisher's r-to-z transformation was used to compare the partial correlation coefficients between patients and controls across the techniques

2.3.5 Analysis of potential technique biases: Bland – Altman plots

The volumetric bias estimations for the caudate and hippocampus were examined separately for each hemisphere. Compared to manual estimates, a relatively small bias range estimate was noted for the right (-1171.78 to -860.55) and left (-990.69 to -727.17) caudate. In contrast, a large bias range estimate was demonstrated for the right and left hippocampus; (-124.45 to 1902.38) and (187.56 to 1877.69) respectively. The regression analysis revealed a trend of significant negative bias in all the techniques across both structures within each hemisphere (Fig. 2.4, 2.5 and Table 2.4).

2.3.6 Consideration of Labour

Manual segmentation was the most resource intensive of the techniques requiring 40 minutes per caudate and 60 minutes per hippocampus respectively for accurate bilateral segmentation. Stereological segmentation required approximately 50% of this time for each structure. FSL-FIRST required approximately 30% of the time of manual segmentation to segment the brain into 15 structures inclusive of both the caudate and hippocampus bilaterally. Furthermore, volBrain required approximately 15% of the time of manual segmentation to segment all the subcortical structures in addition to the ventricles, regional macroscopic structures (hemispheres, cerebellum and brainstem) and volume of intracranial tissues (CSF, GM, WM). Finally, FreeSurfer required approximately 700% of the time of manual segmentation (12 hours) to segment the brain into 40 subcortical regions (including both the caudate and hippocampus) and other global brain measures such as intracranial volume. In addition, several output measures of FreeSurfer cortical reconstruction are generated during this time. FSL-FIRST and volBrain required no amount of manual intervention, however, FreeSurfer required 15 minutes per participant (including both the caudate and hippocampus) to undertake a thorough quality check of the outputs as per the standardised ENIGMA protocols, with an additional 30 minutes per participant required if they failed the skull strip test. Processing was entirely carried out on our system configuration: Intel(R) Xeon(R) CPU E5-2697 v3, 128GB @ 2.60GHz.

Fig. 2.4a: Right Caudate Bland - Altman plots for bias estimation between manual segmentation and A: Stereology, B: FSL, C: volBrain and D: FreeSurfer

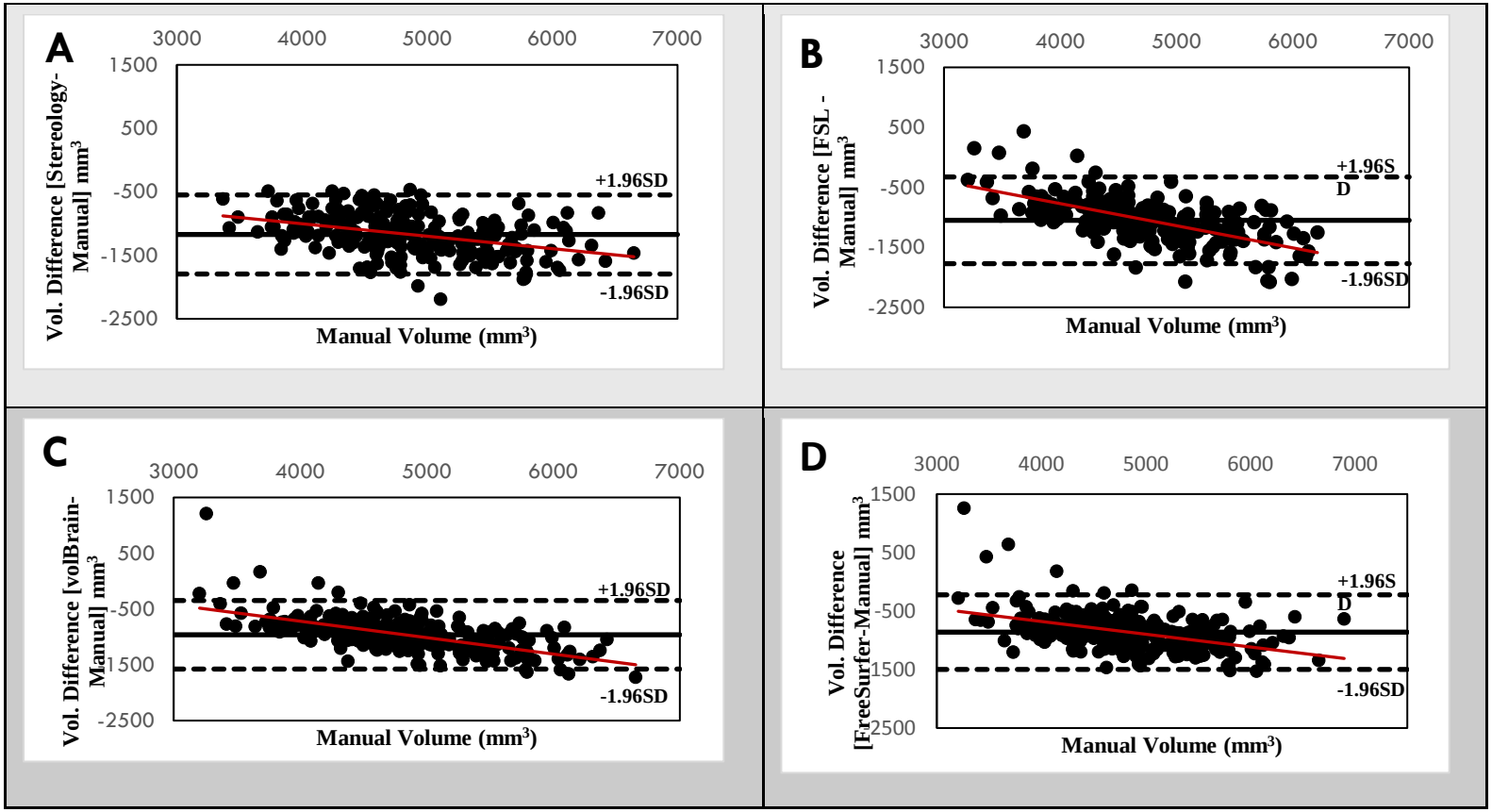

Fig. 2.4a Legend: The red regression lines were fit to show potential bias in volume estimation, the mean is represented with the continuous line while the lower (-1.96 x standard deviation) and upper limits (+1.96 x standard deviation) of agreement are represented with broken lines.

Fig. 2.4b: Left Caudate Bland - Altman plots for bias estimation between manual segmentation and A: Stereology, B: FSL, C: volBrain and D: FreeSurfer

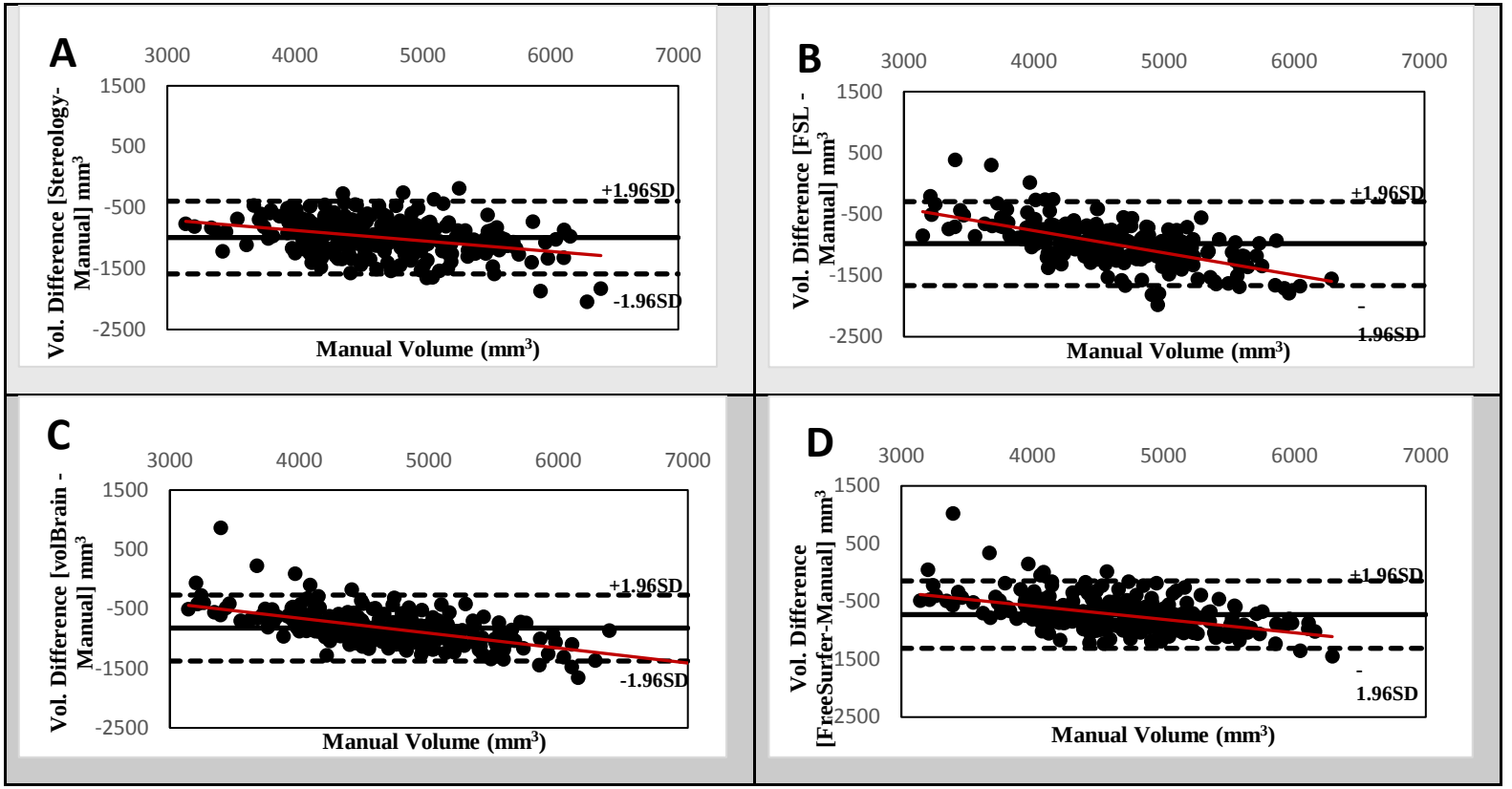

Fig. 2.4b Legend: The red regression lines were fit to show potential bias in volume estimation, the mean is represented with the continuous line while the lower (-1.96 x standard deviation) and upper limits (+1.96 x standard deviation) of agreement are represented with broken lines.

Fig. 2.5a: Rt Hippocampus Bland-Altman plots for bias estimation between manual segmentation and A: Stereology, B: FSL, C: volBrain, D: FreeSurfer

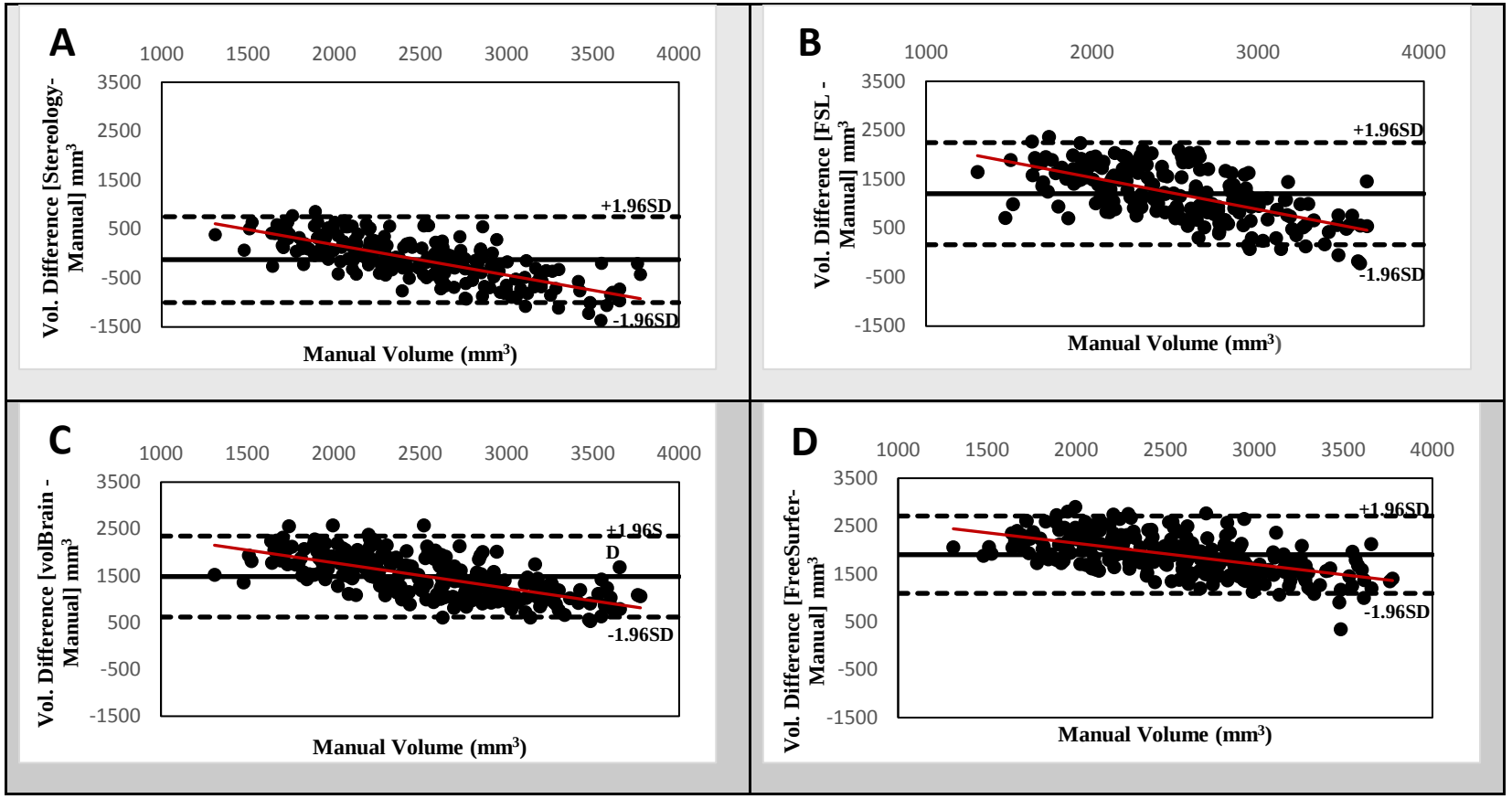

Fig. 2.5a Legend: The red regression lines were fit to show potential bias in volume estimation, the mean is represented with the continuous line while the lower (-1.96 x standard deviation) and upper limits (+1.96 x standard deviation) of agreement are represented with broken lines.

Fig. 2.5b: Lt Hippocampus Bland-Altman plots for bias estimation between manual segmentation and A: Stereology, B: FSL, C: volBrain D: FreeSurfer

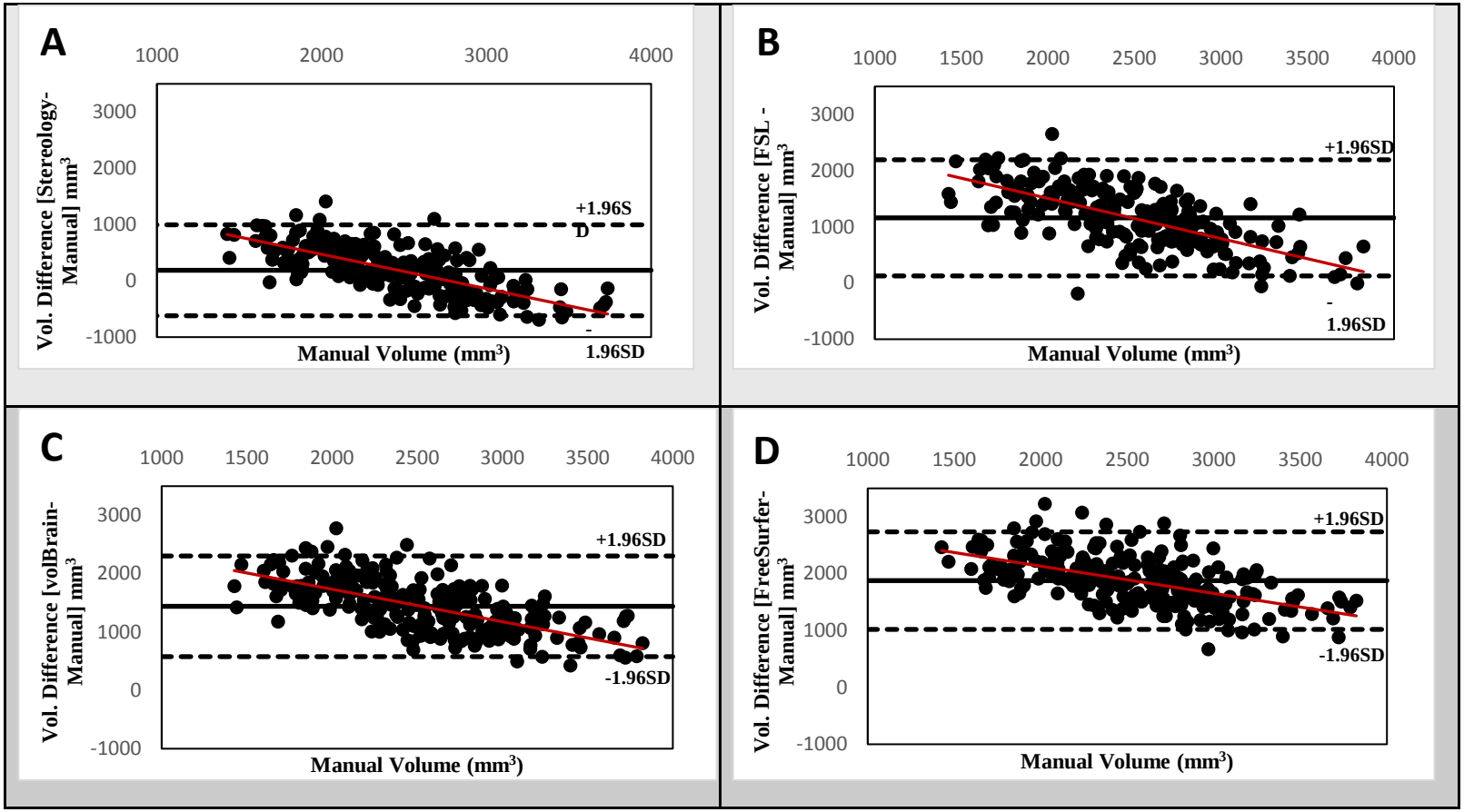

Fig. 2.5b Legend: The red regression lines were fit to show potential bias in volume estimation, the mean is represented with the continuous line while the lower (-1.96 x standard deviation) and upper limits (+1.96 x standard deviation) of agreement are represented with broken lines.

Table 2.4: Quantitative bias estimation and regression analysis of techniques across structures

Anatomy/Structure	Estimation of Bias		Regression Analysis	
	Bias (mm^3)	SD	r	p
Right Caudate				
Stereology	-1171.78	317.64	-0.39	<0.0001
FSL-FIRST	-1049.23	368.57	-0.62	<0.0001
volBrain	-961.81	313.36	-0.62	<0.0001
FreeSurfer	-860.55	325.29	-0.45	<0.0001
Left Caudate				
Stereology	-990.69	304.63	-0.35	<0.0001
FSL-FIRST	-980.41	349.56	-0.62	<0.0001
volBrain	-821.20	282.98	-0.57	<0.0001
FreeSurfer	-727.17	297.46	-0.48	<0.0001
Right Hippocampus				
Stereology	-124.45	447.46	-0.72	<0.0001
FSL-FIRST	1204.37	531.99	-0.62	<0.0001
volBrain	1482.54	440.99	-0.66	<0.0001
FreeSurfer	1902.38	412.09	-0.57	<0.0001
Left Hippocampus				
Stereology	187.56	412.22	-0.72	<0.0001
FSL-FIRST	1160.71	527.54	-0.67	<0.0001
volBrain	1440.31	440.07	-0.65	<0.0001
FreeSurfer	1877.69	437.74	-0.57	<0.0001

Table 2.4 Legend: Bias - the mean difference between the manually traced and the volumes from the other techniques. Pearson's Correlation (r) was computed between the mean differences and their corresponding manual volumes

Table 2.5: Advantages and disadvantages of the techniques at segmenting subcortical structures

Technique	Advantages	Disadvantages
ITK-SNAP	• Provides reliable estimates of brain regions/structures. • Flexibility at defining anatomical boundaries prior to segmentation. • Produces segmentation masks for other brain imaging analysis. E.g. these can be co-registered unto fractional anisotropy/mean diffusivity maps for DTI analysis.	• Require investigator expertise of anatomy. • Thorough training required before analysis using intra and inter-rater studies. • High time consumption • High labour intensity • Limited morphometric measures e.g. volume.
Stereology	• Low bias and time efficient means of estimating brain volumes. • Permits the prediction of coefficient of error which provides information to infer the precision of the volumetric extraction. • Permits assessment of regional profiles of structures by virtue of the individual sectioning along slides. • Flexibility at defining anatomical boundaries prior to segmentation.	• Require investigator expertise of anatomy. • Manual intervention required for point counting of the voxels. • Pilot is usually essential to define an exact sampling design to optimise workload for a particular project. • Precision prediction is complex due to the spatial dependence of the observations. • Limited morphometric measures e.g. volume. • Cannot perform shape analysis to investigate localised shape differences. • Does not provide segmentation masks for other brain analysis tasks.
FSL-FIRST	• No need for anatomical expertise. • Freely available for download. • Relatively fast and time efficient (~25mins). • Allows vertex/shape [mesh (vtk)] analysis of subcortical structures to investigate localised shape differences from segmentation masks. • Statistical maps and analysis e.g. multiple comparison correction and other design matrices. • FSLView–visualisation and data management tool	• Relatively fewer segmented output of the brain regions. • Limited options to manually/automatically fix improperly segmented structures. • Output maps/files are in native anatomical space only. • No flexibility at defining subcortical boundaries.
volBrain	• Faster and time efficient (5-12mins) • Freely available for online use without requiring a local computer for installation of software. • Produces subcortical segmentation masks/maps in both MNI and native anatomical space. • Automatic asymmetric indices output. • Provides additional neuroanatomical information such as regional macroscopic (hemisphere, cerebellum and brainstem) and intracranial tissue (CSF, WM, GM) volumes. • Relatively lower segmentation failure rate (0.4%) recorded from this study.	• Limited number (n=10) of cases to be processed daily per user. • Cannot perform statistical analysis. • Need other visualisation tools e.g. ITK-SNAP to visualise output data. • Cannot perform shape analysis to investigate localised shape differences. • No flexibility at defining subcortical boundaries. • Minimal anatomical descriptions available defining boundaries employed except the hippocampus (EADC-ADNI Harmonised protocol).
FreeSurfer	• Multiple measures: (volume, area, thickness etc.) of both cortical and subcortical structures. • Frequent software maintenance (upgrades), information and support via a dedicated wikipage plus a quick email response support system. • Freely available for download. • Statistical maps and analysis e.g. cohort comparisons between brains/hemispheres. • Freeview and QDEC-visualisation, analysis and data management tools. • Reconstructed information of cortical surfaces can be obtained based on the segmentation of GM and WM. • Subject-specific parcellation algorithm. • In the field of brain network analyses, it can be used to define brain structures (i.e. nodes) to increase the anatomical sensitivity of findings compared to anatomical templates. It values inter-subject anatomical variability by producing cortico-subcortical measures that are in the individual's own coordinate space, and therefore subject-specific.	• Relatively longer processing time. • High computational power requirement. • Output maps/files are in native anatomical space. • Needs additional toolboxes e.g. LDDMM to perform vertex analysis [as previously described on the semi-automated shape analysis (SASHA) project] and ENIGMA-Shape Pipeline (ENIGMA Shape Analysis).

2.4 Discussion

The objective of this study was to compare the performance of stereological (Measure®), fully automated [model-based (FSL-FIRST v.5.0.4) and patch-based (volBrain v.1.0)] and semi–automated (FreeSurfer v.5.1) segmentation techniques to the current gold-standard method: manual segmentation (ITK-SNAP v.1.8) using representative brain structures, the caudate (*easy-to-segment)* and hippocampus (*difficult-to-segment*). The findings from this study demonstrate that automated techniques are fairly reliable in delineating the volumes of an *easy-to-segment* structure such as caudate in a relatively large cohort. Furthermore, we demonstrate that stereology shows high reliability in measuring both *easy*- and *difficult-to-segment* structures. Additionally, we found stereology to have a notably reduced labour intensity relative to manual segmentation whilst preserving the anatomical accuracy; a considerable merit of the manual approach. We further demonstrated, that volBrain was the preferred (Table 2.5) technique for segmentation of the caudate as it was least labour intensive and was fairly accurate anatomically. The extent to which each of these techniques rival the anatomical accuracy and efficiency of manual segmentation varies between caudate and hippocampus as detailed below. Taken together, our findings should help to inform other researchers about the considerable advantages and caveats (Table 2.5) of using each of these segmentation techniques in decision making for the now standard, large-scale brain morphometric studies ongoing in the field of neuropsychiatry.

Hippocampal volume estimates were anatomically accurate demonstrating an almost perfect spatial overlap (93 to 95%) and only slightly under/overestimated (-7 to 5%) using stereology relative to manual segmentation. Previous studies (Gundersen *et al.* 1988; Yuen *et al.* 2001; García-Fiñana *et al.* 2003) and the Measure® user guide indicated this volumetric difference to be acceptable especially in structures where greater variation is evident in the normal population. Furthermore, stereology demonstrated the highest observed absolute agreement (0.47-0.49) for estimation of the hippocampus. The hippocampus was significantly overestimated (44-75%) by the automated methods employed with spatial overlap of 57-69% recorded. Thus, the high volume overlaps obtained with stereology when segmenting the hippocampus resulted from the slight under/overestimation in volume. Furthermore, the relatively low MRI contrast at the voxel level within the region of the hippocampus, has potentially contibuted to a large methodological variance when segmenting a single participant resulting in a low partial correlation (consistency) with the manually segmented volumes. Of note, the poor voxel-to-voxel correspondence across the automated techniques that were tested in this study against manual segmentation and the variable

neuroanatomical protocols used to define our structures of interest have potentially contributed to a high percentage volume overlap, overestimation and low correlations with manual segmentation. The substantial overestimation of hippocampal volume observed is however, consistent with previous studies comparing both automated techniques to manual segmentation in adult (Doring *et al.* 2011; Cherbuin *et al.* 2009; Tae *et al.* 2008) and preadolescent (Schoemaker *et al.* 2016) populations. The trend of overestimation and poor reliability is however not peculiar to preadolescent populations but is similarly noted in adult populations, as previously reported. This study reported higher hippocampal volumes using the automated techniques [FreeSurfer (74-75%), volBrain (57-58%) and FSL-FIRST (44-47%)], partially as a result of a strict neuroanatomical definition of the structural boundaries for manual segmentation (Fig.2.6a). In particular, the alveus and fimbria were excluded, contrary to what was adopted by Schoemaker and colleagues demonstrating 28% (FSL-FIRST) and 60% (FreeSurfer) overestimations. Inclusion of these regions, together with anatomically mis-assigned surrounding grey and WM voxels (especially at the hippocampal head in some slices) and variance in the inclusion of the Andreas-Retzius and the Fasciolar gyrus from the tail region of the hippocampus across studies appear to account for the vast majority of the overestimation of volume that is evident when using the fully automated techniques. We noted (Fig.2.7) the greatest amount of voxel misclassification using FreeSurfer, however application of manual interventions (skullstrip/control-point corrections) would likely significantly improve the quality of segmentation minimising these volume estimation errors (McCarthy *et al.* 2015).

Similarly, the even greater overestimation observed using semi-automated segmentation appears to be explained by the above factors with an added variable amount of parahippocampal and subicular/entorhinal cortices included in hippocampal volume estimation. The subiculum alone is reported to account for over 15% of the hippocampal volume when traced on an MRI (Geuze *et al.* 2005) thus its boundary definition will have a substantial effect on hippocampal volume estimation by all approaches and should be assessed carefully as a representative complex region in further development of automated methods. The lack of absolute agreement in volume estimation, although relevant anatomically may not always be essential in large scale neuropsychiatric research studies given the reasonable correlations with manual segmentation noted, which may suffice to detect case-control differences or disease progression markers.

In contrast, our representative *easy-to-segment* structure, the caudate was underestimated by all techniques (16-24%), however, a high (81-83%) spatial overlap was observed. The

relatively uniform shape and strong contrast of the caudate from surrounding WM on MRI, allows its volume to be more susceptible to prior approximation by the rater using stereology. Volumetric estimation with stereology, however, is designed to be unbiased - without shape and volume assumptions of the structure under investigation (García-Fiñana *et al.* 2003). The almost explicit prior information of the caudate (Fig.2.6b) is suspected to have contributed to rater/methodological bias, hence the large discrepancy (21-24%) in the estimation of the volume of the caudate with stereology. The observed total variance (OCV^2) in stereological estimation comprise of variance due to biological variability (CV^2) and methodologically introduced variance (OCE^2) (García-Fiñana *et al.* 2003).

$$OCV^2 = CV^2 + OCE^2 \quad \textit{eqn (4)}$$

Given the relatively low biological variance of the caudate, differences in volume estimation using stereology compared to manual segmentation may relate to methodological or rater bias. In contrast to the hippocampus, the relatively low MRI contrast and the more indistinct border (Fig.2.6a) has reduced its susceptibility to rater bias (Table 2.4). Our findings (-16 to -24%) of underestimation of the caudate is consistent and closely correspond in magnitude with previous studies utilising a semi- automated [-19.4% (Nazir *et al.* 2014)] and fully-automated [-32.7 to 14.0% (Amann *et al.* 2015)] techniques; with volume underestimation here likely related to the exclusion of boundary voxels of the head of the caudate (labelled as nucleus accumbens or surrounding white matter) (Fig.2.6b).

However, the correlation with manual segmentation was high for these techniques (r=0.77-0.87) as previously reported (Perlaki *et al.* 2017), although absolute agreement was relatively poor. Reasons for modest absolute agreement may be explained by neuroanatomical boundary definition differences derived from the different software's employed, with varied sensitivity of tissue voxel classification algorithms (MRF, OPAL, Bayesian) potentially accounting for some of the observed variance.

Despite the underestimation of the caudate by FreeSurfer, it demonstrated a superior (0.45-0.49) absolute agreement relative to FIRST (0.28-0.30) and volBrain (0.37-0.45). This may potentially relate to the robustness of FreeSurfer's segmentation pipeline adopted to assign unique labels to voxels for the spatial localisation of subcortical structures within a defined space based on MRF (Fischl *et al.* 2002). Furthermore, consistency of segmentation derived from volumes across a large sample will influence the sensitivity of the study to detect subtle differences between populations under study, and thus a consistent over/under-estimation

with the segmentation techniques does not necessarily indicate a lack of validity (Schoemaker *et al.* 2016).

To assess the reliability of each technique in terms of consistency of segmentation in the full sample, we calculated correlations between volumes derived from the techniques and manual segmentation volumes for both structures. Despite the under/overestimation of the volumes of the structures of interest relative to manual segmentation, the consistency of the techniques were relatively high for the caudate (0.77-0.87), and fair (FSL-FIRST: 0.35-0.42) or moderate (Stereology: 0.52-0.55, volBrain: 0.60-0.61, FreeSurfer: 0.56-0.62) for the hippocampus. Our findings extend previous works which assessed the operational consistency of automated techniques based on the correlation of volumes derived from automated and manual techniques in which a strong positive correlation indicated optimal consistency (Schoemaker *et al. 2016*; Makowski *et al.* 2017) otherwise, poor consistency or operational errors are assumed (Allen *et al.* 2002) regardless of the absolute volume differences observed across approaches. Our findings of relatively low consistency of FSL-FIRST for hippocampal segmentation are consistent with previous studies (Morey *et al.* 2009; Schoemaker *et al.* 2016). The lower consistency of FSL-FIRST for hippocampal volume estimation may be attributable at least in part to differences in the sensitivity of operational algorithms at classifying voxels.

Fig. 2.6a: Comparison of the segmented output (right hippocampus) from the techniques

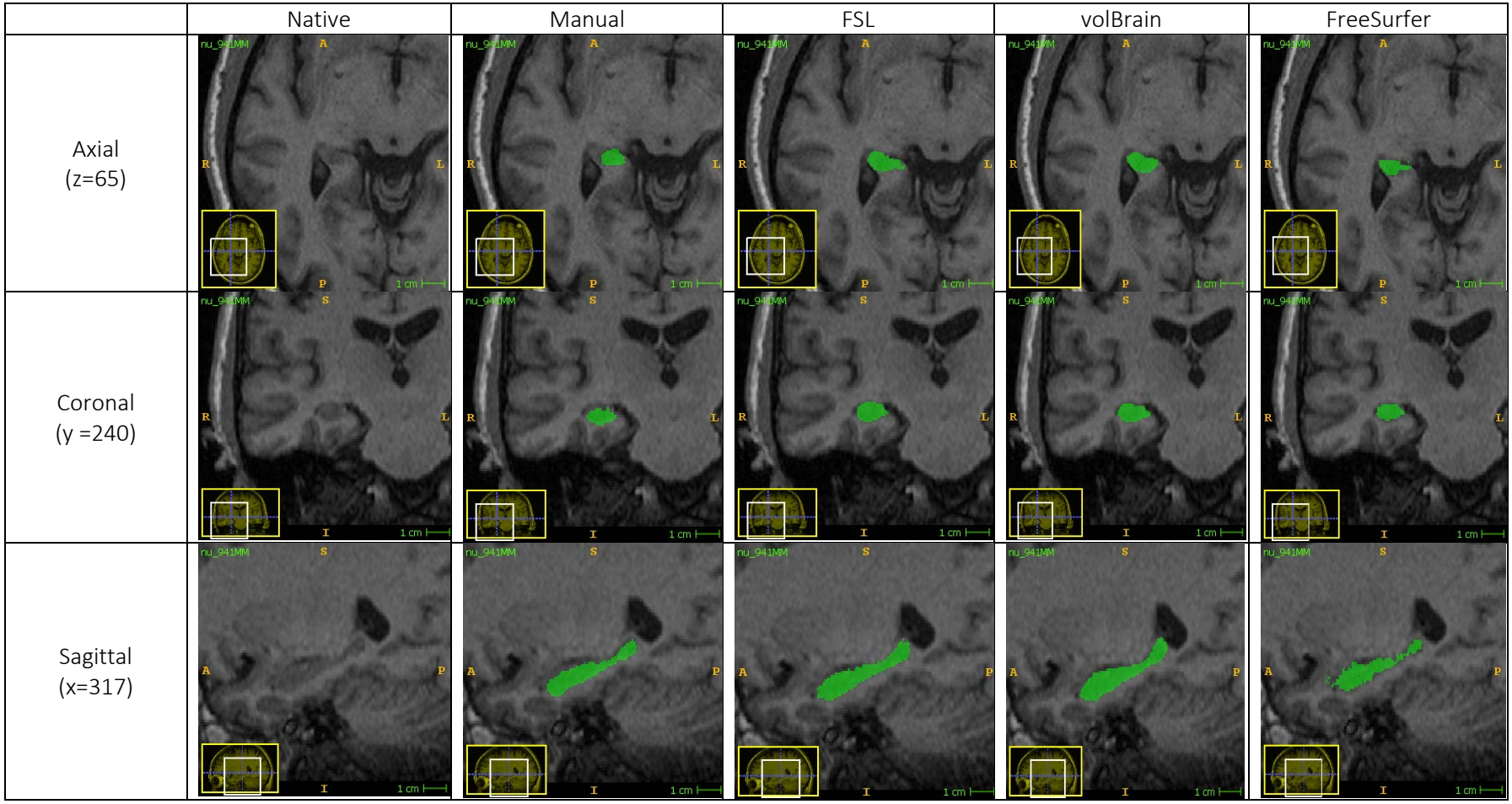

Fig. 2.6a Legend: Images utilising Measure (Stereology) were unfortunately unavailable.

Fig. 2.6b: Comparison of the segmented output (right caudate) from the techniques

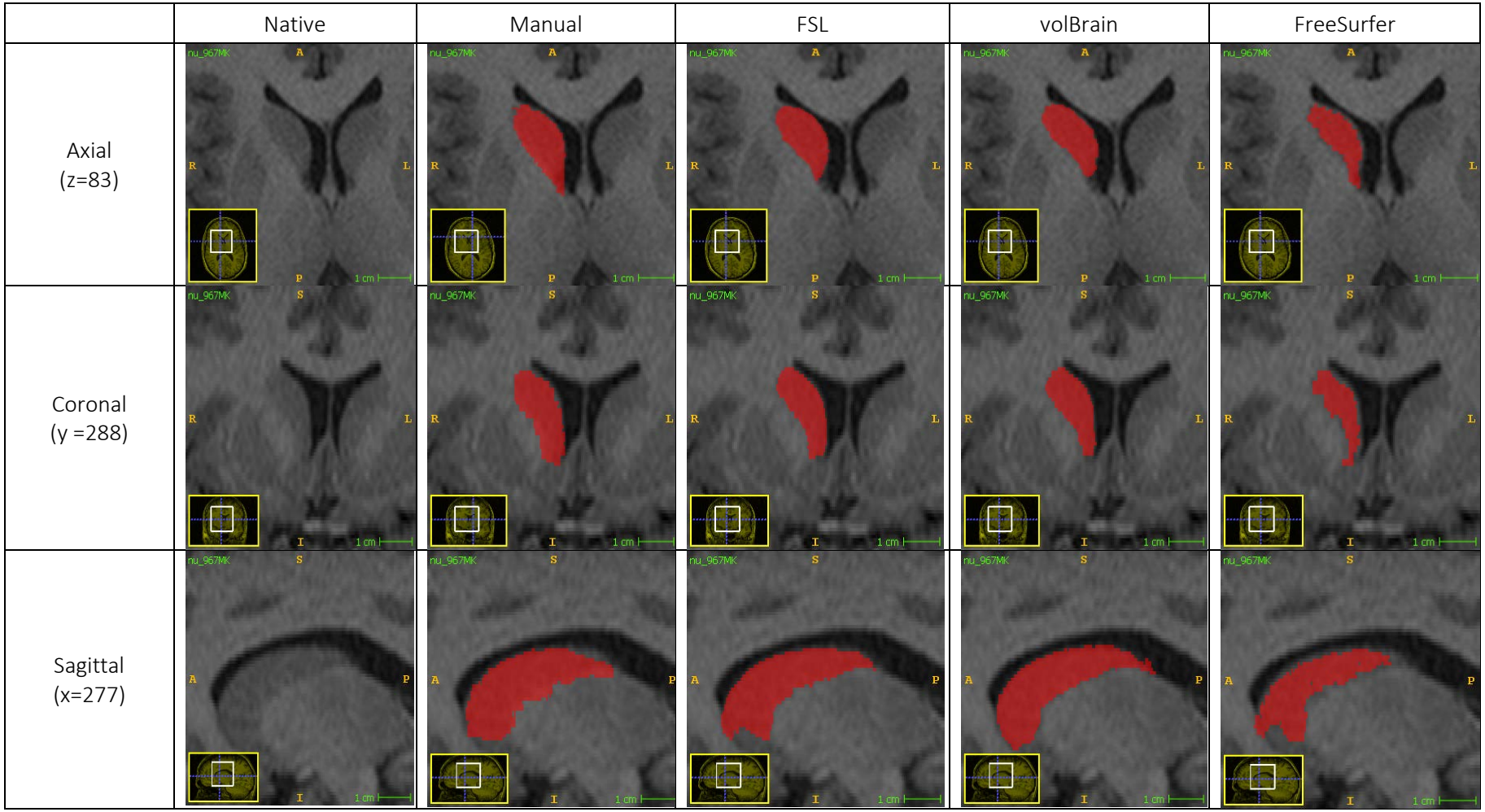

Fig. 2.6b Legend: Images utilising Measure (Stereology) were unfortunately unavailable

Fig. 2.7: Orthogonal view of a subject showing the voxel misclassification of FreeSurfer at estimating the volume of the right hippocampus

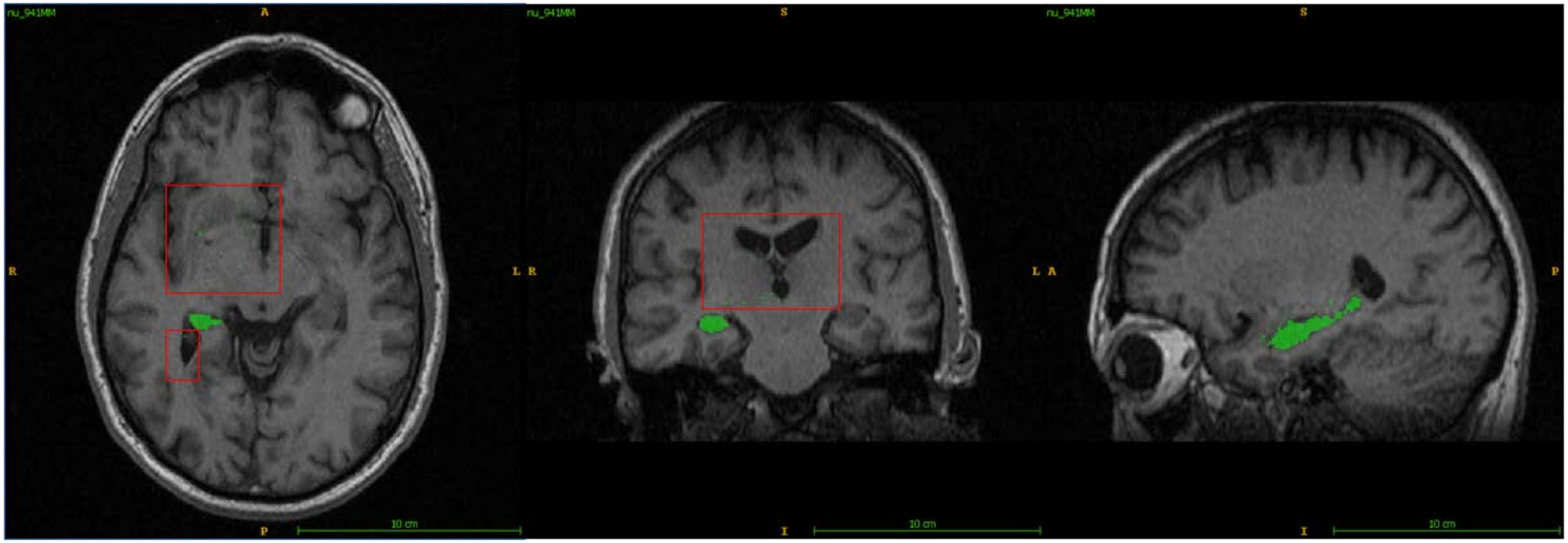

Fig. 2.7 Legend: The regions (in red) of highest voxel misclassification when estimating the volume of the hippocampus by FreeSurfer

Within the diagnostic groups, the consistency of all techniques at segmenting the caudate for the patient and the control group was high, however, a decreasing trend of consistency was observed, particularly for the healthy control group when segmenting the hippocampus (Table 2.1) as reported previously (Sanchez-Benavides *et al.* 2010). Furthermore, the correlation coefficients within the diagnostic groups were compared for significant differences to assess consistency of each of the techniques within the groups. Significant differences were noted between techniques when segmenting the left hippocampus with further differences in consistency noted with volBrain for all structures. This potentially suggests volBrain was particularly sensitive at detecting neuroanatomical differences between groups, however the patient group was heterogeneous in nature and caution is thus required with such an interpretation. Thus, we suggest further that the differing rates/levels and effect size of atrophy (neurodegenerative) and malformations (neurodevelopmental) in brain pathologies together with other essential factors (Table 2.5) must be thoroughly considered when choosing a segmentation technique especially for processing of brain MRI of clinical groups.

The Bland–Altman plots demonstrated relatively few difference points (Fig. 2.4, 2.5) outside of the established limits (± 1.96SD), with regards to the caudate and hippocampal volume bilaterally. Most of these difference points represented images for similar subjects across all techniques. This suggests that operational or systematic errors did not unduly influence segmentation and these subjects were potential outliers. The plots further suggested that biases existed for all the techniques (Fig. 2.4, 2.5 and Table 2.4) relative to manual segmentation across all the structures. The greatest and least biases were observed with stereology and FreeSurfer when segmenting the caudate respectively. The direct reverse of this trend was observed when segmenting the hippocampus. Furthermore, the integrated regression plots demonstrated a significant negative correlation across all the structures with all techniques relative to manual segmentation suggesting a trend of relatively smaller structures being more susceptible to volume overestimation, a finding consistent with some previous studies (Makowski *et al.* 2017; Schoemaker *et al.* 2016).

Manual tracing is the most labour-intensive approach and consequently in large-scale studies where an *easy-to-segment* structure is being examined, automated techniques demonstrate clear advantages. Careful consideration of a wide range of factors including anatomical accuracy, availability of expertise and time, consistency and the number of structures being estimated should, we suggest influence the choice of segmentation technique employed (Table 2.5).

There are a number of limitations associated with this study. Firstly, only two structures were examined; however given that these two structures are implicated in several neuropsychiatric disorders and are at either end of the spectrum in relation to the ease of segmentation, findings in relation to these structures are likely generalisable to several other brain structures. Secondly, data was acquired using a 1.5T MR scanner, and it is possible that automated segmentation may perform more accurately on images acquired with a 3T MR scanner. Thirdly, absolute volumes were used for this study rather than intracranial-corrected volumes however, group difference effects were not under examination in this study and the inclusion of intracranial volume corrections would have excluded the computation of practical performance metrics such as the percentage volume overlap which depends on the actual position of voxels (Sanchez-Benavides *et al.* 2010). Thus, future studies could explore the statistical power required to detect differences between clinical groups as well as the sensitivity and specificity of each technique. This study has several strengths including the comparison of a range of different segmentation techniques (stereology, semi-automated and two automated) with quantified bias estimates across structures, a relatively large sample size and the inclusion of both healthy controls and individuals with significant neuropsychiatric disorders. Thus, these findings are likely generalisable to large-scale global collaborations using semi-automated techniques such as ENIGMA, the Human Connectome Project and the Alzheimer's Disease Neuroimaging Initiative (ADNI) for example (Hibar *et al.* 2016; van Erp *et al.* 2016; Franke *et al.* 2016) which have investigated to date the influence of various demographic and clinical factors on sub/cortical structures. Finally, performance of the emerging segmentation techniques which make use of probabilistic templates from trained computer algorithms and geometric variability of a population is not fully known (Xu *et al.* 2014). It would be of interest to the field if probabilistic segmentation techniques, which are known to efficiently account for partial volume effects (Xu *et al.* 2014), are incorporated in similar future studies to test their performance compared to existing ones.

2.4.1 Conclusion

Our findings indicate that the anatomical accuracy and consistency of subcortical segmentation is dependent upon the anatomical location and adjacency to other grey matter structures which are difficult to differentiate from the structure in question. Furthermore, volumetric estimates from automated techniques are not always comparable to those obtained from manual segmentation especially when examining complex anatomical structures. Consequently, caution is required in interpretation of volume

estimates depending on the structure being examined and the segmentation technique employed. Thus, recognising an optimum segmentation algorithm/technique during the design phase of a study is important as a single approach is not necessarily perfect at segmenting all structures. In a typical dataset of MRI images used in neuropsychiatric studies, standard automated segmentation techniques appear to provide reasonable accuracy for an easy-to-segment structure such as the caudate; however, for a more difficult to segment structure such as the hippocampus, automated techniques provide reasonable correlation with volume but poor absolute approximation. This indicates that manual or stereological volume estimation should be considered for studies that require high levels of precision such as those with small sample sizes, particularly if difficult to segment structures are being examined. A wide range of factors including the number of structures being examined and the availability of expertise and time should additionally be considered prior to the choice of segmentation technique in neuropsychiatric research studies.

References

1. Ahmed, M., Cannon, D. M., Scanlon, C., Holleran, L., Schmidt, H., McFarland, J., et al. (2015). Progressive Brain Atrophy and Cortical Thinning in Schizophrenia after Commencing Clozapine Treatment. Neuropsychopharmacology, 40(10), 2409-2417, doi:10.1038/npp.2015.90.
2. Allen, J. S., Damasio, H., & Grabowski, T. J. (2002). Normal neuroanatomical variation in the human brain: an MRI-volumetric study. Am J Phys Anthropol, 118(4), 341-358, doi:10.1002/ajpa.10092.
3. Altshuler, L. L., Bartzokis, G., Grieder, T., Curran, J., Jimenez, T., Leight, K., et al. (2000). An MRI study of temporal lobe structures in men with bipolar disorder or schizophrenia. Biol Psychiatry, 48(2), 147-162.
4. Altshuler, L. L., Bartzokis, G., Grieder, T., Curran, J., & Mintz, J. (1998). Amygdala enlargement in bipolar disorder and hippocampal reduction in schizophrenia: an MRI study demonstrating neuroanatomic specificity. Arch Gen Psychiatry, 55(7), 663-664.
5. Amann, M., Andělová, M., Pfister, A., Mueller-Lenke, N., Traud, S., Reinhardt, J., et al. (2015). Subcortical brain segmentation of two dimensional T1-weighted data sets with FMRIB's Integrated Registration and Segmentation Tool (FIRST). NeuroImage: Clinical, 7, 43-52, doi:http://dx.doi.org/10.1016/j.nicl.2014.11.010.
6. Bao, S., & Chung, A. C. S. (2017). Feature Sensitive Label Fusion with Random Walker for Atlas-Based Image Segmentation. IEEE Transactions on Image Processing, 26(6), 2797-2810, doi:10.1109/TIP.2017.2691799.
7. Barnes, J., Ridgway, G. R., Bartlett, J., Henley, S. M. D., Lehmann, M., Hobbs, N., et al. (2010). Head size, age and gender adjustment in MRI studies: a necessary nuisance? NeuroImage, 53(4), 1244-1255, doi:https://doi.org/10.1016/j.neuroimage.2010.06.025.
8. Bland, J. M., & Altman, D. G. (1999). Measuring agreement in method comparison studies. Statistical Methods in Medical Research, 8(2), 135-160, doi: 10.1177/096228029900800204.
9. Bland, J. M., & Altman, D. G. (1986). Statistical methods for assessing agreement between two methods of clinical measurement. The Lancet, 327(8476), 307-310, doi:http://dx.doi.org/10.1016/S0140-6736 (86)90837-8.
10. Boccardi, M., Bocchetta, M., Apostolova, L. G., Barnes, J., Bartzokis, G., Corbetta, G., et al. (2015). Delphi definition of the EADC-ADNI Harmonized Protocol for hippocampal segmentation on magnetic resonance. Alzheimer's & Dementia, 11(2), 126-138, doi:https://doi.org/10.1016/j.jalz.2014.02.009.
11. Cahn, W., Pol, H., Lems, E. E., & et al. (2002). Brain volume changes in first-episode schizophrenia: A 1-year follow-up study. Arch Gen Psychiatry, 59(11), 1002-1010, doi:10.1001/archpsyc.59.11.1002.
12. Cherbuin, N., Anstey, K. J., Réglade-Meslin, C., & Sachdev, P. S. (2009). In Vivo Hippocampal Measurement and Memory: A Comparison of Manual Tracing and Automated Segmentation in a Large Community-Based Sample. PLoS ONE, 4(4), e5265, doi:10.1371/journal.pone.0005265.
13. Collins, D. L., Holmes, C. J., Peters, T. M., & Evans, A. C. (1995). Automatic 3-D model-based neuroanatomical segmentation. Hum Brain Mapp, 3(3), 190-208, doi:10.1002/hbm.460030304.
14. Coupé, P., Manjón, J. V., Fonov, V., Pruessner, J., Robles, M., & Collins, D. L. (2011). Patch-based segmentation using expert priors: Application to hippocampus and

ventricle segmentation. NeuroImage, 54(2), 940-954, doi:http://dx.doi.org/10.1016/j.neuroimage.2010.09.018.
15. Dale, A. M., Fischl, B., & Sereno, M. I. (1999). Cortical surface-based analysis. I. Segmentation and surface reconstruction. NeuroImage, 9(2), 179-194, doi:10.1006/nimg.1998.0395.
16. Doring, T. M., Kubo, T. T. A., Cruz, L. C. H., Juruena, M. F., Fainberg, J., & Domingues, R. C. (2011). Evaluation of hippocampal volume based on mr imaging in patients with bipolar affective disorder applying manual and automatic segmentation techniques. J Magn Reson Imaging, 33, doi:10.1002/jmri.22473.
17. Emsell, L., Langan, C., Van Hecke, W., Barker, G. J., Leemans, A., Sunaert, S., et al. (2013). White matter differences in euthymic bipolar I disorder: a combined magnetic resonance imaging and diffusion tensor imaging voxel-based study. Bipolar Disord, 15(4), 365-376, doi:10.1111/bdi.12073.
18. Ertekin, T., Acer, N., İçer, S., Vurdem, Ü. E., Çınar, Ş., & Özçelik, Ö. (2015). Volume estimation of the subcortical structures in Parkinson's disease using magnetic resonance imaging: A methodological study. [Article]. Neurology Asia, 20(2), 143-153.
19. Fenster, A., & Chiu, B. (2005). Evaluation of Segmentation algorithms for Medical Imaging. Conf Proc IEEE Eng Med Biol Soc, 7, 7186-7189, doi:10.1109/iembs.2005.1616166.
20. Filipek, P. A., Richelme, C., Kennedy, D. N., & Caviness, V. S., Jr. (1994). The young adult human brain: an MRI-based morphometric analysis. Cereb Cortex, 4(4), 344-360.
21. Fischl, B., & Dale, A. M. (2000). Measuring the thickness of the human cerebral cortex from magnetic resonance images. Proc Natl Acad Sci U S A, 97(20), 11050-11055, doi:10.1073/pnas.200033797.
22. Fischl, B., Salat, D. H., Busa, E., Albert, M., Dieterich, M., Haselgrove, C., et al. (2002). Whole brain segmentation: automated labeling of neuroanatomical structures in the human brain. Neuron, 33(3), 341-355.
23. Fischl, B., Sereno, M. I., & Dale, A. M. (1999). Cortical surface-based analysis. II: Inflation, flattening, and a surface-based coordinate system. NeuroImage, 9(2), 195-207, doi:10.1006/nimg.1998.0396.
24. Franke, B., Stein, J. L., Ripke, S., Anttila, V., Hibar, D. P., van Hulzen, K. J. E., et al. (2016). Genetic influences on schizophrenia and subcortical brain volumes: large-scale proof of concept. Nature Neuroscience, 19(3), 420–431.
25. Garcia, Y., Breen, A., Burugapalli, K., Dockery, P., & Pandit, A. (2007). Stereological methods to assess tissue response for tissue-engineered scaffolds. Biomaterials, 28(2), 175-186, doi:http://dx.doi.org/10.1016/j.biomaterials.2006.08.037.
26. García-Fiñana, M., Cruz-Orive, L. M., Mackay, C. E., Pakkenberg, B., & Roberts, N. (2003). Comparison of MR imaging against physical sectioning to estimate the volume of human cerebral compartments. NeuroImage, 18(2), 505-516, doi:http://dx.doi.org/10.1016/S1053-8119 (02)00021-6.
27. Geuze, E., Vermetten, E., & Bremner, J. D. (2005). MR-based in vivo hippocampal volumetrics: 1. Review of methodologies currently employed. Mol Psychiatry, 10(2), 147-159, doi:10.1038/sj.mp.4001580.
28. Giraud, R., Ta, V.-T., Papadakis, N., Manjón, J. V., Collins, D. L., & Coupé, P. (2016). An Optimized PatchMatch for multi-scale and multi-feature label fusion. NeuroImage, 124, 770-782, doi:http://dx.doi.org/10.1016/j.neuroimage.2015.07.076.

29. Grimm, O., Pohlack, S., Cacciaglia, R., Winkelmann, T., Plichta, M. M., Demirakca, T., et al. (2015). Amygdalar and hippocampal volume: A comparison between manual segmentation, Freesurfer and VBM. Journal of Neuroscience Methods, 253, 254-261, doi:http://dx.doi.org/10.1016/j.jneumeth.2015.05.024.
30. Gundersen, H. J., Bagger, P., Bendtsen, T. F., Evans, S. M., Korbo, L., Marcussen, N., et al. (1988). The new stereological tools: disector, fractionator, nucleator and point sampled intercepts and their use in pathological research and diagnosis. APMIS, 96(10), 857-881.
31. Hallgren, K. A. (2012). Computing Inter-Rater Reliability for Observational Data: An Overview and Tutorial. Tutorials in quantitative methods for psychology, 8(1), 23-34.
32. Han, X., & Fischl, B. (2007). Atlas renormalization for improved brain MR image segmentation across scanner platforms. IEEE Trans Med Imaging, 26(4), 479-486, doi:10.1109/tmi.2007.893282.
33. Hibar, D. P., Westlye, L. T., van Erp, T. G. M., Rasmussen, J., Leonardo, C. D., Faskowitz, J., et al. (2016). Subcortical volumetric abnormalities in bipolar disorder. [Original Article]. Mol Psychiatry, 21(12), 1710-1716, doi:10.1038/mp.2015.227.
34. Kenney, J., Anderson-Schmidt, H., Scanlon, C., Arndt, S., Scherz, E., McInerney, S., et al. (2015). Cognitive course in first-episode psychosis and clinical correlates: A 4 year longitudinal study using the MATRICS Consensus Cognitive Battery. Schizophr Res, 169(1-3), 101-108, doi:10.1016/j.schres.2015.09.007.
35. Keshavan, M. S., Anderson, S., Beckwith, C., Nash, K., Pettegrew, J. W., & Krishnan, K. R. R. (1995). A comparison of stereology and segmentation techniques for volumetric measurements of lateral ventricles in magnetic resonance imaging. Psychiatry Research: Neuroimaging, 61(1), 53-60, doi:http://dx.doi.org/10.1016/0925-4927 (95)02446-5.
36. Kim H. Y. (2013). Statistical notes for clinical researchers: Evaluation of measurement error 1: using intraclass correlation coefficients. Restorative dentistry & endodontics, 38(2), 98–102.
37. Koo, T. K., & Li, M. Y. (2016). A Guideline of Selecting and Reporting Intraclass Correlation Coefficients for Reliability Research. Journal of Chiropractic Medicine, 15(2), 155-163, doi:https://doi.org/10.1016/j.jcm.2016.02.012.
38. Krouwer, J. S. (2008). Why Bland–Altman plots should use X, not (Y+X)/2 when X is a reference method. Statistics in Medicine, 27(5), 778-780, doi:10.1002/sim.3086.
39. Looi, J. C., Lindberg, O., Liberg, B., Tatham, V., Kumar, R., Maller, J., et al. (2008). Volumetrics of the caudate nucleus: reliability and validity of a new manual tracing protocol. Psychiatry Res, 163(3), 279-288, doi:10.1016/j.pscychresns.2007.07.005.
40. Makowski, C., Béland, S., Kostopoulos, P., Bhagwat, N., Devenyi, G. A., Malla, A. K., et al. (2017). Evaluating accuracy of striatal, pallidal, and thalamic segmentation methods: Comparing automated approaches to manual delineation. NeuroImage, doi:http://dx.doi.org/10.1016/j.neuroimage.2017.02.069.
41. Mamah, D., Alpert, K. I., Barch, D. M., Csernansky, J. G., & Wang, L. (2016). Subcortical neuromorphometry in schizophrenia spectrum and bipolar disorders. NeuroImage: Clinical, 11, 276-286, doi:10.1016/j.nicl.2016.02.011.
42. Mamah, D., Harms, M. P., Barch, D., Styner, M., Lieberman, J. A., & Wang, L. (2012). Hippocampal Shape and Volume Changes with Antipsychotics in Early Stage Psychotic Illness. Frontiers in Psychiatry, 3, 96, doi:10.3389/fpsyt.2012.00096.
43. Manjón, J. V., & Coupé, P. (2016). volBrain: An Online MRI Brain Volumetry System. Frontiers in Neuroinformatics, 10, 30, doi:10.3389/fninf.2016.00030.

44. Mayer, K. N., Latal, B., Knirsch, W., Scheer, I., von Rhein, M., Reich, B., et al. (2016). Comparison of automated brain volumetry methods with stereology in children aged 2 to 3 years. [journal article]. Neuroradiology, 58(9), 901-910, doi:10.1007/s00234-016-1714-x.
45. McCarthy, C. S., Ramprashad, A., Thompson, C., Botti, J.-A., Coman, I. L., & Kates, W. R. (2015). A comparison of FreeSurfer-generated data with and without manual intervention. [Original Research]. Frontiers in Neuroscience, 9(379), doi:10.3389/fnins.2015.00379.
46. McFarland, J., Cannon, D. M., Schmidt, H., Ahmed, M., Hehir, S., Emsell, L., et al. (2013). Association of grey matter volume deviation with insight impairment in first-episode affective and non-affective psychosis. [journal article]. European Archives of Psychiatry and Clinical Neuroscience, 263(2), 133-141, doi: 10.1007/s00406-012-0333-8.
47. Morey, R. A., Petty, C. M., Xu, Y., Pannu Hayes, J., Wagner, H. R., Lewis, D. V., et al. (2009). A comparison of automated segmentation and manual tracing for quantifying hippocampal and amygdala volumes. NeuroImage, 45(3), 855-866, doi:http://dx.doi.org/10.1016/j.neuroimage.2008.12.033.
48. Nazir, M., Cleret de Langavant, L., Brugieres, P., Gaura, V., Lavisse, S., Youssov, K., Bachoud-Levi, A.-C., Remy, P. Comparison of three techniques to measure longitudinally striatal volume in Huntington's disease patients [[abstract]]. Movement Disorders 29(Supple 1), 227.
49. Nordenskjöld, R., Malmberg, F., Larsson, E.-M., Simmons, A., Ahlström, H., Johansson, L., et al. (2015). Intracranial volume normalization methods: Considerations when investigating gender differences in regional brain volume. Psychiatry Research: Neuroimaging, 231(3), 227-235, doi:https://doi.org/10.1016/j.pscychresns.2014.11.011.
50. Okada, N., Fukunaga, M., Yamashita, F., Koshiyama, D., Yamamori, H., Ohi, K., et al. (2016). Abnormal asymmetries in subcortical brain volume in schizophrenia. [Original Article]. Mol Psychiatry, 21(10), 1460-1466, doi:10.1038/mp.2015.209.
51. Pardoe, H. R., Pell, G. S., Abbott, D. F., & Jackson, G. D. (2009). Hippocampal volume assessment in temporal lobe epilepsy: How good is automated segmentation? Epilepsia, 50(12), 2586-2592.
52. Patenaude, B., Smith, S., Kennedy, D., & Jenkinson, M. (2007). Bayesian shape and appearance models, Technical report TR07BP1, FMRIB Centre - University of Oxford
53. Patenaude, B., Smith, S. M., Kennedy, D. N., & Jenkinson, M. (2011). A Bayesian model of shape and appearance for subcortical brain segmentation. NeuroImage, 56(3), 907-922, doi:10.1016/j.neuroimage.2011.02.046.
54. Perlaki, G., Horvath, R., Nagy, S. A., Bogner, P., Doczi, T., Janszky, J., et al. (2017). Comparison of accuracy between FSL's FIRST and Freesurfer for caudate nucleus and putamen segmentation. Scientific Reports, 7, 2418, doi: 10.1038/s41598-017-02584-5.
55. Quigley, S. J., Scanlon, C., Kilmartin, L., Emsell, L., Langan, C., Hallahan, B., et al. (2015). Volume and shape analysis of subcortical brain structures and ventricles in euthymic bipolar I disorder. Psychiatry Research: Neuroimaging, 233(3), 324-330, doi:http://dx.doi.org/10.1016/j.pscychresns.2015.05.012.
56. Razali, N. M. & Wah, Y. B. (2011). Power comparisons of Shapiro-Wilk, Kolmogorov-Smirnov, Lilliefors and Anderson-Darling tests. Journal of Statistical Modeling and Analytics, 2(1), 21-33.

57. Renteria, M. E., Schmaal, L., Hibar, D. P., Couvy-Duchesne, B., Strike, L. T., Mills, N. T., et al. (2017). Subcortical brain structure and suicidal behaviour in major depressive disorder: a meta-analysis from the ENIGMA-MDD working group. [Original Article]. Transl Psychiatry, 7, e1116, doi:10.1038/tp.2017.84.
58. Rodionov, R., Chupin, M., Williams, E., Hammers, A., Kesavadas, C., & Lemieux, L. (2009). Evaluation of atlas-based segmentation of hippocampi in healthy humans. Magn Reson Imaging, 27(8), 1104-1109, doi:10.1016/j.mri.2009.01.008.
59. Sacchet, M. D., Livermore, E. E., Iglesias, J. E., Glover, G. H., & Gotlib, I. H. (2015). Subcortical volumes differentiate Major Depressive Disorder, Bipolar Disorder, and remitted Major Depressive Disorder. Journal of Psychiatric Research, 68, 91-98, doi:http://dx.doi.org/10.1016/j.jpsychires.2015.06.002.
60. Sánchez-Benavides, G., Gómez-Ansón, B., Sainz, A., Vives, Y., Delfino, M., & Peña-Casanova, J. (2010). Manual validation of FreeSurfer's automated hippocampal segmentation in normal aging, mild cognitive impairment, and Alzheimer Disease subjects. Psychiatry Research: Neuroimaging, 181(3), 219-225, doi:http://dx.doi.org/10.1016/j.pscychresns.2009.10.011.
61. Scanlon, C., Anderson-Schmidt, H., Kilmartin, L., McInerney, S., Kenney, J., McFarland, J., et al. (2014). Cortical thinning and caudate abnormalities in first episode psychosis and their association with clinical outcome. Schizophrenia Research, 159(1), 36-42, doi:http://dx.doi.org/10.1016/j.schres.2014.07.030.
62. Schoemaker, D., Buss, C., Head, K., Sandman, C. A., Davis, E. P., Chakravarty, M. M., et al. (2016). Hippocampus and amygdala volumes from magnetic resonance images in children: Assessing accuracy of FreeSurfer and FSL against manual segmentation. NeuroImage, 129, 1-14, doi:http://dx.doi.org/10.1016/j.neuroimage.2016.01.038.
63. Sheline, Y. I., Sanghavi, M., Mintun, M. A., & Gado, M. H. (1999). Depression Duration but Not Age Predicts Hippocampal Volume Loss in Medically Healthy Women with Recurrent Major Depression. The Journal of Neuroscience, 19(12), 5034-5043.
64. Sled, J. G., Zijdenbos, A. P., & Evans, A. C. (1998). A nonparametric method for automatic correction of intensity nonuniformity in MRI data. IEEE Trans Med Imaging, 17(1), 87-97, doi:10.1109/42.668698.
65. Strakowski, S. M., DelBello, M. P., Sax, K. W., & et al. (1999). Brain magnetic resonance imaging of structural abnormalities in bipolar disorder. Arch Gen Psychiatry, 56(3), 254-260, doi:10.1001/archpsyc.56.3.254.
66. Tae, W. S., Kim, S. S., Lee, K. U., Nam, E.-C., & Kim, K. W. (2008). Validation of hippocampal volumes measured using a manual method and two automated methods (FreeSurfer and IBASPM) in chronic major depressive disorder. [journal article]. Neuroradiology, 50(7), 569, doi: 10.1007/s00234-008-0383-9.
67. Taha, A. A., & Hanbury, A. (2015). Metrics for evaluating 3D medical image segmentation: analysis, selection, and tool. [journal article]. BMC Medical Imaging, 15(1), 29, doi: 10.1186/s12880-015-0068-x.
68. van Erp, T. G., Hibar, D. P., Rasmussen, J. M., Glahn, D. C., Pearlson, G. D., Andreassen, O. A., et al. (2016). Subcortical brain volume abnormalities in 2028 individuals with schizophrenia and 2540 healthy controls via the ENIGMA consortium. Mol Psychiatry, 21(4), 547-553, doi:10.1038/mp.2015.63.
69. Velakoulis, D., Wood, S. J., Wong, M. T., McGorry, P. D., Yung, A., Phillips, L., et al. (2006). Hippocampal and amygdala volumes according to psychosis stage and diagnosis: a magnetic resonance imaging study of chronic schizophrenia, first-

episode psychosis, and ultra-high-risk individuals. Arch Gen Psychiatry, 63(2), 139-149, doi:10.1001/archpsyc.63.2.139.
70. Watson, R. (2001). SPSS Survival Manual by Julie Pallant, Open University Press, Buckingham, 2001, 286 pages, ISBN 0 335 20890 8. Journal of Advanced Nursing, 36(3), 478-478, doi:10.1046/j.1365-2648.2001.2027c.x.
71. Xu, H., Thirion, B., Allassonnière, S. (2014). Bayesian estimation of probabilistic atlas for tissue segmentation. IRBM, 35(1), pp.27-32.
72. Yushkevich, P. A., Piven, J., Hazlett, H. C., Smith, R. G., Ho, S., Gee, J. C., et al. (2006). User-guided 3D active contour segmentation of anatomical structures: significantly improved efficiency and reliability. NeuroImage, 31(3), 1116-1128, doi: 10.1016/j.neuroimage.2006.01.015.
73. Zaki, R., Bulgiba, A., Ismail, R., & Ismail, N. A. (2012). Statistical Methods Used to Test for Agreement of Medical Instruments Measuring Continuous Variables in Method Comparison Studies: A Systematic Review. PLoS ONE, 7(5), e37908, doi: 10.1371/journal.pone.0037908

Chapter 3

Study 2

Progression of subcortical changes after first-episode of psychosis: A 3-year longitudinal sMRI study

Theophilus N. Akudjedu[a*], Giulia Tronchin[a], Shane McInerney[a,e], Cathy Scanlon[a], Joanne P.M. Kenney[d], John McFarland[a], Gareth J. Barker[c], Peter McCarthy[b], Dara M. Cannon[a], Colm McDonald[a], Brian Hallahan[a]

[a]Centre for Neuroimaging & Cognitive Genomics (NICOG), Clinical Neuroimaging Laboratory, NCBES Galway Neuroscience Centre, College of Medicine Nursing and Health Sciences, National University of Ireland Galway, H91TK33 Galway, Ireland. [b]Department of Radiology, College of Medicine Nursing and Health Sciences, National University of Ireland Galway, H91TK33 Galway, Ireland. [c]King's College London, Institute of Psychiatry, Psychology & Neuroscience, Department of Neuroimaging, Centre for Neuroimaging Sciences, London, UK. [d]Trinity College Institute of Neuroscience and School of Psychology, Trinity College Dublin, Dublin, Ireland. [e]Department of Psychiatry, University of Toronto, 250 College Street, 8th floor, Toronto, Canada.

Submitted to Schizophrenia Research

Author's Contribution

The original data for this study was acquired prior to commencement of the current PhD research. Authors CMc, DMC and BH designed and supervised the general progress of the study. CS, JPMK, SMc, JM recruited and collected data. GJB and PMc worked to optimise MRI sequences. I carried out all MRI and statistical analyses reported in this study. Furthermore, I wrote the entire manuscript with the input of all authors who have approved the final manuscript under the supervision of CMc, DMC and BH.

Abstract

Background: The extent and location of longitudinal morphometric changes after first-episode of psychosis (FEP) remain unclear. We assessed progressive changes in ventricular and subcortical volumes over a 3-year period in individuals following FEP compared with healthy controls (HC), and whether volumetric changes were associated with clinical outcome.

Methods: High resolution 1.5T T1-weighted MR images were obtained from 28 FEP patients and 28 HCs at baseline and 3-year follow-up and were processed with the longitudinal pipeline in FreeSurfer (v.5.3.0). Repeated-measures ANCOVA and partial correlations were used to compare progressive changes between groups and to determine associations with clinical and functional characteristics. Age, gender and intracranial volume were included as covariates.

Results: A significant group by time interaction was found indicating progressively reduced volume of the caudate [$F(1,51)=5.86$, $p=0.02$, Hedges' $g=0.66$], putamen [$F(1,51)=6.06$, $p=0.02$, $g=0.67$] and thalamus [$F(1,51)=6.99$, $p=0.01$, $g=0.72$] in FEP compared with controls, with a trend for increased lateral ventricular volume [$F(1,51)=3.37$, $p=0.07$, $g=0.50$] more prominent on the right [$F(1, 51)=4.03$, $p=0.05$]. In FEP individuals, greater reduction in putamen volume over time was associated with low cumulative antipsychotic medication dose ($r=0.49$, $p=0.01$), and increasing lateral ventricular volume over time was associated with worsening negative symptoms ($r=0.41$, $p=0.04$) and poorer global assessment of functioning ($r=-0.41$, $p=0.04$).

Conclusions: There is progression of neuroanatomical deficits in dorsal striatal, thalamic and lateral ventricular regions after first-episode of psychosis, indicating a structural disturbance in the subcortical subnetwork of the cortico-striato-thalamo-cortical circuitry. Ventricular volume enlargement over time is a neuroanatomical marker of poorer clinical and functional outcome. This study lends weight to the evidence that there is early regional neuroanatomical progression after FEP.

Keywords first-episode psychosis, schizophrenia, structural MRI, subcortical structures, longitudinal study, progressive changes

3.1 Introduction

Structural magnetic resonance imaging (sMRI) studies have frequently demonstrated that brain volume abnormalities are already present when assessed at the point of first-episode of psychosis (FEP) (Vita *et al.* 2006; Dazzan *et al.* 2012). There is also evidence from longitudinal studies for progression of these brain changes at global and regional levels after FEP (Lieberman *et al.* 2001; Cahn *et al.* 2002). In one early study, greater whole brain volume reduction was demonstrated at follow-up in FEP patients relative to chronic patients suggesting a more pronounced brain change at the initial years of illness (Gur *et al.* 1998). The progression of morphometric abnormalities in the initial years after the onset of psychotic illness may be inherent to the pathogenesis of the illness as well as cumulative antipsychotic medication usage (Lieberman *et al.* 2005; Ho *et al.* 2011), genetic susceptibility (Andreassen *et al.* 2013) and cannabis use (Rais *et al.* 2008). A potential plateau effect on progression of grey matter (GM) deficits after the initial years of psychosis has been suggested from follow-up studies of established schizophrenia, indicating that the initial phase of psychotic illness may be a particularly vulnerable time for progression of neuroanatomical abnormalities (Hulshoff Pol and Kahn, 2008; van Haren *et al.* 2012). On the other hand, this appears less so in relation to lateral ventricular (LV) enlargement, which has been reported to continually increase for approximately two decades after FEP (Kempton *et al.* 2010), suggesting that the neuroprogressive processes may be anatomically region-specific rather than universal throughout the brain. The extent of estimated progressive whole brain tissue reduction in patients (−0.5% per year) has been quantified as approximately twice that of HCs (−0.2% per year) (Hulshoff Pol and Kahn, 2008) and associated with clinical and functional decline (Cahn *et al.* 2006; van Haren *et al.* 2008).

In contrast to ventricular and cortical GM findings, reports of progressive change in subcortical volumes have been inconsistent, with studies reporting conflicting results for the caudate (Lieberman *et al.* 2001; Roiz-Santiánez *et al.* 2014), hippocampus (Schaufelberger *et al.* 2011; Ebdrup *et al.* 2011; Lappin *et al.* 2014;) and thalamus (Theberge *et al.* 2007; van Haren *et al.* 2007; Andreasen *et al.* 2011) as well as no significant progressive changes (Lang *et al.* 2001; Haukvik *et al.* 2016) (see Table 3.1). Inconsistencies in reports of neuroanatomical progression after FEP are potentially due to clinical or methodological heterogeneity embedded in these studies, including variable clinical severity, antipsychotic medication use and follow-up times, and different image acquisition and analysis techniques. Although longitudinal studies are complicated by additional practical factors such as MRI

scanner upgrades and the challenge of re-recruitment, they remain a powerful approach in monitoring intra-individual changes within a cohort over time (Whitwell, 2008).

In our previous cross-sectional report (Scanlon *et al.* 2014), which assessed a cohort of FEP patients shortly after presentation to the mental health services, we found significant bilateral caudate volume reductions in patients compared with healthy volunteers. In the current longitudinal study, we aimed to determine if there were progressive changes in subcortical and ventricular volumes over a 3-year follow-up period and to ascertain if any such changes were related to particular clinical variables including severity of symptoms, use of antipsychotic medications and level of functioning. Based on previous longitudinal MRI studies in FEP, we hypothesised that, compared with controls, individuals with FEP would demonstrate greater ventricular enlargement and a reduction in volume of subcortical structures over time. Additionally, we hypothesised that in individuals with FEP, change in lateral ventricular volumes would be inversely related to changes in volume of subcortical structures overtime. We also hypothesised that volumetric changes over time in the patient group would be associated with measures of poorer outcome including decreased functioning, more negative symptoms and greater use of antipsychotic medication.

Table 3.1: Longitudinal neuroimaging studies that examined volumetric progression of ventricles, subcortical structures, total grey and white matter in first-episode psychosis

Reference	Diagnosis, n, Age (SD) in years		DOI, DUP	Medications/Duration of Treatment		Approx. Average Follow-up period	Study Re-recruitment Rate (%)	MRI/Processing Method	Brain Regions Examined	Findings in relation to ventricles, subcortical structures, total grey and white matter in patients
	Patients	Controls		Duration of Treatment prior to baseline Scan	Treatment during follow-up					
DeLisi *et al.* 1997 †	SCZ; n=50/ (27.4±7.0)	n=20/ (26.5±5.0)	DUP: 48.8 weeks	unclear	FGA, SGA, OM	4 years	50.4	1.5 T/ ANALYZE	Whole hemisphere, temporal lobes, superior temporal gyrus, hippocampus, amygdala, caudate, corpus callosum, cerebellum and lateral ventricles	1. Left ventricular enlargement in patients 2. Greater bilateral caudate reduction in controls † 3. No significant hippocampal, amygdala and caudate volume change in patients
Wood *et al.* 2001	het; n=30/ (21.8 ± 3.6)	n=26/ (23.8±7.9)	Median DUP: 4.2 weeks	up to the day of scan	FGA, SGA	2 years	100.0	1.5 T/ ANALYZE	Hippocampus, temporal lobe, whole brain	No significant hippocampal volume changes were found in patients
Lieberman *et al.* 2001	SCZ; n=107/ (31.17±6.70)	n=20/ (26.00±6.78)	DUP: 68.5 weeks	Naïve	FGA, SGA, OM	18 months	50.4	1.0 T/semi-automated computer mensuration system	Cortex, ventricles, Caudate, Hippocampus	1. Ventricular enlargement in patients 2. No hippocampal volume change in patients 3. Significant caudate volume increase in patients
Puri *et al.* 2001	SCZ; n=24/ (28.47±8.45)	n=12/ (27.92±6.14)	DUP: 59.7 weeks	<12 weeks	FGA, SGA	8 months	100.0	1.0 T/semi-automated computerised technique using image registration and subtraction approaches	Lateral ventricles	1. No significant mean changes in ventricular volume in patients over time 2. Highly variable ventricular volumes
Lang *et al.* 2001	SCZ; n=24/ (22.90±8.45) SCZ; chronic; n=24/ (38.40±11.60)	n=12/ (27.70±7.20)	unclear	<12 weeks 307.1 weeks	SGA	1 year	83.6	1.5 T/ manually segmentation with the interactive Shareware (NIH Image, v.1.61 ppc)	Basal Ganglia	No significant longitudinal basal ganglia volume changes found in the FEP patients
Cahn *et al.* 2002	SCZ; n=34/ (26.20±5.31)	n=36/ (24.5±5.80)	DOI: 72.8 weeks	<16 weeks	FGA, SGA	1 year	92.9	1.5 T/ in-house semi-automated software using intensity histogram analysis algorithms	Total brain, ventricles, cerebellum, cerebral grey and white matter	1. Grey matter volume reduction in patients 2. Lateral ventricular enlargement in patients
Massana *et al.* 2005	SCZ; n=11/ (23.0±4.0)	-	unclear	Naïve	SGA	3 months	100.0	1.5 T /optimised voxel-based morphometry	Basal ganglia, ventricles, cerebellum, cerebral grey and white matter	1. Significant grey matter increase in the left accumbens and the left caudate nuclei 2. No significant ventricular, total cerebral grey and white matter volume changes were demonstrated
Theberge *et al.* 2007*	SCZ; n=16/ (25.0±8.0)	n=16/ (29.0 ±12.0)	DOI: 96.2 weeks DUP: 96.2 weeks	Naïve	FGA, SGA, OM	10 months 30 months	100.0	4T/ Voxel-based morphometry	Whole brain	Greater reductions in total grey mater, right caudate and right thalamus were found in patients
Nakamura *et al.* 2007	FESCZ; n=17/ (26.0±6.80)	n=26/ (25.1 ±4.0)	unclear	3 weeks	FGA, SGA, OM	1.5 years	64.6	1.5 T/ Expectation Maximisation Segmentation	Neocortical Gray Matter, ventricles	1.Significant longitudinal increase of neocortical grey matter volume was observed in the FEAFF group relative to controls

	FEAFF n=21/ (23.70±3.20)			1 week				(EMS) toolbox		2. In the FESCZ group, neocortical grey matter volume reductions were observed in the frontal and temporal regions with enlargement of lateral ventricles which did not reach statistical significance
Glenthoj *et al.* 2007	SCZ; Risperidone; n=11/ (25.7±5.2) SCZ; Zuclopenthixol; n=8/ (26.1±5.3)	n=16/ (29.0 ±12.0)	DUP: 74.8 weeks DUP: 56.4 weeks	Naïve	FGA, SGA	12 weeks	100.0	1.5 T/ Manual and semi-automated approaches were used (DISPLAY software)	Basal Ganglia	1. Significant volume increase in the putamen was demonstrated in patients treated with risperidone 2. Altered asymmetry in caudate volume of patients was observed, with the left caudate being marginally smaller in volume than the right
Deng *et al.* 2009	SCZ; n=20/ (29.9±13.5)	n=11/ (28.0±11.7)	Median DUP: 17.1 weeks	Naïve	FGA, SGA	3 weeks	100.0	1.5 T/ Expectation Maximisation Segmentation (EMS) toolbox	multiple brain regions	Grey matter volume increase in the right caudate and thalamus in patients
de Castro-Manglano *et al.* 2011	het; n=22/ (18.50± 4.00)	n=17/ (18.30 ±5.80)	DUP: 10 weeks	28.5 weeks	FGA, SGA, OM	3 years	90.7	1.5T/ Voxel-based morphometry	Whole brain	No significant longitudinal thalamic volume changes observed
Boonstra *et al.* 2011	SCZ; continued Treatment; n=8/ (29.56±5.72) SCZ; discontinued Treatment; n=8/ (26.20±5.70)	n=20/ (27.97±5.63)	DUP: 73.8 weeks DUP: 49.9 weeks	unclear	SGA	1 year	100.0	1.5 T/ in-house semi-automated software using intensity histogram analysis algorithms and manual tracing for the basal ganglia	Cerebral grey and white matter, ventricles, cerebellum, basal ganglia	1. Significant reduction in volume of cerebral grey matter and caudate was observed over time in patients relative to controls 2. Significant volume reductions in the nucleus accumbens and putamen in patients who discontinued antipsychotic medication, whereas increases were found in patients who continued antipsychotic medication 3. No significant progressive ventricular changes were found
Ebdrup *et al.* 2011	SCZ; Low dose Treatment; n=13/ (26.20±5.70) SCZ; High dose Treatment; n=9/ (27.80±5.10)	n=28/ (28.40±6.00)	DUI: 266.8 weeks DUI: 133.6 weeks	Naïve	SGA	6 months	61.7	3 T/ DARTEL (diffeomorphic anatomical registration through exponentiated lie Algebra) with VBM5 toolbox	Striatum, hippocampus and ventricles	1. Significant progressive bilateral striatal and hippocampal volume reductions were observed in patients relative to controls. 2. The striatal volume loss was most pronounced in the low dose treatment group. 3. Hippocampal volume reductions were more pronounced in the high dose treatment group relative to controls. 4. No significant changes in ventricular, total cerebral grey and white matter were observed in patients.
Schaufelberger *et al.* 2011	SCZ; n=39/ (29.50±9.00)	n=52/ (31.80 ±8.80)	unclear	unclear	FGA,SGA	18 months	61.1	1.5T/ Voxel-based morphometry and manual ventricular tracing with MRICRO v.1.40 software	Whole brain	1. Significant volume increase in right hippocampal volume 2. No significant longitudinal ventricular changes observed 3. No significant change in global brain tissues
Andreasen *et al.* 2011	SCZ; n=202/ (24.56±7.14)	n=125/ (29.69±8.37)	unclear	Naïve (50% of sample)	FGA, SGA, OM	7 years	65.5	1.5 T ♦/ BRAINS2 AutoWorkup software	Global and lobular grey and white, ventricles, thalamus, putamen, caudate	1. Increase in lateral ventricular volume over time in patients 2. Decrease in thalamic volume over time in patients 3. No significant volume changes observed in the caudate and putamen.
Asami *et al.* 2012	SCZ; n=33/ (22.50±6.70)	n=36/ (22.90 ±3.80)	DOI: 19.5 weeks	<20 weeks	FGA, SGA, OM	1.5 years	63.8	1.5T/ Voxel-based morphometry	Superior temporal gyrus, amygdala, hippocampus, bilateral Heschl's gyrus, anterior and posterior cingulate gyrus	No significant longitudinal changes in amygdala and hippocampus found

Roiz-Santiánez *et al.* 2014	SCZ; n=109/ (29.44±8.21)	n=76/ (27.80±7.73)	DOI: 94.6 weeks DUP: 44.0 weeks	<5 weeks	SGA, OM	3 years	82.2	1.5 T/BRAINS2	multiple brain regions	Significant progressive caudate volume increase found in patients compared to controls
Lappin *et al.* 2014	het; n=42/ (27.7 ± 8.8)	n=32/ (29.8±8.6)	Median DUP: 6.7 weeks	unclear	FGA, SGA, OM	6 years	42.5	1.5 T/Longitudinal FreeSurfer (v5.3)	bilateral hippocampi	1. Bilateral hippocampal volume increases were found in 29% of patients, with increased volume associated with a less severe illness course 2. No difference in hippocampal volumes noted between patients and controls
Haukvik *et al.* 2016	het; n=79/ (27.6±7.7)	n=82/ (29.3±7.2)	DUP: 123 weeks	<52 weeks	FGA, SGA, OM	1 year	58.5	1.5 T/Longitudinal FreeSurfer (v5.3)	multiple brain regions	No significant longitudinal subcortical structural changes were found
Bodnar *et al.* 2016	het; Risperidone; n=24/ (22.50±3.50)	n=44/ (n.a)	DOI: 394.6 weeks DUP: 18.6 weeks	< 4 weeks	SGA	1 year	unclear	1.5 T/Longitudinal FreeSurfer (v5.3) and MAGeT-Brain (Multiple Automatically Generated Templates) algorithm	bilateral hippocampi	A significant bilateral hippocampal volume increase in the aripiprazole group compared to the other treatment groups and healthy controls was demonstrated
	het; Olanzapine; n=12/ (22.30±3.20)		DOI: 200.9 weeks DUP:17.8 weeks							
	het; Aripiprazole; n=13/ (23.30±4.10)		DOI: 207.4 weeks DUP:12.8 weeks							
	het; Refused-Treatment; n=13/ (24.30±3.10)		DOI: 255.3 weeks DUP:20.6 weeks							
Li *et al.* 2018	SCZ; n=41/ (23.90 ± 7.72)	n=39/ (24.01±8.18)	DOI: 36 weeks	Naïve	SGA	6 weeks	78.8	3 T/Longitudinal FreeSurfer (v6.0)	bilateral hippocampi and subfields	At the whole hippocampus level, there were no significant volume differences found in patients but significant volume reduction of some subfields were observed

Table 3.1 Legend: *two follow-up times; ϕTwo different 1.5T MRI brands and acquisition sequences were used for this study; SCZ = schizophrenia; FEAFF= First-episode Affective; FESCZ= First-episode Schizophrenia; het = heterogenous sample; DOI = duration of illness; DUP = duration of untreated psychosis; FGA = first-generation antipsychotics; n.a = not available; SGA = second-generation antipsychotics; OM= other medications (mainly, mood stabilisers and antidepressants); † = includes the sample and findings reported in DeLisi et al. 1995; Age = age at baseline.

3.2 Methods

3.2.1 Study design and setting

Participants were included in this study if they have previously participated in the initial phase (Scanlon *et al.* 2014) and had no contraindications to MRI procedures. Exclusion criteria for all participants included presence/history of neurological disorders, learning disability, life-time substance dependency (as defined by DSM-IV-TR), a history of head injury resulting in loss of consciousness for over 5 minutes and oral steroid use in the past 3 months. HCs were excluded if they had a personal or family history of any psychotic illness. Written informed consent was provided by all participants at both time-points and ethical approval was obtained from the National University of Ireland, Galway (NUI Galway) and Galway University Hospitals Research Ethics Committees.

3.2.2 Participants

The original baseline sample comprised of 46 patients and 46 controls (Scanlon *et al.* 2014) and re-recruitment of all participants was attempted. Five patients from the original patient cohort were un-contactable, 11 refused to participate and 2 had relocated to another country. Two individuals in the control group were later excluded as imaging data was acquired on a different MRI scanner, while others within this cohort had either relocated (n=8), were un-contactable (n=4) or declined our invitation to participate (n=4). At follow-up therefore the final successful re-recruitment rate was 61%. There was no significant difference in age, gender, age of illness onset and daily medication dose prescribed at baseline in patients from the original cohort who were successfully re-recruited at follow-up (n=28) compared to those not re-recruited (n=18). The final number of patients and healthy controls re-recruited to the current longitudinal study was identical (n=28).

3.2.3 Clinical assessment

The baseline clinical assessments were described previously in detail (Scanlon *et al.* 2014) and were repeated at follow-up. Briefly, the Structured Clinical Interview (SCID) for DSM-IV Research Version (First *et al.* 2002) was repeated to establish updated diagnostic status given its potential variation (Fusar-Poli *et al.* 2016). Ratings of symptomatology and functioning were carried out using the Positive and Negative Syndrome Scale (PANSS: 0–6 scale) (Kay *et al.* 1987) and the Global Assessment of Functioning score (GAF) (Hall, 1995) respectively. HCs were also re-screened for the presence of psychotic illness using the SCID-NP (non-patient) edition (First *et al.* 2002). Total antipsychotic medication administered during the follow-up period was converted to chlorpromazine (CPZ) equivalents (Lehman *et*

al. 1998; Taylor *et al.* 2007; Woods, 2003) from detailed clinical interviews and review of clinical notes. Similarly, information on cannabis use was collected from clinical interviews and supplemented by a review of clinical notes and categorised via binary coding based on the adapted criteria of the Centre for Addiction and Mental Health (Boak *et al.* 2017) for either heavy use (≥ 12 times on a lifetime basis and at least once during the past year) or none/minimal use (0-11 times on a lifetime basis and none during the past year).

3.2.4 MRI data acquisition

MRI scans at both time-points were acquired at the University Hospital Galway on the same 1.5 Tesla Siemens Magnetom Symphony scanner (Erlangen, Germany), with an identical sequence at each timepoint. Scout sequences were used to confirm each subject's radiological positioning and image field-of-view was in alignment with the AC-PC line. A 4-channel head coil was used to acquire data, using a magnetisation-prepared rapid acquisition of gradient echo (MPRAGE) sequence to provide high resolution volumetric T1-weighted images (160 slices) with the following parameters: repetition time (TR): 1140 ms, echo time (TE): 4.38 ms, inversion time (TI): 600 ms, flip angle 15; matrix size 256 × 256; an in-plane pixel size of 0.9 mm × 0.9 mm and slice thickness of 0.9 mm. There was no major system upgrade during this research period and participants were scanned in a random order at each timepoint in order to minimise any acquisition bias due to any changes in scanner characteristics over time, which could otherwise potentially confound group diagnostic differences.

3.2.5 Image quality assessment and correction

Non-parametric non-uniform intensity normalisation (N3) was used to correct for intensity non-uniformity (Sled *et al.* 1998) identified in some of the structural scans after visual examination for quality as previously described (Emsell *et al.* 2013; Scanlon *et al.* 2014).

3.2.6 Longitudinal image processing

The longitudinal processing pipeline of FreeSurfer (v.5.3.0, http://surfer.nmr.mgh.harvard.edu/) (Reuter *et al.* 2012) was employed for the segmentation of subcortical structures and ventricles. This pipeline operates in a semi-automated fashion, thus providing the option of checking and improving segmentation quality (Akudjedu *et al.* 2018). The technical operation of this validated analysis pipeline had been previously detailed (Reuter *et al.* 2010; Reuter and Fischl, 2011; Reuter *et al.* 2012). The images from both time points were independently analysed with the "recon-all" segmentation pipeline.

Further analysis through an inverse consistent registration (Reuter *et al.* 2010) produced a within-subject neuroanatomical space and template for unbiased volumetric brain estimation over time. Several processing steps, including motion correction, removal of non-brain tissue, Talairach transformation, atlas registration as well as spherical surface mapping and segmentation were then initialised with information from the neuroanatomical template. Further reconstruction of the template was carried out for longitudinal brain volumetry. All the images were visually inspected at each of the analysis stages and segmentation quality improved as deemed necessary in accordance with the FreeSurfer quality check protocols (https://surfer.nmr.mgh.harvard.edu/fswiki/QATools).

Given that FreeSurfer tends to overestimate hippocampal volume (Akudjedu *et al.* 2018), manually segmented hippocampal volumes were also incorporated in our analysis. Bilateral hippocampi were manually segmented as previously described (Akudjedu *et al.* 2018) by anatomically trained raters with inter-rater reliability (Left: 0.89; Right: 0.94) and intra-rater reliability scores greater than 0.85 for all raters.

3.2.7 Statistical analysis

Statistical analyses were performed with the Statistical Package for Social Sciences (SPSS, v.24.0) for Windows (SPSS Inc., IBM, New York, USA)**.** The Kolmogorov-Smirnov test was used to examine the distribution of our data for normality. Clinical and demographic differences between groups over time were assessed using chi-square or independent t-test. Paired t-tests were used to assess longitudinal changes in clinical symptom and functionality scores within FEP individuals. Bilateral brain volumes were summed to reduce multiple comparisons in the analyses. Independent ANCOVAs were used to explore baseline neuroanatomical differences between FEP patients and HCs. Repeated-measures ANCOVA with Greenhouse-Geisser corrections were used to investigate differences in the progression of regional brain morphometric abnormalities over the 3-year follow-up period. In each general linear model, the dependent measures were MRI volumes and the independent measure was group (FEP vs. HC). The within-subject factor was time (baseline vs. follow-up) with hemisphere (left vs. right) added for bilateral structures. Given the potential of age, gender and intracranial volume (ICV) to confound results in brain morphometric investigations (Barnes *et al.* 2010), all analyses were controlled for these covariates. Where there were significant findings, further post-hoc within-group analyses of variances were conducted to identify the direction of lateralised effects. To better quantify the significant findings, effect sizes were calculated from the adjusted percent volume differences at baseline and follow-up for each region of

interest (ROI). Given the relatively small sample size, Hedges' g was adopted (Hedges and Olkin, 1985) for unbiased effect sizes (Calin-Jageman, 2018). The adjusted (for age, gender and ICV) percent volume difference of each ROI was computed as: [(adjusted volume at follow-up – adjusted volume at baseline)/adjusted volume at baseline] x 100%]. For brain regions demonstrating significant progressive volume changes over time, partial correlations controlling for age, gender and ICV were used to determine the strength of potential associations between percent volume change in ROI and change ($Time_2$ - $Time_1$) in clinical or functional variables. A two-tailed α level of 0.05 was used for statistical testing. Given that brain structures are not independent (Haukvik *et al.* 2016) and our study was being driven by *a priori* hypotheses for progressive brain change, we did not apply a Bonferroni correction for these group analyses, as per similar previous studies (Ayesa-Arriola *et al.* 2013; Roiz-Santiánez *et al.* 2014).

3.3 Results

3.3.1 Clinico-demographic characteristics

Demographic and clinical data are presented in Table 3.2. Individuals with FEP were on average younger and had engaged in less years of education. There were no differences between the groups in gender distribution or time between scans. Formal SCID diagnoses of the patients at follow up were: schizophrenia (n=8), bipolar I disorder (n=9), major depressive disorder (n=3), schizoaffective disorder (n=3), psychotic disorder not otherwise specified (NOS) (n=3), delusional disorder (n=1) and substance induced psychotic disorder (n=1). At baseline, 24 patients were taking second-generation antipsychotic (SGA) medication, 1 was taking a first-generation antipsychotic (FGA) medication and 3 participants were not prescribed antipsychotic medication. At follow-up, 16 individuals were treated with SGAs comprising olanzapine (n=6), aripiprazole (n=5), risperidone (n=3), clozapine (n=2), quetiapine (n=2), amisulpride (n=1) and no patients were treated with a FGA medication. Three individuals were treated with more than one SGA. In addition to a SGA, 7 patients were prescribed antidepressants and 4 patients were prescribed mood stabilisers. Nine patients were on no psychotropic medications at the point of the follow-up scan.

Within the patient group, there were significant reductions in positive ($t_{(27)} = 5.41$, $p<0.001$) and general psychopathology ($t_{(27)} = 3.89$, $p<0.001$) subscale symptoms of the PANSS between baseline and follow-up, with a reduction in negative symptoms also demonstrated, that did not reach statistical significance ($t_{(27)} = 1.92$, $p=0.07$). GAF scores increased

significantly ($t_{(27)}$ = -7.87, p<0.001) between baseline and follow-up assessments (see Table 2).

Table 3.2: Sociodemographic and clinical characteristics of participants

Variables		Patients (n=28)	Controls (n=28)	Comparison (T/χ^2, p)
Age at baseline MRI, mean (SD), years		28.5 (9.3)	33.5 (8.8)	-2.07, 0.04
Time between Scans, mean (SD), years		3.2 (1.1)	3.2 (0.9)	0.11, 0.91
Years of Education, mean (SD), years		16.0 (2.7)	17.8 (3.0)	-2.37, 0.02
Gender, n (% male)		18 (64.3)	14 (50.0)	1.15, 0.28
Age of onset, mean (SD), years		25.7 (10.1)		
DUP, mean (SD), months		13.9 (16.5)		
TICV, mean (SD), cm^3		1570.5 (132.1)	1548.8 (153.1)	0.60, 0.56
Cannabis Users, n (%)	Current None/Minimal users: Baseline	16 (57.1)	23 (82.1)	4.14, 0.04
	Current None/Minimal users: Follow-Up	27 (96.4)	28 (100.0)	1.02, 0.31
Antipsychotic Dosage [Total CPZ equiv. (mgs)] †	Daily dose: Baseline [a]	235.5 (198.1)		
	Daily dose: Follow-Up [b]	341.2 (285.9)		
	Cumulative dose: Baseline [c]	6531.1 (8004.9)		
	Cumulative dose: Follow-Up [d]	264912.4 (252121.4)		
PANSS, mean (SD)	Total: Baseline	34.2 (14.2)		
	Total: Follow-Up	16.4 (16.1)		
	Positive: Baseline	10.7 (5.2)		
	Positive: Follow-Up	3.8 (5)		
	Negative: Baseline	7.6 (6.0)		
	Negative: Follow-Up	4.9 (6.2)		
	General psychopathology: Baseline	15.9 (8.0)		
	General psychopathology: Follow-Up	7.7 (7.1)		
GAF, mean (SD)	Baseline	51.3 (11.3)		
	Follow-Up	75.7 (14.8)		

Table 3.2 Legend: ; CPZ= chlorpromazine equivalents; DUP = duration of untreated psychosis; GAF= global assessment of functioning; SD = standard deviation, TICV= Total Intracranial Volume; PANSS= positive and negative syndrome score (0-6 point scale); † = antipsychotic medication was converted to chlorpromazine equivalents (CPZ) [(Lehman *et al.* 1998; Taylor *et al.* 2007; Woods, 2003)]; a Data based on: n=25; b Data based on: n=16; c Data based on: n=25; d Data based on: n = 26.

3.3.2 Group comparison of progressive brain changes over time

There were no significant differences at baseline between FEP patients and HCs for caudate [F(1,51)=0.761, 0.387], putamen [F(1,51)=0.070, 0.792], nucleus accumbens [F(1,51)=0.759, 0.388], globus pallidus [F(1,51)=1.692, 0.199], hippocampus [F(1,51)=1.165, 0.286], and

amygdala [F(1,51)=0.389, 0.536] volumes. However, significant differences were found indicating reduced volume of the thalamus [F(1,51)=5.092, 0.028] and enlargement of the LVs [F(1,51)=4.825, 0.033] in FEP patients compared to HCs. As demonstrated in Table 3.3, significant group x time interactions were found, indicating progressively greater volume reduction of the caudate [F(1,51)=5.86, p=0.02, Hedges' g=0.66], putamen [F(1,51)=6.06, p=0.02, g=0.67] and thalamus [F(1,51)=6.99, p=0.01, g=0.72] in FEP patients compared with healthy volunteers. There was also a trend towards significance for increased LV volume over time in patients [F(1,51)=3.37, p=0.07, g=0.50]. A significant effect of group x time x laterality [F(1,51)=4.38, p=0.04, g=0.57] was demonstrated for LV enlargement in patients compared to controls. Post-hoc analysis demonstrated significant right LV enlargement over time in patients compared to controls [F(1,51)=4.03, p=0.05)] which was not significant for left LV enlargement [F(1,51)=2.66, p=0.11)]. These findings were essentially unaltered when age was removed as a covariate (Miller and Chapman, 2001) and when scan interval time was added as a covariate in all analyses. Furthermore, Figure 3.1 illustrates the significantly progressive changes in ROI's at baseline and follow-up for patients and controls. There were no progressive volume deficits identified in medial temporal lobe structures in the cohort, including in manually segmented hippocampal volume.

Fig. 3.1: Progressive volume change over time in FEP patients and controls

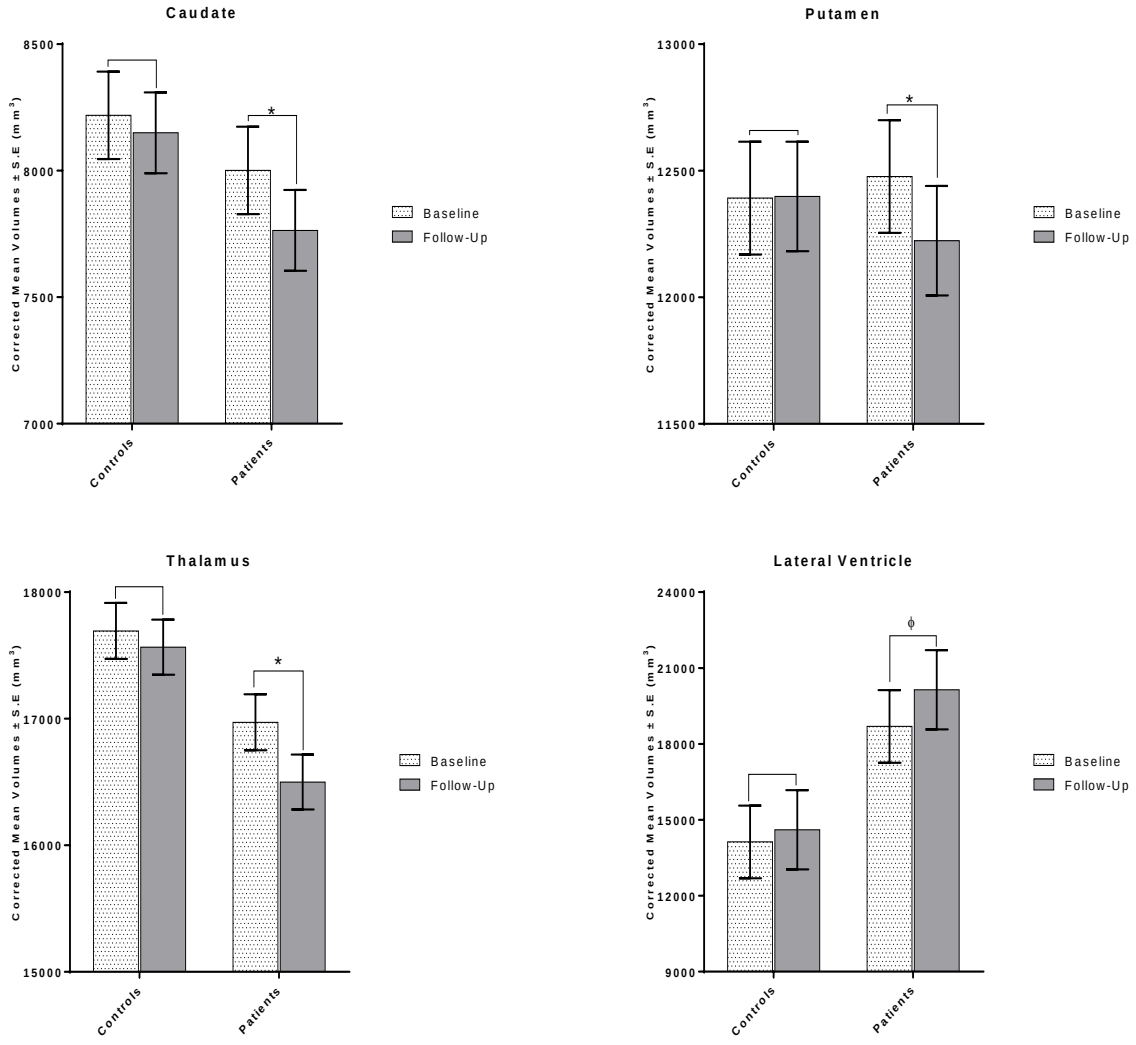

Fig. 3.1 Legend: Plot of corrected mean volumes (± standard error) of the neuroanatomical structures that progressed over time. Comparison of these progressions in first-episode psychosis patients with healthy controls at baseline and after 3-years. The mean volumes were corrected for ICV, gender and age at baseline. *significant change; ϕgreater progressive change that did not reach statistical significance.

Table 3.3: Group comparison of progressive brain change over time

Brain Region	Baseline		Follow-up		Mean Vol. Diff. Over time (mm^3) (95% C.I)	% Vol. Diff. Over time (SD)	Group x Time			Group x Time x Laterality		
	Adjusted Mean Vol. (mm^3) (SE)		Adjusted Mean Vol. (mm^3) (SE)				F (1,51)	p	Hedges' g	F (1,51)	p	Hedges' g
	FEP (n=28)	HC (n=28)	FEP (n=28)	HC (n=28)								
Caudate	8001.04 (172.50)	8218.81 (172.50)	7763.75 (159.74)	8149.83 (159.74)	**-168.31 (-299.57, -37.06)**	**-2.13 (1.51)**	**5.86**	**0.02**	**0.66**	0.23	0.64	0.13
Putamen	12477.22 (222.75)	12391.89 (222.75)	12223.64 (216.12)	12398.61 (216.12)	**-260.30 (-473.66, -46.94)**	**-2.08 (1.47)**	**6.07**	**0.02**	**0.67**	0.03	0.86	0.05
Globus pallidus	3833.15 (85.15)	3993.42 (85.15)	3806.78 (81.17)	4016.26 (81.17)	-49.21 (-136.21, 37.79)	-1.26 (0.89)	1.18	0.28	0.30	0.02	0.89	0.04
Nucleus accumbens	1165.84 (29.75)	1203.34 (29.75)	1160.22 (24.84)	1205.64 (24.84)	-7.92 (-54.88, 39.04)	-0.67 (0.47)	0.11	0.75	0.09	1.00	0.32	0.27
Thalamus	16971.56 (221.22)	17693.80 (221.22)	16499.69 (217.14)	17565.34 (217.14)	**-343.41 (-589.14, -97.68)**	**-3.51 (2.48)**	**6.98**	**0.01**	**0.72**	0.64	0.43	0.22
Hippocampus †	8972.39 (124.01)	9166.01 (124.01)	8866.77 (125.07)	9146.37 (125.07)	-85.98 (-199.41, 27.45)	-0.98 (0.69)	2.06	0.16	0.39	0.01	0.94	0.03
Hippocampus ǂ	5560.83 (112.47)	5724.92 (112.47)	5697.26 (123.55)	5757.06 (123.55)	104.29 (-17.92, 186.49)	1.89 (1.34)	0.53	0.47	0.20	1.18	0.28	0.30
Amygdala	3160.27 (53.46)	3208.51 (53.46)	3205.07 (56.67)	3206.43 (56.67)	46.88 (-10.88,104.64)	1.48 (1.05)	1.81	0.19	0.37	2.58	0.11	0.44
Lateral Ventricle	18694.10 (1436.51)	14128.63 (1436.51)	20140.05 (1563.69)	14607.76 (1563.69)	**966.82 (-39.39, 1973.03)**	**4.34 (3.07)**	**3.37**	**0.07 ϕ**	**0.50**	**4.38**	**0.04**	**0.57**
Third Ventricle	917.33 (63.84)	850.59 (63.84)	973.39 (73.70)	880.15 (73.70)	26.50 (-41.26, 94.26)	2.63 (1.86)	0.54	0.47	0.19	-	-	-
Total White matter	460972.52 (5223.60)	477984.35 (5223.60)	459682.90 (5380.71)	477362.00 (5380.71)	-667.27 (-5 222.46, 3 887.92)	-0.15 (0.11)	0.08	0.78	0.08	-	-	-
Total Grey matter	647495.84 (4723.89)	656765.01 (4723.89)	638932.15 (5151.78)	649329.12 (5151.78)	-1127.80 (-11 314.52, 9 058.92)	-0.19 (0.13)	0.05	0.83	0.06	-	-	-

Table 3.3 Legend: Age, gender and ICV were included as covariates for all the mean adjustments and analyses; SE= standard error; C.I = confidence interval; % Vol. Diff. = percentage volume difference; calculated as follows: 100 × [(adjusted volume at follow-Up − adjusted volume at baseline)/adjusted volume at baseline] and difference between groups over time is presented; Negative value indicates a % volume decrease over time; The percent volume differences in FEP's and HC's at baseline and follow-Up were selected to estimate the effect size (Hedges' g); **Bold** = significant values and/or large effect sizes (>0.5); p-values presented are uncorrected; **ϕ** = a trend towards significance; **†** = Longitudinal FreeSurfer volumes; **ǂ =** manually segmented volumes. Of note, there was no significant difference in the results with regards to hippocampal volume deficit progression when analysis was repeated using the manual segmentation data.

3.3.3 Association of progressive neuroanatomical changes with change in clinical and functional variables

Table 4 displays the correlation coefficients of clinical measures assessed with (change in volume of regions-of-interest in patients). Of note, in FEP patients, a greater reduction of putamen (r=0.49, p=0.01; Fig.2A) and globus pallidum volume (r=0.44, p=0.03) was associated with less cumulative antipsychotic medication (measured in chlorpromazine equivalents) over the 3-year follow-up period. Increased right LV (r=0.43, p=0.03), total LV (r=0.41, p=0.04; Fig. 2B) and 3rd ventricular (r=0.55, p=0.004) volume over time was associated with worsening negative symptoms on the PANSS. Additionally, increased right LV (r=-0.43, p=0.03), total LV (r=0.41, p=0.04; Fig.2C) and 3rd ventricular (r=-0.49, p=0.01) volume over time was associated with reduced GAF scores. A moderate correlation between antipsychotic medication use and total GM loss over time was also noted (r=-0.45, p=0.02).

3.3.4 Association of lateral ventricular changes with change in subcortical structures

The relationship between percentage volume change in lateral ventricles and the subcortical structures that were significantly reduced in volume over time in individuals with FEP are displayed in Fig.3.3. Of note, in FEP individuals, there was a significant inverse relationship between percentage volume change in lateral ventricles with the thalamus (r=-0.48, p=0.02; Fig.3A) and caudate (r=-0.52, p=0.01; Fig.3B) over the 3-year follow-up period. A similar relationship was demonstrated between the lateral ventricles and putamen, however this finding was not significant (r=-0.27, p=0.19; Fig.3C).

Table 3.4: Partial correlation of brain volume changes with change in clinical and functional variables in FEP patients

Brain Region	CPZ (Time $_2$ – Time $_1$) (r, p)	PANSS (Time $_2$ – Time $_1$) (r, p)			GAF (Time $_2$ – Time $_1$) (r, p)
		Positive	Negative	General	
Caudate	0.11, 0.59	-0.14, 0.50	-0.32, 0.12	-0.18, 0.40	0.15, 0.48
Putamen	**0.49, 0.01**	0.01, 0.95	0.003, 0.99	0.06, 0.78	-0.17, 0.43
Globus pallidus	**0.44, 0.03**	-0.13, 0.55	0.06, 0.79	-0.05, 0.80	-0.08, 0.72
Nucleus Accumbens	0.09, 0.68	0.01, 0.96	0.26, 0.21	0.15, 0.47	-0.09, 0.69
Thalamus	-0.01, 0.98	-0.11, 0.61	-0.16, 0.45	-0.01, 0.98	0.21, 0.31
Hippocampus †	-0.10, 0.65	0.23, 0.27	-0.14, 0.52	0.35, 0.09	0.02, 0.94
Hippocampus ǂ	0.02, 0.94	0.36, 0.08	-0.38, 0.06	0.07, 0.75	0.02, 0.93
Amygdala	0.04, 0.85	0.02, 0.93	0.10, 0.64	-0.08, 0.71	0.33, 0.11
Total White matter	0.02, 0.92	0.003, 0.99	-0.24, 0.25	-0.32, 0.12	**0.42, 0.04**
Total Grey matter	**-0.45, 0.02**	0.05, 0.82	-0.39, 0.06	0.04, 0.87	0.32, 0.12
Third Ventricle	0.31, 0.13	-0.03, 0.87	**0.55, 0.004**	0.22, 0.30	**-0.49, 0.01**
Lateral Ventricle	0.10, 0.64	-0.17, 0.43	**0.41, 0.04**	0.14, 0.52	**-0.41, 0.04**
Left	0.07, 0.76	-0.18, 0.40	0.39, 0.06	0.13, 0.54	**-0.39, 0.05**
Right	0.14, 0.50	-0.15, 0.47	**0.43, 0.03**	0.14, 0.51	**-0.44, 0.03**

Table 3.4 Legend: Change was computed as: cumulative medication dosage (CPZ equiv.) = ($Time_2$ - $Time_1$), negative symptoms = ($Time_2$ - $Time_1$), and change in global assessment of functioning scores = ($Time_2$ - $Time_1$). **Bold** = significant values; p-values presented are uncorrected; PANSS= positive and negative syndrome score (0-6 point scale); GAF= global assessment of functioning; CPZ= chlorpromazine equivalents; † = brain volume change (Longitudinal FreeSurfer); ǂ = brain volume change (manual segmentation). Similar associations were found for both FreeSurfer and manually segmented volume changes of the hippocampus. Note: All correlations were controlled for age, gender and ICV; % volume change in brain volume = [($Time_2$ - $Time_1$)/$Time_1$)] x 100.

Fig. 3.2: Association of progressive neuroanatomical volume change with clinical variables in FEP patients

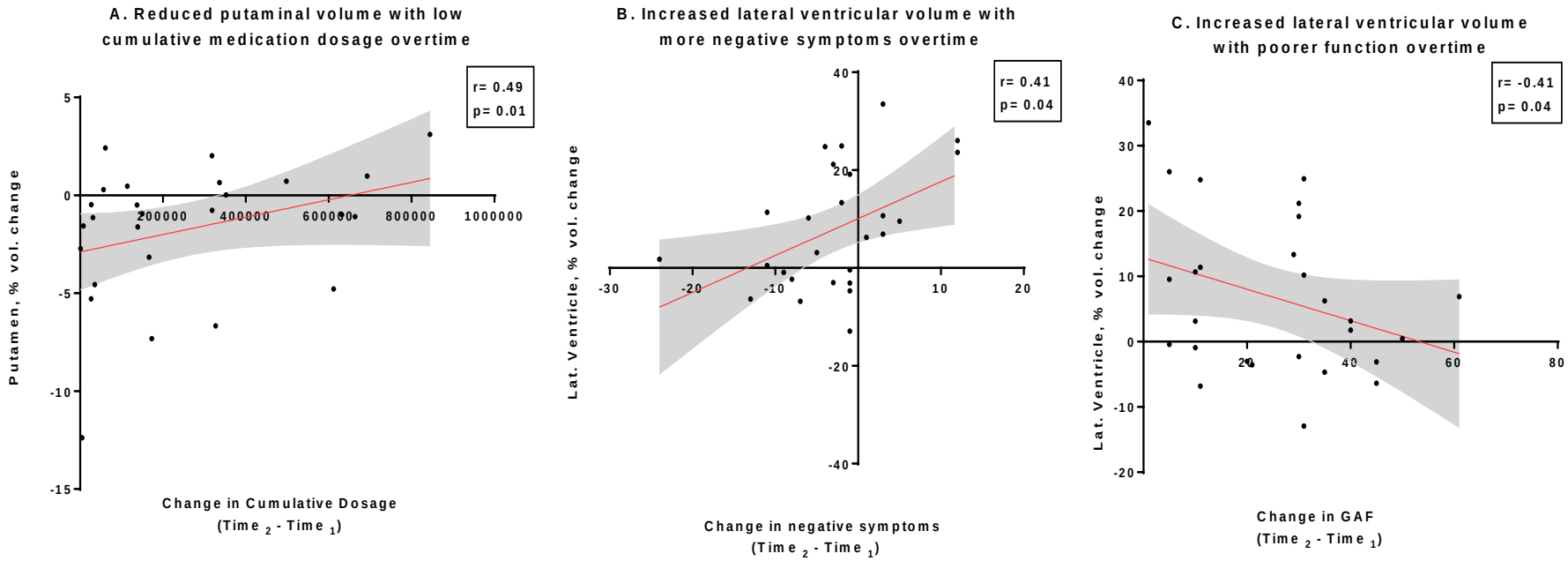

Fig. 3.2 Legend: A. Reduced putaminal volume associated with low cumulative medication dosage over time - change ($Time_2$ - $Time_1$) in total cumulative medication dosage (CPZ equiv.) significantly associate with % volume change in putamen. Increased lateral ventricular volume associated with: **B. Worsening negative symptoms over time -** change ($Time_2$ - $Time_1$) in negative symptoms significantly associate with % volume change in lateral ventricles. **C. Poorer global assessment of functioning over time -** change ($Time_2$ - $Time_1$) in global assessment of functioning scores significantly associate with % volume change in lateral ventricles in patients experiencing their first episode of psychosis during the 3-year period. Note: % volume change in brain volume = [($Time_2$ - $Time_1$)/$Time_1$)] x 100.

Fig. 3.3: Relationship between change in total volume of lateral ventricles and subcortical structures in FEP patients

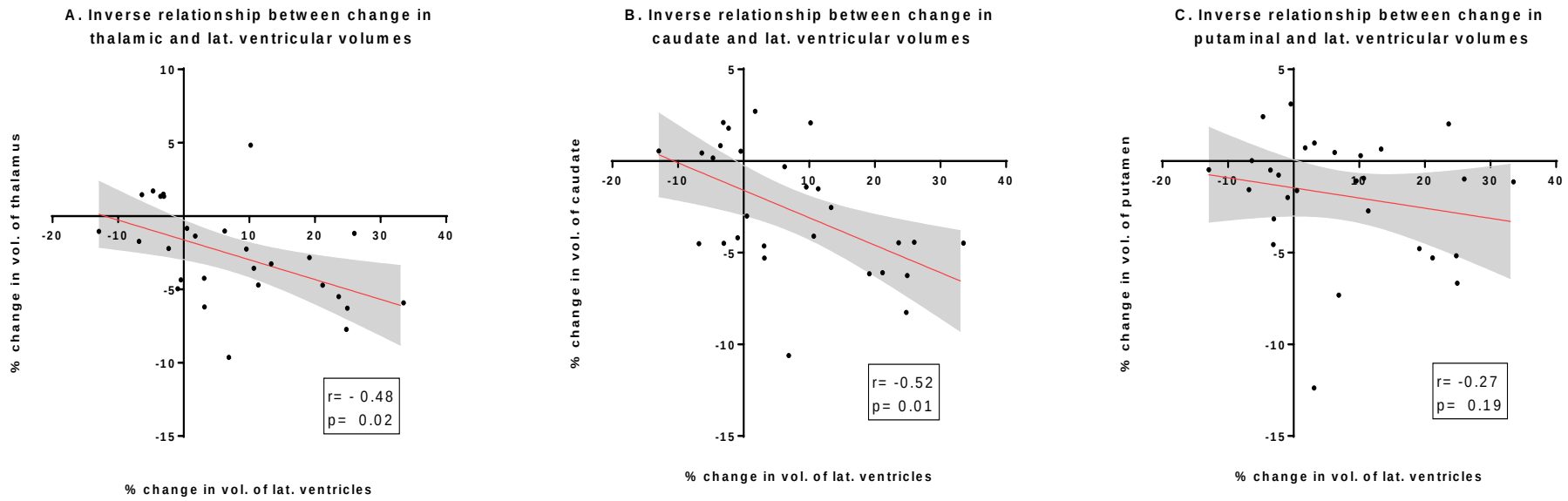

Fig. 3.3 Legend: A. Inverse relationship between change in lateral ventricular volume and thalamus – reduction in total thalamic volume significantly associate with enlargement in lateral ventricular volume over time. **B. Inverse relationship between change in lateral ventricular volume and caudate –** reduction in total caudate volume significantly associate with enlargement in lateral ventricular volume over time. **C. Inverse relationship between change in lateral ventricular volume and putamen –** reduction in total putamen volume significantly associate with enlargement in lateral ventricular volume over time. Note: All correlations were controlled for age, gender and ICV: % volume change in brain volume = $[(Time_2 - Time_1)/Time_1)] \times 100$.

3.4 Discussion

Our results indicate that there is regionally specific progression of neuroanatomical deficits amongst patients in the years after their first-episode of psychosis in this cohort. These deficits are characterised by progressive changes within dorsal striatal and thalamic regions and by right lateral ventricular enlargement. In contrast, there was relative preservation of global tissue volumes and of medial temporal lobe structures. Additionally, the progressive changes in LV volume were associated with indices of poorer outcome amongst patients as evidenced by worsening negative symptoms and functioning scores.

3.4.1 Progressive neuroanatomical changes after first-episode psychosis

Striatal volume reductions over time have been reported in some previous studies of FEP patients (Theberge *et al.* 2007; Boonstra *et al.* 2011; Ebdrup *et al.* 2011) and of treatment naive individuals at ultra-high risk of psychosis (Smieskova *at al.* 2013). However, these findings are in contrast with other studies that have reported increased putaminal and caudate volume (Massana *et al.* 2005; Glenthoj *et al.* 2007; Deng *et al.* 2009; Roiz-Santiánez *et al.* 2014) or no significant volumetric differences between FEP patients and healthy controls (Lang *et al.* 2001; Haukvik *et al.* 2016) (see Table 3.1). One potential source of this heterogeneity may relate to differential treatment with antipsychotic medications. Striatal volume reduction compared with controls is much more prominent in those who are neuroleptic naïve than in medicated patients with schizophrenia (Haijma *et al.* 2012). Long exposure to antipsychotic medications have also been linked to increased striatal volume (Corson *et al.* 1999; Okugawa *et al.* 2007; van Haren *et al.* 2007). Other longitudinal studies examining treatment naïve individuals with ultra-high risk for psychosis have reported reduced striatal volumes compared to those treated with antipsychotic medication (Smieskova *at al.* 2013; Katagiri *et al.* 2019). Thus, the use of antipsychotic medication in some cohorts may be obscuring basal ganglia reduction which is more readily detected in medication naïve sample or in those with minimal medication exposure. Patients in the present study were minimally medicated (<3 weeks) prior to their baseline scan, and only 57% were treated with SGAs at the time of the follow-up MRI scan (none with FGAs). In further support of this interpretation, high cumulative antipsychotic medication during the interscan period was correlated with increased putaminal and pallidal volumes over time in the FEP patients.

The progressive thalamic volume reduction observed in this study is consistent with some longitudinal studies of FEP (Theberge *et al.* 2007; Andreasen *et al.* 2011) and established

psychosis (van Haren *et al.* 2007; Cobia *et al.* 2017). Moreover, reduced thalamic volume has also been observed over time in individuals at high risk for psychosis (Harrisberger *et al.* 2016) and in those at high genetic liability for schizophrenia (Lawrie *et al.* 2001; McDonald *et al.* 2004). Others have reported increased thalamic volume after a short period of antipsychotic treatment (Deng *et al.* 2009; Dazzan *et al.* 2005) and no significant thalamic changes were observed in an adolescent cohort after a 3-year follow-up (de Castro-Manglano *et al.* 2011) (see Table 3.1). In this study, progressive thalamic volume reductions were not associated with the measurements of clinical outcome that were included. However other measurements of functional and cognitive performance were not assessed. The thalamus is a critical neuroanatomical hub for integration of diverse information throughout the cerebral cortex (Hwang *et al.* 2017). Our findings suggest a regional disturbance in the structural integrity of the subcortical GM sub-network involved in information transfer, that is related to an ongoing disease process in the early years of psychotic illness and the implications of which warrant further research in longitudinal studies.

We observed a trend towards a progressively increased volume of the right LV over time of a medium effect size in FEP patients compared to HCs which is consistent with a number of previous longitudinal studies (DeLisi *et al.* 1997; Lieberman *et al.* 2001; Cahn *et al.* 2002; Andreasen *et al.* 2011; Suárez-Pinilla *et al.* 2015). However, other studies failed to demonstrate significant LV enlargement over time (Puri *et al.* 2001; Massana *et al.* 2005; Nakamura *et al.* 2007; Ebdrup *et al.* 2011; Boonstra *et al.* 2011) potentially due to its highly variable structure. Our findings further indicate that the neuroprogressive process of LVs in poor clinical outcome patients, possibly relates to the observed regionally specific shrinkage of adjacent (thalamus and caudate) and remote (putamen) subcortical GM structures (Gaser *et al.* 2004) over time, considering the significant association between LVs and these subcortical structures. Thus, these associations suggest that these volumetric progressions could potentially be viewed as a biomarker of the illness. Additionally, LV enlargement over time has previously been associated with poorer clinical outcomes in a number of previous studies (Lieberman *et al.* 2001; Saijo *et al.* 2008; Ebdrup *et al.* 2011) however, this is not a consistent finding (Cahn *et al.* 2002; DeLisi *et al.* 2004; Andreasen *et al.* 2011).

3.4.2 Anatomically preserved regions after first-episode psychosis

In this study, there were observed neuroanatomical differences at baseline between FEP patients and HCs only evident for the thalamus and LV amongst the structures examined. Thus, these indicate that some baseline changes may remain static and not necessarily progress throughout illness (Schaufelberger *et al.* 2011; Olabi *et al.* 2011). The relative volume preservation of the medial temporal lobe structures (amygdala and hippocampus) over time, observed in this study is consistent with some previous studies which examined neuroanatomical progression in FEP patients (DeLisi *et al.* 1997; Wood *et al.* 2001; Lieberman *et al.* 2001; Asami *et al.* 2012). However, other studies have reported progressive hippocampal volume increment (Schaufelberger *et al.* 2011; Lappin *et al.* 2014; Bodnar *et al.* 2016) or volume reductions over time (Ebdrup *et al.* 2011). Again, differential antipsychotic medication use may contribute to these conflicting findings. For example, Ebdrup and colleagues (2011) demonstrated a dose-dependent volumetric effect of SGA on hippocampal volume, whereby FEP patients treated with more antipsychotic medication displayed hippocampal volume reductions compared to those treated with less antipsychotic medication. Of course, in observational studies it may be that patients with more severe or poorly responsive illness receive larger amounts of antipsychotic medication. It may also be that hippocampal progression is more likely in more severe schizophrenic illness (Velakoulis *et al.* 2006) than in the broader psychosis phenotype included in the current study. Indeed, differential medication usage in affective psychosis could attenuate hippocampal deficit in these patients (Hallahan *et al.* 2011). Alternatively, anatomical preservation of this region may be a potential characteristic feature of the initial stages of psychosis (Wood *et al.* 2001; Zipursky *et al.* 2004). While the FreeSurfer-acquired hippocampal volumes were relatively larger compared to manually-segmented volumes (Akudjedu *et al.* 2018), comparable case-control differences were found with both approaches, indicating that this finding does not relate to methodological bias. Interestingly, there was a moderate correlation at a statistical trend level between progressive volumetric deficit of manually segmented hippocampal volume and poorer clinical outcome as measured by positive and negative symptoms, which was not evident in the larger FreeSurfer segmented structure. This may be because the manually segmented hippocampus focusses upon the functionally specific hippocampus proper and dentate, whereas FreeSurfer segmented hippocampus includes more functionally diverse structures such as variable amounts of subiculum and tail (Akudjedu *et al.* 2018). If confirmed in a larger sample, this would be consistent with the study of Lappin and colleagues (2014) that hippocampal volume enlargement after FEP is a marker of good clinical outcome.

Global brain tissue volumes were preserved in agreement with some other studies (Schaufelberger *et al.* 2011; Roiz-Santiánez *et al.* 2014). However, some longitudinal studies report progressive decreases in global GM volume in early (Cahn *et al.* 2002; Zipparo *et al.* 2008; Andreasen *et al.* 2011) and chronic (Mathalon *et al.* 2001) stages of the disease, and others have reported a reversal of brain volume reductions over time in FEP patients (Keshavan *et al.* 1998; Schaufelberger *et al.* 2011). Despite overall preservation within the patient sample, GM volume changes were associated with cumulative antipsychotic medication use, consistent with meta-analytical findings (Vita *et al.* 2015) of a significant association between progressive loss of cortical GM volume and cumulative antipsychotic intake.

3.4.3 Strengths and Limitations

The main strength of the study is its application of a longitudinal design to a cohort of psychotic patients who were originally assessed very shortly after presentation to mental health services and with minimal antipsychotic exposure. We were also able to employ the same MRI scanner and acquisition sequences without any major software or hardware upgrades during the study period. We used the longitudinal FreeSurfer pipeline which has the advantage, compared to other analysis approaches, of accounting for inter-subject variability by creating an unbiased subject-specific anatomical template (Reuter *et al.* 2010) from the images at both time-points resulting in higher anatomical accuracy in identifying subtle changes over time. We recruited a broad psychosis phenotype for our study, rather than focus on schizophrenia spectrum disorders alone, which is more generally representative of FEP patients presenting to the mental health services. Despite the potential increase in clinical heterogeneity associated with this approach, we were able to detect regions of subcortical progression and link these with measures of clinical outcome that were not confined to a non-affective psychosis category.

The main limitation of the study was the relatively small sample size and consequent risk of error and generalisability of the results, which require confirmation in larger carefully acquired samples. We did not employ a stringent statistical approach to control for multiple comparison, however, our major findings were hypothesised a priori based on current literature. Due to inadequate data availability we were not able to assess the contribution of environmental exposures other than antipsychotic medication (e.g. cannabis use) on the neuroanatomical measures acquired.

3.4.4 Conclusion

In conclusion, this study demonstrated the existence of localised progressive neuroanatomical changes in the years after a first-episode of psychosis characterised by volume deficits in dorsal striatal and thalamic regions and by right lateral ventricular enlargement. The progressive enlargement in ventricular volume was associated with poorer clinical outcome. The progressive caudate deficits were attenuated by antipsychotic medication and the progressive thalamic deficits were not related to clinical measures. Taken together, the structural integrity of the subcortical grey matter sub-network of the cortico-striato-thalamo-cortical circuitry appears to be compromised in a progressive manner over the initial years after first presentation of a psychotic illness. As such the impact of pharmacological and non-pharmacological interventions on the anatomy of this circuit should be assessed in future larger longitudinal studies.

References

1. Akudjedu, T.N., Nabulsi, L., Makelyte, M., Scanlon, C., Hehir, S., Casey, H., Ambati, S., Kenney, J., O'Donoghue, S., McDermott, E., Kilmartin, L., Dockery, P., McDonald, C., Hallahan, B., Cannon, D.M., 2018. A comparative study of segmentation techniques for the quantification of brain subcortical volume. Brain Imaging and Behavior 12(6), 1678-1695.
2. Andreasen, N.C., Nopoulos, P., Magnotta, V., Pierson, R., Ziebell, S., Ho, B.-C., 2011. Progressive brain change in schizophrenia: a prospective longitudinal study of first-episode schizophrenia. Biological psychiatry 70(7), 672-679.
3. Andreassen, O.A., Thompson, W.K., Schork, A.J., Ripke, S., Mattingsdal, M., Kelsoe, J.R., Kendler, K.S., O'Donovan, M.C., Rujescu, D., Werge, T., Sklar, P., Psychiatric Genomics, C., Bipolar, D., Schizophrenia Working, G., Roddey, J.C., Chen, C.-H., McEvoy, L., Desikan, R.S., Djurovic, S., Dale, A.M., 2013. Improved detection of common variants associated with schizophrenia and bipolar disorder using pleiotropy-informed conditional false discovery rate. PLoS genetics 9(4), e1003455-e1003455.
4. Asami, T., Bouix, S., Whitford, T.J., Shenton, M.E., Salisbury, D.F., McCarley, R.W., 2012. Longitudinal loss of gray matter volume in patients with first-episode schizophrenia: DARTEL automated analysis and ROI validation. NeuroImage 59(2), 986-996.
5. Ayesa-Arriola, R., Roiz-Santiañez, R., Pérez-Iglesias, R., Ferro, A., Sainz, J., Crespo-facorro, B., 2013. Neuroanatomical Differences between First-Episode Psychosis Patients with and without Neurocognitive Deficit: A 3-Year Longitudinal Study. Frontiers in Psychiatry 4(134).
6. Barnes, J., Ridgway, G.R., Bartlett, J., Henley, S.M.D., Lehmann, M., Hobbs, N., Clarkson, M.J., MacManus, D.G., Ourselin, S., Fox, N.C., 2010. Head size, age and gender adjustment in MRI studies: a necessary nuisance? NeuroImage 53(4), 1244-1255.
7. Boak, A., Hamilton, H. A., Adlaf, E. M., Mann, R. E., 2017. Drug use among Ontario students,1977-2017: Detailed findings from the Ontario Student Drug Use and Health Survey (OSDUHS) (CAMH Research Document Series No. 46). Toronto, ON: Centre for Addiction and Mental Health.
8. Bodnar, M., Malla, A.K., Makowski, C., Chakravarty, M.M., Joober, R., Lepage, M., 2016. The effect of second-generation antipsychotics on hippocampal volume in first episode of psychosis: longitudinal study. BJPsych open 2(2), 139-146.
9. Boonstra, G., van Haren, N.E.M., Schnack, H.G., Cahn, W., Burger, H., Boersma, M., de Kroon, B., Grobbee, D.E., Hulshoff Pol, H.E., Kahn, R.S., 2011. Brain Volume Changes After Withdrawal of Atypical Antipsychotics in Patients with First-Episode Schizophrenia. Journal of Clinical Psychopharmacology 31(2), 146-153.
10. Cahn, W., Pol, H., Lems, E.E., et al., 2002. Brain volume changes in first-episode schizophrenia: A 1-year follow-up study. Archives of General Psychiatry 59(11), 1002-1010.
11. Cahn, W., van Haren, N.E.M., Pol, H.E.H., Schnack, H.G., Caspers, E., Laponder, D.A.J., Kahn, R.S., 2006. Brain volume changes in the first year of illness and 5-year outcome of schizophrenia. British Journal of Psychiatry 189(4), 381-382.

12. Calin-Jageman, R.J., 2018. The New Statistics for Neuroscience Majors: Thinking in Effect Sizes. Journal of undergraduate neuroscience education : JUNE : a publication of FUN, Faculty for Undergraduate Neuroscience 16(2), E21-E25.
13. Corson, P.W., Nopoulos, P., Miller, D., Arndt, S., Andreasen, N.C., 1999. Change in Basal Ganglia Volume Over 2 Years in Patients with Schizophrenia: Typical Versus Atypical Neuroleptics. American Journal of Psychiatry 156(8), 1200-1204.
14. Dazzan, P., Morgan, K.D., Orr, K., Hutchinson, G., Chitnis, X., Suckling, J., Fearon, P., McGuire, P.K., Mallett, R.M., Jones, P.B., Leff, J., Murray, R.M., 2005. Different Effects of Typical and Atypical Antipsychotics on Grey Matter in First Episode Psychosis: the ÆSOP Study. Neuropsychopharmacology 30, 765.
15. Dazzan, P., Soulsby, B., Mechelli, A., Wood, S.J., Velakoulis, D., Phillips, L.J., Yung, A.R., Chitnis, X., Lin, A., Murray, R.M., McGorry, P.D., McGuire, P.K., Pantelis, C., 2012. Volumetric Abnormalities Predating the Onset of Schizophrenia and Affective Psychoses: An MRI Study in Subjects at Ultrahigh Risk of Psychosis. Schizophrenia Bulletin 38(5), 1083-1091.
16. de Castro-Manglano, P., Mechelli, A., Soutullo, C., Gimenez-Amaya, J., Ortuño, F., McGuire, P., 2011. Longitudinal changes in brain structure following the first episode of psychosis. Psychiatry Research: Neuroimaging 191(3), 166-173.
17. DeLisi, L.E., Sakuma, M., Maurizio, A.M., Relja, M., Hoff, A.L., 2004. Cerebral ventricular change over the first 10 years after the onset of schizophrenia. Psychiatry Research: Neuroimaging 130(1), 57-70.
18. DeLisi, L.E., Sakuma, M., Tew, W., Kushner, M., Hoff, A.L., Grimson, R., 1997. Schizophrenia as a chronic active brain process: a study of progressive brain structural change subsequent to the onset of schizophrenia. Psychiatry Research: Neuroimaging 74(3), 129-140.
19. DeLisi, L.E., Tew, W., Xie, S.-h., Hoff, A.L., Sakuma, M., Kushner, M., Lee, G., Shedlack, K., Smith, A.M., Grimson, R., 1995. A prospective follow-up study of brain morphology and cognition in first-episode schizophrenic patients: Preliminary findings. Biological Psychiatry 38(6), 349-360.
20. Deng, M.Y., McAlonan, G.M., Cheung, C., Chiu, C.P.Y., Law, C.W., Cheung, V., Sham, P.C., Chen, E.Y.H., Chua, S.E., 2009. A naturalistic study of grey matter volume increase after early treatment in anti-psychotic naïve, newly diagnosed schizophrenia. Psychopharmacology 206(3), 437-446.
21. Ebdrup, B.H., Aggernaes, B., Glenthoj, B., Oranje, B., Rasmussen, H., Lublin, H., Skimminge, A., Baaré, W., 2011. Progressive striatal and hippocampal volume loss in initially antipsychotic-naive, first-episode schizophrenia patients treated with quetiapine: relationship to dose and symptoms. International Journal of Neuropsychopharmacology 14(1), 69-82.
22. Emsell, L., Langan, C., Van Hecke, W., Barker, G.J., Leemans, A., Sunaert, S., McCarthy, P., Nolan, R., Cannon, D.M., McDonald, C., 2013. White matter differences in euthymic bipolar I disorder: a combined magnetic resonance imaging and diffusion tensor imaging voxel-based study. Bipolar Disorders 15(4), 365-376.
23. First, M.B., Spitzer, R.L., Gibbon, M., Williams, J.B., 2002. Structured clinical interview for DSM-IV-TR axis I disorders, research version, patient edition. (SCID-I/P) New York: Biometrics Research, New York State Psychiatric Institute.
24. First, M.B., Spitzer, R.L., Gibbon, M., Williams, J.B., 2002. Structured clinical interview for DSM-IV-TR axis I disorders, research version, non-patient edition. (SCID-I/NP) New York: Biometrics Research, New York State Psychiatric Institute.

25. Fusar-Poli, P., Cappucciati, M., Rutigliano, G., Heslin, M., Stahl, D., Brittenden, Z., Caverzasi, E., McGuire, P., Carpenter, W.T., 2016. Diagnostic Stability of ICD/DSM First Episode Psychosis Diagnoses: Meta-analysis. Schizophrenia Bulletin 42(6), 1395-1406.
26. Gaser, C., Nenadic, I., Buchsbaum, B.R., Hazlett, A.E., Buchsbaum. M.S., 2004. Ventricular Enlargement in Schizophrenia Related to Volume Reduction of the Thalamus, Striatum, and Superior Temporal Cortex. American Journal of Psychiatry 161(1), 154-156.
27. Glenthoj, A., Glenthoj, B.Y., Mackeprang, T., Pagsberg, A.K., Hemmingsen, R.P., Jernigan, T.L., Baaré, W.F.C., 2007. Basal ganglia volumes in drug-naive first-episode schizophrenia patients before and after short-term treatment with either a typical or an atypical antipsychotic drug. Psychiatry Research: Neuroimaging 154(3), 199-208.
28. Gur, R.E., Cowell, P., Turetsky, B.I., et al., 1998. A follow-up magnetic resonance imaging study of schizophrenia: Relationship of neuroanatomical changes to clinical and neurobehavioral measures. Archives of General Psychiatry 55(2), 145-152.
29. Haijma, S.V., Van Haren, N., Cahn, W., Koolschijn, P.C.M.P., Hulshoff Pol, H.E., Kahn, R.S., 2012. Brain Volumes in Schizophrenia: A Meta-Analysis in Over 18 000 Subjects. Schizophrenia Bulletin 39(5), 1129-1138.
30. Hall, R.C.W., 1995. Global Assessment of Functioning: A Modified Scale. Psychosomatics 36(3), 267-275.
31. Hallahan, B., Newell, J., Soares, J.C., Brambilla, P., Strakowski, S.M., Fleck, D.E., Kieseppä, T., Altshuler, L.L., Fornito, A., Malhi, G.S., McIntosh, A.M., Yurgelun-Todd, D.A., Labar, K.S., Sharma, V., MacQueen, G.M., Murray, R.M., McDonald, C., 2011. Structural Magnetic Resonance Imaging in Bipolar Disorder: An International Collaborative Mega-Analysis of Individual Adult Patient Data. Biological Psychiatry 69(4), 326-335.
32. Harrisberger, F., Buechler, R., Smieskova, R., Lenz, C., Walter, A., Egloff, L., Bendfeldt, K., Simon, A.E., Wotruba, D., Theodoridou, A., Rössler, W., Riecher-Rössler, A., Lang, U.E., Heekeren, K., Borgwardt, S., 2016. Alterations in the hippocampus and thalamus in individuals at high risk for psychosis. Npj Schizophrenia 2, 16033.
33. Haukvik, U.K., Hartberg, C.B., Nerland, S., Jørgensen, K.N., Lange, E.H., Simonsen, C., Nesvåg, R., Dale, A.M., Andreassen, O.A., Melle, I., Agartz, I., 2016. No progressive brain changes during a 1-year follow-up of patients with first-episode psychosis. Psychological Medicine 46(3), 589-598.
34. Hedges, L.V., Olkin, I., 1985. Statistical methods for meta-analysis. San Diego, CA: Academic Press.
35. Ho, B.-C., Andreasen, N.C., Ziebell, S., Pierson, R., Magnotta, V., 2011. Long-term antipsychotic treatment and brain volumes: a longitudinal study of first-episode schizophrenia. Archives of general psychiatry 68(2), 128-137.
36. Hulshoff Pol, H.E., Kahn, R.S., 2008. What Happens After the First Episode? A Review of Progressive Brain Changes in Chronically Ill Patients with Schizophrenia. Schizophrenia Bulletin 34(2), 354-366.
37. Hwang, K., Bertolero, M.A., Liu, W.B., D'Esposito, M., 2017. The Human Thalamus Is an Integrative Hub for Functional Brain Networks. The Journal of Neuroscience 37(23), 5594-5607.
38. Katagiri, N., Pantelis, C., Nemoto, T., Tsujino, N., Saito, J., Hori, M., Yamaguchi, T., Funatogawa, T., Mizuno, M., 2019. Longitudinal changes in striatum and sub-

threshold positive symptoms in individuals with an 'at risk mental state' (ARMS). Psychiatry Research: Neuroimaging 285, 25-30.
39. Kay, S.R., Fiszbein, A., Opler, L.A., 1987. The Positive and Negative Syndrome Scale (PANSS) for Schizophrenia. Schizophrenia Bulletin 13(2), 261-276.
40. Kempton, M.J., Stahl, D., Williams, S.C.R., DeLisi, L.E., 2010. Progressive lateral ventricular enlargement in schizophrenia: A meta-analysis of longitudinal MRI studies. Schizophrenia Research 120(1), 54-62.
41. Keshavan, M.S., Haas, G.L., Kahn, C.E., Eduardo, A., Dick, E.L., Schooler, N.R., Sweeney, J.A., Pettegrew, J.W., 1998. Superior temporal gyrus and the course of early schizophrenia: Progressive, static, or reversible? Journal of Psychiatric Research 32(3), 161-167.
42. Lang, D. J., Kopala, L.C., Vandorpe, R.A., Rui, Q., Smith, G.N., Goghari, V.M., Honer, W.G., 2001. An MRI Study of Basal Ganglia Volumes in First-Episode Schizophrenia Patients Treated with Risperidone. American Journal of Psychiatry 158(4), 625-631.
43. Lappin, J.M., Morgan, C., Chalavi, S., Morgan, K.D., Reinders, A.A.T.S., Fearon, P., Heslin, M., Zanelli, J., Jones, P.B., Murray, R.M., Dazzan, P., 2014. Bilateral hippocampal increase following first-episode psychosis is associated with good clinical, functional and cognitive outcomes. Psychological Medicine 44(6), 1279-1291.
44. Lawrie, S.M., Whalley, H.C., Abukmeil, S.S., Kestelman, J.N., Donnelly, L., Miller, P., Best, J.J.K., Owens, D.G.C., Johnstone, E.C., 2001. Brain structure, genetic liability, and psychotic symptoms in subjects at high risk of developing schizophrenia. Biological Psychiatry 49(10), 811-823.
45. Lehman, A.F., Steinwachs, D.M., The Survey Co-Investigators of the, P.P., 1998. Patterns of Usual Care for Schizophrenia: Initial Results from the Schizophrenia Patient Outcomes Research Team (PORT) Client Survey. Schizophrenia Bulletin 24(1), 11-20.
46. Li, W., Li, K., Guan, P., Chen, Y., Xiao, Y., Lui, S., Sweeney, J.A., Gong, Q., 2018. Volume alteration of hippocampal subfields in first-episode antipsychotic-naïve schizophrenia patients before and after acute antipsychotic treatment. NeuroImage: Clinical 20, 169-176.
47. Lieberman, J., Chakos, M., Wu, H., Alvir, J., Hoffman, E., Robinson, D., Bilder, R., 2001. Longitudinal study of brain morphology in first episode schizophrenia. Biological Psychiatry 49(6), 487-499.
48. Lieberman, J.A., Stroup, T.S., McEvoy, J.P., Swartz, M.S., Rosenheck, R.A., Perkins, D.O., Keefe, R.S.E., Davis, S.M., Davis, C.E., Lebowitz, B.D., Severe, J., Hsiao, J.K., 2005. Effectiveness of Antipsychotic Drugs in Patients with Chronic Schizophrenia. New England Journal of Medicine 353(12), 1209-1223.
49. Massana, G., Salgado-Pineda, P., Junqué, C., Pérez, M., Baeza, I., Pons, A., Massana, J., Navarro, V., Blanch, J., Morer, À., Mercader, J.M., Bernardo, M., 2005. Volume changes in gray matter in first-episode neuroleptic-naive schizophrenic patients treated with risperidone. Journal of Clinical Psychopharmacology 25(2), 111-117.
50. Mathalon, D.H., Sullivan, E.V., Lim, K.O., Pfefferbaum, A., 2001. Progressive Brain Volume Changes and the Clinical Course of Schizophrenia in Men: A Longitudinal Magnetic Resonance Imaging Study. Archives of General Psychiatry 58(2), 148-157.
51. McDonald, C., Bullmore, E.T., Sham, P.C., Chitnis, X., Wickham, H., Bramon, E., Murray, R.M., 2004. Association of Genetic Risks for Schizophrenia and Bipolar

Disorder with Specific and Generic Brain Structural Endophenotypes. Archives of General Psychiatry 61(10), 974-984.
52. Miller, G.A., Chapman, J.P., 2001. Misunderstanding analysis of covariance. Journal of Abnormal Psychology 110(1), 40-48.
53. Nakamura, M., Salisbury, D.F., Hirayasu, Y., Bouix, S., Pohl, K.M., Yoshida, T., Koo, M.-S., Shenton, M.E., McCarley, R.W., 2007. Neocortical gray matter volume in first-episode schizophrenia and first-episode affective psychosis: a cross-sectional and longitudinal MRI study. Biological psychiatry 62(7), 773-783.
54. Okugawa, G., Nobuhara, K., Takase, K., Saito, Y., Yoshimura, M., Kinoshita, T., 2007. Olanzapine Increases Grey and White Matter Volumes in the Caudate Nucleus of Patients with Schizophrenia. Neuropsychobiology 55(1), 43-46.
55. Puri, B.K., Hutton, S.B., Saeed, N., Oatridge, A., Hajnal, J.V., Duncan, L.-J., Chapman, M.J., Barnes, T.R.E., Bydder, G.M., Joyce, E.M., 2001. A serial longitudinal quantitative MRI study of cerebral changes in first-episode schizophrenia using image segmentation and subvoxel registration. Psychiatry Research: Neuroimaging 106(2), 141-150.
56. Rais, M., Cahn, W., van Haren, N., Schnack, H., Caspers, E., Hulshoff Pol, H., Kahn, R., 2008. Excessive Brain Volume Loss Over Time in Cannabis-Using First-Episode Schizophrenia Patients. American Journal of Psychiatry 165(4), 490-496.
57. Reuter, M., Fischl, B., 2011. Avoiding asymmetry-induced bias in longitudinal image processing. NeuroImage 57(1), 19-21.
58. Reuter, M., Rosas, H.D., Fischl, B., 2010. Highly accurate inverse consistent registration: A robust approach. NeuroImage 53(4), 1181-1196.
59. Reuter, M., Schmansky, N.J., Rosas, H.D., Fischl, B., 2012. Within-subject template estimation for unbiased longitudinal image analysis. NeuroImage 61(4), 1402-1418.
60. Roiz-Santiánez, R., Ayesa-Arriola, R., Tordesillas-Gutiérrez, D., Ortiz-García de la Foz, V., Pérez-Iglesias, R., Pazos, A., Sánchez, E., Crespo-Facorro, B., 2014. Three-year longitudinal population-based volumetric MRI study in first-episode schizophrenia spectrum patients. Psychological Medicine 44(8), 1591-1604.
61. Saijo, T., Abe, T., Someya, Y., Sassa, T., Sudo, Y., Suhara, T., Shuno, T., Asai, K., Okubo, Y., 2008. Ten year progressive ventricular enlargement in schizophrenia: An MRI morphometrical study. Psychiatry and Clinical Neurosciences 55(1), 41-47.
62. Scanlon, C., Anderson-Schmidt, H., Kilmartin, L., McInerney, S., Kenney, J., McFarland, J., Waldron, M., Ambati, S., Fullard, A., Logan, S., Hallahan, B., Barker, G.J., Elliott, M.A., McCarthy, P., Cannon, D.M., McDonald, C., 2014. Cortical thinning and caudate abnormalities in first episode psychosis and their association with clinical outcome. Schizophrenia Research 159(1), 36-42.
63. Schaufelberger, M.S., Lappin, J.M., Duran, F.L.S., Rosa, P.G.P., Uchida, R.R., Santos, L.C., Murray, R.M., McGuire, P.K., Scazufca, M., Menezes, P.R., Busatto, G.F., 2011. Lack of progression of brain abnormalities in first-episode psychosis: a longitudinal magnetic resonance imaging study. Psychological Medicine 41(8), 1677-1689.
64. Sled, J.G., Zijdenbos, A.P., Evans, A.C., 1998. A nonparametric method for automatic correction of intensity nonuniformity in MRI data. IEEE Transactions on Medical Imaging 17(1), 87-97.
65. Smieskova, R., Marmy, J., Schmidt, A., Bendfeldt, K., Riecher-Rossler, A., Walter, M., Lang, U.E., Borgwardt, S., 2013. Do Subjects at Clinical High Risk for Psychosis Differ from those with a Genetic High Risk? - A Systematic Review of Structural and Functional Brain Abnormalities. Current Medicinal Chemistry 20(3), 467-481.

66. Suárez-Pinilla, P., Roiz-Santiánez, R., Mata, I., Ortiz-García de la Foz, V., Brambilla, P., Fañanas, L., Valle-San Román, N., Crespo-Facorro, B., 2015. Progressive Structural Brain Changes and NRG1 Gene Variants in First-Episode Nonaffective Psychosis. Neuropsychobiology 71(2), 103-111.
67. Taylor, D.A., Paton, C., Kerwin, R., 2007. Maudsley Prescribing Guidelines. CRC Press
68. Theberge, J., Williamson, K.E., Aoyama, N., Drost, D.J., Manchanda, R., Malla, A.K., Northcott, S., Menon, R.S., Neufeld, R.W.J., Rajakumar, N., Pavlosky, W., Densmore, M., Schaefer, B., Williamson, P.C., 2007. Longitudinal grey-matter and glutamatergic losses in first-episode schizophrenia. British Journal of Psychiatry 191(4), 325-334.
69. van Haren, N., Cahn, W., Hulshoff Pol, H., Kahn, R., 2012. The course of brain abnormalities in schizophrenia: can we slow the progression? Journal of Psychopharmacology 26(5_suppl), 8-14.
70. van Haren, N.E.M., Cahn, W., Hulshoff Pol, H.E., Kahn, R.S., 2008. Schizophrenia as a progressive brain disease. European Psychiatry 23(4), 245-254.
71. van Haren, N.E.M., Hulshoff Pol, H.E., Schnack, H.G., Cahn, W., Mandl, R.C.W., Collins, D.L., Evans, A.C., Kahn, R.S., 2007. Focal Gray Matter Changes in Schizophrenia across the Course of the Illness: A 5-Year Follow-Up Study. Neuropsychopharmacology 32, 2057.
72. Velakoulis, D., Wood, S.J., Wong, M.T.H., McGorry, P.D., Yung, A., Phillips, L., Smith, D., Brewer, W., Proffitt, T., Desmond, P., Pantelis, C., 2006. Hippocampal and Amygdala Volumes According to Psychosis Stage and Diagnosis: A Magnetic Resonance Imaging Study of Chronic Schizophrenia, First-Episode Psychosis, and Ultra–High-Risk Individuals. Archives of General Psychiatry 63(2), 139-149.
73. Vita, A., De Peri, L., Deste, G., Barlati, S., Sacchetti, E., 2015. The Effect of Antipsychotic Treatment on Cortical Gray Matter Changes in Schizophrenia: Does the Class Matter? A Meta-analysis and Meta-regression of Longitudinal Magnetic Resonance Imaging Studies. Biological Psychiatry 78(6), 403-412.
74. Vita, A., De Peri, L., Silenzi, C., Dieci, M., 2006. Brain morphology in first-episode schizophrenia: A meta-analysis of quantitative magnetic resonance imaging studies. Schizophrenia Research 82(1), 75-88.
75. Whitwell, J.L., 2008. Longitudinal imaging: change and causality. Current Opinion in Neurology 21(4), 410-416.
76. Wood, S.J., Velakoulis, D., Smith, D.J., Bond, D., Stuart, G.W., McGorry, P.D., Brewer, W.J., Bridle, N., Eritaia, J., Desmond, P., Singh, B., Copolov, D., Pantelis, C., 2001. A longitudinal study of hippocampal volume in first episode psychosis and chronic schizophrenia. Schizophrenia Research 52(1), 37-46.
77. Woods, S.W., 2003. Chlorpromazine equivalent doses for the newer atypical antipsychotics. J. Clin. Psychiatry, 64, 663-667
78. Zipparo, L., Whitford, T.J., Redoblado Hodge, M.A., Lucas, S., Farrow, T.F.D., Brennan, J., Gomes, L., Williams, L.M., Harris, A.W.F., 2008. Investigating the neuropsychological and neuroanatomical changes that occur over the first 2–3 years of illness in patients with first-episode schizophrenia. Progress in Neuro-Psychopharmacology and Biological Psychiatry 32(2), 531-538.
79. Zipursky, R.B., Christensen, B.K., Mikulis, D.J., 2004. Stable deficits in gray matter volumes following a first episode of schizophrenia. Schizophrenia Research 71(2), 515-516.

Chapter 4

Study 3

Progression of cortical changes after first-episode of psychosis: A 3-year longitudinal sMRI study

Theophilus N. Akudjedu[a*], Giulia Tronchin[a], Shane McInerney[a,e], Cathy Scanlon[a], Joanne P.M. Kenney[d], John McFarland[a], Gareth J. Barker[c], Peter McCarthy[b], Dara M. Cannon[a], Brian Hallahan[a], Colm McDonald[a]

[a]Centre for Neuroimaging & Cognitive Genomics (NICOG), Clinical Neuroimaging Laboratory, NCBES Galway Neuroscience Centre, College of Medicine Nursing and Health Sciences, National University of Ireland Galway, H91TK33 Galway, Ireland. [b]Department of Radiology, College of Medicine Nursing and Health Sciences, National University of Ireland Galway, H91TK33 Galway, Ireland. [c]King's College London, Institute of Psychiatry, Psychology & Neuroscience, Department of Neuroimaging, Centre for Neuroimaging Sciences, London, UK. [d]Trinity College Institute of Neuroscience and School of Psychology, Trinity College Dublin, Dublin, Ireland. [e]Department of Psychiatry, University of Toronto, 250 College Street, 8th floor, Toronto, Canada.

for submission to Psychological Medicine

Author's Contribution

The original data for this study was acquired prior to commencement of the current PhD research. Authors CMc, DMC and BH designed and supervised the general progress of the study. CS, JPMK, SMc, JM recruited and collected data. GJB and PMc worked to optimise MRI sequences. I carried out all MRI and statistical analyses reported in this study. Furthermore, I wrote the entire manuscript with the input of all authors who have approved the final manuscript under the supervision of CMc, DMC and BH.

Abstract

Background: The progressive profile of cortical abnormalities after the first-episode of psychosis (FEP) remains unclear. We assessed progressive changes across the cortical mantle over a 3-year period in individuals following FEP compared with healthy controls (HC), and whether cortical changes were associated with clinical and functional outcome.

Methods: Twenty-eight individuals with FEP and 28 HCs underwent 1.5T MRI imaging at baseline and 3-year follow-up. The longitudinal FreeSurfer pipeline (v.5.3.0) was used for cortical reconstructions and vertex-wise linear regression analyses were used to compare rates of progressive thickness change. Independent group analyses of covariance was used to compare rates of thickness change of the abnormal cortical regions (ROI). Partial correlations were used to determine associations between rates of cortical thickness change from the ROI and clinical/functional characteristics. Age and gender were included as covariates.

Results: In FEP patients relative to HCs, there was a significantly increased rate of cortical thinning [$F(1,52)=5.11$, $p=0.028$)] at a mean difference of 0.844% [95% CI (0.095, 1.593)] (Fig.4.3A) in the left lateral orbitofrontal region (LLOFR) over the 3-year period. Rates of cortical thinning in the LLOFR of FEP patients did not associate with changes in clinical or functional measures over time.

Conclusions: Our results indicate progressive rates of cortical thinning in the LLOFR after FEP suggestive of a disturbance in the structural integrity of the associative/cognitive component of the cortico-striato-thalamo-cortical circuitry. Cortical thinning in the LLOFR of FEP patients is not a neuroanatomical marker of clinical or functional outcome. This study lends weight to the evidence that there is early regional neuroanatomical progression after FEP.

Keywords: first-episode psychosis, structural MRI, cortical thickness, longitudinal study, progressive changes

4.1 Introduction

Neuroanatomical abnormalities are already present at the time of first-episode of psychosis (FEP) as demonstrated by structural magnetic resonance imaging studies (Pantelis *et al.* 2003; Andreasen *et al.* 2011; Olabi *et al.* 2011). The period of time after the onset of psychosis may represent a critical phase for clinical intervention considering evidence from longitudinal studies for progression of brain changes across the cortical mantle after FEP (Cahn *et al.* 2002; Andreasen *et al.* 2011; Guo *et al.* 2015). Despite extensive research, the progressive profile of cortical abnormalities after FEP and the clinical and environmental factors associated with neuroprogression are not fully understood. Cortical thickness change has been demonstrated to strongly influence volumetric reductions (Panizzon *et al.* 2009). Given that cortical thickness is highly heritable and may be influenced by specific cellular mechanisms (Winkler *et al.* 2010) such as synaptic pruning and myelination (Goldstone *et al.* 2018), it therefore represents an important morphometric measure for the identification of prognostically meaningful biological markers in patients experiencing their FEP.

In some longitudinal FEP studies, cortical thinning was observed in the frontal and prefrontal regions over time (Andreasen *et al.* 2011; Roiz-Santianez *et al.* 2014; Gutiérrez-Galve *et al.* 2015). Similarly, a meta-analytic investigation of longitudinal MRI studies of FEP schizophrenia patients showed a significant pattern of progressive grey matter volume reduction in the frontal, temporal, parietal lobes and in the Heschl's gyrus relative to healthy controls (HCs) (Vita *et al.* 2012). In a more established schizophrenia cohort followed-up after two years, an exaggerated cortical thinning of the middle frontal, superior temporal, and middle temporal gyri was revealed (Cobia *et al.* 2012). Furthermore, in individuals with an "at risk mental state" (ARMS) who subsequently developed psychosis, a progressive reduction of the right superior frontal, middle frontal and medial orbitofrontal regions relative to HCs and ARMS individuals who did not develop psychosis was observed (Cannon *et al.* 2015). Thus, the diagnostic transitioning from ARMS to the time of FEP is characterised by excessive cortical changes over time, mostly pronounced in the frontal and temporal regions (Nakamura *et al.* 2007) and may be attributable to cortical grey matter tissue loss over time across the entire course of the illness (van Haren *et al.* 2011). Additionally, a number of other studies have similarly demonstrated increased global cortical thinning, particularly pronounced in the frontal cortex (Roiz-Santianez *et al.* 2014; Guo *et al.* 2015) with significant tissue loss in the frontal, temporal and parietal cortices of FEP patients compared to HCs over time (de Castro-Manglano *et al.* 2011). However, this is not a consistent finding with no significant cortical changes demonstrated over time (Dickey *et al.*

2004; Haukvik *et al.* 2016) (Table 4.1 and 4.2). These inconsistencies regarding cortical progression after FEP are potentially due to embedded study heterogeneities of a clinical (e.g. variable clinical severity, antipsychotic medication use and follow-up times) and methodological (e.g. different image acquisition and analysis techniques) nature.

Some longitudinal studies initiated at FEP indicate that the disease process of excessive cortical thinning may be partly moderated or related to environmental factors such as cannabis use over time (Rais *et al.* 2010), clinical factors such as illness severity and medication dose (van Haren *et al.* 2011; Vita *et al.* 2012) and genetic susceptibility (Vazquez-Bourgon *et al.* 2016).

Although several studies have investigated the cross-sectional relationship between cortical changes and clinical/functional measures in FEP, few have carried out longitudinal analyses to clarify the extent and location of progressive changes and their associations over time. The current naturalistic longitudinal study therefore seeks to investigate the progressive profile of cortical thickness changes in individuals with FEP compared to HCs over a 3-year period. Additionally, we wanted to ascertain if any such changes would be related to a number of clinical variables including severity of symptoms, antipsychotic medications and level of functioning.

Table 4.1: Longitudinal neuroimaging studies initiated in first-episode psychosis that examined cortical thickness change over time

Reference	Diagnosis, n, Age (SD) in years		DOI, DUP	Medications/Duration of Treatment		Approx. Average Follow-up period	Study Re-recruitment Rate (%)	MRI/Processing Method	Brain Regions Examined	Findings in relation to cortical thickness change in patients and controls over time
	Patients	Controls		Duration of Treatment prior to baseline Scan	Treatment during follow-up					
Rais *et al.* 2010	SCZ; Cannabis+ n=19/ (29.44±8.21)	n=31/ (24.72±6.66)	DOI: 61.3 weeks	17 weeks	FGA, SGA	5 years	92.9	1.5T /The CLASP algorithm was used to estimate change in cortical thickness for every vertex in individual space, then transformed to the ICBM template for visualisation.	multiple brain regions	Progressive cortical thinning of the right supplementary motor cortex, inferior frontal cortex, superior temporal gyrus, angular gyrus, occipital and parietal lobe was found in patients compared to controls after controlling for cannabis use.
	SCZ; Cannabis- n=32/ (23.28±5.10)		DOI: 50.1 weeks	11 weeks						
Roiz-Santiánez *et al.* 2015	SCZ; n=109/ (29.44±8.21)	n=76/ (27.80±7.73)	DOI: 94.6 weeks DUP: 44.0 weeks	<5 weeks	SGA, OM	3 years	82.2	1.5 T/BRAINS2	multiple brain regions	At baseline, patients demonstrated cortical thinning in the frontal, temporal, parietal and occipital lobes. Increased cortical thinning globally and in particular in the frontal cortex was demonstrated in the control group over time.
Gutiérrez-Galve *et al.* 2015	het; n=27/ (25.9±6.5)	n=25/ (26.8±7.1)	unclear	≤12 weeks	FGA, SGA	2 years	69.3	1.5T /Longitudinal FreeSurfer version 4.5.0 was used for surface-based morphometric parcellation and estimation of thickness change over time based on the Desikan-Killarney Atlas.	multiple brain regions	Progressive cortical thinning was found in the superior and inferior frontal and, to a lesser extent in the superior temporal cortex in the patient group compared to controls.
Haukvik *et al.* 2016	het; n=79/ (27.6±7.7)	n=82/ (29.3±7.2)	DUP: 123 weeks	< 52 weeks	FGA, SGA, OM	1 year	58.5	1.5T /Longitudinal FreeSurfer (v5.3.0) was used to estimate cortical thickness change over time and expressed as annual percentage change (PC) from the baseline at each vertex.	Multiple brain regions	No significant longitudinal cortical thickness changes were found between patients and controls.
Vázquez-Bourgon *et al.* 2016	rs6675281;Leu/leu; n=46 (29.3±7.5)	-	DUP: 55.6 weeks DOI: 124.8 weeks	unclear	SGA, OM	3 years	unclear	1.5 T/BRAINS2	multiple brain regions	Patients homozygous for the Leu allele of the rs6675281 SNP had a significant progressive cortical thinning while those carrying the Phe allele presented an increase in thickness. When combining the two SNPs a synergic effect on thickness progression was observed, presenting those patients homozygous for Leu607 +Ser704 a more pronounced cortical thinning.
	Rs6675281;Phe-Ca; n=17 (32.7±9.7)		DUP: 66.4 weeks DOI: 89.6 weeks							
	rs821616;Ser/Ser; n=4 (27.7±2.6)		DUP: 13.6 weeks DOI: 47.6 weeks							
	rs821616;Cys-Car; n=56 (29.7±7.9)		DUP: 56.4 weeks DOI: 110.4 weeks							

Buchy *et al.* 2017*	het; n=128/ (24.2±4.0)	-	DUP: 49.1 weeks DOI: 306.8 weeks	<4 weeks	FGA, SGA	1 years 2 years	57.0 34.0	1.5T / CIVET (v2.0.0) was used for vertex-based corticometric analysis using the Surf Stat toolbox within MATLAB to assess differences in cortical thickness.	multiple brain regions	A worsening of insight between 1 and 2 years follow-up was associated with cortical thinning in the right dorsal pre-central and postcentral gyri
Buchy *et al.* 2018*	het; n=130/ (24.1±4.1)	n=52/ (24.3±3.4)	DUP: 48.3 weeks DOI: 301.6 weeks	<4 weeks						Progressive increase in cortical thickness was found in the precentral gyrus bilaterally, extending to the right premotor cortex and paracentral lobule in patients. In controls, progressive increase in cortical thickness was found in the right posterior cingulate gyrus after one year.
Pawełczyk *et al.* 2018	SCZ; PUFA, n=18/ (23.06 ±4.90) SCZ; Placebo, n=11 (22.00±3.77)	-	Mean DUP:11.9 weeks Mean DUP: 9.8 weeks	Not stated	FGA, SGA, PUFA	6 months	62.0	1.5T /Longitudinal FreeSurfer (v5.3.0) was used to estimate cortical thickness change over time and expressed as symmetrised percentage change (SPC) at each vertex.	multiple brain regions	The placebo group demonstrated significantly greater cortical thinning in the parieto-occipital cortex of the left hemisphere on the border of Brodmann areas 7 and 19 than the PUFA-treated group.

Table 4.1 Legend: *two follow-up times; SCZ = schizophrenia; het = heterogenous sample; DOI = duration of illness; DUP = duration of untreated psychosis; Tx = treatment; FGA = first-generation antipsychotics; SGA = second-generation antipsychotics; OM= other medications (mainly, mood stabilisers and antidepressants); PUFA = n-3 polyunsaturated fatty acids as add-on therapy; Disrupted-in-Schizophrenia 1 (DISC1) gene variant type for SNP rs6675281, and Disrupted-in-Schizophrenia 1 (DISC1) gene variant type for SNP rs821616; Age = age at baseline.

Table 4.2: Longitudinal neuroimaging studies initiated in first-episode psychosis that examined cortical grey matter volume change over time

Reference	Diagnosis, n, Age (SD) in years		DOI, DUP	Medications/Duration of Treatment		Approx. Average Follow-up period	Study Re-recruitment Rate (%)	MRI/Processing Method	Brain Regions Examined	Findings in relation to cortical volume changes in patients and controls
	Patients	Controls		Duration of Treatment prior to baseline Scan	Treatment during follow-up					
Kasai *et al.* 2003	SCZ; n=13/ (27.3±8.5) AFF; n=15/ (21.8±2.9)	n=22/ (25.0 ±4.3)	unclear	1 week ≤1 week	FGA, SGA, OM	1.5 years	75.8	1.5T/manual tracing (3D Slicer software package)	Heschl's gyrus, planum temporale, temporal lobe	Patients showed a progressive decrease in grey matter volume of the left superior temporal gyrus, Heschl's gyrus and the planum temporale.
Dickey *et al.* 2004	SCZ; n=12/ (28.1±8.4) AFF; n=10/ (22.9±2.8)	n=15/ (25.4 ±4.5)	unclear	unclear	FGA, SGA	1.5 years	45.9	1.5T/manual tracing	prefrontal cortex	Prefrontal grey matter was reduced at baseline in volume in the schizophrenia group compared to the other two groups. No difference in change in prefrontal cortical volume over time between the groups was demonstrated
Whitford *et al.* 2006	SCZ; n=25/ (22.1±3.2)	n=26/ (22.0±4.4)	DUP: 23.6 weeks	unclear	SGA	2–3 years	58.0	1.5T/ Voxel-based morphometry	multiple brain regions	Greater progressive grey matter volume reduction, especially in the parietal and temporal cortices in patients compared to controls.
Theberge *et al.* 2007*	SCZ; n=16/ (25.0±8.0)	n=16/ (29.0 ±12.0)	DOI: 96.2 weeks DUP: 96.2 weeks	Naïve	FGA, SGA, OM	10 months 30 months	100.0	4T/ Voxel-based morphometry	multiple brain regions	Limited cortical grey matter reductions were seen in patients at 10 months followed by widespread grey matter volume reduction at 30 months especially in the temporal and limbic lobes
Nakamura *et al.* 2007	SCZ; n=17/ (24.7±7.0) AFF; n=21/ (22.4±3.2)	n=26/ (23.6 ±4.1)	unclear	3 weeks 1 week	FGA, SGA, OM	1.5 years	64.6	1.5T/Expectation-maximization atlas tissue segmentation and manual segmentation	neocortex	Frontal and temporal cortical grey matter volume reductions were found in the schizophrenia patient group. In contrast, the affective patient group showed a greater cortical grey matter volume increase compared to the SCZ group.
Salisbury *et al.* 2007	SCZ; n=16/ (26.4±8.1) AFF; n=17/ (22.4±3.6)	n=20/ (24.5±4.1)	unclear	1 week ≤1 week	FGA, SGA, OM	1.5 years	50.7	1.5T/manual tracing (3D Slicer software package)	Heschl's gyrus	Individuals with schizophrenia demonstrated reduced volume of the Heschls gyrus compared to the individuals with an affective psychosis and healthy controls.
Koo *et al.* 2008	SCZ; n=17/ (23.9±5.5) AFF; n=18/ (22.8±4.5)	n=18/ (23.0 ±3.2)	DOI: 11.2 weeks DOI: 8.2 weeks	3 weeks 1 week	FGA, SGA, Other	1.5 years	44.2	1.5T/ manual tracing on a workstation	Cingulate gyrus	FESZ patients showed progressive gray matter volume reductions in the subgenual, affective , cognitive and posterior cingulate subregions compared with HCs. In contrast, patients with FEAFF showed progressive volume reductions in the subgenual sub-region compared to healthy controls.
Mane *et al*. 2009	SCZ; n=15/ (25.56±5.77)	n=11/ (30.31±4.36)	DUP: 23.1 weeks	Naïve	FGA, SGA	4 years	57.8	1.5T/ Voxel-based morphometry	multiple brain regions	Excessive decrease in grey matter was found in patients as compared to controls in the left superior temporal gyrus, right orbitofrontal gyrus with excessive increase in the bilateral lingual gyrus and right cuneus.
Takahashi *et al.* 2009	SCZ; FEP, n=23/ (21.6 ± 3.5)	n=26/ (25.6 ± 9.1)	DOI: 9.4 weeks	<4 weeks	FGA, SGA, OM	2 years	unclear	1.5T/Manual parcellation (Dr View	insular cortex	FEP patients showed significant gray matter reduction of the insular cortex over time (4.3%) compared to controls (0.3%). Individuals with chronic

	SCZ; chronic, n=11 (32.7 ± 7.6)		DOI: 624 weeks	unclear				software)		schizophrenia (1.7%) did not differ significantly from FEP patients or healthy controls in relation to reduced volume of the insula.
Takahashi *et al.* 2010, 2011	FEP, n=18/ (23.1 ± 4.7)	n=20/ (23.2 ± 5.7)	DOI: 43.2 weeks	< 4 weeks	FGA, SGA, OM	3 years	unclear	1.5T/Manual parcellation (Dr View 5 software package)	Superior temporal gyrus, Fusiform gyrus, middle temporal gyrus, inferior temporal gyrus	FEP patients showed significantly greater reductions in volume of the fusiform and superior temporal gyrus compared to healthy controls and individuals with schizotypal personality disorder.
	Schizotypal, n=13 (22.8 ± 5.0)		DOI: 265.2 weeks	unclear						
de Castro-Manglano *et al.* 2011	het; n=22/ (18.50± 4.00)	n=17/ (18.30 ±5.80)	DUP: 10 weeks	28.46 weeks	FGA, SGA, OM	3 years	90.7	1.5T/ Voxel-based morphometry	multiple brain regions	There were significant reductions in the frontal, temporal and parietal cortices in the controls but not in the patients. Similar longitudinal reductions in regional brain volumes were demonstrated in patients with affective psychoses but not in individuals with schizophrenia.
Asami *et al.* 2012	SCZ; n=33/ (22.50±6.70)	n=36/ (22.90 ±3.80)	DOI: 19.5 weeks	<20 weeks	FGA, SGA, OM	1.5 years	63.8	1.5T/ Voxel-based morphometry	multiple brain regions	Patients showed significant grey matter volume reductions compared to controls in the left superior temporal gyrus including Heschl's gyrus, and in widespread brain neocortical regions of frontal, parietal, and limbic regions including the cingulate gyrus.
Ohtani *et al.* 2018	SCZ; n=21/ (25.5±8.2)	n=23/ (23.0 ±3.6)	DUP: 0.9 week	2 weeks	FGA, SGA, OM	1.5 years	100.0	1.5T/FreeSurfer and manual parcellation techniques	prefrontal cortex	The SCZ group showed significant progressive grey matter volume reduction in the left superior frontal gyrus, bilateral middle frontal gyrus and bilateral inferior frontal gyrus while the AFF group showed no significant difference in grey matter volume compared with healthy controls.
	AFF; n=24/ (23.3±4.9)		DUP: 0.2 week	1 week						

Table 4.2 Legend: *two follow-up times; SCZ = schizophrenia; het = heterogenous sample; DOI = duration of illness; DUP = duration of untreated psychosis; Tx = treatment; FGA = first-generation antipsychotics; SGA = second-generation antipsychotics; OM= other medications (mainly, mood stabilisers and antidepressants). If treatment naïve, DOI = DUP; Age = age at baseline.

4.2 Methods

4.2.1 Participants and clinical assessment

Participants for this study were recruited from the Galway University Hospital (GUH) and the Mental Health Services within the West of Ireland. For this study, however, all the participants were drawn from the broader research project: "The Galway First Episode Psychosis Study" and were included only if they have previously participated in the first phase of the study and had no contraindications to MRI procedures. The recruitment and clinical assessment strategies employed were previously described in detail by Scanlon and colleagues (2015) and briefly summarised in sections 3.2.1, 3.2.2 and 3.2.3 of chapter 3. As stated previously (Kenney et al. 2015), schizophrenia, schizoaffective disorder, psychotic disorder not otherwise specified (NOS), substance induced psychosis and delusional disorder were defined as non-affective types of psychoses whereas bipolar I disorder and major depressive disorder were defined as affective types of psychoses for further subcategory analyses in patients.

4.2.2 MRI data acquisition and pre-processing

The MRI data acquisition protocol used on the 1.5 Tesla Siemens Magnetom Symphony scanner (Erlangen, Germany) and the image pre-processing approach employed with the non-parametric non-uniform intensity normalisation (N3) at both baseline and follow-up phases of the study were described previously by Scanlon and colleagues (2015) as per sections 3.2.4 and 3.2.5 of chapter 3.

4.2.3 Image analysis

As per section 3.2.6 of chapter 3, the longitudinal pipeline of the FreeSurfer (v.5.3.0) processing pipeline (http://surfer.nmr.mgh.harvard.edu/)(Reuter *et al.* 2012) was employed for preparation of the cortical surfaces and to track its progression after FEP within groups over time.

4.2.3.1 Cortical reconstruction and measurement of thickness

Cortical reconstruction of the MRI data from each time-point was independently processed with the default workflow using the *recon-all* function in FreeSurfer as per section 2.2.8 of chapter 2 (Akudjedu *et al.* 2018). Briefly, the steps included the automatic removal of non-brain tissues such as the skull, brain stem and cerebellum (Segonne *et al.* 2004; Desikan *et al.* 2006) and transformation of all data into the Talairach space. Based on a linear combination

of voxel intensities and local geometric constraints, reconstruction of the grey/white matter boundary and the cortical surfaces (Dale *et al.* 1999; Han *et al.* 2006) were segmented to reduce intra-subject morphological variability (Reuter *et al.* 2010) and divided into the two hemispheres. The surfaces were then tessellated into approximately 160,000 vertices per hemisphere resulting in a triangulated cortical surface which was refined to minimise the voxel-based nature of the initial curvature. These were spherically inflated and registered to a common space for spherical deformation and automatic identification of gyral and sulcal regions with reference to a population atlas (Fischl *et al.* 1999). The resulting surfaces were transferred to Talairach space, allowing direct and anatomically accurate measurement of thickness. With information from both time-points, an unbiased average anatomical template was created as an initial guess for initialisation of the longitudinal runs as described previously (chapter 3, section 3.2.6).

For quality control, all parcellations and cortical reconstructions for each participant were visually inspected for gross topological defects and inaccuracies. When deemed necessary, these were corrected according to the established FreeSurfer quality check and control guidelines (http://surfer.nmr.mgh.harvard.edu/) using a combination of automatic and manual methods (Segonne *et al.* 2007). Cortical thickness was calculated at each vertex from a specified triangulated surface as the average distance between a point on the grey/white matter boundary and the pial surface (Fischl and Dale, 2000; Han *et al.* 2006). The accuracy of this measurement approach was previously validated by direct comparison with cortical thickness measures from post-mortem brains (Rosas *et al.* 2002).

For computation of cortical thickness maps, differences between groups over time were computed from the longitudinal runs for each participant over the two time-points. The longitudinal temporal data from each subject was then transformed to the symmetrised rate of change maps using the *mris_slopes* function of the longitudinal two-stage model (Reuter *et al.* 2012) in FreeSurfer for group comparisons. The metric of symmetrised percent change (spc) per year (in % per year) reflects the total change in thickness, scaled by the interscan interval, expressed as a percentage of the average thickness (in millimetres) across the two time points. Presented mathematically as;

$$\text{spc} = 100 \times [\text{rate of cortical thickness change} / \text{temporal average cortical thickness}] \quad \textit{eqn (1)}$$

However, percent change (pc1) is the rate with respect to the thickness at the baseline, thus;

$$\text{pc1} = [\text{rate of cortical thickness change} / \text{thickness at baseline}] \quad \textit{eqn (2)}$$

Following the FreeSurfer recommendations (http://surfer.nmr.mgh.harvard.edu/) for a robust measure of cortical thickness change with increased statistical power, the spc in average cortical thickness was used in the current study. Cortical thickness at baseline is relatively noisier than the temporal average over the two time-points, furthermore, computation of spc is sensitive to the ordering of thickness values from the various time-points within the equation. Thus, the symmetrised percentage change (spc) was considered optimal for this study because it is relatively less prone to the effects of noise, it is symmetric and finally as recommended in the FreeSurfer guidelines for its efficient use, this study has equal number of participants at both time-points.

Prior to statistical analyses, all the longitudinal cortical thickness maps were smoothed using a 20-mm full width of half maximum (FWHM) Gaussian kernel to alleviate the voxel-based nature of the initial curvature and mapped to an average surface (*fsaverage*) as previously done by Zak and colleagues (2019).

4.2.4 Statistical analysis

4.2.4.1 Group comparison of cortical thickness changes over time

In QDEC®, global longitudinal vertex-wise linear regressions were conducted to determine the effect of diagnosis on the dependent variable of symmetrised percent thickness change (% per year) across the cortical mantle while controlling for age at baseline. Scan interval was not included in the rate of change model as it was already accounted for in the calculation of the dependent variable (spc). Furthermore, spc does not depend on intracranial volume, and is less dependent on baseline values than measures such as percent change (pc1) (Berry, 1989; Berry and Ayers, 2001). For the group effect of diagnosis on progressive cortical thickness change, participants were contrasted as FEP patients and HCs. The Monte Carlo null-z (a permutation-based) strategy which employs 10,000 vertex-wise iterations (Hagler *et al.* 2006) with an initial cluster-forming threshold of $p<0.05$ was implemented for multiple comparisons to reduce the probability of type I errors. The identified clusters were extracted and averaged for further analyses.

4.2.4.2 Analyses of clinico-demographic measures and association with clinical variables

Additional statistical analyses were performed with the Statistical Package for Social Sciences (SPSS, v.24.0) for Windows (SPSS Inc., IBM, New York, USA). Detailed descriptions of the analytic approaches for comparing clinico-demographic differences between groups over time were previously presented (chapter 3, section 3.2.7). We conducted independent

ANCOVAs to compute group (FEP vs HCs) and (affective vs non-affective vs HCs) comparisons over the extracted ROI cortical thickness at baseline and the change measure (spc). Furthermore, we used partial correlations to assess the association of thickness change over time (spc) in the patient group with change ($Time_2 – Time_1$) in clinical and functional variables. A two-tailed α level of 0.05 was used for statistical testing. Age at baseline and gender were added as covariates.

4.3 Results

4.3.1 Clinico-demographic characteristics

The demographic and clinical data of this cohort were presented in detail in Chapter 3, section 3.3.1. Briefly, the FEP patients were on average younger and had engaged in less years of education. There were no differences between the groups in gender distribution or time between scans. Within the patient group, there were significant reductions in the positive ($t_{(27)}$=5.41,p<0.001) and general psychopathology ($t_{(27)}$=3.89,p<0.001) subscales of the PANSS between baseline and follow-up, with a reduction in negative symptoms also demonstrated, that did not reach statistical significance ($t_{(27)}$=1.92,p=0.07). GAF scores increased significantly ($t_{(27)}$=-7.87,p<0.001) between baseline and follow-up assessments.

4.3.2 Group comparison of rates of progressive cortical brain change

There were no significant cortical thickness differences [F(1,52)=0.643, 0.426] in the LLOFR between FEP patients and HC at baseline. Increased rates of progressive cortical thinning were observed in FEP patients relative to HCs, mostly in the left frontal and temporal regions, specifically significant clusters were observed in the regions of the left lateral orbitofrontal, superiorparietal, lingual, superiortemporal, the banks of the superior temporal sulcus, fusiform gyrus and the bilateral superiorfrontal gyrus (Fig.4.1 and Table 4.3, all uncorrected, p<0.05). Furthermore, a cluster of progressive cortical thinning was observed after multiple comparison correction [Fig.4.2 and Table 4.4, all corrected p<0.05] in FEP patients at the left lateral orbitofrontal cortex extending into aspects of the left pars orbitalis, pars triangularis, rostral middle frontal gyrus and frontal pole.

4.3.2.1 Group comparison of symmetrised percentage change in cortical thickness of the LLOFR

The spc measures of thickness from the ROI (left lateral orbitofrontal cortex extending into aspects of the left pars orbitalis, pars triangularis, rostral middle frontal gyrus and frontal pole) (Fig. 4.2) was compared between groups. There was an increased rate of cortical

thinning of this ROI as evidenced by a significantly reduced spc [F(1,52)=5.11, p=0.028)] in all individuals with FEP relative to HCs, a mean difference of 0.844% [95% CI (0.095, 1.593)] (Fig.4.3A) over the 3-year period was observed. Furthermore, a trend towards significance for increased progressive rate of thinning [F(2,51)=2.868, p=0.066)] in this ROI was observed with a mean difference of 1.006% [95% CI (0.154, 1.858), p=0.022] more in the non-affective and 0.580% [95% CI (-0.415, 1.576), p=0.247] more in the affective subgroups relative to HCs (Fig.4.3B), indicating that the mean spc in cortical thickness of the ROI in the non-affective subgroup differ from controls. Further pairwise comparisons showed no significant mean difference [0.426%, 95 CI (-0.629,1.481), p=0.422] in cortical thickness of this ROI between the affective and non-affective subgroups (Fig.4.3B).

4.3.3 Association of rates of cortical thinning in the LLOFR with change in clinical and functional variables

Table 4.5 displays the partial correlation coefficients of change in clinical and functional measures assessed with the spc of the ROI in FEP patients. The spc in the LLOFR did not associate with changes in clinical or functional measures over time.

Fig. 4.1: Uncorrected *p*-value maps showing regional neuroanatomical clusters with different symmetrised rates for progressive cortical thickness change in FEP patients relative to HCs over time.

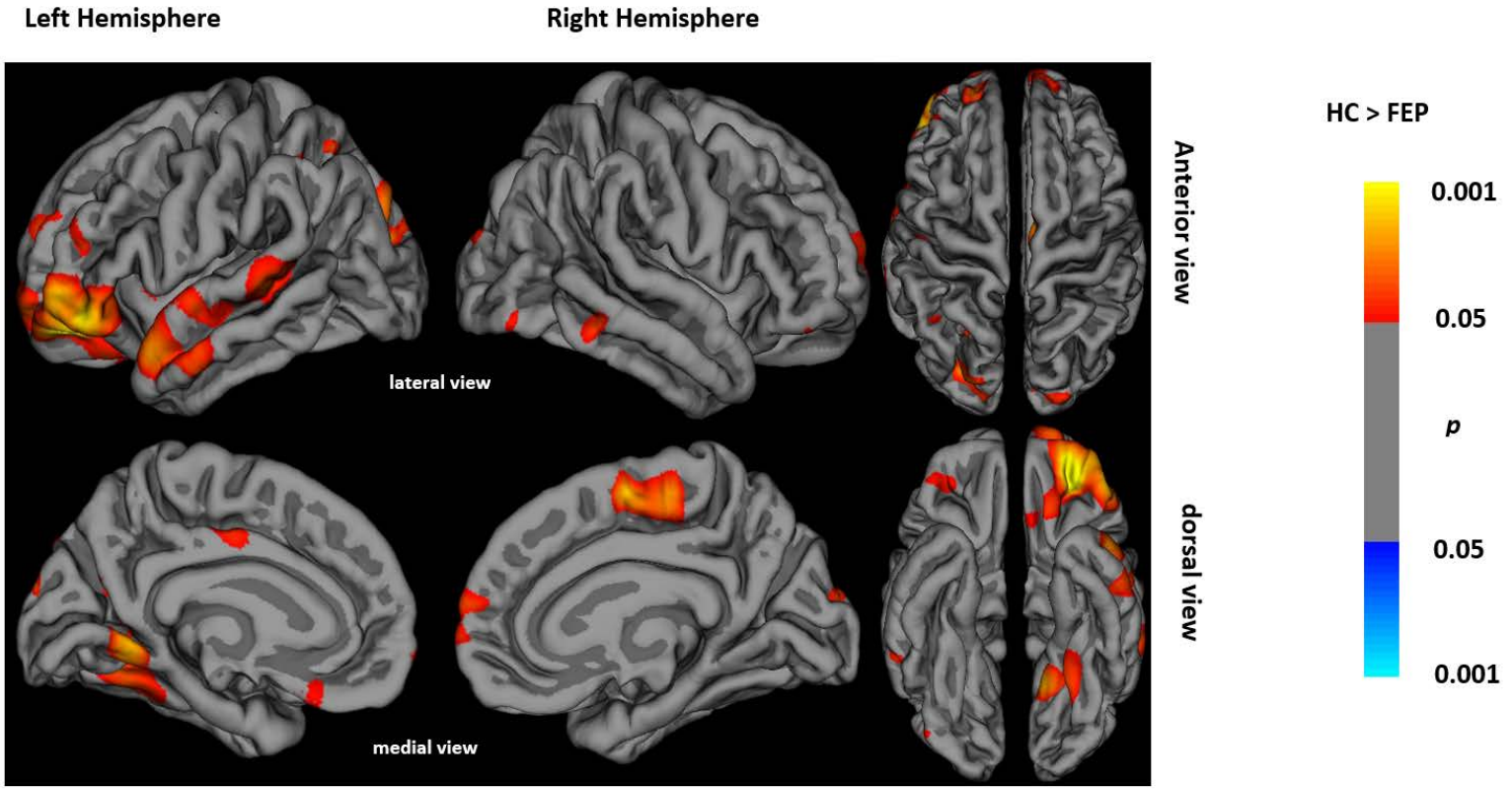

Fig. 4.1 Legend: The symmetrised rate of progressive cortical thickness change in FEP patients relative to healthy controls per year, mostly in the left frontal and temporal regions. Regions of cortical thinning are displayed in RED-YELLOW and reduced cortical thinning over time in BLUE.

Table 4.3: Clusters showing neuroanatomical regions with different symmetrised rates of progressive cortical thickness change in FEP patients relative to HCs over time.

Cluster No.	Cluster Location*	Cluster Probability (p-value)	Number of Vertices in cluster	Cluster Size (mm^2)	Talairach coordinates of maxima		
					TalX	TalY	TalZ
Left Hemisphere							
1	Lateral orbitofrontal	<0.0001	4152	2565.55	-25.5	43.9	-9.5
2	superiorparietal	0.0107	1097	718.87	-21.9	-82.5	17.6
3	lingual	0.0114	1084	560.68	-11.3	-56.9	-2.0
4	superiortemporal	0.0199	1701	1030.02	-48.7	8.6	-23.6
5	superiorfrontal	0.0321	346	241.61	-17.7	54.5	20.7
7	banks of the superior temporal sulcus	0.0477	1640	717.70	-60.8	-33.7	3.3
8	fusiform	0.0536	846	493.23	-30.3	-59.6	-12.3
9	precuneus	0.0590	414	208.64	-19.4	-62.1	24.1
10	insula	0.0770	464	169.39	-32.5	7.5	13.2
11	rostral middle frontal	0.0785	176	116.42	-37.5	39.7	16.1
12	posterior cingulate	0.1000	326	125.24	-4.6	-11.4	38.8
13	postcentral	0.1073	97	59.22	-50.1	-17.3	35.6
14	inferiorparietal	0.1471	118	52.14	-41.4	-57.1	37.7
15	medial orbitofrontal	0.1567	177	87.25	-5.7	25.7	-23.4
Right Hemisphere							
1	superiorfrontal	0.0092	1258	648.59	7.8	-4.5	58.0
2	lateral occipital	0.0657	265	207.91	14.8	-92.3	15.7
3	middle temporal	0.0808	233	161.05	59.1	-43.0	-12.7
4	pars orbitalis	0.1318	193	152.61	35.0	39.8	-8.0
5	inferiorparietal	0.1606	39	15.64	45.3	-54.4	29.5
6	cuneus	0.1726	9	7.69	7.9	-89.4	14.5
7	paracentral	0.1806	3	1.16	12.6	-27.1	47.8
8	precentral	0.1839	3	1.19	23.9	-4.2	45.8
9	superiorparietal	0.1888	1	0.45	35.5	-46.1	52.7

Table 4.3 Legend: The cluster-wise p-values presented are uncorrected; * The cortical regions of the Desikan-Killiany atlas were employed

Fig. 4.2: Corrected *p*-value maps showing regional neuroanatomical clusters with increased symmetrised rates of progressive cortical thinning in FEP patients relative to HCs over time. Cluster-wise correction for multiple comparison at p=0.05.

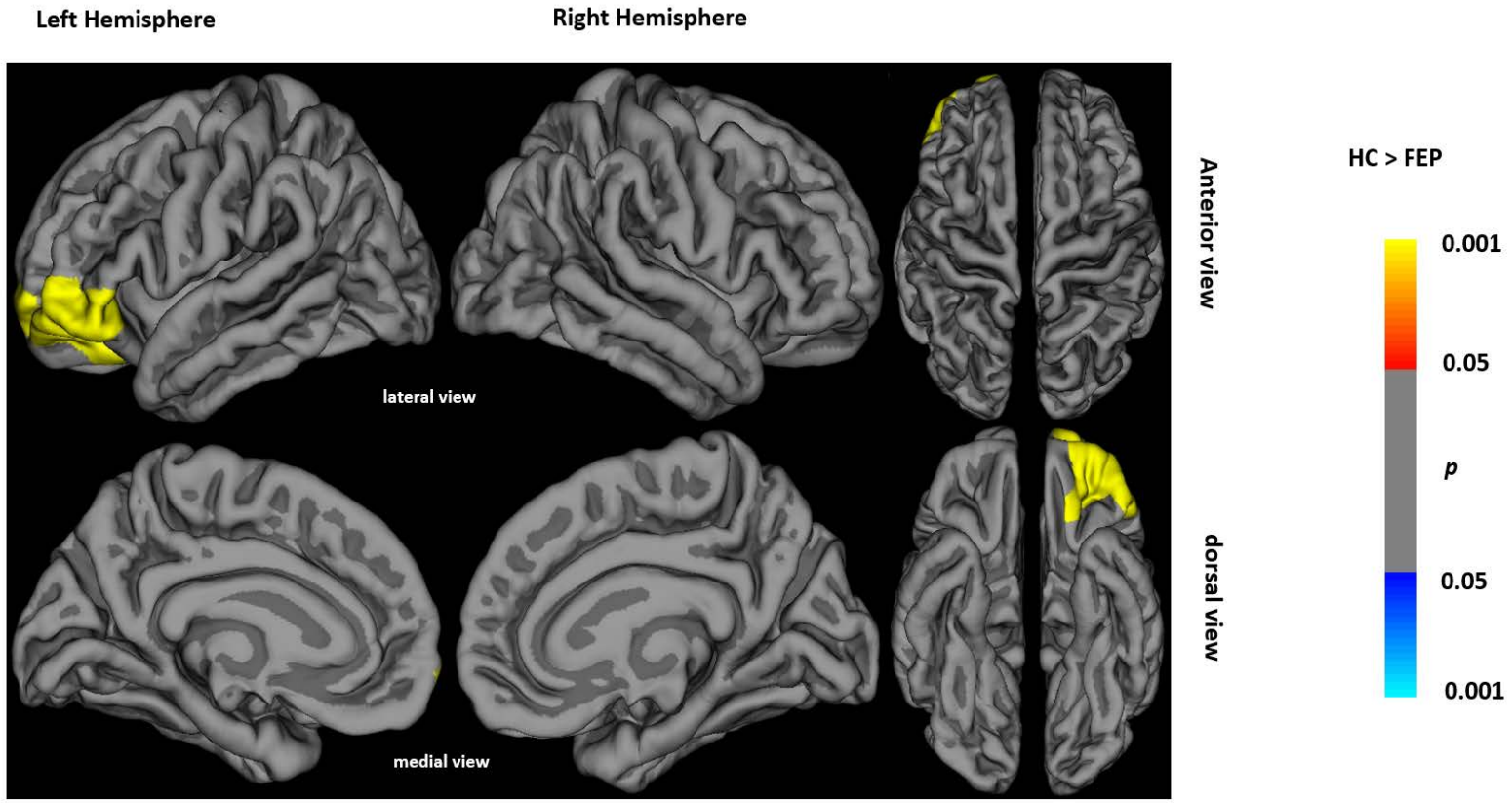

Fig. 4.2 Legend: The symmetrised rate of progressive cortical thickness change in FEP patients relative to healthy controls per year. The regional neuroanatomical clusters that survived cluster-wise correction for multiple comparison (p=0.05) for cortical thinning are displayed in YELLOW. This region coincides with the left lateral orbitofrontal cortex extending into aspects of the left pars orbitalis, pars triangularis, rostral middle frontal gyrus and frontal pole.

Table 4.4. Cluster showing the neuroanatomical region that survived cluster-wise correction for multiple comparisons for symmetrised rate of progressive change in cortical thickness in FEP patients relative to HCs.

Cluster No.	Cluster Location*	Cluster Probability (p-value)	Number of Vertices in cluster	Cluster Size (mm^2)	Talairach coordinates of maxima		
					TalX	TalY	TalZ
1	Left lateral orbitofrontal	<0.0001	4152	2565.55	-25.3	42.1	-10.1

Table 4.4 Legend: * The cortical regions of the Desikan-Killiany atlas were employed

Fig. 4.3: Comparison of symmetrised percentage change in cortical thickness of the left lateral orbitofrontal region

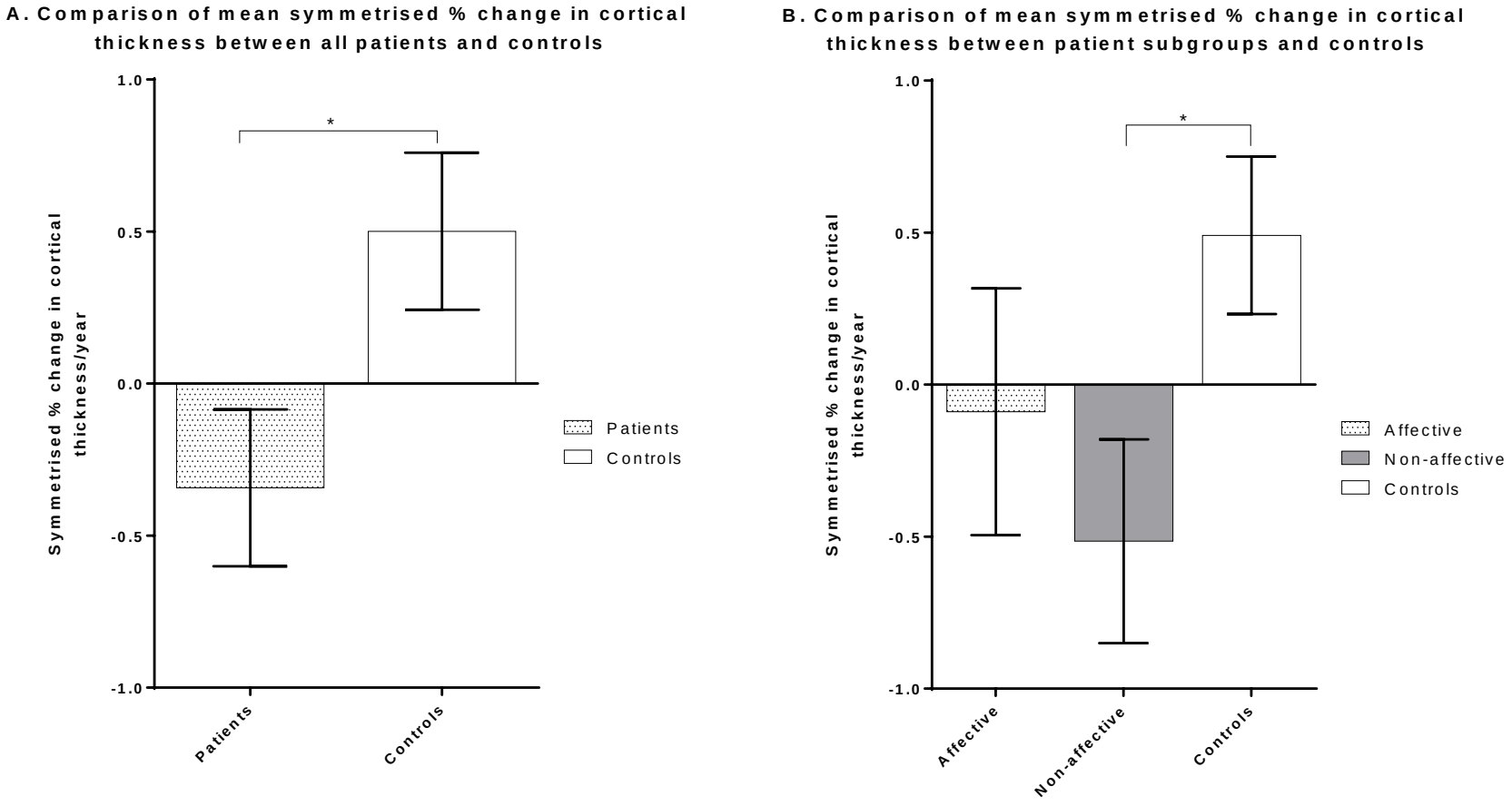

Fig. 4.3 Legend: Plot of corrected mean symmetrised % change (± standard error) of cortical thickness/year of the left lateral orbitofrontal region in first-episode psychosis A. patients (all) relative to healthy controls and B. patient subgroups (affective and non-affective) relative to healthy controls. The mean symmetrised % change in thickness was corrected for age at baseline and gender *significant difference

Table 4.5: Partial correlations of the mean symmetrised % change in cortical thickness of the left lateral orbitofrontal region with change in clinical and functional variables in all FEP patients

Change in clinical measures	r	p
CPZ	0.156	0.447
PANSS Positive	-0.129	0.530
PANSS Negative	0.129	0.532
PANSS General	0.071	0.729
PANSS Total	0.042	0.840
GAF	-0.239	0.240

Table 4.5 Legend: Change was computed as: cumulative medication dosage (CPZ equiv.) = ($Time_2$ – $Time_1$), PANSS scores = ($Time_2$ – $Time_1$), and change in global assessment of functioning scores = ($Time_2$ – $Time_1$). PANSS= positive and negative syndrome score (0-6 point scale); GAF= global assessment of functioning; CPZ= chlorpromazine equivalents; Note: All correlations were controlled for age at baseline and gender

4 Discussion

This longitudinal study identified a cortical region (left lateral orbitofrontal cortex extending into aspects of the left pars orbitalis, pars triangularis, rostral middle frontal gyrus and frontal pole) that demonstrated a relatively greater progressive rate for cortical thinning mainly in FEP patients relative to HCs. The rate of cortical thinning in the LLOFR of FEP patients did not associate with changes in clinical or functional measures over the 3-year follow-up period.

4.4.1 Progressive cortical grey matter changes after first-episode psychosis

Cortical thinning was identified most prominently in the left prefrontal region of the brain after the first 3-years of FEP. This study lends weight to the evidence that there is progression after FEP as previously demonstrated in prefrontal cortical subregions of progressive thinning in FEP patients (Andreasen *et al.* 2011; Gutiérrez-Galve *et al.* 2015; Buchy *et al.* 2017), ARMS patients (Cannon *et al.* 2015) and in those with more established illness (van Haren *et al.* 2011; Cobia *et al.* 2012) over time. Of note, cortical thinning was present in this broad sample of psychosis, as distinct from just non-affective psychosis. Indeed, we found similar rates of cortical thinning in affective and non-affective psychosis. On the contrary, Haukvik and colleagues (2016) found no significant cortical thickness changes in another heterogenous FEP sample followed-up after 1-year. Additionally, a 2-year follow-up study (Palaniyappan *et al.* 2019) reported thickness sparing of the prefrontal cortex over time in a cohort of adolescent-onset schizophrenia relative to HCs. This inconsistency may be due to the relatively small sample size (n=18; Palaniyappan *et al.* 2019) or the relatively short follow-up period (1-year, Haukvik *et al.* 2016) in these studies. Progression of cortical deficits amongst FEP patients in the years after their FEP is considered a major neurobiological trait of psychotic illness (Keshavan *et al.* 2008; Cobia *et al.* 2012), however, the specific mechanisms underlying progressive loss of frontal lobe thickness still remain unclear. Some evidence suggests neuropil pruning as a potential cause of progressive reduction of grey matter in schizophrenia (Selemon and Goldman-Rakic, 1999) resulting in a distributed cortical reorganisation mostly leading to synaptic dysfunction in response to psychosis (Palaniyappan, 2017; Palaniyappan *et al.* 2018). Thus, our reported pattern of progressive change is suggestive of an active but inefficient cortical reorganisation which is likely initiated from the left prefrontal cortex in the early years after FEP with further progression to other cortices across the entire course of illness (van Haren *et al.* 2011). We speculate further, that these cortical reorganisations may indicate progression of abnormalities in the functional neuroanatomical units of the trans-thalamic circuitries which involve the lateral orbitofrontal regions of the prefrontal cortex. Furthermore, it has also

been suggested that antipsychotic medication influences total grey matter tissues (Vita *et al.* 2015; Guo *et al.* 2015), however, our finding of progressive cortical thinning in the left lateral orbitofrontal region do not relate to cumulative antipsychotic medication taken as assessed by chlorpromazine equivalents (Woods, 2003). This further suggests that this regional cortical thinning is an inherent feature of progressive psychotic illness (Nesvag *et al.* 2008) which potentially reflects an underlying neuropathophysiological process associated with the onset of FEP. Taken together, these may be indicative of a structural disturbance in subnetworks of the associative/cognitive component of the cortico-striato-thalamo-cortical circuitry (Ellison-Wright *et al.* 2008; Galvan *et al.* 2015).

4.4.2 Preserved cortical grey matter regions after first-episode psychosis

In the current study, global cortical grey matter tissues were preserved, a finding concordant with some other studies (Schaufelberger *et al.* 2011; Haukvik *et al.* 2016). However, assessment of this cohort of a relatively larger sample size (Scanlon *et al.* 2014), showed a cluster of cortical thinning in the right superior temporal gyrus and sulcus extending into the middle temporal gyrus in FEP patients. This is consistent with a recent ENIGMA cross-sectional study (van Erp *et al.* 2018) that reported large effect sizes for cortical thinning in the frontal and temporal lobe regions of schizophrenia patients. However, our hypothesis-free longitudinal vertex-wise analyses approach failed to demonstrate progressive thinning in this region. Of note, we observed in the contralateral region, progressive thinning in the banks of the superior temporal sulcus that did not survive corrections for multiple comparisons. In this study, there were no significant cortical thickness differences observed in the LLOFR between FEP patients and HC at baseline. Taken together, these findings indicate that some baseline changes may be preserved or remain static and not necessarily progress throughout illness or indeed may be reversible (Keshavan *et al.* 1998; Schaufelberger *et al.* 2011; Olabi *et al.* 2011) and thus, other regions may emerge in a progressive manner over time.

4.4.3 Association of clinical measures with cortical thickness changes

In this study, the observed rates of cortical thinning in the LLOFR do not associate with change in clinical or functional measures over time. Similarly, other longitudinal studies also failed to find any such associations over time in FEP patients (Gutiérrez-Galve *et al.* 2015) and in established illness (Cobia *et al.* 2012). Of note, a large cross-sectional ENIGMA study reported significant associations between left lateral orbitofrontal thinning and negative symptom severity in a schizophrenia cohort (Walton *et al.* 2018). Furthermore, the findings

of Mathalon and colleagues (2001) demonstrated significant associations between greater negative symptom severity and increased rates of frontal brain tissue changes. Neuroinflammation is an integral component of the pathogenic mechanisms underlying the onset of several psychiatric disorders and results in increased regional blood flow, vascular permeability, microglial activation and high expression of inflammatory cytokines (Radtke *et al.* 2017). These processes result in an initial increase in volume of brain tissues, since cortical grey matter volume is a product of cortical thickness and surface area, it is likely that the neuroinflammatory processes contributed to the "normal" baseline cortical thickness of the LLOFR (Scanlon *et al.* 2014). A human postmortem study (Zhang *et al.* 2016) found significantly reduced cortical grey matter volumes in the prefrontal cortex of schizophrenia brains with high inflammation status relative to those with low inflammatory status. This results suggest that the reduction in cortical grey matter volume in people with schizophrenia is exaggerated in those who have high expression of inflammatory cytokines. Thus, it is likely that progressive cortical thinning of the LLOFR has resulted from the anti-inflammatory effect of antipsychotic treatment over time (Al-min *et al.* 2013). Of note, cortical thinning of the LLOFR do not relate to cumulative antipsychotic medication taken as assessed by chlorpromazine equivalents (Woods, 2003). However, the "normal" baseline cortical thickness of the LLOFR (Scanlon *et al.* 2014) is reflective of an initial neuroinflammation at illness onset. Furthermore, the weak associations of the rate of cortical thinning in the LLOFR with clinical and functional measures suggest that cortical thinning in the LLOFR of FEP patients is not a neuroanatomical marker of clinical outcome. Albeit speculative, cortical thinning in the LLOFR may imply an increase in cognitive impairments over the course of the illness considering the high involvement of the orbitofrontal cortex in emotional and social cognition (Beer *et al.* 2006; Nestor *et al.* 2013). Of note, measurements of cognitive performance were not assessed in this study.

4.4.4 Strengths and Limitations

The main strength of this study is its application of a global longitudinal vertex-wise analyses approach to a cohort of psychotic patients who were originally assessed very shortly after presentation to the mental health services and with minimal antipsychotic exposure. The vertex-wise group analyses, unlike the surface-based approaches which are less reliable at localising changes within specific lobular subregions (DeLisi, 2008; Cercignani *et al.* 2018) has enabled a hypothesis-free investigation over the entire cortical mantle. We used the longitudinal FreeSurfer pipeline which has the advantage, compared to other analysis approaches, of accounting for inter-subject variability by creating an unbiased subject-

specific anatomical template (Reuter *et al.* 2010) from the images at both time-points resulting in higher anatomical accuracy in identifying subtle changes over time. We were also able to employ the same MRI scanner and acquisition sequences without any major software or hardware upgrades during the study period. We recruited a broad psychosis phenotype for our study, rather than focus on schizophrenia spectrum disorders alone, which is more generally representative of FEP patients presenting to the mental health services. Despite the potential increase in clinical heterogeneity associated with this approach, we were able to detect regional cortical progression and link these with measures of clinical outcome that were not confined to a non-affective psychosis category.

The main limitation of the study was the relatively small sample size and consequent risk of type II errors and generalisability of the results, which require confirmation in larger carefully acquired samples. Furthermore, there has been a concern that a cluster-forming threshold of <0.05 might be too low, however, after repeating the analyses using a cluster-forming threshold of <0.01, the main group difference remained significant (Fig.4.5). Due to inadequate data availability we were not able to assess the influence of environmental exposures other than antipsychotic medication (e.g. cannabis use) on the observably thinned regions of the prefrontal cortex.

4.4.5 Conclusion

In conclusion, this study demonstrated the existence of localised progressive cortical thinning which is most prominent in the left lateral orbitofrontal regions after the early years of first-episode of psychosis to indicate that thinning was present across the psychosis phenotype. Cortical thinning in the LLOFR of FEP patients is not a neuroanatomical marker of clinical or functional outcome. Taken together, these may be indicative of a progressive disturbance in the structural integrity of a subnetwork of the associative/cognitive component of the cortico-striato-thalamo-cortical circuitry, that involve specifically, the lateral orbitofrontal regions of the prefrontal cortex. This finding lends weight to the evidence that there is early regional neuroanatomical progression after FEP and thus such knowledge could potentially contribute to the identification of imaging biomarkers for psychosis which would be particularly beneficial in the critical early stages of the disorder.

Fig. 4.4: Corrected *p*-value maps showing regional neuroanatomical clusters with increased symmetrised rates of progressive cortical thinning in FEP patients relative to HCs over time. Cluster-wise correction for multiple comparison at p=0.01.

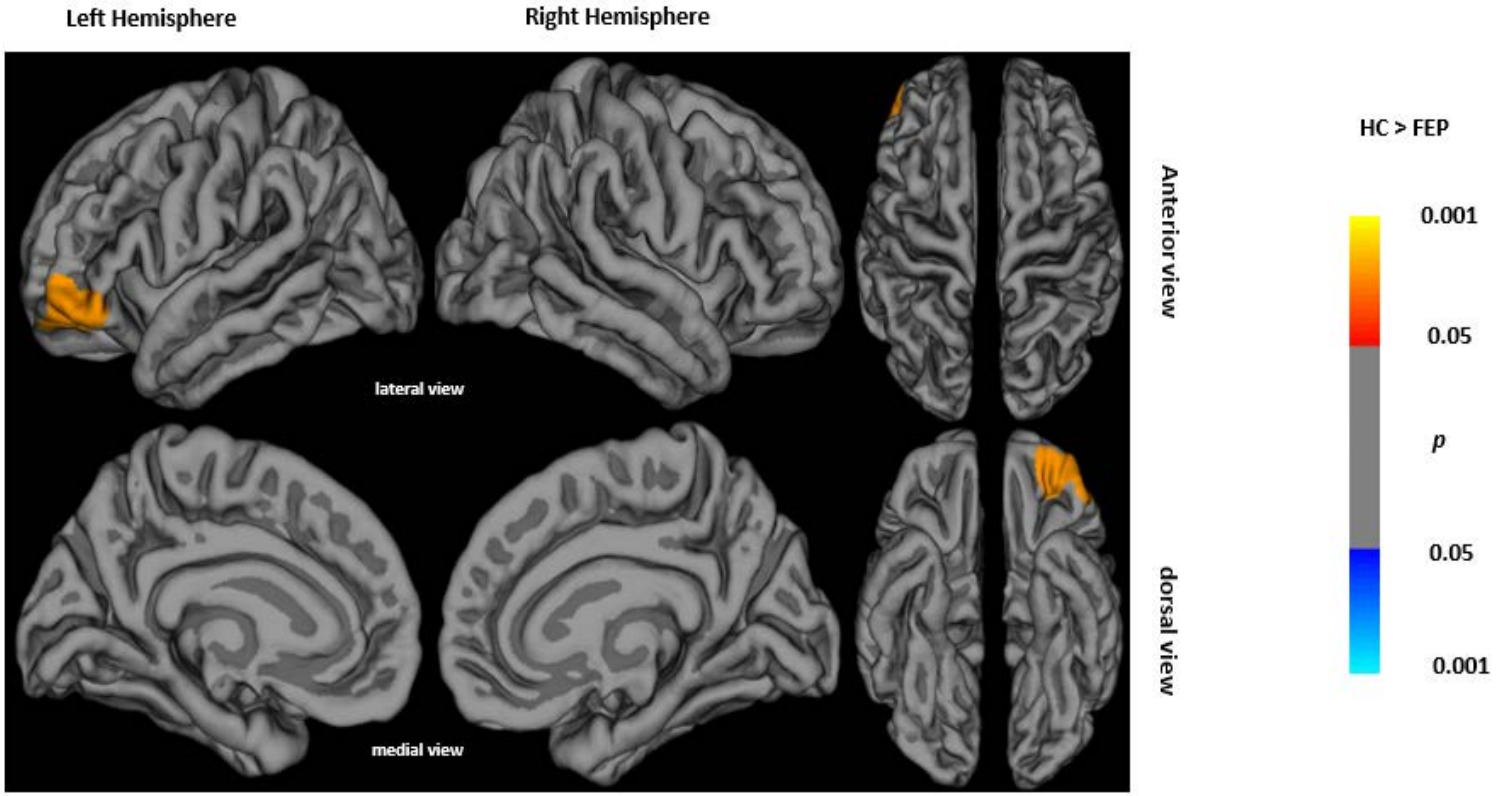

Fig. 4.4 Legend: The symmetrised rate of progressive cortical thickness change in FEP patients relative to healthy controls per year. The regional neuroanatomical clusters that survived cluster-wise correction for multiple comparison (p=0.01) for cortical thinning are displayed in ORANGE. This region coincides with the left lateral orbitofrontal cortex extending into aspects of the left pars orbitalis, pars triangularis, rostral middle frontal gyrus and frontal pole.

References

1. Akudjedu, T.N., Nabulsi, L., Makelyte, M., Scanlon, C., Hehir, S., Casey, H., Ambati, S., Kenney, J., O'Donoghue, S., McDermott, E., Kilmartin, L., Dockery, P., McDonald, C., Hallahan, B., Cannon, D.M., 2018. A comparative study of segmentation techniques for the quantification of brain subcortical volume. Brain Imaging and Behavior 12(6), 1678-1695.
2. Al-Amin, M.M., Nasir Uddin, M.M., Mahmud Reza, H., 2013. Effects of antipsychotics on the inflammatory response system of patients with schizophrenia in peripheral blood mononuclear cell cultures. Clin Psychopharmacol Neurosci 11(3), 144-151.
3. Andreasen, N.C., Nopoulos, P., Magnotta, V., Pierson, R., Ziebell, S., Ho, B.-C., 2011. Progressive brain change in schizophrenia: a prospective longitudinal study of first-episode schizophrenia. Biological psychiatry 70(7), 672-679.
4. Asami, T., Bouix, S., Whitford, T.J., Shenton, M.E., Salisbury, D.F., McCarley, R.W., 2012. Longitudinal loss of gray matter volume in patients with first-episode schizophrenia: DARTEL automated analysis and ROI validation. NeuroImage 59(2), 986-996.
5. Beer, J.S., John, O.P., Scabini, D., Knight, R.T., 2006. Orbitofrontal Cortex and Social Behavior: Integrating Self-monitoring and Emotion-Cognition Interactions. Journal of Cognitive Neuroscience 18(6), 871-879.
6. Berry, D.A., 1989. Statistical Methodology in the Pharmaceutical Sciences. Marcel Dekker, New York.
7. Berry, D.A., Ayers, G.D., 2006. Symmetrized Percent Change for Treatment Comparisons. The American Statistician 60(1), 27-31.
8. Buchy, L., Makowski, C., Malla, A., Joober, R., Lepage, M., 2017. Longitudinal trajectory of clinical insight and covariation with cortical thickness in first-episode psychosis. Journal of Psychiatric Research 86, 46-54.
9. Buchy, L., Makowski, C., Malla, A., Joober, R., Lepage, M., 2018. A longitudinal study of cognitive insight and cortical thickness in first-episode psychosis. Schizophrenia Research 193, 251-260.
10. Cahn, W., Pol, H.E.H., Lems, E.B.T.E., van Haren, N.E.M., Schnack, H.G., van der Linden, J.A., Schothorst, P.F., van Engeland, H., Kahn, R.S., 2002. Brain Volume Changes in First-Episode Schizophrenia: A 1-Year Follow-up Study. JAMA Psychiatry 59(11), 1002-1010.
11. Cannon, T.D., Chung, Y., He, G., Sun, D., Jacobson, A., van Erp, T.G.M., McEwen, S., Addington, J., Bearden, C.E., Cadenhead, K., Cornblatt, B., Mathalon, D.H., McGlashan, T., Perkins, D., Jeffries, C., Seidman, L.J., Tsuang, M., Walker, E., Woods, S.W., Heinssen, R., 2015. Progressive Reduction in Cortical Thickness as Psychosis Develops: A Multisite Longitudinal Neuroimaging Study of Youth at Elevated Clinical Risk. Biological Psychiatry 77(2), 147-157.
12. Cercignani, M., Dowell, G.N., Tofts, P.S., 2018. Quantitative MRI of the Brain: Principles of Physical Measurement, 2nd Edition edn., Boca Raton: CRC Press.
13. Cobia, D.J., Smith, M.J., Wang, L., Csernansky, J.G., 2012. Longitudinal progression of frontal and temporal lobe changes in schizophrenia. Schizophrenia Research 139(1), 1-6.
14. Dale, A.M., Fischl, B., Sereno, M.I., 1999. Cortical Surface-Based Analysis: I. Segmentation and Surface Reconstruction. NeuroImage 9(2), 179-194.

15. de Castro-Manglano, P., Mechelli, A., Soutullo, C., Gimenez-Amaya, J., Ortuño, F., McGuire, P., 2011. Longitudinal changes in brain structure following the first episode of psychosis. Psychiatry Research: Neuroimaging 191(3), 166-173.
16. DeLisi, L.E., 2008. The concept of progressive brain change in schizophrenia: implications for understanding schizophrenia. Schizophr Bull 34(2), 312-321.
17. Desikan, R.S., Ségonne, F., Fischl, B., Quinn, B.T., Dickerson, B.C., Blacker, D., Buckner, R.L., Dale, A.M., Maguire, R.P., Hyman, B.T., Albert, M.S., Killiany, R.J., 2006. An automated l135abelling system for subdividing the human cerebral cortex on MRI scans into gyral based regions of interest. NeuroImage 31(3), 968-980.
18. Dickey, C.C., Salisbury, D.F., Nagy, A.I., Hirayasu, Y., Lee, C.U., McCarley, R.W., Shenton, M.E., 2004. Follow-up MRI study of prefrontal volumes in first-episode psychotic patients. Schizophrenia research 71(2-3), 349-351.
19. Ellison-Wright ,I ., Glahn , D.C., Laird , R.A., Thelen , M.S., Ed Bullmore , E., 2008. The Anatomy of First-Episode and Chronic Schizophrenia: An Anatomical Likelihood Estimation Meta-Analysis. American Journal of Psychiatry 165(8), 1015-1023.
20. Fischl, B., Dale, A.M., 2000. Measuring the thickness of the human cerebral cortex from magnetic resonance images. Proc Natl Acad Sci U S A 97(20), 11050-11055.
21. Fischl, B., Sereno, M.I., Dale, A.M., 1999. Cortical Surface-Based Analysis: II: Inflation, Flattening, and a Surface-Based Coordinate System. NeuroImage 9(2), 195-207.
22. Galvan, A., Devergnas, A., Wichmann, T., 2015. Alterations in neuronal activity in basal ganglia-thalamocortical circuits in the parkinsonian state. Frontiers in Neuroanatomy 9(5).
23. Goldstone, A., Willoughby, A.R., de Zambotti, M., Franzen, P.L., Kwon, D., Pohl, K.M., Pfefferbaum, A., Sullivan, E.V., Müller-Oehring, E.M., Prouty, D.E., Hasler, B.P., Clark, D.B., Colrain, I.M., Baker, F.C., 2018. The mediating role of cortical thickness and gray matter volume on sleep slow-wave activity during adolescence. Brain Struct Funct 223(2), 669-685.
24. Guo, J.Y., Huhtaniska, S., Miettunen, J., Jääskeläinen, E., Kiviniemi, V., Nikkinen, J., Moilanen, J., Haapea, M., Mäki, P., Jones, P.B., Veijola, J., Isohanni, M., Murray, G.K., 2015. Longitudinal regional brain volume loss in schizophrenia: Relationship to antipsychotic medication and change in social function. Schizophrenia research 168(1-2), 297-304.
25. Gutiérrez-Galve, L., Chu, E.M., Leeson, V.C., Price, G., Barnes, T.R.E., Joyce, E.M., Ron, M.A., 2014. A longitudinal study of cortical changes and their cognitive correlates in patients followed up after first-episode psychosis. Psychological Medicine 45(1), 205-216.
26. Hagler, D.J., Saygin, A.P., Sereno, M.I., 2006. Smoothing and cluster thresholding for cortical surface-based group analysis of fMRI data. NeuroImage 33(4), 1093-1103.
27. Han, X., Jovicich, J., Salat, D., van der Kouwe, A., Quinn, B., Czanner, S., Busa, E., Pacheco, J., Albert, M., Killiany, R., Maguire, P., Rosas, D., Makris, N., Dale, A., Dickerson, B., Fischl, B., 2006. Reliability of MRI-derived measurements of human cerebral cortical thickness: The effects of field strength, scanner upgrade and manufacturer. NeuroImage 32(1), 180-194.
28. Haukvik, U.K., Hartberg, C.B., Nerland, S., Jørgensen, K.N., Lange, E.H., Simonsen, C., Nesvåg, R., Dale, A.M., Andreassen, O.A., Melle, I., Agartz, I., 2015. No progressive brain changes during a 1-year follow-up of patients with first-episode psychosis. Psychological Medicine 46(3), 589-598.

29. IBM Corp. Released 2016. IBM SPSS Statistics for Windows, Version 24.0. Armonk, NY: IBM Corp.
30. Kasai, K., Shenton, M.E., Salisbury, D.F., Hirayasu, Y., Onitsuka, T., Spencer, M.H., Yurgelun-Todd, D.A., Kikinis, R., Jolesz, F.A., McCarley, R.W., 2003. Progressive Decrease of Left Heschl Gyrus and Planum Temporale Gray Matter Volume in First-Episode Schizophrenia: A Longitudinal Magnetic Resonance Imaging Study. Archives of General Psychiatry 60(8), 766-775.
31. Kenney, J., Anderson-Schmidt, H., Scanlon, C., Arndt, S., Scherz, E., McInerney, S., McFarland, J., Byrne, F., Ahmed, M., Donohoe, G., Hallahan, B., McDonald, C., Cannon, D.M., 2015. Cognitive course in first-episode psychosis and clinical correlates: A 4year longitudinal study using the MATRICS Consensus Cognitive Battery. Schizophrenia Research 169(1), 101-108.
32. Keshavan, M.S., Haas, G.L., Kahn, C.E., Eduardo, A., Dick, E.L., Schooler, N.R., Sweeney, J.A., Pettegrew, J.W., 1998. Superior temporal gyrus and the course of early schizophrenia: Progressive, static, or reversible? Journal of Psychiatric Research 32(3), 161-167.
33. Keshavan, M.S., Tandon, R., Boutros, N.N., Nasrallah, H.A., 2008. Schizophrenia, "just the facts": What we know in 2008: Part 3: Neurobiology. Schizophrenia Research 106(2), 89-107.
34. Koo, M.-S., Levitt, J.J., Salisbury, D.F., Nakamura, M., Shenton, M.E., McCarley, R.W., 2008. A cross-sectional and longitudinal magnetic resonance imaging study of cingulate gyrus gray matter volume abnormalities in first-episode schizophrenia and first-episode affective psychosis. Archives of general psychiatry 65(7), 746-760.
35. Kuperberg, G.R., Broome, M.R., McGuire, P.K., David, A.S., Eddy, M., Ozawa, F., Goff, D., West, W.C., Williams, S.C.R., van der Kouwe, A.J.W., Salat, D.H., Dale, A.M., Fischl, B., 2003. Regionally Localized Thinning of the Cerebral Cortex in Schizophrenia. JAMA Psychiatry 60(9), 878-888.
36. Lawrie, S.M., 2018. Are structural brain changes in schizophrenia related to antipsychotic medication? A narrative review of the evidence from a clinical perspective. Ther Adv Psychopharmacol 8(11), 319-326.
37. Mane, A., Falcon, C., Mateos, J.J., Fernandez-Egea, E., Horga, G., Lomeña, F., Bargalló, N., Prats-Galino, A., Bernardo, M., Parellada, E., 2009. Progressive gray matter changes in first episode schizophrenia: A 4-year longitudinal magnetic resonance study using VBM. Schizophrenia Research 114(1), 136-143.
38. Mathalon, D.H., Sullivan, E.V., Lim, K.O., Pfefferbaum, A., 2001. Progressive Brain Volume Changes and the Clinical Course of Schizophrenia in Men: A Longitudinal Magnetic Resonance Imaging Study. JAMA Psychiatry 58(2), 148-157.
39. Nakamura, M., Nestor, P.G., Levitt, J.J., Cohen, A.S., Kawashima, T., Shenton, M.E., McCarley, R.W., 2008. Orbitofrontal volume deficit in schizophrenia and thought disorder. Brain 131(Pt 1), 180-195.
40. Nakamura, M., Salisbury, D.F., Hirayasu, Y., Bouix, S., Pohl, K.M., Yoshida, T., Koo, M.-S., Shenton, M.E., McCarley, R.W., 2007. Neocortical Gray Matter Volume in First-Episode Schizophrenia and First-Episode Affective Psychosis: A Cross-Sectional and Longitudinal MRI Study. Biological Psychiatry 62(7), 773-783.
41. Nestor, P.G., Nakamura, M., Niznikiewicz, M., Thompson, E., Levitt, J.J., Choate, V., Shenton, M.E., McCarley, R.W., 2013. In search of the functional neuroanatomy of sociality: MRI subdivisions of orbital frontal cortex and social cognition. Soc Cogn Affect Neurosci 8(4), 460-467.

42. Nesvag, R., Lawyer, G., Varnäs, K., Fjell, A.M., Walhovd, K.B., Frigessi, A., Jönsson, E.G., Agartz, I., 2008. Regional thinning of the cerebral cortex in schizophrenia: Effects of diagnosis, age and antipsychotic medication. Schizophrenia Research 98(1), 16-28.
43. Ohtani, T., del Re, E., Levitt, J.J., Niznikiewicz, M., Konishi, J., Asami, T., Kawashima, T., Roppongi, T., Nestor, P.G., Shenton, M.E., Salisbury, D.F., McCarley, R.W., 2018. Progressive symptom-associated prefrontal volume loss occurs in first-episode schizophrenia but not in affective psychosis. Brain Structure and Function 223(6), 2879-2892.
44. Olabi, B., Ellison-Wright, I., McIntosh, A.M., Wood, S.J., Bullmore, E., Lawrie, S.M., 2011. Are There Progressive Brain Changes in Schizophrenia? A Meta-Analysis of Structural Magnetic Resonance Imaging Studies. Biological Psychiatry 70(1), 88-96.
45. Palaniyappan, L., 2017. Progressive cortical reorganisation: A framework for investigating structural changes in schizophrenia. Neuroscience & Biobehavioral Reviews 79, 1-13.
46. Palaniyappan, L., Das, T.K., Winmill, L., Hough, M., James, A., 2019. Progressive post-onset reorganisation of MRI-derived cortical thickness in adolescents with schizophrenia. Schizophrenia Research 208, 477-478.
47. Palaniyappan, L., Hodgson, O., Balain, V., Iwabuchi, S., Gowland, P., Liddle, P., 2018. Structural covariance and cortical reorganisation in schizophrenia: a MRI-based morphometric study. Psychological Medicine 49(3), 412-420.
48. Panizzon, M.S., Fennema-Notestine, C., Eyler, L.T., Jernigan, T.L., Prom-Wormley, E., Neale, M., Jacobson, K., Lyons, M.J., Grant, M.D., Franz, C.E., Xian, H., Tsuang, M., Fischl, B., Seidman, L., Dale, A., Kremen, W.S., 2009. Distinct Genetic Influences on Cortical Surface Area and Cortical Thickness. Cerebral Cortex 19(11), 2728-2735.
49. Pantelis, C., Velakoulis, D., McGorry, P.D., Wood, S.J., Suckling, J., Phillips, L.J., Yung, A.R., Bullmore, E.T., Brewer, W., Soulsby, B., Desmond, P., McGuire, P.K., 2003. Neuroanatomical abnormalities before and after onset of psychosis: a cross-sectional and longitudinal MRI comparison. The Lancet 361(9354), 281-288.
50. Pawełczyk, T., Piątkowska-Janko, E., Bogorodzki, P., Gębski, P., Grancow-Grabka, M., Trafalska, E., Żurner, N., Pawełczyk, A., 2018. Omega-3 fatty acid supplementation may prevent loss of gray matter thickness in the left parieto-occipital cortex in first episode schizophrenia: A secondary outcome analysis of the OFFER randomized controlled study. Schizophrenia Research 195, 168-175.
51. Radtke, F.A., Chapman, G., Hall, J., Syed, Y.A., 2017. Modulating Neuroinflammation to Treat Neuropsychiatric Disorders. Biomed Res Int 2017, 5071786-5071786.
52. Rais, M., van Haren, N.E.M., Cahn, W., Schnack, H.G., Lepage, C., Collins, L., Evans, A.C., Hulshoff Pol, H.E., Kahn, R.S., 2010. Cannabis use and progressive cortical thickness loss in areas rich in CB1 receptors during the first five years of schizophrenia. European Neuropsychopharmacology 20(12), 855-865.
53. Reuter, M., Rosas, H.D., Fischl, B., 2010. Highly accurate inverse consistent registration: A robust approach. NeuroImage 53(4), 1181-1196.
54. Reuter, M., Schmansky, N.J., Rosas, H.D., Fischl, B., 2012. Within-subject template estimation for unbiased longitudinal image analysis. NeuroImage 61(4), 1402-1418.
55. Roiz-Santiánez, R., Ayesa-Arriola, R., Tordesillas-Gutiérrez, D., Ortiz-García de la Foz, V., Pérez-Iglesias, R., Pazos, A., Sánchez, E., Crespo-Facorro, B., 2014. Three-year longitudinal population-based volumetric MRI study in first-episode schizophrenia spectrum patients. Psychological Medicine 44(8), 1591-1604.

56. Roiz-Santiánez, R., Ortiz-García de la Foz, V., Ayesa-Arriola, R., Tordesillas-Gutiérrez, D., Jorge, R., Varela-Gómez, N., Suárez-Pinilla, P., Córdova-Palomera, A., Navasa-Melado, J.M., Crespo-Facorro, B., 2015. No progression of the alterations in the cortical thickness of individuals with schizophrenia-spectrum disorder: a three-year longitudinal magnetic resonance imaging study of first-episode patients. Psychological Medicine 45(13), 2861-2871.
57. Rosas, H.D., Liu, A.K., Hersch, S., Glessner, M., Ferrante, R.J., Salat, D.H., van der Kouwe, A., Jenkins, B.G., Dale, A.M., Fischl, B., 2002. Regional and progressive thinning of the cortical ribbon in Huntington's disease. Neurology 58(5), 695-701.
58. Salisbury, D.F., Kuroki, N., Kasai, K., Shenton, M.E., McCarley, R.W., 2007. Progressive and interrelated functional and structural evidence of post-onset brain reduction in schizophrenia. Archives of general psychiatry 64(5), 521-529.
59. Scanlon, C., Anderson-Schmidt, H., Kilmartin, L., McInerney, S., Kenney, J., McFarland, J., Waldron, M., Ambati, S., Fullard, A., Logan, S., Hallahan, B., Barker, G.J., Elliott, M.A., McCarthy, P., Cannon, D.M., McDonald, C., 2014. Cortical thinning and caudate abnormalities in first episode psychosis and their association with clinical outcome. Schizophrenia Research 159(1), 36-42.
60. Schaufelberger, M.S., Lappin, J.M., Duran, F.L.S., Rosa, P.G.P., Uchida, R.R., Santos, L.C., Murray, R.M., McGuire, P.K., Scazufca, M., Menezes, P.R., Busatto, G.F., 2010. Lack of progression of brain abnormalities in first-episode psychosis: a longitudinal magnetic resonance imaging study. Psychological Medicine 41(8), 1677-1689.
61. Ségonne, F., Dale, A.M., Busa, E., Glessner, M., Salat, D., Hahn, H.K., Fischl, B., 2004. A hybrid approach to the skull stripping problem in MRI. NeuroImage 22(3), 1060-1075.
62. Segonne, F., Pacheco, J., Fischl, B., 2007. Geometrically Accurate Topology-Correction of Cortical Surfaces Using Nonseparating Loops. IEEE Transactions on Medical Imaging 26(4), 518-529.
63. Selemon, L.D., Goldman-Rakic, P.S., 1999. The reduced neuropil hypothesis: a circuit based model of schizophrenia. Biological Psychiatry 45(1), 17-25.
64. Takahashi, T., Suzuki, M., Zhou, S.-Y., Tanino, R., Nakamura, K., Kawasaki, Y., Seto, H., Kurachi, M., 2010. A follow-up MRI study of the superior temporal subregions in schizotypal disorder and first-episode schizophrenia. Schizophrenia Research 119(1), 65-74.
65. Takahashi, T., Wood, S.J., Soulsby, B., McGorry, P.D., Tanino, R., Suzuki, M., Velakoulis, D., Pantelis, C., 2009. Follow-up MRI study of the insular cortex in first-episode psychosis and chronic schizophrenia. Schizophrenia Research 108(1), 49-56.
66. Takahashi, T., Wood, S.J., Yung, A.R., Soulsby, B., McGorry, P.D., Suzuki, M., Kawasaki, Y., Phillips, L.J., Velakoulis, D., Pantelis, C., 2009. Progressive Gray Matter Reduction of the Superior Temporal Gyrus During Transition to Psychosis. Archives of General Psychiatry 66(4), 366-376.
67. Takahashi, T., Zhou, S.-Y., Nakamura, K., Tanino, R., Furuichi, A., Kido, M., Kawasaki, Y., Noguchi, K., Seto, H., Kurachi, M., Suzuki, M., 2011. A follow-up MRI study of the fusiform gyrus and middle and inferior temporal gyri in schizophrenia spectrum. Progress in Neuro-Psychopharmacology and Biological Psychiatry 35(8), 1957-1964.
68. Théberge, J., Williamson, K.E., Aoyama, N., Drost, D.J., Manchanda, R., Malla, A.K., Northcott, S., Menon, R.S., Neufeld, R.W.J., Rajakumar, N., Pavlosky, W., Densmore, M., Schaefer, B., Williamson, P.C., 2007. Longitudinal grey-matter and glutamatergic losses in first-episode schizophrenia. British Journal of Psychiatry 191(4), 325-334.

69. van Erp, T.G.M., Walton, E., Hibar, D.P., Schmaal, L., Jiang, W., Glahn, D.C., Pearlson, G.D., Yao, N., Fukunaga, M., Hashimoto, R., Okada, N., Yamamori, H., Bustillo, J.R., Clark, V.P., Agartz, I., Mueller, B.A., Cahn, W., de Zwarte, S.M.C., Hulshoff Pol, H.E., Kahn, R.S., Ophoff, R.A., van Haren, N.E.M., Andreassen, O.A., Dale, A.M., Doan, N.T., Gurholt, T.P., Hartberg, C.B., Haukvik, U.K., Jørgensen, K.N., Lagerberg, T.V., Melle, I., Westlye, L.T., Gruber, O., Kraemer, B., Richter, A., Zilles, D., Calhoun, V.D., Crespo-Facorro, B., Roiz-Santiañez, R., Tordesillas-Gutiérrez, D., Loughland, C., Carr, V.J., Catts, S., Cropley, V.L., Fullerton, J.M., Green, M.J., Henskens, F.A., Jablensky, A., Lenroot, R.K., Mowry, B.J., Michie, P.T., Pantelis, C., Quidé, Y., Schall, U., Scott, R.J., Cairns, M.J., Seal, M., Tooney, P.A., Rasser, P.E., Cooper, G., Shannon Weickert, C., Weickert, T.W., Morris, D.W., Hong, E., Kochunov, P., Beard, L.M., Gur, R.E., Gur, R.C., Satterthwaite, T.D., Wolf, D.H., Belger, A., Brown, G.G., Ford, J.M., Macciardi, F., Mathalon, D.H., O'Leary, D.S., Potkin, S.G., Preda, A., Voyvodic, J., Lim, K.O., McEwen, S., Yang, F., Tan, Y., Tan, S., Wang, Z., Fan, F., Chen, J., Xiang, H., Tang, S., Guo, H., Wan, P., Wei, D., Bockholt, H.J., Ehrlich, S., Wolthusen, R.P.F., King, M.D., Shoemaker, J.M., Sponheim, S.R., De Haan, L., Koenders, L., Machielsen, M.W., van Amelsvoort, T., Veltman, D.J., Assogna, F., Banaj, N., de Rossi, P., Iorio, M., Piras, F., Spalletta, G., McKenna, P.J., Pomarol-Clotet, E., Salvador, R., Corvin, A., Donohoe, G., Kelly, S., Whelan, C.D., Dickie, E.W., Rotenberg, D., Voineskos, A.N., Ciufolini, S., Radua, J., Dazzan, P., Murray, R., Reis Marques, T., Simmons, A., Borgwardt, S., Egloff, L., Harrisberger, F., Riecher-Rössler, A., Smieskova, R., Alpert, K.I., Wang, L., Jönsson, E.G., Koops, S., Sommer, I.E.C., Bertolino, A., Bonvino, A., Di Giorgio, A., Neilson, E., Mayer, A.R., Stephen, J.M., Kwon, J.S., Yun, J.-Y., Cannon, D.M., McDonald, C., Lebedeva, I., Tomyshev, A.S., Akhadov, T., Kaleda, V., Fatouros-Bergman, H., Flyckt, L., Farde, L., Flyckt, L., Engberg, G., Erhardt, S., Fatouros-Bergman, H., Cervenka, S., Schwieler, L., Piehl, F., Agartz, I., Collste, K., Victorsson, P., Malmqvist, A., Hedberg, M., Orhan, F., Busatto, G.F., Rosa, P.G.P., Serpa, M.H., Zanetti, M.V., Hoschl, C., Skoch, A., Spaniel, F., Tomecek, D., Hagenaars, S.P., McIntosh, A.M., Whalley, H.C., Lawrie, S.M., Knöchel, C., Oertel-Knöchel, V., Stäblein, M., Howells, F.M., Stein, D.J., Temmingh, H.S., Uhlmann, A., Lopez-Jaramillo, C., Dima, D., McMahon, A., Faskowitz, J.I., Gutman, B.A., Jahanshad, N., Thompson, P.M., Turner, J.A., 2018. Cortical Brain Abnormalities in 4474 Individuals with Schizophrenia and 5098 Control Subjects via the Enhancing Neuro Imaging Genetics Through Meta-Analysis (ENIGMA) Consortium. Biological Psychiatry 84(9), 644-654.
70. van Haren, N.E.M., Schnack, H.G., Cahn, W., van den Heuvel, M.P., Lepage, C., Collins, L., Evans, A.C., Pol, H.E.H., Kahn, R.S., 2011. Changes in Cortical Thickness During the Course of Illness in Schizophrenia. JAMA Psychiatry 68(9), 871-880.
71. Vázquez-Bourgon, J., Roiz-Santiañez, R., Papiol, S., Ferro, A., Varela-Gómez, N., Fañanás, L., Crespo-Facorro, B., 2016. Variations in Disrupted-in-Schizophrenia 1 gene modulate long-term longitudinal differences in cortical thickness in patients with a first-episode of psychosis. Brain Imaging and Behavior 10(3), 629-635.
72. Vita, A., De Peri, L., Deste, G., Barlati, S., Sacchetti, E., 2015. The Effect of Antipsychotic Treatment on Cortical Gray Matter Changes in Schizophrenia: Does the Class Matter? A Meta-analysis and Meta-regression of Longitudinal Magnetic Resonance Imaging Studies. Biological Psychiatry 78(6), 403-412.
73. Vita, A., De Peri, L., Deste, G., Sacchetti, E., 2012. Progressive loss of cortical gray matter in schizophrenia: a meta-analysis and meta-regression of longitudinal MRI studies. Translational Psychiatry 2, e190.

74. Walton, E., Hibar, D.P., van Erp, T.G.M., Potkin, S.G., Roiz-Santiañez, R., Crespo-Facorro, B., Suarez-Pinilla, P., van Haren, N.E.M., de Zwarte, S.M.C., Kahn, R.S., Cahn, W., Doan, N.T., Jørgensen, K.N., Gurholt, T.P., Agartz, I., Andreassen, O.A., Westlye, L.T., Melle, I., Berg, A.O., Morch-Johnsen, L., Færden, A., Flyckt, L., Fatouros-Bergman, H., Karolinska Schizophrenia Project, C., Jönsson, E.G., Hashimoto, R., Yamamori, H., Fukunaga, M., Jahanshad, N., De Rossi, P., Piras, F., Banaj, N., Spalletta, G., Gur, R.E., Gur, R.C., Wolf, D.H., Satterthwaite, T.D., Beard, L.M., Sommer, I.E., Koops, S., Gruber, O., Richter, A., Krämer, B., Kelly, S., Donohoe, G., McDonald, C., Cannon, D.M., Corvin, A., Gill, M., Di Giorgio, A., Bertolino, A., Lawrie, S., Nickson, T., Whalley, H.C., Neilson, E., Calhoun, V.D., Thompson, P.M., Turner, J.A., Ehrlich, S., 2018. Prefrontal cortical thinning links to negative symptoms in schizophrenia via the ENIGMA consortium. Psychological medicine 48(1), 82-94.
75. Whitford, T.J., Grieve, S.M., Farrow, T.F.D., Gomes, L., Brennan, J., Harris, A.W.F., Gordon, E., Williams, L.M., 2006. Progressive grey matter atrophy over the first 2–3 years of illness in first-episode schizophrenia: A tensor-based morphometry study. NeuroImage 32(2), 511-519.
76. Winkler, A.M., Kochunov, P., Blangero, J., Almasy, L., Zilles, K., Fox, P.T., Duggirala, R., Glahn, D.C., 2010. Cortical thickness or grey matter volume? The importance of selecting the phenotype for imaging genetics studies. NeuroImage 53(3), 1135-1146.
77. Woods, S.W., 2003. Chlorpromazine equivalent doses for the newer atypical antipsychotics. J. Clin. Psychiatry, 64, 663-667
78. Zak, N., Bøen, E., Boye, B., Andreassen, O.A., Doan, N.T., Malt, U.F., Westlye, L.T., Elvsåshagen, T., 2019. Mood episodes are associated with increased cortical thinning: A longitudinal study of bipolar disorder type II. Bipolar Disorders 0(0).
79. Zhang, Y., Catts, V.S., Sheedy, D., McCrossin, T., Kril, J.J., Shannon Weickert, C., 2016. Cortical grey matter volume reduction in people with schizophrenia is associated with neuro-inflammation. Translational Psychiatry 6(12), e982-e982.

Chapter 5

General Discussion

5.1 Introduction

This thesis explored the progressive profile of neuroanatomical changes in ventricles and the cortico-subcortical regions of the brain after the first 3-years of first-episode of psychosis. We further ascertained if these changes were related to clinical and functional measures including severity of symptoms, use of antipsychotic medications and level of functioning. In order to accurately measure the neuroanatomical changes, performance in terms of anatomical accuracy, consistency and required labour intensity of various types of brain segmentation techniques were compared to choose an optimal segmentation tool for this project. This chapter will therefore provide a summary of each of the study findings, provide an integrated discussion emerging from the various studies, examine the strengths and limitations of the work and finally, make recommendations for future research directions that may be beneficial to this area of work.

5.2 Summary of main findings

Study 1 - This study highlighted that in a typical neuropsychiatric MRI study, the anatomical accuracy and consistency of subcortical segmentation is dependent upon the anatomical location and adjacency to other grey matter structures. This study further demonstrated that automated segmentation techniques provide a good accuracy for an *easy-to-segment* structure such as the caudate, whereas for a *difficult-to-segment* structure such as the hippocampus, a reasonable correlation with volume but poor absolute agreement exist. Thus, volumetric estimates from automated techniques are not always comparable to those obtained from manual segmentation especially when examining complex anatomical structures. It is therefore recommended that manual or stereological volume estimation should be considered for studies that require high levels of precision such as those with small sample size. However, these segmentation techniques require high human resource in terms of technical skills, anatomical knowledge and labour intensity, thus although FreeSurfer required approximately seven times longer (12 hours on our system) of computational processing time relative to manual segmentation, it was considered the optimal segmentation tool for this study because:

1. FreeSurfer generates numerous morphometric measures of both cortical and subcortical regions (volume, thickness and surface area etc) in a single analysis and has additional tools (e.g. QDEC) for whole-brain cortical analysis with in-built statistical controls for multiple comparison.
2. FreeSurfer demonstrates a relatively good reliability/reproducibility at segmenting both sets of (*easy/difficult-to-segment*) structures compared to

the fully-automated techniques.

3. FreeSurfer provides an option for the automated FreeSurfer segmentation procedure and its outputs to be quality checked and corrected to minimise errors related to the morphometric estimation of brain tissues. Reports from other studies showed a significantly improved quality of segmentation which was comparable to the gold standard of manual tracing after engaging the semi-automated features of FreeSurfer (e.g. application of control-points and/or skullstripping) to edit the outputs (McCarthy *et al.* 2015).

4. FreeSurfer has a robust and validated (Reuter *et al.* 2010; Reuter and Fischl, 2011) longitudinal data processing pipeline (https://surfer.nmr.mgh.harvard.edu) which has the advantage, compared to other longitudinal analysis approaches, of accounting for inter-subject variability by creating an unbiased subject-specific anatomical template from the images at both time-points resulting in higher anatomical accuracy in identifying subtle changes over time. Therefore, this was deemed appropriate for analysis of our data.

Study 2 - Based on the findings and recommendations of study 1, the longitudinal FreeSurfer analysis approach was applied to data acquired from our first-episode of psychosis cohort that was assessed and scanned very early after presenting to the mental health services and after 3-years. This study highlighted the existence, extent and location of longitudinal morphometric changes in subcortical grey matter structures after first-episode of psychosis. Specifically, this study demonstrated the existence of localised progressive changes characterised by volume deficits in the dorsal striatum and thalamic regions and by right lateral ventricular enlargement. The progressive enlargement in ventricular volume was associated with poorer clinical outcome. Thus, ventricular volume enlargement over time could be a neuroanatomical marker of poorer clinical and functional outcome.

Study 3 - Following on from study 2, this further study examined the progressive profile of abnormalities after the first-episode of psychosis across the cortical mantle. Our findings highlighted the existence of localised progressive rates of cortical thinning most prominent in the left lateral orbitofrontal regions after the early years of first-episode of psychosis to indicate that thinning was present across the psychosis phenotype. Taken together, the highlights from study 2 and 3 is suggestive of a disturbance in the structural integrity of the associative/cognitive component of the cortico-striato-thalamo-cortical circuitry which

appears to be compromised in a progressive manner over the initial years after the first presentation of a psychotic illness.

5.3 Impact of volume segmentation on associations with clinical and functional measures

In study 1, we demonstrated a lack of absolute agreement in volume estimation, particularly of the hippocampus when using the automated techniques including FreeSurfer. Although this is relevant anatomically, it may not always be essential in large scale neuropsychiatric research studies given the reasonable correlations with manual segmentation noted, which may suffice to detect case-control differences or disease progression markers. Furthermore, given that FreeSurfer tends to overestimate hippocampal volume (Akudjedu *et al.* 2018), manually segmented hippocampal volumes were also incorporated in our analyses that focused on progression of subcortical structures after FEP (study 2). We observed that the FreeSurfer-acquired hippocampal volumes in the FEP patients (study 2) were relatively larger compared to manually-segmented volumes, even after rigorous quality controls and corrections. Despite the volumetric overestimations, comparable case-control differences were found with both approaches, indicating that this finding does not relate to methodological bias.

However, the volumetric mean differences may be explained by the varied neuroanatomical boundary definitions employed by these segmentation approaches of the hippocampus. Interestingly, there was a moderate correlation at a statistical trend level between progressive volumetric deficit of manually segmented hippocampal volume and poorer clinical outcome as measured by positive and negative symptoms, which was not evident in the larger FreeSurfer segmented structure. This may be because the manually segmented hippocampus focuses upon the functionally specific hippocampus proper and dentate, whereas FreeSurfer segmented hippocampus includes more functionally diverse structures such as variable amounts of subiculum and the Andreas-Retzius and the Fasciolar gyrus from the tail region as reported in study 1 (Akudjedu *et al.* 2018). If these findings are confirmed in a larger sample, this would be consistent with the study of Lappin and colleagues (2014) that hippocampal volume enlargement after FEP is a marker of good clinical outcome. These findings further support the relevance of manual segmentation to indicate its essential role in smaller studies where greater precision is required in maximising available statistical power, whereas automated segmentation remains optimal for large sample studies and collaborative consortia.

5.4 Progression of the cortico-striato-thalamo-cortical circuitry after first-episode of psychosis

We additionally demonstrated in study 2, a regionally selective volumetric reduction in dorsal striatum and thalamic regions which strongly correlated with LV enlargement over time. Interestingly, the observed associations between LV enlargement and the regionally specific shrinkage of the adjacent subcortical GM structures (thalamus and caudate) were more significant while a similar relationship was observed with the putamen (a relatively remote structure with reference to LV), this was not significant. These findings are in agreement with that of Gaser and colleagues (2004) that reported similar associations between ventricular enlargement and volume reductions of the thalamus, striatum and the superior temporal cortex in a schizophrenia cohort.

Furthermore, study 3 findings demonstrated the full extent of cortical thickness change and differences across the entire cortical mantle between groups over time. There were widespread cortical changes noted at an uncorrected level, mainly within the frontal and temporal regions, however, a focally distinct cortical pathology of thinning was found, specifically, in the left lateral orbitofrontal cortex which extended into aspects of the left pars orbitalis, pars triangularis, rostral middle frontal gyrus and frontal pole (ROI) of FEP patients over time. This agrees with several other longitudinal studies that previously demonstrated progressive thinning in subregions of the prefrontal cortex in FEP patients (Andreasen *et al.* 2011; Gutiérrez-Galve *et al.* 2015; Buchy *et al.* 2017), ARMS patients (Cannon *et al.* 2015) and in those with more established illness (van Haren *et al.* 2011; Cobia *et al.* 2012) over time.

In order to explore whether the subcortical and cortical deficits identified in chapters 3 and 4 were related, I performed correlations on the extracted changes over time in these structures in the same FEP patients (Table 5.1). However, we found no significant associations between the symmetrised percentage change in cortical thickness from the abnormally thinned ROI and LV enlargement or caudate, putamen and thalamic volume reduction (Table 5.1).

Our observation of progressive thalamic volume reduction in study 2 is consistent with some longitudinal studies of FEP (Theberge *et al.* 2007; Andreasen *et al.* 2011) and established psychosis (van Haren *et al.* 2007; Cobia *et al.* 2017). Moreover, reduced thalamic volume has also been observed over time in individuals at high risk for psychosis (Harrisberger *et al.* 2016) and in those at high genetic liability for schizophrenia (Lawrie *et al.* 2001; McDonald *et*

al. 2004). Despite, the finding of no significant associations in thalamic volume reduction and left lateral orbitofrontal regional thinning (Table 5.1), the observed changes in these structures indicate an early emergence of an aberrant functional coupling in neuroanatomy after FEP (Steullet, 2019). These findings are corroborated by another first-episode of psychosis study (Cho *et al.* 2019) that employed diffusion imaging techniques to observe microstructural alterations in the mediodorsal and pulvinar regions of the thalamus, that directly connect to the orbitofrontal and latero-temporal cortices. The thalamus is a neuroanatomical hub for integration of diverse information throughout the cortex (Hwang *et al.* 2017) and other subcortical regions. Albeit speculative, there is progression of abnormalities in the functional neuroanatomical units of the trans-thalamic circuitries which seem to be initiated with an active but inefficient cortical reorganisation (Palaniyappan, 2017; Palaniyappan *et al.* 2018) in the lateral orbitofrontal regions of the prefrontal cortex. Previous findings in chronic schizophrenia demonstrate significant cortical thinning in the orbitofrontal cortices bilaterally, inferior frontal, inferior temporal and occipitotemporal cortices (Kuperberg *et al.* 2003). Thus, our findings of cortical thinning in the left lateral orbitofrontal region is supported by the findings of Kuperberg and colleagues (2003) to indicate a pattern of thinning across the cortical mantle due to psychosis which is likely initiated from the left lateral orbitofrontal cortex before progressing further to other cortices across the entire course of illness (van Haren *et al.* 2011).

The trans-thalamic circuitries involve connections between the thalamus, cortex and other subcortical structures, particularly, the striatum. In study 2, we observed a progressive caudate and putaminal volume reduction over time which is consistent with some other longitudinal studies of FEP (Massana *et al.* 2005; Glenthoj *et al.* 2007; Deng *et al.* 2009; Roiz-Santiánez *et al.* 2014). Similarly, the observed cortical thinning in the left lateral orbitofrontal region do not associate with the volume changes in the dorsal striatum (caudate and putamen) (Table 5.1). However, considering reports (Amato *et al.* 2019; McCutcheon *et al.* 2019) that antipsychotic medication affect brain structure, especially the regions of high dopamine D_2 receptor density such as the basal ganglia, it is likely that our observation of no significant association between thinning of the LLOFR and volume reduction in the dorsal striatum were obscured by subregional striatal responses to antipsychotic medication (Massana *et al.* 2005; Glenthoj *et al.* 2007; Deng *et al.* 2009; Roiz-Santiánez *et al.* 2014). The use of antipsychotic medication in some cohorts may be obscuring the full extent of basal ganglia reduction which is more readily detected in medication naïve sample (Haijma *et al.* 2013) or in those with minimal medication exposure (Glenthoj *et al.* 2007; Deng *et al.* 2009).

In fact, others have also reported increased thalamic volume after a short period of antipsychotic treatment (Deng *et al.* 2009; Dazzan *et al.* 2005). In further support of this interpretation, the findings of study 2 demonstrate a strong association between increased putaminal and pallidal volumes and high cumulative antipsychotic medication taken during the interscan period in these same patients. However, our finding of progressive cortical thinning in the left lateral orbitofrontal region do not relate to cumulative antipsychotic medication taken during the interscan period as assessed by chlorpromazine equivalents (Woods, 2003). In contrast, there have been suggestions that antipsychotic medication influences total grey matter tissues (Vita *et al.* 2015; Guo *et al.* 2015) with a report demonstrating significant associations between prefrontal cortical thinning and short-term antipsychotic treatment in a first-episode schizophrenia cohort (Lesh *et al.* 2015). This further suggests that this regional cortical thinning is an inherent feature of progressive psychotic illness (Nesvag *et al.* 2008) which is potentially reflecting an underlying neuropathophysiological process associated with the onset of FEP and may not necessarily progress in a linear nature with volume changes in the subcortical structures. Taken together, these may be indicative of a structural neuroanatomical disturbance, particularly in the associative/cognitive component of the cortico-striato-thalamo-cortical circuitry (Ellison-Wright *et al.* 2008; Galvan *et al.* 2015). Thus, perhaps to better understand the progressive relationship of structure-function after FEP, it will be imperative to consider the structural changes in the neural information processing pathways, involving the trans-thalamic circuitries.

Table 5.1: Correlation of mean symmetrised percentage change (spc) in cortical thickness of the left lateral orbitofrontal region with the significantly changed subcortical structures and lateral ventricles in FEP patients over time

% Change in Structure	Hemisphere	Correlations with thickness (spc) in the LLOFR	
		r	p
Caudate	L	0.163	0.427
	R	0.159	0.437
Putamen	L	-0.078	0.703
	R	0.218	0.285
Thalamus	L	-0.134	0.516
	R	0.273	0.177
Lateral ventricle	L	-0.071	0.721
	R	-0.048	0.815

Table 5.1 Legend: % volume change in each structure was computed as = [(Time $_2$ – Time $_1$)/Time $_1$)] x 100. L = left hemisphere; R = right hemisphere. Note: All correlations were controlled for age at baseline and gender.

5.5 Strengths and Limitations

The strengths and limitations will be discussed in relation to each study. To the best of our knowledge, study 1 compared the largest number (n=5) of different segmentation (stereology, semi-automated and two fully-automated) techniques in the largest heterogenous sample (n=281) with significant neuropsychiatric disorders to-date. It also provided quantified segmentation technique bias estimates across structures. Thus, these findings are likely generalisable to the current trend of large-scale global collaborations which are using semi-automated techniques on their research projects such as the Enhancing Neuroimaging Genetics through Meta-analysis (ENIGMA), the Human Connectome Project (HCP) and the Alzheimer's Disease Neuroimaging Initiative (ADNI) for example (Hibar *et al.* 2016; van Erp *et al.* 2016; Franke *et al.* 2016) which have investigated to date the influence of various demographic and clinical factors on sub/cortical structures. There are a number of limitations associated with study 1 of this thesis. Of note, only two structures were examined, however given that these two structures are implicated in several neuropsychiatric disorders and are at either end of the spectrum in relation to the ease of segmentation, findings in relation to these structures are likely generalisable to several other brain structures. Secondly, data was acquired using a 1.5T MR scanner, and it is possible that automated segmentation techniques may perform more accurately on images acquired with a ≥3T MR scanner. Thirdly, absolute volumes were used for this study rather than intracranial-corrected volumes however, group difference effects were not under examination in this study and the inclusion of intracranial volume corrections would have excluded the computation of practical performance metrics such as the percentage volume overlap which depends on the actual position of voxels (Sanchez-Benavides *et al.* 2010).

The main strength of studies 2 and 3 is the application of a longitudinal design to a cohort of psychotic patients who were originally assessed very shortly after presentation to the mental health services and with minimal antipsychotic exposure. The recruited sample for these studies consist of a broad array of psychosis phenotypes, rather than focus on schizophrenia spectrum disorders alone like other groups have done previously (Cahn *et al.* 2002; Asami *et al.* 2012; Roiz-Santianez *et al.* 2015; Li *et al.* 2018). Thus, we recruited a sample that is more generally representative of FEP patients presenting to the mental health services. Although several studies have investigated the cross-sectional relationship between sub/cortical neuroanatomical changes and clinical/functional measures in FEP, few have carried out longitudinal analyses to clarify the existence, extent and location of progressive changes and their associations over time with clinical and functional measures. Despite the potential

increase in clinical heterogeneity associated with this sample, we were able to detect regions of sub/cortical progression and link these with measures of clinical outcome that were not confined to a non-affective psychosis category alone. In relation to MRI data acquisition, the same scanner and acquisition sequences were employed without any major software or hardware upgrades during the study period and the participants were scanned in a random order at each time-point, thus, minimising any acquisition bias due to changes in scanner characteristics over time, which is known to potentially confound group diagnostic differences. Furthermore, we used the longitudinal FreeSurfer pipeline (v.5.3) which has the advantage, compared to other longitudinal analysis approaches, of accounting for inter-subject variability by creating an unbiased subject-specific anatomical template (Reuter *et al.* 2010) from the images at both time-points resulting in higher anatomical accuracy in identifying subtle changes over time. In relation to progressive cortical change analysis, the application of a global longitudinal vertex-wise analyses approach and our ability to extract individual cortical metric values of thickness of the abnormally thinned regions is a key strength. The group vertex-wise analyses, unlike the surface-based approaches which are less reliable at localising changes within specific lobular subregions (DeLisi, 2008; Cercignani *et al.* 2018) has enabled a hypothesis-free investigation over the entire cortical mantle to outline specific abnormal regions and thus, the need for future studies to move beyond the conventional volume-based approaches when investigating cortical morphometry.

The main limitation in the design of study 2 and 3 was the relatively small sample size and consequent risk of type II error and generalisability of the results, which require confirmation in larger carefully acquired samples. We did not employ a stringent statistical approach to control for multiple comparisons in our analysis relating to subcortical structures, however, our major findings were hypothesised *a priori* based on current available literature in this area. In relation to the global vertex-wise cortical analysis, a cluster-forming threshold of <0.05 may be considered too low, however, after repeating the analyses using a cluster-forming threshold of <0.01 (Fig.4.5), the main group difference remained significant. Finally, due to inadequate data availability we were not able to assess the influence of environmental exposures other than antipsychotic medication (e.g. cannabis use) on the ventricles, subcortical structures and the observably thinned regions of the prefrontal cortex. The collection of such data would have provided further insight into the impact of environmental exposures on neuroanatomical progression over time including for example, the influence of cannabis use on sub/cortical and ventricular progression over time.

5.6 Recommendations and future directions

Future work could aim to replicate the findings of study 1 in a dataset acquired on a scanner of higher acquisition strength (≥3T) to re-assess the performance of a set of segmentation techniques. Additional focus on the performance of each technique at segmenting subregional morphometry of subcortical structures in a large heterogenous sample of psychiatric disorders could be explored. Findings from such a study would enable selection of an optimal segmentation tool to assess the progression of neuroanatomical abnormalities in an FEP cohort with focus to progression of detailed regional abnormalities such as those reported, mostly in cross-sectional studies in schizophrenia and other neuropsychiatric disorders as well as replicating the findings of the current study. For example, hippocampal subfields (Iglesias *et al.* 2016; Li *et al.* 2018; Brown *et al.* 2019), amygdala subfields (Brown *et al.* 2019) and thalamic subfields (Cobia *et al.* 2017). Additionally, this could form the basis for research in computing and engineering into the development of tools for subfield segmentation of other structures like the caudate, putamen and globus pallidus which are currently not available. Furthermore, replication of findings from the current study utilising the latest version of FreeSurfer (v.6.0) would be beneficial, given that concerns have previously been expressed that newer versions of FreeSurfer have not replicated previous findings of earlier FreeSurfer versions (Iglesias *et al.* 2016). Additionally, replication of findings utilising other image processing tools such as SIENA (Structural Image Evaluation, using Normalisation, of Atrophy)(Smith et al. 2002; 2004) and CAT12 (http://www.neuro.uni-jena.de/cat/) will further strengthen evidence of progressive temporal cortical brain changes after FEP.

To further elucidate the profile of progressive neuroanatomical changes in much detail, future studies could aim to replicate the findings of study 2 and 3 in a carefully recruited FEP cohort such as those who present to the mental health services shortly after their first-episode and follow them up at multiple time-points in a larger cohort of individuals with affective and non-affective psychosis over a long period. This replication is necessary to clearly determine whether progressive changes continue in a linear, nonlinear, sporadic and/or curvilinear nature as suggested in at least two previous studies (DeLisi *et al*. 1998; van Haren *et al.* 2008) that focused solely on non-affective psychotic phenotypes mostly at the established stages of the illness.

Additionally, future studies could also aim to extensively assess the impact of other clinical and major environmental exposures on brain progression over time. For example, cannabis use during the follow-up period, changes in cognitive performance and urbanicity (rural vs.

urban dwelling) to allow exploratory investigations in the future. It would also be of interest to the field if future studies would assess the progression of white matter abnormalities over a relatively longer period using structural and functional connectivity as well as other emerging graph theory approaches. For example, in a recent study by Ganella and colleagues (2018), a first-episode psychosis cohort was followed-up after 12 months using brain network approaches and observed no evidence of abnormal brain topology in FEP patients relative to HCs. Thus, a longer follow-up time may further outline the natural progression of white matter topology in relation to the disease process. Finally, future studies may also consider elucidating the functional consequences of anatomical progression by incorporating multimodal imaging and cognitive/functional measures in larger longitudinal studies with multiple assessment points.

5.7 Conclusion

Taken together, our findings from the comparative analyses of brain segmentation techniques should inform the field about the considerable advantages and caveats of using each type of segmentation technique in decision making especially for the now standard, large-scale brain morphometric studies ongoing in the field of neuropsychiatry. Furthermore, our findings from studies that focused on FEP demonstrate the existence of localised progressive cortical thinning which is most prominent in the left lateral orbitofrontal region and characterised by volume deficits in the dorsal striatum, thalamic regions and right lateral ventricular enlargement after the early years of first episode of psychosis across the psychosis phenotype. Taken together, these may be indicative of a progressive disturbance in the structural integrity of a subnetwork of the associative/cognitive component of the cortico-striato-thalamo-cortical circuitry involving the lateral orbitofrontal regions of the prefrontal cortex. Thus, this circuitry appears to be compromised in a progressive manner over the initial years after the first presentation of a psychotic illness. This thesis therefore highlights the importance of elucidating the underlying neurobiology of the progression of psychotic illness as indexed by clinical and functional deficits. Such knowledge could potentially contribute to the identification of imaging biomarkers for psychosis which would be particularly beneficial in the critical early stages of the disorder.

References

1. Akudjedu, T.N., Nabulsi, L., Makelyte, M., Scanlon, C., Hehir, S., Casey, H., Ambati, S., Kenney, J., O'Donoghue, S., McDermott, E., Kilmartin, L., Dockery, P., McDonald, C., Hallahan, B., Cannon, D.M., 2018. A comparative study of segmentation techniques for the quantification of brain subcortical volume. Brain Imaging and Behavior 12(6), 1678-1695.
2. Amato, D., Kruyer, A., Samaha, A.-N., Heinz, A., 2019. Hypofunctional Dopamine Uptake and Antipsychotic Treatment-Resistant Schizophrenia. Front Psychiatry 10, 314-314.
3. Andreasen, N.C., Nopoulos, P., Magnotta, V., Pierson, R., Ziebell, S., Ho, B.-C., 2011. Progressive brain change in schizophrenia: a prospective longitudinal study of first-episode schizophrenia. Biological psychiatry 70(7), 672-679.
4. Asami, T., Bouix, S., Whitford, T.J., Shenton, M.E., Salisbury, D.F., McCarley, R.W., 2012. Longitudinal loss of gray matter volume in patients with first-episode schizophrenia: DARTEL automated analysis and ROI validation. NeuroImage 59(2), 986-996.
5. Brown, S.S.G., Rutland, J.W., Verma, G., Feldman, R.E., Alper, J., Schneider, M., Delman, B.N., Murrough, J.M., Balchandani, P., 2019. Structural MRI at 7T reveals amygdala nuclei and hippocampal subfield volumetric association with Major Depressive Disorder symptom severity. Scientific Reports 9(1), 10166.
6. Buchy, L., Makowski, C., Malla, A., Joober, R., Lepage, M., 2017. Longitudinal trajectory of clinical insight and covariation with cortical thickness in first-episode psychosis. Journal of Psychiatric Research 86, 46-54.
7. Cahn, W., Pol, H.E.H., Lems, E.B.T.E., van Haren, N.E.M., Schnack, H.G., van der Linden, J.A., Schothorst, P.F., van Engeland, H., Kahn, R.S., 2002. Brain Volume Changes in First-Episode Schizophrenia: A 1-Year Follow-up Study. JAMA Psychiatry 59(11), 1002-1010.
8. Cannon, T.D., Chung, Y., He, G., Sun, D., Jacobson, A., van Erp, T.G.M., McEwen, S., Addington, J., Bearden, C.E., Cadenhead, K., Cornblatt, B., Mathalon, D.H., McGlashan, T., Perkins, D., Jeffries, C., Seidman, L.J., Tsuang, M., Walker, E., Woods, S.W., Heinssen, R., 2015. Progressive Reduction in Cortical Thickness as Psychosis Develops: A Multisite Longitudinal Neuroimaging Study of Youth at Elevated Clinical Risk. Biological Psychiatry 77(2), 147-157.
9. Cercignani, M., Dowell, G.N., Tofts, P.S., 2018. Quantitative MRI of the Brain: Principles of Physical Measurement, 2nd Edition edn., Boca Raton: CRC Press.
10. Cho, K.I.K., Kwak, Y.B., Hwang, W.J., Lee, J., Kim, M., Lee, T.Y., Kwon, J.S., 2019. Microstructural Changes in Higher-Order Nuclei of the Thalamus in Patients with First-Episode Psychosis. Biological Psychiatry 85(1), 70-78.
11. Cobia, D.J., Smith, M.J., Salinas, I., Ng, C., Gado, M., Csernansky, J.G., Wang, L., 2017. Progressive deterioration of thalamic nuclei relates to cortical network decline in schizophrenia. Schizophrenia research 180, 21-27.
12. Cobia, D.J., Smith, M.J., Wang, L., Csernansky, J.G., 2012. Longitudinal progression of frontal and temporal lobe changes in schizophrenia. Schizophrenia Research 139(1), 1-6.
13. Dazzan, P., Morgan, K.D., Orr, K., Hutchinson, G., Chitnis, X., Suckling, J., Fearon, P., McGuire, P.K., Mallett, R.M., Jones, P.B., Leff, J., Murray, R.M., 2005. Different Effects of Typical and Atypical Antipsychotics on Grey Matter in First Episode Psychosis: the ÆSOP Study. Neuropsychopharmacology 30, 765.

14. DeLisi, L.E., 2008. The concept of progressive brain change in schizophrenia: implications for understanding schizophrenia. Schizophr Bull 34(2), 312-321.
15. DeLisi, L.E., Sakuma, M., Ge, S., Kushner, M., 1998. Association of brain structural change with the heterogeneous course of schizophrenia from early childhood through five years subsequent to a first hospitalization. Psychiatry Research: Neuroimaging 84(2), 75-88.
16. Deng, M.Y., McAlonan, G.M., Cheung, C., Chiu, C.P.Y., Law, C.W., Cheung, V., Sham, P.C., Chen, E.Y.H., Chua, S.E., 2009. A naturalistic study of grey matter volume increase after early treatment in anti-psychotic naïve, newly diagnosed schizophrenia. Psychopharmacology 206(3), 437-446.
17. Ellison-Wright ,I ., Glahn , D.C., Laird , R.A., Thelen , M.S., Ed Bullmore , E., 2008. The Anatomy of First-Episode and Chronic Schizophrenia: An Anatomical Likelihood Estimation Meta-Analysis. American Journal of Psychiatry 165(8), 1015-1023.
18. Franke, B., Stein, J. L., Ripke, S., Anttila, V., Hibar, D. P., van Hulzen, K. J. E., et al., 2016. Genetic influences on schizophrenia and subcortical brain volumes: large-scale proof of concept. Nature Neuroscience, 19(3), 420–431.
19. Galvan, A., Devergnas, A., Wichmann, T., 2015. Alterations in neuronal activity in basal ganglia-thalamocortical circuits in the parkinsonian state. Frontiers in Neuroanatomy 9(5).
20. Ganella, E.P., Seguin, C., Pantelis, C., Whittle, S., Baune, B.T., Olver, J., Amminger, G.P., McGorry, P.D., Cropley, V., Zalesky, A., Bartholomeusz, C.F., 2018. Resting-state functional brain networks in first-episode psychosis: A 12-month follow-up study. Australian & New Zealand Journal of Psychiatry 52(9), 864-875.
21. Gaser, C., Nenadic, I., Buchsbaum, B.R., Hazlett, A.E., Buchsbaum. M.S., 2004. Ventricular Enlargement in Schizophrenia Related to Volume Reduction of the Thalamus, Striatum, and Superior Temporal Cortex. American Journal of Psychiatry 161(1), 154-156.
22. Glenthoj, A., Glenthoj, B.Y., Mackeprang, T., Pagsberg, A.K., Hemmingsen, R.P., Jernigan, T.L., Baaré, W.F.C., 2007. Basal ganglia volumes in drug-naive first-episode schizophrenia patients before and after short-term treatment with either a typical or an atypical antipsychotic drug. Psychiatry Research: Neuroimaging 154(3), 199-208.
23. Guo, J.Y., Huhtaniska, S., Miettunen, J., Jääskeläinen, E., Kiviniemi, V., Nikkinen, J., Moilanen, J., Haapea, M., Mäki, P., Jones, P.B., Veijola, J., Isohanni, M., Murray, G.K., 2015. Longitudinal regional brain volume loss in schizophrenia: Relationship to antipsychotic medication and change in social function. Schizophrenia research 168(1-2), 297-304.
24. Gutiérrez-Galve, L., Chu, E.M., Leeson, V.C., Price, G., Barnes, T.R.E., Joyce, E.M., Ron, M.A., 2014. A longitudinal study of cortical changes and their cognitive correlates in patients followed up after first-episode psychosis. Psychological Medicine 45(1), 205-216.
25. Harrisberger, F., Buechler, R., Smieskova, R., Lenz, C., Walter, A., Egloff, L., Bendfeldt, K., Simon, A.E., Wotruba, D., Theodoridou, A., Rössler, W., Riecher-Rössler, A., Lang, U.E., Heekeren, K., Borgwardt, S., 2016. Alterations in the hippocampus and thalamus in individuals at high risk for psychosis. Npj Schizophrenia 2, 16033.
26. Hibar, D. P., Westlye, L. T., van Erp, T. G. M., Rasmussen, J., Leonardo, C. D., Faskowitz, J., et al., 2016. Subcortical volumetric abnormalities in bipolar disorder. [Original Article]. Mol Psychiatry, 21(12), 1710-1716, doi:10.1038/mp.2015.227.
27. Hwang, K., Bertolero, M.A., Liu, W.B., D'Esposito, M., 2017. The Human Thalamus Is an Integrative Hub for Functional Brain Networks. The Journal of Neuroscience 37(23), 5594-5607.

28. Iglesias, J.E., Van Leemput, K., Augustinack, J., Insausti, R., Fischl, B., Reuter, M., Alzheimer's Disease Neuroimaging, I., 2016. Bayesian longitudinal segmentation of hippocampal substructures in brain MRI using subject-specific atlases. Neuroimage 141, 542-555.
29. Kuperberg, G.R., Broome, M.R., McGuire, P.K., David, A.S., Eddy, M., Ozawa, F., Goff, D., West, W.C., Williams, S.C.R., van der Kouwe, A.J.W., Salat, D.H., Dale, A.M., Fischl, B., 2003. Regionally Localized Thinning of the Cerebral Cortex in Schizophrenia. JAMA Psychiatry 60(9), 878-888.
30. Lappin, J.M., Morgan, C., Chalavi, S., Morgan, K.D., Reinders, A.A.T.S., Fearon, P., Heslin, M., Zanelli, J., Jones, P.B., Murray, R.M., Dazzan, P., 2014. Bilateral hippocampal increase following first-episode psychosis is associated with good clinical, functional and cognitive outcomes. Psychological Medicine 44(6), 1279-1291.
31. Lawrie, S.M., 2018. Are structural brain changes in schizophrenia related to antipsychotic medication? A narrative review of the evidence from a clinical perspective. Ther Adv Psychopharmacol 8(11), 319-326.
32. Lawrie, S.M., Whalley, H.C., Abukmeil, S.S., Kestelman, J.N., Donnelly, L., Miller, P., Best, J.J.K., Owens, D.G.C., Johnstone, E.C., 2001. Brain structure, genetic liability, and psychotic symptoms in subjects at high risk of developing schizophrenia. Biological Psychiatry 49(10), 811-823.
33. Lesh, T.A., Tanase, C., Geib, B.R., Niendam, T.A., Yoon, J.H., Minzenberg, M.J., Ragland, J.D., Solomon, M., Carter, C.S., 2015. A Multimodal Analysis of Antipsychotic Effects on Brain Structure and Function in First-Episode Schizophrenia Antipsychotics in First-Episode Schizophrenia Antipsychotics in First-Episode Schizophrenia. JAMA Psychiatry 72(3), 226-234.
34. Li, W., Li, K., Guan, P., Chen, Y., Xiao, Y., Lui, S., Sweeney, J.A., Gong, Q., 2018. Volume alteration of hippocampal subfields in first-episode antipsychotic-naïve schizophrenia patients before and after acute antipsychotic treatment. NeuroImage: Clinical 20, 169-176.
35. Massana, G., Salgado-Pineda, P., Junqué, C., Pérez, M., Baeza, I., Pons, A., Massana, J., Navarro, V., Blanch, J., Morer, À., Mercader, J.M., Bernardo, M., 2005. Volume changes in gray matter in first-episode neuroleptic-naive schizophrenic patients treated with risperidone. Journal of Clinical Psychopharmacology 25(2), 111-117.
36. McCarthy, C. S., Ramprashad, A., Thompson, C., Botti, J.-A., Coman, I. L., & Kates, W. R., 2015. A comparison of FreeSurfer-generated data with and without manual intervention. [Original Research]. Frontiers in Neuroscience, 9(379), doi:10.3389/fnins.2015.00379.
37. McCutcheon, R.A., Abi-Dargham, A., Howes, O.D., 2019. Schizophrenia, Dopamine and the Striatum: From Biology to Symptoms. Trends in Neurosciences 42(3), 205-220.
38. McDonald, C., Bullmore, E.T., Sham, P.C., Chitnis, X., Wickham, H., Bramon, E., Murray, R.M., 2004. Association of Genetic Risks for Schizophrenia and Bipolar Disorder with Specific and Generic Brain Structural Endophenotypes. Archives of General Psychiatry 61(10), 974-984.
39. Nesvag, R., Lawyer, G., Varnäs, K., Fjell, A.M., Walhovd, K.B., Frigessi, A., Jönsson, E.G., Agartz, I., 2008. Regional thinning of the cerebral cortex in schizophrenia: Effects of diagnosis, age and antipsychotic medication. Schizophrenia Research 98(1), 16-28.

40. Palaniyappan, L., 2017. Progressive cortical reorganisation: A framework for investigating structural changes in schizophrenia. Neuroscience & Biobehavioral Reviews 79, 1-13.
41. Palaniyappan, L., Hodgson, O., Balain, V., Iwabuchi, S., Gowland, P., Liddle, P., 2018. Structural covariance and cortical reorganisation in schizophrenia: a MRI-based morphometric study. Psychological Medicine 49(3), 412-420.
42. Reuter, M., Rosas, H.D., Fischl, B., 2010. Highly accurate inverse consistent registration: A robust approach. NeuroImage 53(4), 1181-1196.
43. Reuter, M., Fischl, B., 2011. Avoiding asymmetry-induced bias in longitudinal image processing. NeuroImage 57(1), 19-21.
44. Roiz-Santiánez, R., Ortiz-García de la Foz, V., Ayesa-Arriola, R., Tordesillas-Gutiérrez, D., Jorge, R., Varela-Gómez, N., Suárez-Pinilla, P., Córdova-Palomera, A., Navasa-Melado, J.M., Crespo-Facorro, B., 2015. No progression of the alterations in the cortical thickness of individuals with schizophrenia-spectrum disorder: a three-year longitudinal magnetic resonance imaging study of first-episode patients. Psychological Medicine 45(13), 2861-2871.
45. Sanchez-Benavides, G., Gómez-Ansón, B., Sainz, A., Vives, Y., Delfino, M., & Peña-Casanova, J., 2010. Manual validation of FreeSurfer's automated hippocampal segmentation in normal aging, mild cognitive impairment, and Alzheimer Disease subjects. Psychiatry Research: Neuroimaging, 181(3), 219-225.
46. Smith, S.M., Jenkinson, M., Woolrich, M.W., Beckmann, C.F., Behrens, T.E.J., Johansen-Berg, H., Bannister, P.R., De Luca, M., Drobnjak, I., Flitney, D.E., Niazy, R.K., Saunders, J., Vickers, J., Zhang, Y., De Stefano, N., Brady, J.M., Matthews, P.M., 2004. Advances in functional and structural MR image analysis and implementation as FSL. Neuroimage 23, S208-S219.
47. Smith, S.M., Zhang, Y., Jenkinson, M., Chen, J., Matthews, P.M., Federico, A., De Stefano, N., 2002. Accurate, Robust, and Automated Longitudinal and Cross-Sectional Brain Change Analysis. Neuroimage 17(1), 479-489.
48. Steullet, P., 2019. Thalamus-related anomalies as candidate mechanism-based biomarkers for psychosis. Schizophrenia Research. https://doi.org/10.1016/j.schres.2019.05.027
49. Theberge, J., Williamson, K.E., Aoyama, N., Drost, D.J., Manchanda, R., Malla, A.K., Northcott, S., Menon, R.S., Neufeld, R.W.J., Rajakumar, N., Pavlosky, W., Densmore, M., Schaefer, B., Williamson, P.C., 2007. Longitudinal grey-matter and glutamatergic losses in first-episode schizophrenia. British Journal of Psychiatry 191(4), 325-334.
50. van Erp, T. G., Hibar, D. P., Rasmussen, J. M., Glahn, D. C., Pearlson, G. D., Andreassen, O. A., et al., 2016. Subcortical brain volume abnormalities in 2028 individuals with schizophrenia and 2540 healthy controls via the ENIGMA consortium. Mol Psychiatry, 21(4), 547-553, doi:10.1038/mp.2015.63.
51. van Haren, N.E.M., Pol, H.E.H., Schnack, H.G., Cahn, W., Brans, R., Carati, I., Rais, M., Kahn, R.S., 2008. Progressive Brain Volume Loss in Schizophrenia Over the Course of the Illness: Evidence of Maturational Abnormalities in Early Adulthood. Biological Psychiatry 63(1), 106-113.
52. Vita, A., De Peri, L., Deste, G., Barlati, S., Sacchetti, E., 2015. The Effect of Antipsychotic Treatment on Cortical Gray Matter Changes in Schizophrenia: Does the Class Matter? A Meta-analysis and Meta-regression of Longitudinal Magnetic Resonance Imaging Studies. Biological Psychiatry 78(6), 403-412.
53. Woods, S.W., 2003. Chlorpromazine equivalent doses for the newer atypical antipsychotics. J. Clin. Psychiatry, 64, 663-667